

THE EFFECTS OF NITRIC ACID AND SILANE SURFACE TREATMENTS ON
CARBON FIBERS AND CARBON/VINYL ESTER COMPOSITES BEFORE AND
AFTER SEAWATER EXPOSURE

by

Tye A. Langston

A Dissertation Submitted to the Faculty of
The College of Engineering and Computer Science
in Partial Fulfillment of the Requirements for the Degree of
Doctor of Philosophy

Florida Atlantic University

Boca Raton, Florida

December, 2008

Copyright by Tye Langston 2008

THE EFFECTS OF NITRIC ACID AND SILANE SURFACE TREATMENTS ON
CARBON FIBERS AND CARBON/VINYL ESTER COMPOSITES BEFORE AND
AFTER SEAWATER EXPOSURE

by

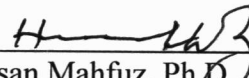
Tye A. Langston

This dissertation was prepared under the direction of the candidate's dissertation advisor, Prof. Richard Granata, Department of Ocean Engineering, and has been approved by the members of his supervisory committee. It was submitted to the faculty of the College of Engineering and Computer Science and was accepted in partial fulfillment of the requirements for the degree of Doctor of Philosophy.

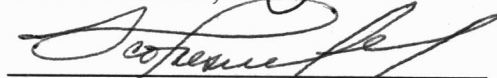
SUPERVISORY COMMITTEE:



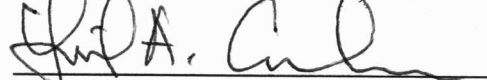
Richard Granata, Ph.D.
Dissertation Advisor



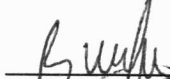
Hassan Mahfuz, Ph.D.



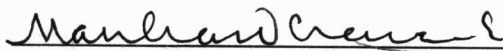
Francisco Presuel-Moreno, Ph.D.



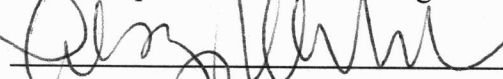
Lef Carlsson, Ph.D.



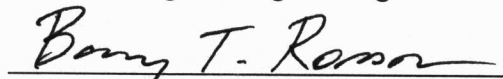
Betiana Acha, Ph.D.



Manhar R. Dhanak, Ph.D.
Chair, Department of Ocean Engineering



Karl K. Stevens, Ph.D.
Dean, College of Engineering and Computer Science



Barry T. Rosson, Ph.D.
Dean, Graduate College

Nov. 19, 2008

Date

ACKNOWLEDGEMENTS

I wish to express my deepest thanks to Prof. Richard Granata for the guidance, support and time he has contributed to this work. He has always kept this a learning experience and helped me to overcome the numerous obstacles I encountered along the way. I am grateful for the invaluable opportunity I have been afforded.

I would like to extend my gratitude to my committee members: Dr. Hassan Mahfuz, Dr. Leif Carlsson, Dr. Francisco Presuel-Moreno, and Dr. Betiana Acha, each of whom provided unique input that helped me to develop this document and myself as a better engineer. It is a rare opportunity to have access to advice from a group with such expertise and diverse engineering backgrounds.

Thanks to Prof. Howard Fairbrother at John's Hopkins University for the cooperative research he and his group provided. Their cooperation boosted my research and opened doors for future studies. Thanks to Ed Drown, Mike Rich and Prof. Drzal at Michigan State University for giving me access to their laboratory equipment, supplies and time. They helped me to complete an integral portion of this research.

And I could not forget my wife, who provided the most support of all. She must have infinite patience to put up with me.

I would also like to acknowledge the U.S. Office of Naval Research for the financial support provided under grant No. N00014-05-1-0341.

ABSTRACT

Author: Tye A. Langston

Title: The effects of nitric acid and silane surface treatments on carbon fibers and carbon/vinyl ester composites before and after seawater exposure

Institution: Florida Atlantic University

Thesis Advisor: Prof. Richard D. Granata

Degree: Doctor of Philosophy

Year: 2008

This research focuses on carbon fiber treatment by nitric acid and 3-(trimethoxysilyl)propyl methacrylate silane, and how this affects carbon/vinyl ester composites. These composites offer great benefits, but it is difficult to bond the fiber and matrix together, and without a strong interfacial bond, composites fall short of their potential. Silanes work well with glass fiber, but do not bond directly to carbon fiber because its surface is not reactive to liquid silanes. Oxidizing surface treatments are often prescribed for improved wetting and bonding to carbon, but good results are not always achieved. Furthermore, there is the unanswered question of environmental durability.

This research aimed to form a better understanding of oxidizing carbon fiber treatments, determine if silanes can be bonded to oxidized surfaces, and how these treatments affect composite strength and durability before and after seawater exposure.

Nitric acid treatments on carbon fibers were found to improve their tensile strength to a constant level by smoothing surface defects and chemically modifying their surfaces by increasing carbonyl and carboxylic acid concentrations. Increasing these surface group concentrations raises fiber polar energy and causes them to cohere. This impedes wetting, resulting in poor quality, high void content composites, even though there appeared to be improved adhesion between the fibers and matrix.

Silane was found to bond to the oxidized carbon fiber surfaces, as evidenced by changes in both fiber and composite properties. The fibers exhibited low polarity and cohesion, while the composites displayed excellent resin wetting, low void content, and low seawater weight gain and swelling. On the contrary, the oxidized fibers that were not treated with silane exhibited high polarity and fiber cohesion. Their composites displayed poor wetting, high void content, high seawater weight gain, and low swelling.

Both fiber treatment types resulted in great improvements in dry transverse tensile strength over the untreated fibers, but the oxidized fiber composites lost strength as the acid treatment time was extended, due to poor wetting. The acid/silane treated composites lost some transverse tensile strength after seawater exposure, but the nitric acid oxidized fiber composites appeared to be more seawater durable.

TABLE OF CONTENTS

LIST OF TABLES	ix
LIST OF FIGURES	xi
1. THEORY AND LITERATURE REVIEW	1
1.1 Introduction.....	1
1.2 Reinforcement/Matrix Bonding.....	7
1.3 Composite Degradation in Marine Environments	11
1.4 Sorption in Composites.....	17
1.5 Reinforcement (Fiber) Surface Modifications.....	19
1.5.1 Silane Treatment.....	20
1.5.2 Carbon Fiber Surface Treatments	28
2. MATERIALS.....	36
2.1 Carbon Fiber	36
2.2 Vinyl Ester Resin.....	41
3. RESEARCH.....	47
3.1 Theoretical Basis.....	47
3.1.1 Carbon Fiber Surface Treatment to Improve Fiber/matrix Adhesion and Durability	47
3.1.2 Carbon Fiber Surface Treatment and Silane Application to Improve Fiber/matrix Adhesion and Hydrolytic Stability.....	56
3.2 Experimental Methods and Results	57
3.2.1 Fiber Treatment.....	58

3.2.2	Fiber Surface Morphology and Diameter	63
3.2.3	Fiber Tensile Properties	72
3.2.4	Resin Tensile Properties	86
3.2.5	Fiber Surface Functional Chemistry	93
3.2.6	Fiber-fiber Interaction	103
3.2.7	Fiber Surface Wettability	113
3.2.8	Fiber Bundle Wettability	123
3.2.9	Composite Fiber Volume Fraction and Void Content	126
3.2.10	Composite Transverse Tensile Strength	137
3.2.11	Transverse Tensile Failure Analysis	147
3.2.12	Composite Seawater Weight Gain and Swelling	169
3.2.13	Composite Cross-sectional Analysis and Seawater Damage	176
3.3	Discussion	195
3.4	Conclusions	209
APPENDICES		220
A1	Fiber Diameter Measurements	220
A2	Fiber Tensile Test Measurements	222
A3	Resin Tensile Test Measurements	226
A4	Fiber Bundle Cohesion Test Measurements	228
A5	Fiber Surface Energy Measurements	229
A6	Transverse Tensile Strength Measurements	231
REFERENCES		244

LIST OF TABLES

Table 1 – Properties of sized and unsized carbon fibers used	41
Table 2– Resin property comparisons.....	44
Table 3– Typical liquid resin properties of Derakane Momentum™ 411-350 epoxy vinyl ester resin	45
Table 4– Typical cured properties of Derakane Momentum™ 411-350 epoxy vinyl ester resin.....	46
Table 5 - Fiber diameter change equation constants.....	71
Table 6 – Sized fiber (T700) average diameter	71
Table 7 – Unsized (AS4) fiber average diameter.....	72
Table 8 - Fiber compliance and Young's modulus results	85
Table 9 - Derakane 411-350 manufacturer-reported tensile properties	86
Table 10 - Measured tensile properties of Derakane 411-350 Momentum	90
Table 11 - Fiber surface functional oxygen percentages	100
Table 12 - Surface tension properties of water and diiodomethane.....	120
Table 13 - Density of composite specimens determined by ASTM D 792	130
Table 14 - Composite weight and volume percents.....	135
Table 15 - Untreated and acid-treated fiber transverse tensile specimen failure types ..	161
Table 16 - Silane-treated transverse tensile specimen failure types	162
Table 17 - Constants for composite weight gain equations	173
Table 18 - Constants for composite length change equations.....	173

Table 19 - Weight gain and length change order rankings	174
Table 20 - Composite wet and dry problem table.....	190

LIST OF FIGURES

Figure 1– 24.3 m (80 ft) yacht and 5.3 m (17.5 ft) pleasure boat with composite hulls ^{4,5}	2
Figure 2 - Royal Norwegian Navy Skjold class patrol boat. ¹⁰	3
Figure 3 –Royal Swedish Navy Visby class corvette. ¹¹	4
Figure 4 – Sandown with single-skin, framed composite hull. ¹⁹	5
Figure 5 – Current status of the application of composite structures to naval ships and submarines, as of 2001. ⁹	6
Figure 6 – Interface bonds formed by (a) mechanical interlocking; (b) chemical bonding; (c) reaction bonding after the formation of new compounds at the interface; (d) electrostatic attraction; (e) molecular entanglement; (f) interdiffusion of elements.....	8
Figure 7 – Composite material damage modes.....	11
Figure 8 – Source of shrinkage stresses: (a) rigid fiber embedded in a matrix; (b) resin pockets surrounded by fibers in hexagonal and square arrays. ²⁰	15
Figure 9 – Functionalities of Silane Groups	22
Figure 10 - Action of a coupling agent: (1) hydrolysis of organosilane to corresponding silanol; (2) hydrogen bonding between hydroxyl groups of silanol and glass surface; (3) condensation and bonding to glass surface; (4) organofunctional R-group reaction with polymer.	23
Figure 11 - Proposed reversible hydrolysis silane mechanism.....	25
Figure 12 - Interdiffusion and interpenetrating network in a silane-treated glass fiber-polymer matrix composite ⁷²	27
Figure 13 - Structure of the silane remnant remaining on glass fiber surface after extractive hydrolysis with hot water ⁷³	28
Figure 14 - Carbon fiber structure of layered graphite crystallites ⁸⁷	37

Figure 15 - Carbon fiber basal plane angle ⁸⁷	38
Figure 16 – Toray Industries carbon fiber production process ⁸⁷	39
Figure 17– Carbon fiber drawing ⁸⁷	40
Figure 18 – Formation of the vinyl ester molecule.....	42
Figure 19 - Vinyl ester cross-linking	43
Figure 20 – Cross-linked vinyl ester resin	45
Figure 21 – Surface groups that likely result from ammonia and nitrogen plasma treatment	50
Figure 22 – Surface groups that likely result from oxygen plasma treatment and nitric acid treatment.....	51
Figure 23 – Vinyl ester structure	52
Figure 24 – Styrene structure.....	52
Figure 25 – 3-(trimethoxysilyl)propyl methacrylate.....	57
Figure 26 – Carbon fiber nitric acid treatment configuration.....	59
Figure 27 – Fiber bundle treatment glass rod frame.....	59
Figure 28 – Fiber mat treatment assembly diagram.....	61
Figure 29 – Fiber mat treatment assembly photograph	61
Figure 30 – Quanta 200 ESEM used in this research	64
Figure 31 - Unsized fiber acid-treated SEM images.....	67
Figure 32 - Sized fiber acid-treated SEM images.....	69
Figure 33 – Fiber diameter as a function of acid treatment time	70
Figure 34 – Single fiber tensile test fixture.....	73
Figure 35 - MTS Insight 1kN test machine in the fiber tensile testing configuration	73
Figure 36 - Typical fiber tensile test plot (sized(T700) untreated).....	75

Figure 37 - Fiber load at break.....	75
Figure 38 - Fiber strength	76
Figure 39 - Sized (T700) fiber failure load as a function of test gage length.....	78
Figure 40 - Sized (T700) fiber Weibull plots, scale parameters and shape parameters....	80
Figure 41 - Unsized (AS4) fiber Weibull plots, scale parameters and shape parameters.	81
Figure 42 - Sized (T700) fiber predicted strength as a function of length.....	82
Figure 43 - Unsized (AS4) fiber predicted strength as a function of length.....	82
Figure 44 - System compliance chart.....	85
Figure 45 – Resin tensile test coupon dimensions	87
Figure 46 - Mold for resin tensile test specimens	88
Figure 47 - MTS 50 Insight test machine configured for resin tensile-testing	89
Figure 48 - MTS extensometer used for resin tensile-testing.....	90
Figure 49 - 411-350 catalyzed immediately after mixing resin and promoter	91
Figure 50 - 411-350 catalyzed one hour after mixing resin and promoter	91
Figure 51 - Vinyl ester type comparison.....	92
Figure 52 - Chemical derivatization reactions	95
Figure 53 - C(1s) and O(1s) XPS measurements on Sized (T700) fiber and various treatments of unsized (AS4) fiber	98
Figure 54 - Surface functional group type distribution from chemical derivatization and XPS (percentage of total surface concentration)	100
Figure 55 - Nitrogen percentage of total surface concentration from XPS	102
Figure 56 – Fiber cohesion test depiction.....	103
Figure 57 – In-progress fiber cohesion test.....	104
Figure 58 - Work of separation required for acid-treated fiber bundles.....	105

Figure 59 - Work of separation (acid-treated vs. water-treated).....	105
Figure 60 - Work of separation plotted against a linear time scale	106
Figure 61 - Fiber cohesion markings on acid treated fibers: (a) 120-minute treated unsized fiber, and (b) 160-minute treated sized fiber	107
Figure 62 - Work of separation for acid treated and acid/silane treated fiber bundles...	108
Figure 63 – Textile fiber cohesion test from ASTM D 2612.....	110
Figure 64 - Separation angle during fiber cohesion test	111
Figure 65 - Typical fiber bundle force-displacement curve.....	112
Figure 66 - Surface tension and surface energy	113
Figure 67 – Contact angle of a liquid drop on a solid surface	114
Figure 68 – Fiber contact angle measurement through tensiometry.....	118
Figure 69 - Cahn DCA-322 dynamic contact angle analyzer	119
Figure 70 - Mitutoyo LSM-6200 Laser Scan Micrometer.....	119
Figure 71 - Advancing contact angles with water and diiodomethane.....	120
Figure 72 - Receding contact angles with water and diiodomethane	121
Figure 73 - Total, polar, and dispersive fiber surface energies.....	121
Figure 74 - Bundle wettability test.....	124
Figure 75 - Fiber bundle wettability test in resin.....	125
Figure 76 - Setup used to weigh composites in water	128
Figure 77 - Composite densities as determined by water displacement	129
Figure 78 - Filter setup for matrix acid digestion	131
Figure 79 - Composite fiber and matrix weight percents	133
Figure 80 - Composite fiber and matrix volume percents	134

Figure 81 - Composite void volume percents	134
Figure 82 - Single-bundle transverse tensile test	138
Figure 83 - Single-bundle transverse tensile silicone mold	139
Figure 84 - MTS Insight 1kN test machine in the transverse tensile testing configuration	140
Figure 85 - Transverse tensile strength of the untreated and acid-treated fiber types	141
Figure 86 - Nitric acid-treated transverse tensile strength before and after seawater exposure	143
Figure 87 - Acid/Silane-treated transverse tensile strength	144
Figure 88 - Silane-treated transverse tensile strength before and after seawater exposure	145
Figure 89 - Interfacial fiber/matrix failure types	148
Figure 90 - Sized (T700) transverse tensile failure dry (L) and 2 months seawater exposure (R).....	149
Figure 91 - Unsized (AS4) fiber transverse tensile failure dry (L) and after seawater exposure (R).....	150
Figure 92 - 2.5 minute treated unsized fiber transverse tensile failure dry (L) and after seawater exposure (R).....	151
Figure 93 – 5 minute treated unsized fiber transverse tensile failure dry (L) and after seawater exposure (R).....	152
Figure 94 - 10 minute treated unsized fiber transverse tensile failure dry (L) and after seawater exposure (R).....	153
Figure 95 - 20 minute treated unsized fiber transverse tensile failure dry (L) and after seawater exposure (R).....	154
Figure 96 - 40 minute treated unsized fiber transverse tensile failure dry (L) and after seawater exposure (R).....	155
Figure 97 – Silane-treated sized fiber (no acid treatment) transverse tensile failure dry (L) and after seawater exposure (R).....	156

Figure 98 – Silane-treated unsized fiber (no acid treatment) transverse tensile failure dry (L) and after seawater exposure (R).....	157
Figure 99 – Silane-treated unsized fiber (2.5 minute acid treatment) transverse tensile failure dry (L) and after seawater exposure (R).....	158
Figure 100 – Silane-treated unsized fiber (20 minute acid treatment) transverse tensile failure dry (L) and after seawater exposure (R).....	159
Figure 101 – Silane-treated unsized fiber (40 minute acid treatment) transverse tensile failure dry (L) and after seawater exposure (R).....	160
Figure 102 - Example of fiber/matrix debonding observed.....	163
Figure 103 - Example of resin interfacial failure in dry acid-treated composite	164
Figure 104 - Example of resin interfacial failure in seawater-exposed acid-treated composite	164
Figure 105 - Brittle fracture seen in dry specimens.....	165
Figure 106 - Ductile fracture seen in seawater-exposed specimens	166
Figure 107 - Ductile fracture seen in seawater-exposed specimens	166
Figure 108 - Example of resin interfacial failure in a silane-treated composite.....	167
Figure 109 - Example of resin interfacial failure in a silane-treated composite.....	168
Figure 110 - Composite weight gain and swelling specimen	171
Figure 111 - Percentage weight gain of composites in seawater with different fiber surface treatments	172
Figure 112 - Percentage length change of composites in seawater with different fiber surface treatments	172
Figure 113 – Dry, sized fiber composite cross-sectional views.....	178
Figure 114 – Dry, unsized fiber composite cross-sectional views.....	179
Figure 115 – Dry, 2.5-minute acid-treated sized fiber composite cross-sectional views	180
Figure 116 – Dry, 5-minute acid-treated sized fiber composite cross-sectional views ..	181
Figure 117 – Dry, 10-minute acid-treated sized fiber composite cross-sectional views	182

Figure 118 – Dry, 5-minute acid-treated and silane-treated sized fiber composite cross-sectional views	183
Figure 119 – Seawater-exposed, sized fiber composite cross-sectional views.....	184
Figure 120 – Seawater-exposed, unsized fiber composite cross-sectional views.....	185
Figure 121 – Seawater-exposed, 2.5-minute acid-treated sized fiber composite cross-sectional views	186
Figure 122 – Seawater-exposed, 5-minute acid-treated sized fiber composite cross-sectional views	187
Figure 123 – Seawater-exposed, 10-minute acid-treated sized fiber composite cross-sectional views	188
Figure 124 – Seawater-exposed, 5-minute acid-treated and silane-treated sized fiber composite cross-sectional views	189
Figure 125 - Probable interphase characteristics	209

1. THEORY AND LITERATURE REVIEW

1.1 Introduction

There is a growing interest in the use of composite materials in many aspects of the marine environment, including infrastructure, offshore oil, navy and commercial ships. Considerable oil reserves are found in deep-water offshore areas where drilling and recovery cannot be economically performed due to the impracticality of current drilling platforms in deep-water locations. For example, it is known that considerable oil reserves are located off the continental United States at depths of 1800 m or greater, but it is currently not feasible to construct offshore platforms of the current state of technology at these ocean depths. Efforts are currently underway to develop new varieties of oil productions systems that can operate in these deeper areas, such as floating platforms and tension leg platforms. In these envisioned approaches, weight is a critical issue and the use of high-strength and lightweight composite materials for risers and tendon legs could help open the door to realizing these concepts. Reducing the weight of these components by replacing metals with composites would significantly reduce the buoyancy requirements and therefore the size and overall cost of the structure.^{1,2,3}

Composite materials are a common hull material choice in the pleasure-boating industry and various navies are using more composite materials on increasingly larger vessels. In pleasure boats, hulls are often made of a glass/polyester material with a protective gel coat overlay. In order to further protect against water damage, a vinyl ester

skin coat is sometimes used over the polyester composite, because vinyl ester is more water resistant.



Figure 1– 24.3 m (80 ft) yacht and 5.3 m (17.5 ft) pleasure boat with composite hulls^{4, 5}

Naval use of fully composite ships extends to large patrol boats, hovercraft, corvettes, and mine counter-measure ships. Composites are ideal for mine counter-measure vessels because they do not trigger magnetically-activated underwater mines. Several navy studies have been conducted to evaluate the feasibility of composite ships with regard to cost, weight and performance. In the case of patrol boats, it was projected that the use of a graphite-reinforced polymer sandwich composite would result in structural weight reductions of approximately 10% and 36% when compared to similar

aluminum and steel boats, respectively.^{6, 7} It has also been suggested that improved fabrication methods and increased use of carbon fiber may serve to further boost the weight savings.^{6, 8} Life-cycle costs of composite ships are also predicted to be less. A life-cycle cost reduction of approximately 7% for a composite boat versus a steel boat was predicted, due to less corrosion and fuel consumption.⁷ The Royal Norwegian Navy currently operates an all-composite patrol boat (commissioned in 1999) with a catamaran hull form that is 46.8 m long, 13.5 m wide and 270 tonnes full-load displacement. These patrol boats are known as the Skjold class of vessels and a picture is shown in Figure 2. The Skjold is built entirely of a sandwich composite consisting of glass- and carbon fiber laminate skins with a polyvinyl chloride foam core.⁹



Figure 2 - Royal Norwegian Navy Skjold class patrol boat.¹⁰

The longest and heaviest naval ship currently being built from composite materials is the Visby class corvette by the Royal Swedish Navy. The Visby is 72 m (236 .2 ft) long, 10.4 m (34.1 ft) wide and has a full-load displacement of 620 tonnes. It is built from a sandwich composite material, having skins of hybrid carbon and glass fiber polymer laminates and a polyvinyl chloride foam core. In addition to its size and weight,

another notable characteristic regarding the Visby construction is that it makes significant use of carbon fiber in the hull. While carbon fiber is more expensive than glass, the design studies for the Visby predicted that a weight reduction of about 30% could be achieved by replacing some glass fiber with carbon fiber, without a significant increase in fabrication cost. The Visby is designed to be a multi-purpose ship with capabilities for surveillance, combat, mine laying, mine countermeasures, and anti-submarine operations.⁹ The Visby is shown in Figure 3.



Figure 3 –Royal Swedish Navy Visby class corvette.¹¹

The US Navy has also conducted feasibility studies to evaluate building corvette ships up to 85 m (278.9 ft) long and 1200 tonnes displacement with composite material, instead of steel. They concluded that reductions in structural weight and full-load displacement of approximately 30% and 7-21% could be achieved, respectively. They also anticipated a cost savings of up to 15%.^{12, 13, 14}

While sandwich-type composite hulls are currently a popular design choice, single-skin designs are also in use. The UK Royal Navy's Hunt and Sandown class have a single-skin structure, consisting of composite frames and girders that are bonded to a laminated graphite-reinforced polymer hull.^{15, 16, 17, 18} An example of the Sandown class can be seen in Figure 4.



Figure 4 – Sandown with single-skin, framed composite hull.¹⁹

In addition to all-composite ships, several navies are considering the incorporation of composite parts or segments into ships, including topside superstructures, masts, propellers, propulsors, propeller and propulsion shafts, machinery and engine components, fittings, bulkheads, decks, floors, doors, rudders, piping, ducts, and pressure hulls.

Figure 5 describes the locations under consideration for the application of composite structures to naval ships and submarines, as of 2001.

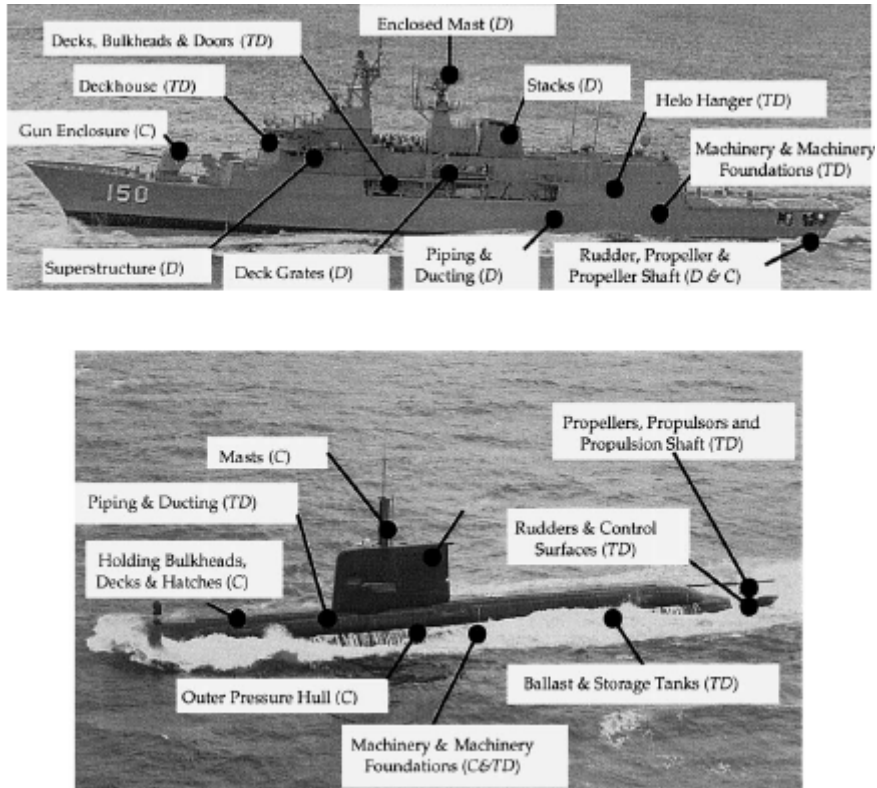


Figure 5 – Current status of the application of composite structures to naval ships and submarines, as of 2001.⁹

A composite is a material system consisting of two or more independent phases, combined to produce a bulk material that provides more desirable properties than the constituents alone. Not only do the properties of the composite surpass those of its individual components, but they also often possess superior properties to other material options, such as metals and ceramics. Composites offer such desirable properties as low density, high specific strength and corrosion resistance. The different phases of a composite can be categorized into a continuous phase (matrix) and dispersed phases (reinforcement). The matrix is often a polymer and the dispersed phases are frequently in the form of continuous fibers, which is the focus of this work. The matrix helps to

maintain the form of the material and keep the reinforcement in proper position. The fiber adds strength and stiffness. Fiber reinforcement benefits are mostly ascertained in tensile loading along their axes, while the matrix is responsible for most of the material's transverse tensile and compressive strengths.

1.2 Reinforcement/Matrix Bonding

The combined materials of a composite are essentially insoluble in each other, but adhesion between them is crucial to the performance of the bulk material. The matrix must be able to transfer loading to the reinforcement. The point where the matrix and reinforcement meet is deemed the “interface”, and several different methods are possible to accomplish bonding and load transfer, including the interdiffusion of elements, chemical reaction between surface elements, chemical reaction between new compounds formed on the surfaces, electrostatic attraction, molecular entanglement, and mechanical interlocking.²⁰ These types of bonds are shown in Figure 6.

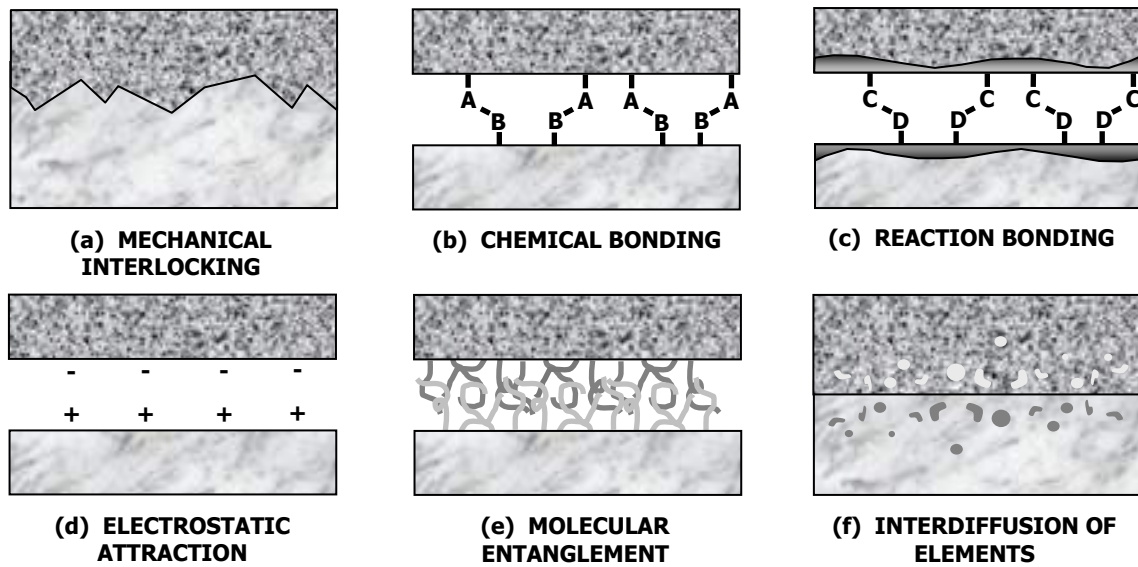


Figure 6 – Interface bonds formed by (a) mechanical interlocking; (b) chemical bonding; (c) reaction bonding after the formation of new compounds at the interface; (d) electrostatic attraction; (e) molecular entanglement; (f) interdiffusion of elements.

Mechanical interlocking (Figure 6, a) refers to two different aspects, a geometrical one and a residual stress-induced one. Geometrical mechanical interlocking refers to how the surface irregularities of the reinforcement grip the surrounding matrix. For geometrical mechanical interlocking to occur, the matrix must be able to pervade the surface irregularities, without bubbles or voids. This process is referred to as “wetting”. Geometrical mechanical interlocking is often promoted by surface treatments of the reinforcement that produce a large number of pits, corrugations and more surface area for reinforcement/matrix bonding. The other aspect of mechanical interlocking, the residual stress one, involves the shrinkage of the matrix. After manufacturing, when the matrix cools, the thermal contraction of the reinforcement and the matrix are not the same, often causing the matrix to “clamp” the reinforcement.²⁰ In the case of fiber reinforcement, cure shrinkage often results in compressive residual stresses on the fibers in both axial

and radial directions.^{1,2} A residual clamping stress, normal to the fiber direction, can add a synergistic effect to the geometrical mechanical anchoring aspect.²⁰

Interfacial chemical bonding in composite systems (Figure 6, b) occurs when the constituents of the matrix are chemically reactive with a coating on the fiber, chemical groups that have been implanted, or the fiber material itself. Usually, the fiber is not reactive with the polymer matrix and chemical bonding is dependent on modification of the fiber surface to introduce compatible chemistries in order to produce primary bonding. The forces in this type of bonding are high-energy covalent, ionic or metal bonds, usually falling within the order of 40 to 400 kJ/mol.²¹ Several methods are available to modify the fiber surface, including the deposition of organic coatings (sizings) and oxidation of the fiber surface through various types of plasma and liquid treatments. Chemical bonding can also occur following the formation of new compounds at the interface (Figure 6, c). This is known as reaction bonding and is particularly prevalent in metal-matrix composites, notably in those manufactured by molten metal infiltration processes.²⁰

When the interface strength depends on charge density, an electrostatic attraction component is considered (Figure 6, d). This may result when there is a difference in the electrostatic charge between the two constituents at the interface. This is usually a small component of the final bond strength, but it can be important when the reinforcement is treated with a coupling agent.²⁰ These forces include mostly London dispersion forces, dipolar interactions and hydrogen bonding. The energy of these forces is usually between 8 and 16 kJ/mol.²¹

Molecular entanglement (Figure 6, e) may contribute to the interfacial bond when both the fiber and matrix have long-chain molecules that can penetrate each other. Additionally, this may result when the fiber has been coated with a suitable material. Usually, either the fiber or coating is a polymeric material.

The interdiffusion of elements (Figure 6, f) involves crossing of atoms or molecules across the interface into the other material. This depends on molecular conformation, constituents involved and the ease of molecular motion. It may also be promoted by the presence of a solvent. When interdiffusion occurs, the interface region is different from the reinforcement and matrix in chemical, physical or mechanical properties. This is referred to as the “interphase” region. The interphase region usually extends into the matrix (instead of the fiber) and has been found to be softer than the bulk matrix by some researchers,^{22, 23} while Drzal has suggested that the interphase is more rigid than the bulk material^{24, 25}. Furthermore, both cases may be true at once. Williams et al. used a nano-indenter to determine the material modulus of an epoxy resin near a graphite fiber. They found that there was an overall softening effect within 500 nm of the fiber, which they postulated to be a result of chemical effects. However, nearer to the fiber (within approximately 100 nm), there was an apparent stiffening of the interphase. This stiffening was attributed to restricted deformation due to mechanical effects. Therefore, they concluded that there are two opposing effects in the interphase that result in both softening and stiffening.²²

1.3 Composite Degradation in Marine Environments

Due to their excellent properties and lightweight, composite materials are appealing to many industries, including the marine industry. There is, however, a drawback regarding the use of composite materials in marine environments: they degrade in the presence of water, seawater and humidity. The matrix, interface, interphase, and sometimes, even the fiber, degrade. This degradation occurs in many forms, including chemical bond loss at the interface, chemical degradation of the matrix, reduction in the matrix glass transition temperature (T_g), reduction of the beneficial residual stresses that result from cure shrinkage, leaching of the matrix, and swelling that causes microcracks and phase debonding. These damage types are depicted in Figure 7.

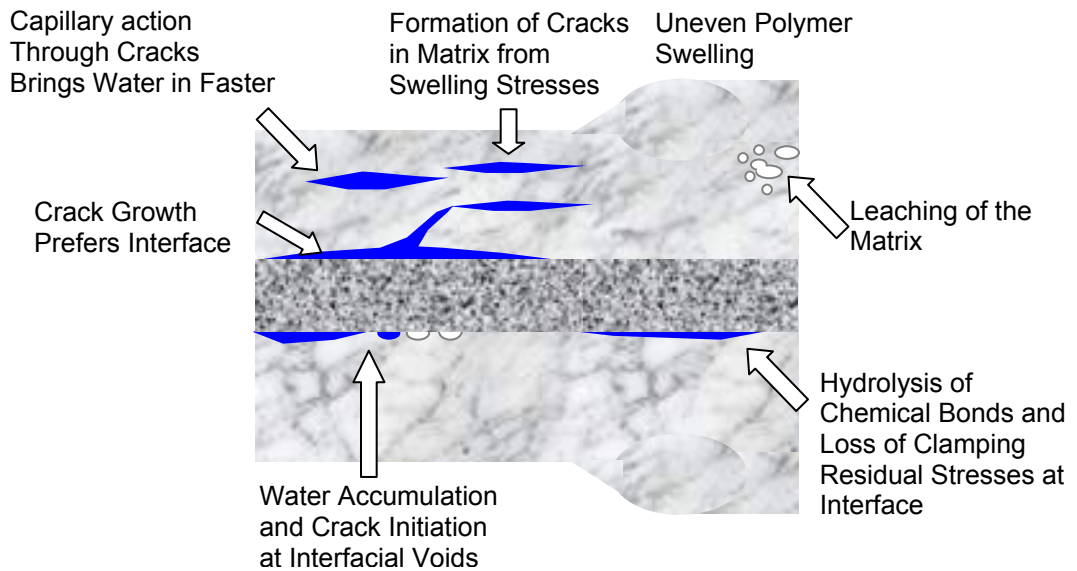


Figure 7 – Composite material damage modes

Chemical Bond Reduction at the Interface/Interphase

The interface/interphase region of polymeric composite materials degrades in the presence of water and seawater.^{1, 2, 26} Composites that previously failed by matrix failure have been observed to shift to an interfacial failure mode when exposed to seawater.¹ This failure is most likely the result of hydrolysis reactions within this region that disrupt the chemical bonds that link the fiber and matrix.²⁶ Hydrolysis is a chemical reaction or process in which a chemical compound reacts with water to break the compound into different parts. Hydrolysis can be considered to be the reverse of condensation, in which two molecular fragments are joined for each water molecule produced.^{27, 28} The amount of interface/interphase chemical degradation also depends on the ability of water or seawater to migrate through the polymer matrix. Composites with accelerated diffusion mechanisms, such as internal cracking and increased void content, lead to faster interface/interphase degradation.

Chemical Degradation of the Matrix

Like the interface/interphase region, the matrix material is often vulnerable to hydrolysis of unsaturated groups by water.^{26, 29} In the case of vinyl ester matrices, hydrolysis reactions may attack the ester groups in the vinyl ester polymer structure.³⁰

Along with hydrolysis, polymer matrices are also subject to plasticization when small molecules such as moisture or organic molecules penetrate them.^{1, 2, 26, 29, 31, 32, 33, 34} Plasticization weakens the intermolecular forces between macromolecules and results in greater freedom of movement, increasing the flexibility and plasticity of the matrix, but also reducing the tensile strength and chemical resistance.³⁵ Water that sorbs into a

polymer disrupts hydrogen bonding between the polymer molecules and allows these molecules to slip past one another more easily.³⁶ This process is reversible.²⁹ Another consequence of plasticization is reduction of the glass transition temperature (T_g).^{29, 31, 35, 36} The T_g is the temperature where the polymer transforms from a viscous to a rigid and brittle material.³⁵ At this point, the free movement of segments of molecules that previously occurred in amorphous regions becomes more difficult.³⁷ The decrease in mobility is a result of the more efficient packing of the polymer chains into crystalline regions.³⁸ Plasticization is more prevalent in more tightly cross-linked polymer systems. Cross-linked systems often contain more hydrogen bonding sites, which lead to more water absorption.³¹ In the case of vinyl ester, the hydroxyl groups along the vinyl ester chain length are particularly affinitive to hydrogen bonding and attractive to water. In addition to affecting the polymer properties, plasticization also induces swelling, which in turn can lead to cracking and reinforcement/matrix debonding.³⁸

Leaching of the Matrix

Not only can water pass into the matrix and chemically modify it, but it can also remove chemical species through leaching. The leaching of vinyl ester matrices is low in comparison to other polymers, such as polyester, but several variables are involved, such as the degree of curing. Undercured vinyl ester has been shown to be more susceptible to leaching than fully cured material, due to the loss of unreacted chemical species.²⁶ Mouritz et al. investigated the loss of chemical species from polyester and vinyl ester matrix composites into seawater. For the polyester-based composites, they found significant amounts of organic species released into the seawater after prolonged

immersion, in addition to an initial weight gain, followed by gradual weight loss.³⁹ This weight loss behavior of polyesters was also noted by Baley et al.⁴⁰ The vinyl ester-based composites showed a classical Fickian water uptake and much less organic residue left behind in the seawater bath. In both vinyl ester and polyester composites, it was seen that the undercured samples gained weight more slowly, presumably due to the loss of weight through leaching.³⁹ Leaching of polymers, such as polyester and vinyl ester, occurs by the removal of ester species with hydroxyl end groups and other low molecular weight species.²⁶ Leaching likely affects the interface as well as bulk matrix material. It has been shown that matrix/reinforcement debonding can be correlated with the amount of matrix leaching.⁴¹

Reduction of Beneficial Residual Stresses

During fabrication of composite materials, the polymer matrix shrinks during curing and cooling. Residual stresses in the reinforcement/matrix interface region can result from differential coefficients of thermal expansion of the reinforcement and matrix, with the reinforcement usually having the lower coefficient.⁴⁰ Shrinkage of the matrix during cooling also causes several stress states that depend on the geometry and packing of the reinforcement. In the case of a single, round fiber surrounded by matrix, shrinkage of the matrix causes radial compressive stresses, which clamp the fiber (Figure 8, a).²⁰ For a square array of circular fibers in a matrix, the residual stresses in the region between adjacent fibers are found to be compressive while they are tensile in the resin pocket between the fibers. With a high fiber volume fraction and small fiber spacing, and when the fiber is much stiffer than the matrix, the tensile stresses in the matrix pocket

may become compressive, resulting in compression around the fibers. (Figure 8, b).²⁰ Along with the radial compressive stresses on the fibers, the shrinkage also results in longitudinal tensile stresses in the matrix, which in turn results in longitudinal compressive stresses on reinforcing fibers.^{1, 2, 40}

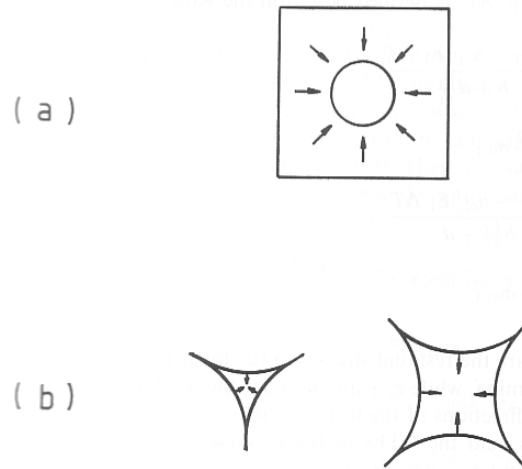


Figure 8 – Source of shrinkage stresses: (a) rigid fiber embedded in a matrix; (b) resin pockets surrounded by fibers in hexagonal and square arrays.²⁰

When exposed to water or seawater, polymeric matrices tend to swell and plasticize, counter-acting the mechanical anchoring benefit gained from matrix shrinkage during curing and cooling.^{26, 36, 40} Polymers are prone to swelling in water because of their polar nature. More moisture is absorbed when there is a higher density of polar molecules in the system, because the water itself is a polar molecule and is attracted to the hydrophilic sites on the polymer structure. This results in greater water uptake than can be accounted for by free volume considerations under the theory of solvent diffusion.^{35, 36, 42}

Swelling Damage

As discussed, the polar nature of polymers leads to more water absorption than is predicted by free volume considerations, which leads to swelling of the material.^{1, 33, 34, 43, 44, 45} Since the diffusion of the water into the composite takes place first at the edges and then progresses into the center, swelling is not uniform and differential stresses occur. The swollen edges result in compressive stress at the edges and tensile stress at a distance into the interior.⁴⁶ This tensile stress acts to enhance diffusion into the composite by creating microcracks, which act as capillary channels for water flow, and this capillary flow is much faster than diffusion. These micro-cracks grow with more absorption and tend to migrate to and continue along matrix/reinforcement interface boundaries, resulting in debonding to further weaken the composite. Not only does absorption result in composite damage, but desorption does as well. Desorption has been found to cause even more damage than that which occurs during the absorption stage. During the absorption stage, the tensile stress that arises in the inner regions of the composite results in micro-cracking. It is the opposite in desorption. During desorption, water first exits the outer regions of the composite, leaving inner regions that are still swollen with water. This results in compressive stresses in the inner regions and tensile stresses in the outer regions, which result in outer region micro-cracks.^{47, 48, 49}

In addition to the uneven absorption of water in the composite, the inhomogeneous character of polymers can also introduce differential stresses. The resin structure contains regions of high-density polymer separated by narrow boundary regions of lower molecular weight material (crystallinity per se).⁵⁰ Less highly cross-linked regions of the matrix have been found to absorb more water than highly cross-linked

regions.⁵¹ This may be due to the higher availability of unreacted polar sites in the less highly cross-linked regions.

McBagonluri et al. also identified irreversible damage in a glass/vinyl ester pultruded system after moisture exposure.⁵²

1.4 Sorption in Composites

The absorption of water into composites isn't easily predicted with classical (Fickian) diffusion theory.^{53, 54} Instead, it is subject to several different processes. A component of classical diffusion exists, but it alone does not accurately represent absorption and desorption seen in composites and must be combined with other methods of water uptake to correspond with actual data. Water uptake and loss may also occur via wicking along fiber boundaries and non-Fickian diffusion through cracks or voids.^{32, 36, 51, 55, 56, 57, 58} Wicking allows for accelerated transport along the fiber/matrix interface that can result from fiber/matrix debonding, the type of sizing (coating) that is applied to the fibers during processing, or the different chemical makeup that results in the interphase region.^{26, 59} As previously mentioned, micro-cracks may form in composites due to the tensile stresses that result from nonuniform water absorption and desorption. When water is absorbed, the edges swell first, placing the interior of the material in tension, and when water is desorbed from the edges, they shrink and undergo tensile stress, imparted from the still-swollen interior. These micro-cracks serve to further aggravate the water sorption problem by allowing capillary flow into and out of the composite. Capillary flow through micro-cracks has been noted to proceed at an exceedingly faster rate than classical diffusion and is affected by tensile stress on the composite. Capillary flow has

been described to be as fast as 7mm/min.^{36, 57, 60} Tensile stress increases the free volume in the resin according to the free volume theory, thereby increasing the rate and amount of absorption.^{36, 61} In composites, this increase is linear when stressed in the transverse direction and unchanged when stressed in the fiber direction.⁶¹ This is a generalized statement and may vary, depending on the extent of the fiber/matrix debonding.

The chemical nature of the composite resin itself often makes it attractive to water. Polymer matrices absorb water because of their polar constituents, which results in swelling and plasticization. Plasticization in thermoset composites of interest herein, such as epoxy, polyester and vinyl ester, occurs when the water disrupts the hydrogen bonding between the polymer molecules and allows these molecules to slip past one another more easily.³⁶ More moisture is absorbed when there is a higher density of polar molecules in the system.^{31, 35} This directly affects cross-linked polymers, such as vinyl ester, polyester and epoxy. The more capable the system is of cross-linking, the more hydrogen bonding sites there are available, and the more water is absorbed.³¹ The system's ability for greater degrees of cross-linking exposes it to greater amounts of water absorption because there are more water-attractive sites, but the degree of cross-linking completion that actually occurs can mitigate this. Increased water resistance has been shown to occur when more curing agent was used, leading to a higher degree of cross-linking completion, leaving fewer sites free.⁵¹

Furthermore, the absorption of distilled water differs from the absorption of seawater into polymer-based composites, with seawater absorption being slower. It has been postulated that the relatively large salt molecules in seawater slow the diffusion into the matrix.⁴⁰ Leidheiser and Granata conducted studies on ion transport through

polymeric coatings in aqueous solutions, and showed that ion transport takes place by two paths, one through the homogeneous material, and the other through small aqueous pathways. They also showed that ions in aqueous solutions affected the diffusion rates of other (hydrogen) ions into the coating, and that the ion size further affects this rate.⁶² Turoscy, Leidheiser, Jr., and Roberts later confirmed these two types of ion transport by studying polymeric coatings that were exposed to aqueous solutions of sodium ions.⁶³

Measurement of composite water absorption is not always straightforward, due to the potential for water to leach material out of the matrix. Composite moisture level is often determined via weight measurement. Composite weight can be deceiving if leaching occurs, because the removed polymer mass acts to lessen the composite weight, indicating less water absorption, when more has actually occurred. In vinyl ester, it has been shown that leaching is more prevalent in undercured specimens than in fully cured ones, due to the loss of unreacted chemical species.²⁶ It has been shown that there is no direct relationship between weight change and mechanical property variation in glass reinforced polyester, vinyl ester and epoxy.⁴⁰

1.5 Reinforcement (Fiber) Surface Modifications

Of the composite degradation modes discussed, degradation of the interface/interphase is one of the most detrimental, as it prevents the matrix from transferring load to the fibers. Depending on the interface design, this degradation involves chemical bond reduction, loss of compressive residual stresses, and/or swelling-induced debonding. Swelling-induced debonding occurs because the amount of moisture absorbed by the matrix is significantly different than that of the reinforcement, creating a

mismatch in volumetric expansion. In addition to interface degradation, it is also important to consider how well the interface between the matrix and reinforcement was initially formed. If the matrix does not fully wet the reinforcement, the interface will contain voids where no load transfer is possible and extensive interface debonding is likely to initiate. These voids will also likely accelerate diffusion of moisture into this region.⁶⁰ Excellent wetting may occur, but poor bonding may still result if no method of fiber/matrix adhesion is successfully employed, such as chemical reaction, electrostatic attraction, molecular entanglement, or mechanical interlocking.²⁰

Surface treatments of fibers are often applied to improve the fiber/matrix bond. This is especially necessary for carbon fiber/vinyl ester composite systems, which normally bond poorly. While surface treatments are often designed to improve the interfacial bonding, they are also intended for other purposes, such as improving the ease of processing. Very rarely is the surface treatment designed to prevent the adverse effects of water absorption. Several current fiber surface treatments are in practice, with the surface treatment being applied depending on the fiber type.

1.5.1 Silane Treatment

Glass fibers, for example, are most frequently treated with silane coupling agents, which has proven to be a great success in glass fiber composites. In addition to promoting adhesion with the resin, they are intended to act as a protective coating, reduce viscosity during processing, alter the catalytic effect of the surfaces, and improve the dispersion of particulate fillers. Silane coupling agents also improve the performance and hygrothermal stability of glass fiber composites when applied correctly. It is not exactly

known how this benefit is imparted, but theories include chemical bonding, preferential absorption, constrained layer, coefficient of friction, wettability and surface energy effect. The chemical bonding theory is the most widely accepted, which points to a reaction between the inorganic reinforcement and the organic matrix.²⁰ While silane coupling agents can improve the hydrolytic stability of glass fiber composites, they can also serve to degrade water resistance if not applied correctly.

Silane coupling agents are hybrid organic-inorganic compounds that bridge the interface between the fibers and matrix. Organofunctional silanes have groups that can form covalent bonds with the matrix resin while hydroxyl (or alkoxy) groups on the silicon moiety are available to form oxane bonds to the fiber.⁶⁴ It is, however, necessary for the fibers to have a sufficiently reactive surface to bond to silanes. Silanes can be represented by the formula $R_nSiX_{(4-n)}$. R is a nonhydrolysable organofunctional group, which can react with the organic resin. X is a group, which can hydrolyze to form a silanol in aqueous solution and thus react with a hydroxyl group of the glass surface. Silanes can be classified according to the type (-chloro, -methoxy, -ethoxy) and functionality (mono-, di-, tri-) of the hydrolysable group, X, the non-hydrolyzable group, R (amino-, epoxy-, vinyl-, chloro-, γ -aminopropyl, γ -methacryloxypropyl, etc.), and the chain length. The reactivity of the silanes decreases in the order - chloro => - methoxy => - ethoxy. The functionality of silanes refers to the number of hydrolysable groups connected to the Si atom that likely form bonds with the substrate. Various silane functionalities are represented in Figure 9.⁶⁵

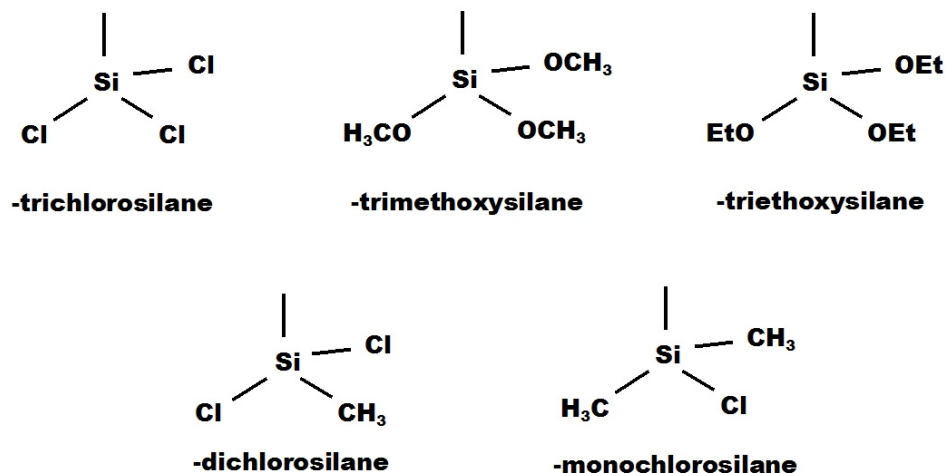


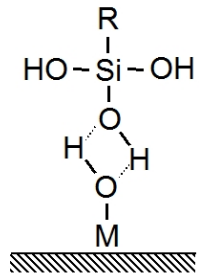
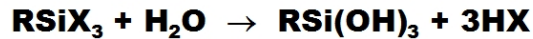
Figure 9 – Functionalities of Silane Groups

Mono-functional silanes have been found to have poor hydrolytic stability and form a single monolayer on glass surfaces.⁶⁵ Tri-functional silanes impart high hydrolytic stability and form multi-layers on glass surfaces.^{65, 66} Bi-functional silanes are more flexible than the tri-functional type. Longer chain lengths promote a better degree of silane molecule orientation on the surface, due to the van der Waals forces acting between neighboring chains.⁶⁵

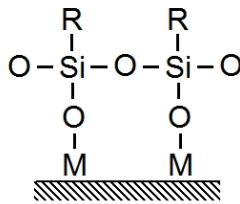
The chemical bonding theory leads to the conclusion that the silane molecules form a chemical bond with the glass surface through a siloxane bridge, while its organofunctional group bonds to the polymer. Thus, strong covalent bonds are formed which connect both the fiber and matrix. Four steps are postulated to take place in silane groups applied to glass substrates: (1) hydrolysis of the X groups attached to the Si atom; (2) Hydrogen bonding occurs between the reactive oligomers and silanol groups on the glass surface; (3) Condensation of the hydrolyzed molecules to form reactive oligomers, which bond to each other and to the glass surface; (4) During drying or curing, covalent

bonding with the substrate is achieved.⁶⁵ Figure 10 shows this silane chemical bonding theory.

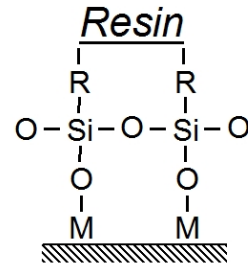
1. HYDROLYSIS



2. HYDROGEN BONDING



3. CONDENSATION AND BONDING



4. BONDING TO RESIN

Figure 10 - Action of a coupling agent: (1) hydrolysis of organosilane to corresponding silanol; (2) hydrogen bonding between hydroxyl groups of silanol and glass surface; (3) condensation and bonding to glass surface; (4) organofunctional R-group reaction with polymer.

Although commonly accepted, the silane chemical bonding theory does not fully explain the gains in mechanical strength and there must be other mechanisms occurring in the interphase region to constitute such an improvement. Several other theories have been put forth, including the surface wetting theory, deformable layer theory, restrained layer theory, and the reversible hydrolysis mechanism.

The surface wetting theory states that adhesion between the lower-energy organic resins and the high-energy substrate surfaces is strong because the system is driven to achieve as low a surface energy as possible.

The deformable layer theory attributes improved composite strength to a flexible interlayer formed by the silane in between the matrix and substrate. It is believed that this flexible layer improves composite toughness by allowing deformation at the

interface, rather than failure during loading or differential expansion between the composite constituents. The amount of silane in a typical glass fiber finish is not believed to be sufficient to provide the necessary modulus changes at the interface through interpenetration, but it has been proposed that the silane-treated surface may serve to modify the surrounding resin by attracting specific ingredients for adsorption more than others.⁶⁷

The reversible hydrolysis mechanism purports that the silane bonds to the substrate break and reform reversibly in order to relieve interfacial stresses. Evidence for the reversible hydrolysis mechanism has been obtained from acid/base exposure. Both acids and bases are known to aid the processes of hydrolysis and re-formation of siloxane bonds. If bonding depended on permanent (non-reversible) covalent bonds between the resin and glass, the mechanical properties of reinforced composite materials would be expected to degrade faster in the presence of acids or bases than in the presence of pure water. However, if the resin/glass bonds were reversible, the addition of acids or bases would increase the rate of hydrolysis and condensation, but the equilibrium would remain the same and the degradation of the fiber/matrix bond would be no worse than in pure water. Studies have been conducted that showed when the pH of the water was varied, the flexural strength of epoxy and polyester glass composites showed little variation.⁶⁸

The proposed reversible hydrolysis mechanism is shown in Figure 11.

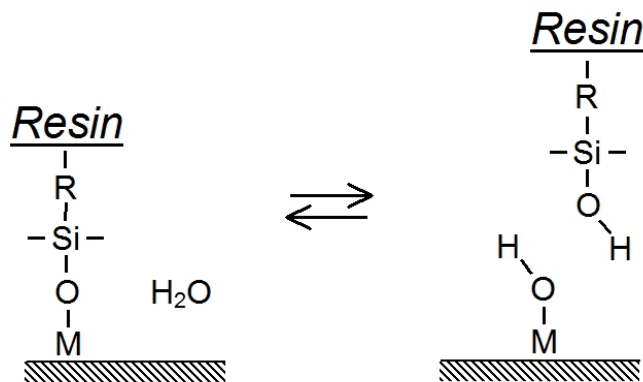
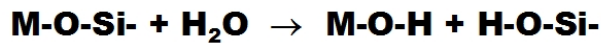


Figure 11 - Proposed reversible hydrolysis silane mechanism.

The restrained layer theory suggests the formation of an interphase region near the interface that has a different modulus value than that of the resin and substrate. Similar theories refer to this region as an interpenetrating network.⁶⁵ Thus, if one assumes that the sizing produces an interphase region within the matrix, compatibility of the silane and the resin is important. A description of an interpenetrating network is shown in Figure 12. Some researchers have concluded that the interphase region produced by silanes tends to have a lower transition temperature, larger tensile modulus, a greater tensile strength, a reduced strain to failure and a decreased toughness than the bulk matrix.⁶⁹ Drown et al. conducted experiments in which they mixed epoxy resin with silane sizing to evaluate the resin property changes. These properties were not measured in the interphase, but they believed that the silane-modified bulk resin represented the chemical formulations that would be expected there. To evaluate the expected fracture toughness in the interphase region, they calculated the toughness of the bulk resin/silane mixture by

integrating the area under the stress vs. strain curve. As additional investigation, they embedded single glass fibers within epoxy matrices, with and without sizing, and observed the failure modes by way of a polarized microscope. They found that the failure mode with silane sizing was more consistent with decreased interphase fracture toughness than that without sizing. They observed that the initial cracks perpendicular to the fiber were larger in the sized system than without sizing, and the cracks continued into the matrix to failure, whereas in the unsized system, the cracking gave way to interfacial debonding. Improved interfacial adhesion likely plays a large role in this behavior, but it was concluded that reduced fracture toughness also contributed. It was assumed that no interphase was created with unsized fibers.⁶⁹

Conversely, other researchers found that large amounts of siloxane in a polyester resin reduced the resin modulus and compressive pressure on the fibers, while increasing the fracture toughness of the interphase region.^{70, 71} Chua et al. arrived at this conclusion by varying the amount of silane in resin blocks and testing them for Young's modulus, compressive strength and Izod fracture energy. They also used a fiber pullout test and a curve-fitting technique to estimate the pressure on the fiber. They concluded that the shrinkage pressure was reduced and pointed out that other researchers have shown that the fracture toughness is enhanced when the shrinkage pressure is reduced.⁷¹

When altered, the resultant properties of the interphase region are of great importance because the interphase is a major player in the performance of the composite as a whole.

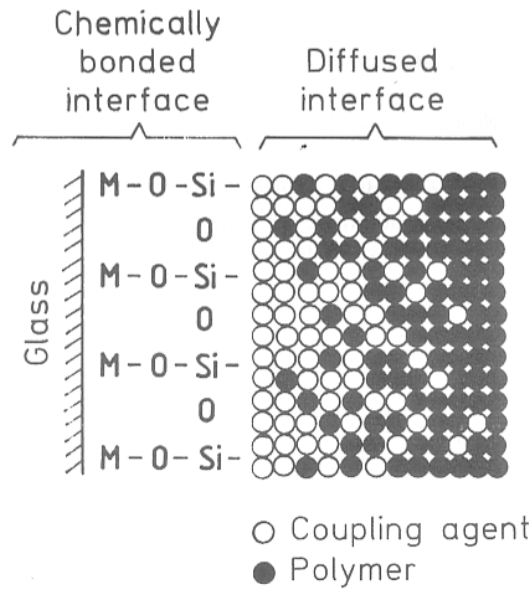


Figure 12 - Interdiffusion and interpenetrating network in a silane-treated glass fiber-polymer matrix composite⁷²

While they are not completely understood, silane treatments are one of the few treatments that have been shown to provide protection from water-related interface adhesion loss. Without the treatment, glass fiber interfaces are seriously degraded. Water molecules migrate to the interface of untreated fibers by diffusion, filtering through cracks or voids, or by capillary wicking along the fibers. Water molecules adsorb to the fiber and hydrolyze the chemical bonds at the interface.²⁰ It is believed that there are three major sublayers of the glass-matrix interphase region. These are the physisorbed, chemisorbed and chemically reacted regions. The physisorbed region, the outermost region, consists of most of the bulk of deposited silane, and its contribution to the performance of the composite is not precisely known, but removal of it has improved the flexural strength of composites in a few cases. However, it has been observed that there is an optimal concentration for this. The chemisorbed region, the middle layer, consists

of mainly higher oligomeric siloxanols and may be responsible for the reinforcement mechanisms.⁶⁴ The innermost region, the chemically reacted region, is most likely responsible for the high resistance of the interfacial bond to attack by water. The physisorbed region can be extracted with water at room temperature, the chemisorbed region can be extracted by prolonged immersion in boiling water, and the chemically reacted region remains after exposure to boiling water.²⁰ Figure 13 illustrates the structure of the chemically reacted region that remains on the glass surface after exposure to boiling water.

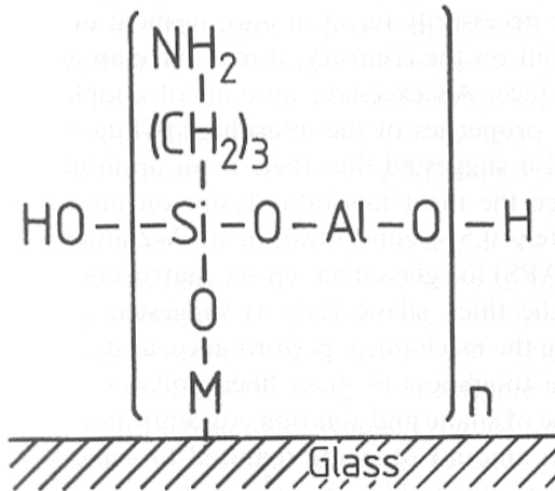


Figure 13 - Structure of the silane remnant remaining on glass fiber surface after extractive hydrolysis with hot water⁷³

1.5.2 Carbon Fiber Surface Treatments

Like glass fibers, carbon fibers are often subjected to surface treatments, which are intended to improve processing as well as fiber/matrix adhesion. It can help processing by binding the fibers together, lubricating the fibers so they can withstand

abrasion, and imparting anti-electrostatic properties. The treatments can also protect the fibers from surface damage and provide a chemical fiber/matrix link.

Carbon fiber surface treatments can be roughly grouped into two categories, oxidative and non-oxidative, with the goals of improving wetting, chemical bonding, fiber strength and/or mechanical anchoring. Oxidative surface treatments can be categorized into dry oxidation in the presence of gases, plasma etching and wet oxidation. Dry oxidation in the presence of gases is usually carried out with air, oxygen or oxygen-containing gases such as ozone and carbon dioxide. The surface layers simply burn away unevenly to create pits in lines that coalesce into channels, which improves surface roughness for mechanical anchoring. While this improves mechanical anchoring, it can also result in excessive pitting that reduces the fiber tensile strength.²⁰

In plasma etching of carbon fibers, energy such as direct current, alternating current, radio frequency and microwave are applied to a gas to create high-energy plasma. Plasma, in this context, is a region of space in which high-energy species, like electrons, ions, radicals, ionized atoms and molecules are present. Immersion of the fibers in this region induces strong interactions at the surface with the energetic species. Many chemical bonds are broken, forming very reactive species. The most frequently used plasma types are thermal plasma, glow discharge and corona discharge.²⁰ Different inorganic gases are used with different results in the plasma etching of carbon fibers, including oxygen, argon, ammonia, nitrogen, hydrogen and helium. All of these are believed to improve interfacial strength to some extent in carbon fiber composites, but by different means and to differing extents. These plasma types work by creating surface roughness, introducing functional chemical groups, and removing surface defects on the

fibers through the implantation of atoms, radical generation and etching reactions. The increase in surface roughness obtained through plasma etching improves the fiber/matrix frictional coefficient as well as increases the total surface area of the fiber that the matrix can bond to. However, this burning away of the surface can also serve to lower the fiber's tensile strength.⁷⁴

Oxygen plasma is believed to improve interfacial bond strength in carbon fiber composites through a combination of chemical bonding, improved wetting and mechanical anchoring.^{74, 75, 76} Several researchers have found that treatment with oxygen plasma increases the concentration of oxygen-containing functional groups. It is difficult to discriminate between types of oxygen surface groups that result, but many researchers suggest that they are likely carboxylic, carbonylic, hydroxylic and ester groups, as well as carbon dioxide and carbon monoxide.^{74, 75, 77, 78, 79, 80, 81} Chang reported an increased surface oxidation level by oxygen plasma treatment, as well as an increase in interfacial adhesion between unsized carbon fibers and bismaleimide (BMI) resin.⁷⁴ He postulated that the surface oxidation was comprised of a significant increase in carboxylic acid and/or ester groups. Nohara et al. showed an increased oxygen/carbon ratio on the fiber surface and suggested that the surface groups consisted of hydroxyl, carbonyl, carboxylic acid and carbon dioxide constituents.⁸⁰ Yuan et al. showed improved interfacial shear strength of sized carbon fibers and PPS resin after fiber treatment with oxygen plasma, pointing to increased hydroxyl and ether groups on the surface.⁷⁵ These surface compounds are polar and, as such, fiber surface polarity, surface energy and wettability have been found to consistently improve, although not as much as with ammonia plasma treatment.^{74, 76} Removal of weak boundary layers were noted in early stages of treatment,

which would serve to improve fiber tensile strength by eliminating defects, however the mechanical properties of the fibers decreased with increasing treatment time.^{74, 75, 76} With sufficient treatment time, it has been proposed that the surface defect removal effect vanishes and the population of critical surface flaws begins to increase.⁸⁰ While this etching was found to reduce the fiber tensile strength, it also acts as a primary aid to interfacial bonding through mechanical anchoring, thus improving composite performance.^{74, 76, 78} Although many researchers have identified bonding functional groups on carbon fiber surfaces after oxygen plasma treatment, it is believed that much of the energetic oxygen species serve to remove carbon atoms from the fiber surface through carbon monoxide and carbon dioxide evolution, and a large proportion of the interfacial shear strength improvement observed is due to mechanical anchoring from the etching effect.⁸⁰

Nitrogen plasma treatment of carbon fibers has also been found to improve interfacial shear strength in carbon fiber based composites, but unlike oxygen plasma treatment, results in very little fiber etching and pitting. One researcher identified no effect on fiber diameter and no loss in strength.⁷⁷ Another researcher identified a loss in strength only after prolonged exposure.⁷⁶ Nitrogen plasma was found to form amines (-NH₂ and -C=NH groups) on the fiber surfaces, which likely act as functional groups to bond to the matrix resin.⁷⁷

Ammonia plasma was found to produce similar results to nitrogen plasma. It has been shown to improve interfacial bond strength with no loss in fiber strength in BMI resin. No surface roughening was observed and therefore, no benefit from mechanical anchoring in interfacial shear strength was assumed. Surface energy and wettability were

found to improve to a larger extent than with oxygen plasma treatment.^{74, 76} In one of these experiments, however, oxygen content was found to increase on the surface, along with nitrogen. The increase in oxygen content was attributed to a leak of atmospheric air into the plasma reactor. It is believed that amines (-NH₂) were created on the fiber surface, similar to that seen with nitrogen plasma treatment.⁷⁴

Argon plasma was observed to improve interfacial shear strength, but whether any chemical bonding is responsible is debated. One researcher reported that no functional groups were introduced,⁸⁰ while another reported the addition of oxygen-containing groups, increased surface energy and polarity, and improved wettability.⁷⁶ Argon plasma treatment definitely adds to interfacial shear strength through mechanical anchoring by contributing additional surface roughness through etching.^{74, 80} It has been shown to remove surface flaws at low treatment periods, but progresses to fiber tensile strength reduction at longer times.^{75, 76, 80} The reduction in tensile stress that results was found to be less than that which resulted from oxygen plasma treatment.⁸⁰

Wet oxidation of carbon fibers is carried out chemically or electrolytically. Oxidizing agents are used, such as nitric acid, acidic potassium permanganate, acidic potassium dichromate, dichromate permanganate, hydrogen peroxide, ammonium bicarbonate and potassium persulfate. This method usually does not result in as much pitting, such as that which can result from dry oxidation methods, but can still remove the outer weak layer that contains defects, leading to improved fiber strength. Electrolytic or anodic oxidation of fibers is fast and uniform. The oxidation mechanism of most carbon fibers is characterized by the simultaneous formation of carbon dioxide and degradation

products that are dissolved in the electrolyte of alkaline solution or adhere to the carbon fiber surface in nitric acid.²⁰

Oxidation with nitric acid (HNO_3) is believed to produce similar surface functional groups on carbon fiber as oxygen plasma, but with higher concentrations. It has been suggested that nitric acid treatment of carbon fibers likely introduces hydroxyl, carbonyl, carboxyl and phenolic groups onto the surface.^{20, 77, 80, 82} Nohora et al. found that nitric acid treatment resulted in higher oxygen/carbon surface ratios than oxygen plasma, argon plasma, and hydrochloric acid treatments. Using X-ray photoelectron spectroscopy (XPS), they concluded that the surface groups consisted of C-O-R, C-NR₂, C=O, and O-C=O types. At the same time, they found that the nitric acid surface treatment was less damaging to the fiber tensile strength than the oxygen plasma treatment, which degraded the fiber tensile strength much more quickly. However, the nitric acid treatment degraded the tensile strength faster than the argon plasma or hydrochloric acid treatment.⁸⁰ The extent of fiber tensile strength loss also depends on the fibers themselves. Jain et al. found that the variation in tensile strength of nitric acid-treated type I fibers differed from that of type II fibers. They also found that type II fibers readily pitted from the acid treatment, whereas type I fibers were never etched, even after 5 hours of treatment. These differences were explained with the dissimilarity in structure between the two types of fibers. The type I fibers have a more uniform and aligned structure than type II fibers.⁸³ Fitzer et al. studied nitric acid-oxidized carbon fiber composites made with epoxy resins, and found a good correlation between the amount of carbonyl, carboxyl and phenolic groups and the improvement of mechanical properties.⁸⁴ Drzal et al. concluded that graphite fiber oxidative surface treatments

increase the fiber/matrix shear strength through a two-part mechanism. First, an outer, weak defect-laden layer is removed, resulting in a surface capable of supporting higher shear loadings. Secondly, the surface oxygen groups added are able to interact with the polar epoxy matrix.²⁴ Other researchers have also used nitric acid oxidation to introduce a number of acidic functions (carboxyl and phenolic) onto carbon fibers.^{85, 86}

Surface oxidation of carbon fibers with hydrochloric acid (HCl) was found to produce a smoother, more uniform surface, when compared to other acid treatments. HCl treatment resulted in less tensile strength loss than nitric acid treatment, but also resulted in significantly less surface functional groups.⁸⁰

Non-oxidative surface treatments of carbon and graphite fibers involve the deposition of additional material on the fiber surface, such as whiskerization or the deposition of organic and polymer coatings. Whiskerization is the nucleation and growth of very thin and high strength single crystals, perpendicular to the fiber axis. The whisker crystals have been formed of silicon carbide (SiC), titanium dioxide (TiO₂), and silicon nitride (Si₃N₄). The whiskers usually originate at defects, compositional heterogeneities, metallic inclusions or structural irregularities and imperfections.²⁰ Whiskers are grown from the vapor phase in a method similar to chemical vapor phase deposition (CVD), but unlike CVD, whiskerization is not surface-dependent. Whiskers can be grown in the absence of a carbon fiber substrate. The substrate just acts as a site for nucleation and growth of the crystals. Whiskerization on graphite fibers is carried out in the 1100 to 1700 C range, which is high enough for some diffusion of the silicon carbide into the graphite.⁸² Temperatures in this range also approach graphitization temperatures and may change the properties of the fibers.^{87, 88} Whiskers have been found

to not only grow on the external fibers of strand bundles, but to penetrate into the bundles and whiskerize the individual filaments. Whiskerization has proven to be very effective in improving the interfacial shear strength in graphite fiber polymeric composites.⁸² However, whiskerization also adds additional weight to the composite.⁷⁶

Plasma deposition of organic polymers coatings uses polymerizable organic vapors, such as polyamide, polyimide, organosilanes, alternating block polymers like styrene and maleic anhydride, propylene, and acrylonitrile and styrene monomers. Plasma polymerization increases the polar component of the surface free energy of the carbon fiber.⁸⁰ Dagli and Sung treated carbon fibers with acrylonitrile and styrene plasmas and reported improvement in the inter-laminar shear strength.⁸⁹ Chen et al. used a radio frequency glow discharge plasma reactor to apply styrene plasma to pyrex glass slides that had been aluminum evaporated to produce a clean aluminum surface, and identified a high concentration of phenyl groups on the surface.⁹⁰ Phenyl groups are hydrophobic.⁹¹

2. MATERIALS

Due to current interest in the use of carbon fiber/vinyl ester polymer composites in marine environments by the US Navy and others, this work focuses on the carbon/vinyl ester composite system.

2.1 Carbon Fiber

Carbon fibers offer high strength and greater stiffness than any other fiber.⁸⁷ Carbon fibers can be made from a number of different precursors, including rayon, polyacrylonitrile (PAN), and petroleum pitch.⁸⁷ The basic requirement to be converted into carbon fibers is that the precursor fibers carbonize rather than melt when heated.⁹² The first filaments used in Edison's incandescent electric lamps were carbon fibers made by carbonizing cotton fibers, but they were extremely brittle and rapidly were replaced by tungsten wire.⁸⁷ The majority of fibers available today are based on PAN,²⁰ and due to this prevalence, this work utilizes PAN-based fibers.

The basic structure of carbon fiber material is made up of graphite crystallites, which in turn are composed of layered basal planes, as shown in Figure 14. Within the basal planes, the carbon atoms are strongly bonded to each other. Between the basal planes, there is only weak van der Waals bonding.

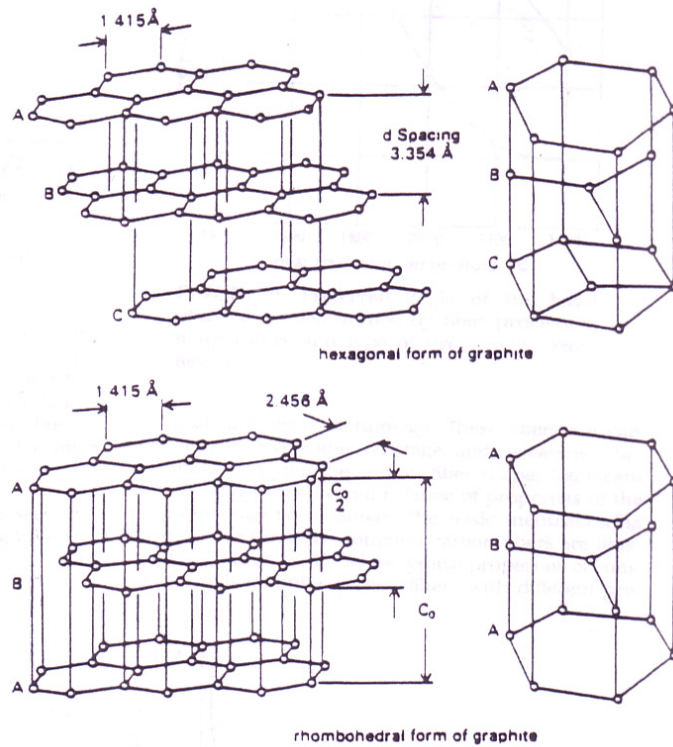


Figure 14 - Carbon fiber structure of layered graphite crystallites⁸⁷

The graphitic structure of carbon fibers lends them to very anisotropic behavior. The high bond strength between the carbon atoms in the basal plane results in extremely high modulus in this direction (along the fiber axis), while the weak van der Waals type of bonding between the adjacent layers produces a low modulus along the edge plane. The graphitic structure of carbon fibers is not perfectly ordered and usually not perfectly aligned with the fiber axis. To achieve a high modulus, a high degree of preferred basal plane orientation along the fiber axis must be achieved. To improve the orientation of the graphite crystals, various kinds of thermal and stretching treatments are employed.²⁰ As the processing temperature increases, the basal plane preferred angle (Figure 15) decreases, aligning closer to the fiber axis.

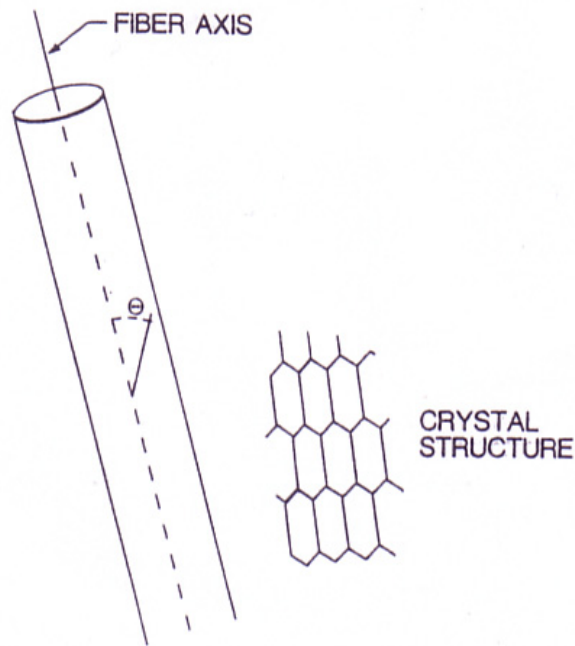


Figure 15 - Carbon fiber basal plane angle⁸⁷

Processing variations lead to three general groups of carbon fibers: high strength (Type I), high modulus (Type II) and ultra-high modulus (Type III) types. Type I, II, and III types have tensile strength ranges of 3000-6400, 4500-6200, and 2400-4400 MPa and Young's modulus ranges of 235-295, 296-344 and 345-540 GPa, respectively.^{20, 93, 94} The type of fiber attained primarily depends on the temperature of pyrolysis used.^{88, 95} This study utilizes Type I fibers. PAN, pitch and rayon based carbon fibers are all processed similarly. They are heated in the presence of oxygen at temperatures up to about 400° C and then carbonized in the presence of an inert gas at temperatures up to 1700° C. They are sometimes then graphitized in the presence of an inert gas at temperatures up to approximately 2800° C.⁸⁷ Figure 16 shows the production method

used by one of the largest carbon fiber manufacturers, Toray Industries, in making PAN based carbon fibers.

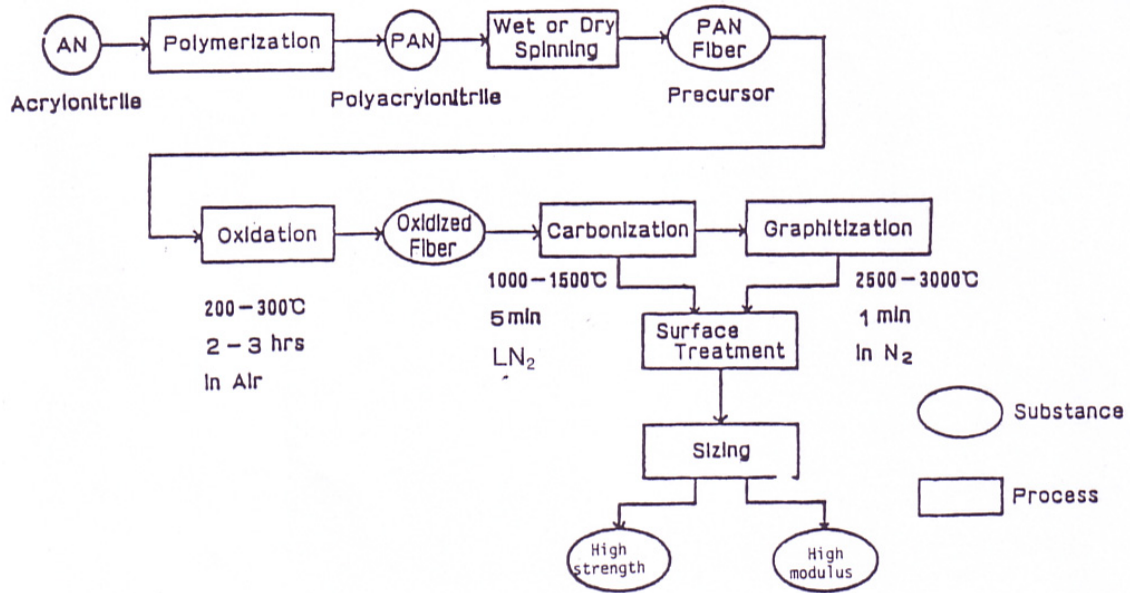


Figure 16 – Toray Industries carbon fiber production process⁸⁷

The structure resulting from the pyrolysis of PAN based fiber is highly anisotropic, with the hexagonally bonded carbon atom basal planes being aligned with the fiber axis. There is no rotational order in the radial direction and the carbon atoms stack poorly so that a graphite structure is never totally achieved.⁸⁷ Figure 17 shows a schematic drawing of a three-dimensional model of a carbon fiber.⁹⁶

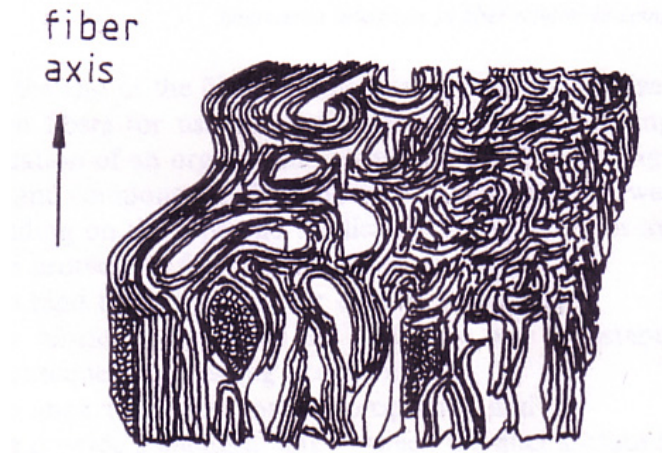


Figure 17– Carbon fiber drawing⁸⁷

Two types of carbon fiber are used in this research. The first is the T700S fiber with sizing “FOE”, produced by Toray Industries. This is a high strength, standard modulus fiber, and the sizing is a proprietary sizing, which is used in vinyl ester composite systems. This fiber is used in this research for comparison purposes, because several parallel experiments are currently underway which involve the carbon/vinyl ester system with this fiber. These other experiments are different in focus than this research, but it may be useful to compare those results with the results found through this effort. Furthermore, it will be useful to see if similar results are obtained using sized and unsized fiber types, even when the sizing composition is unknown. For the additional T700S sized fiber research, the reader is referred to the work of F. A. Ramirez⁹⁷, and the progressing work of M. U. Farooq and B. A. Acha.

The second type of carbon fiber used is an unsized fiber with similar properties to the Toray fiber. It is an AS4-type fiber, produced by Hexcel Corporation. Its properties were chosen to be similar to the Toray fiber, which was already available at the initiation

of this study. Table 1 provides a comparison of the two fiber types. Unsized fiber is being used so that experimental control is maintained and conclusions can more easily be drawn. With an unknown sizing, interpretation of interface test results becomes difficult. Surface methods may provide an indication of what is contained in the sizing, but it cannot be precisely determined.

CARBON FIBER PROPERTIES		
Property	Sized Fiber (Toray T700)	Unsized Fiber (Hexcel AS4D)
Tensile Strength (MPa)	4900	4692
Tensile Modulus (GPa)	230	245
Strain (%)	2.1	1.92
Density (g/cc)	1.80	1.79

Table 1 – Properties of sized and unsized carbon fibers used

2.2 Vinyl Ester Resin

Vinyl ester has become a popular resin for use in marine environments. It is a thermosetting polymer, meaning that it undergoes an irreversible chemical reaction when mixed with a catalyst, in which it becomes hard and will not melt. The beginning components of a vinyl ester matrix are an unsaturated carboxylic acid, such as methacrylic or acrylic acid, and an epoxy resin, which react to produce an unsaturated resin.^{98, 99} Methacrylic acid is most commonly used for vinyl ester resins intended for

composite applications while acrylic acid finds use in resins intended for application coatings.⁹⁹

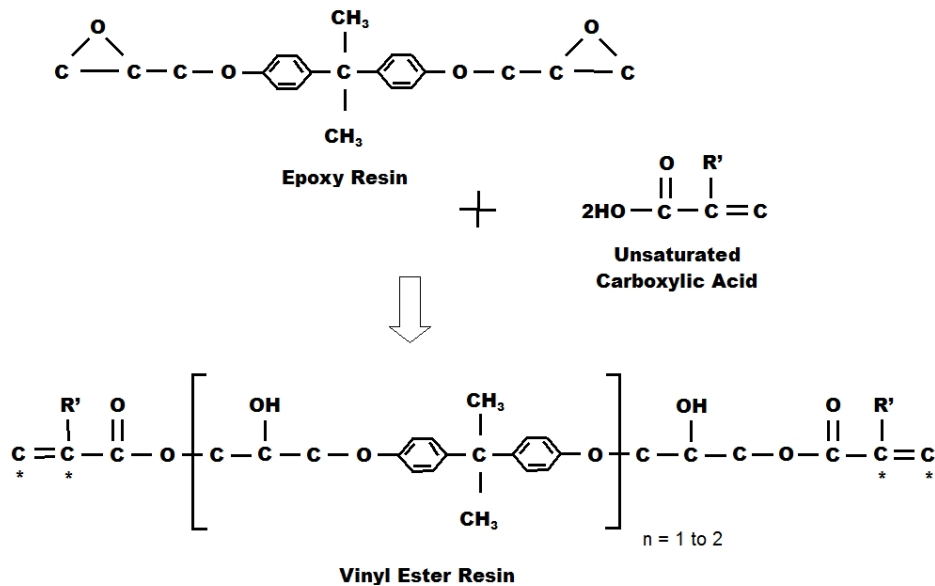


Figure 18 – Formation of the vinyl ester molecule

The curing reaction of vinyl ester resins is similar to that of polyester resins, both being dissolved in styrene monomer. The styrene reduces the resin viscosity and during polymerization, it reacts with the resin to form cross-links between the unsaturated points on adjacent vinyl ester molecules.^{98, 100} In addition to copolymerization with the unsaturated styrene monomers, the unsaturated points can also react through homopolymerization of the vinyl ester resin with itself to give cross-linking.⁹⁹

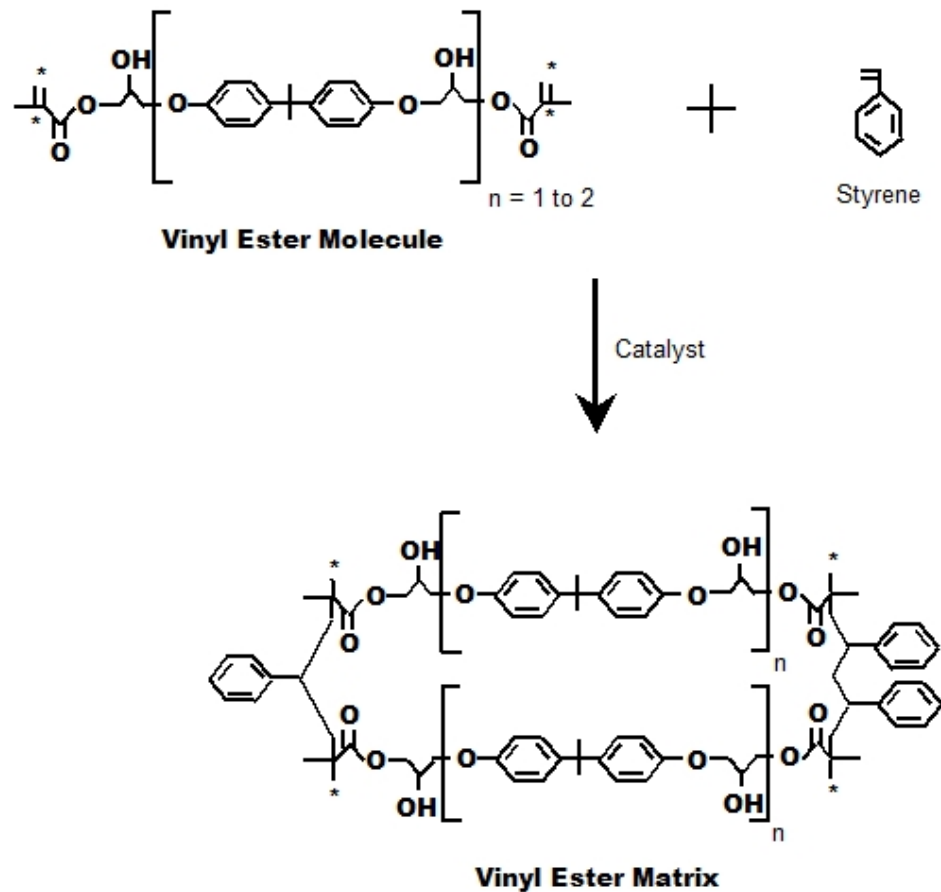


Figure 19 - Vinyl ester cross-linking

Vinyl ester resins possess many of the desirable characteristics of epoxy resins, such as chemical resistance and tensile strength, and of unsaturated polyester resins, such as low viscosity and fast curing.⁹⁸ Because vinyl esters only have reactive sites at the ends of their molecular chains, these are the only sites where cross-linking can occur and the entire length of the molecular chain is available to absorb shock. Fewer cross-links make them tougher, more flexible and more resilient than similar polymers having more bonding sites throughout their chain length, such as polyesters.^{30, 98} The vinyl ester molecule also features relatively fewer ester groups, which are susceptible to water

degradation by hydrolysis.³⁰ Further, if the vinyl ester molecules are terminated with methacrylate groups, the relatively large methyl moiety on the methacrylate group sterically protects the ester linkage from chemical attack.⁹⁹ However, vinyl ester is not completely devoid of ester groups, leaving it less water-resistant than its parent epoxy, which accomplishes bonding through epoxy groups instead.³⁰ Another down-point of vinyl ester is that it exhibits volumetric shrinkage in the range of 5-10%, which is higher than epoxy resins, and it falls short of epoxies with respect to adhesive strength.⁹⁸ Table 2 provides a comparison between vinyl ester, polyester and epoxy resins.

RESIN PROPERTY COMPARISONS			
Property	Polyester	Epoxy	Vinyl Ester
Chemical Resistance	Poor	Best	Better
Tensile Strength (MPa)	34.5 – 103.5	55 – 130	73 – 81
Tensile Modulus (GPa)	2.10 – 4.10	2.75 – 4.10	3.0 – 3.5
Fracture Toughness	Better	Poor	Best
Cure Shrinkage	5 – 12%	1 – 5%	5 – 10%
Adhesive Strength	Fair	Best	Better

Table 2– Resin property comparisons

Another unique characteristic of a vinyl ester molecule is that it contains a number of hydroxyl (OH) molecules along its length, which may be available for hydrogen or primary bonding.⁹⁸ Figure 20 below shows a schematic representation of a cross-linked vinyl ester resin.

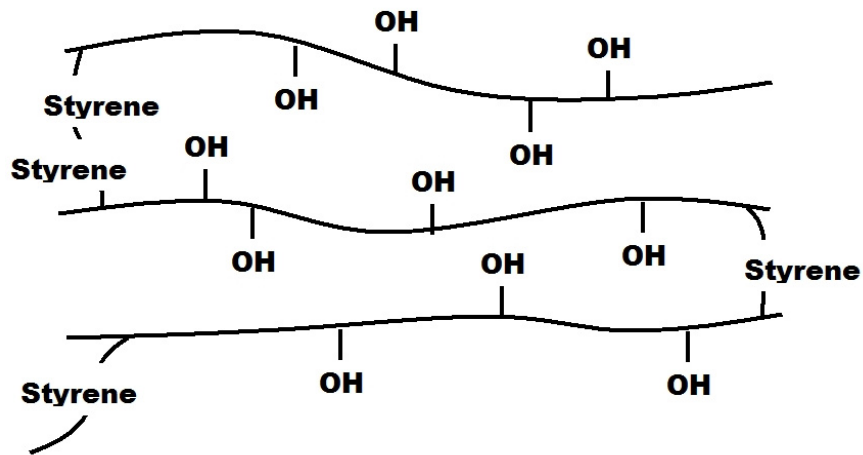


Figure 20 – Cross-linked vinyl ester resin

The vinyl ester type used in this research is Derakane Momentum™ 411-350 epoxy vinyl ester resin, which is based on a bisphenol-A epoxy resin. Typical liquid resin properties can be found in Table 3.

DERAKANE MOMENTUM 411-350 VINYL ESTER LIQUID RESIN PROPERTIES	
Property	Value
Density (25° C/77° F)	1.046 g/ml
Dynamic Viscosity (25° C/77° F)	370 mPa·s
Kinematic Viscosity	350 cSt
Styrene Content	45%

Table 3– Typical liquid resin properties of Derakane Momentum™ 411-350 epoxy vinyl ester resin

Typical properties of postcured resin are shown in Table 4.

DERAKANE MOMENTUM 411-350 VINYL ESTER CURED RESIN PROPERTIES	
Property	Value
Tensile Strength	86 MPa
Tensile Modulus	3.2 GPa
Elongation	5-6 %
Flexural Strength	150 MPa
Flexural Modulus	3.4 GPa
Density	1.14 g/cm ³
Volume Shrinkage	7.8 %
Heat Distortion Temperature	105° C
Glass Transition Temperature	120° C
Barcol Hardness	35

Table 4– Typical cured properties of Derakane Momentum™ 411-350 epoxy vinyl ester resin

In addition to the vinyl ester resin, a catalyst and promoter are used. Methyl Ethyl Ketone Peroxide (MEKP) is used as the catalyst and cobalt napthenate as the promoter. The amounts used, expressed as parts per hundred resin (phr), are 1phr and 0.05 phr (6% solution), respectively.

3. RESEARCH

3.1 Theoretical Basis

This research focuses on two separate, but related goals. The first is to select a fiber surface treatment that may provide benefits with respect to composite fiber/matrix adhesion and seawater durability, develop a better understanding of how the treatment affects the fibers, and evaluate it in composites before and after marine exposure. The second part is an attempt to alter the carbon fiber surface so that a silane coupling agent can be applied. Silane coupling agents are often applied to glass fibers, resulting in improved hydrolytic stability, but carbon fibers do not provide the surface reactivity necessary for silane bonding.

3.1.1 Carbon Fiber Surface Treatment to Improve Fiber/matrix Adhesion and Durability

Numerous studies have been undertaken to understand and improve the bonding of carbon fibers to different polymeric matrices with varying degrees of success. Several efforts have focused on evaluating the degree of degradation of several composite systems in aqueous environments. However, the literature review has not uncovered any indication of repeatable success with composite materials made using these surface treatments, and the problem is not well understood. Some researchers report success while some do not, and no clear theoretical answer is apparent based on the mixed

results. Additionally, while much effort has been put forth to attempt to understand the effects of fiber surface treatments and the effects of water degradation, there has been little effort put forth to evaluate the durability of carbon fiber surface modifications in composites that are exposed to wet environments. More specifically, no information was uncovered in the literature review about the water/seawater performance and durability of fiber surface modifications in the carbon/vinyl ester composite system. One of the goals of this research is to select and investigate a particular carbon fiber surface treatment and how it affects a carbon/vinyl ester composite system before and after seawater exposure. Several types of surface treatments have been reviewed, including dry oxidation, wet oxidation, plasma etching, whiskerization and plasma deposition of organic polymers. Oxidation in nitric acid has been chosen as the surface treatment method because of its ease of use, oxidation effectiveness and the introduction of highly polar and reactive species. The reasoning behind this choice is explained more specifically in the remainder of this section.

From the literature review, it has become apparent that surface treatments on carbon fibers are believed to accomplish several different things. They can (1) improve mechanical anchoring by increasing surface roughness and rugosity, (2) improve fiber strength by removing a weak defect-laden layer of the fiber, (3) improve matrix wetting of the fibers by increasing the surface energy and polarity, and (4) provide a means of chemical bonding through the implantation of reactive functional groups. Several methods of surface modification have been successfully employed to accomplish one or more of these changes. However, many treatments also degrade the fiber and reduce its

tensile strength, as well as resulting in poor quality composites, all of which are undesirable.

The improvement of mechanical interlocking through surface morphology modification is not focused upon herein. The primary reason for not going in this direction is because of literature indicating the dependence of these methods on fiber-clamping residual stresses, and the fact that water-induced matrix swelling and plasticization are known to relax these beneficial residual stresses. There is minimal benefit to be gained in dimensionally modifying the fiber surface if water absorption in the polymer will reduce the hold on these surface irregularities. Fiber surface geometric changes that occur during the course of this research are reviewed and considered, but they are not a goal.

Without focusing on mechanical interlocking, the focus shifts to evaluating the changes in wettability and chemical bonding resulting from a surface treatment, and to a lesser extent, the effects on fiber strength and size. Surface modifications have been shown to both increase the strength of the fibers and decrease them. Several non-polymer forming, dry-oxidation treatments have been found to improve single-fiber wettability and to introduce functional chemical groups. Nitrogen and ammonia plasma treatments were believed to have introduced amines on carbon fiber surfaces, which may be available for bonding and increasing the surface energy. It is possible that the available surface groups are $-C-NH_2$ and $-C=N-H$ groups. The unsaturated $C=N$ bond may provide a possible bonding site with the vinyl ester matrix. The nitrogen moiety of these groups also carries two unbonded electrons, making the groups nucleophiles, meaning that the central nitrogen has a tendency to donate electrons and attract positively

charged chemical entities. The basic structure of these groups is shown in Figure 21. Bonding angles are not considered in this figure.



Figure 21 – Surface groups that likely result from ammonia and nitrogen plasma treatment

Electronegativity is a measure of the ability of an atom or a compound to attract electrons in the context of a chemical bond. The higher the electronegativity, the stronger an electron is attracted to an atom. The type of bond formed is dependent on the difference in electronegativity between the atoms involved. Atoms with similar electronegativities will share an electron and form a covalent bond. As the electronegativity difference grows, the tendency for complete transfer of an electron from the atom with the lower electronegativity to the one with the larger electronegativity grows.¹⁰¹ The electronegativity of the surface groups that are implanted likely affects the tendency toward primary chemical bonding and hydrogen bonding between the fiber and resin. It may also affect the polarity of the fiber surface and change wettability. Being somewhat balanced in electronegativity means that the group is less polar, although it is still polar to an extent. Comparing the electronegativity of the surface groups in Figure 21 finds them somewhat balanced. The electronegativity of hydrogen, according to the Pauling scale, is 2.20 and that of nitrogen is 3.04. Carbon has an electronegativity of 2.55.¹⁰² The hydrogen ends of these groups are somewhat positive and can attract more

electronegative bodies, such as the oxygen end of water or the oxygen portion of hydroxyl (OH), resulting in hydrogen bonding. Nitrogen and ammonia plasma treatments were also shown to produce very little etching effect, which means little or no fiber strength loss and mechanical anchoring.

Oxygen plasma treatment is believed to introduce carbonyl groups (carboxylic acid and esters) on the fiber surface, leaving C-OH, C=OH, C=O, COOH and CO₂ for interaction with the matrix. Carbonyl groups contain a strong carbon/oxygen dipole.¹⁰³ Schematic drawings of these groups are shown in Figure 22. R' represents an organic group.

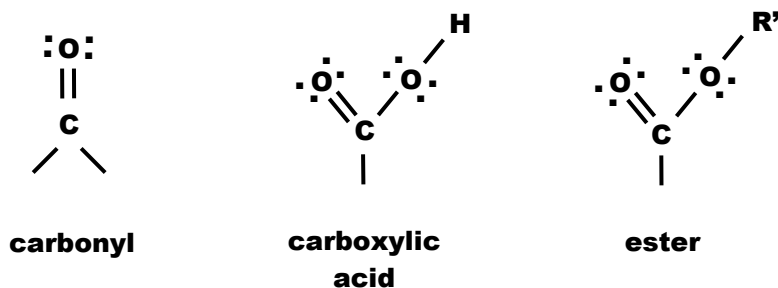


Figure 22 – Surface groups that likely result from oxygen plasma treatment and nitric acid treatment

The unsaturated C=O bonds may be available for bonding to the matrix and these surface groups exhibit much more polarity and electronegativity than those deposited with nitrogen and ammonia plasmas (according to the Pauling scale).¹⁰² Oxygen is more electronegative than nitrogen. Also, the oxygens of these groups can be seen to have more unbonded electrons than the nitrogens of the ammonia and nitrogen treatment groups, making them even more nucleophilic. These oxygens are free to bond with the unsaturated carbons on the ends of the vinyl ester matrix, as well as participate in

hydrogen bonding with the hydroxyls along the matrix chains. The vinyl ester molecule is shown below in Figure 23.

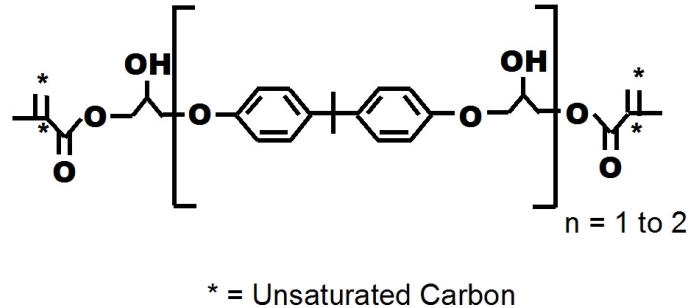


Figure 23 – Vinyl ester structure

Because styrene is also a constituent of the matrix resin that participates in cross-linking, these oxygens may also bond with styrene through primary or hydrogen bonding. Styrene can be seen in Figure 24.

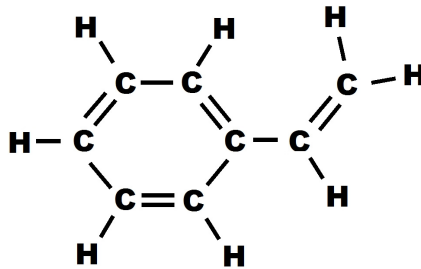


Figure 24 – Styrene structure

Furthermore, the hydrogen of the carboxylic acid group (Figure 22) can also participate in hydrogen bonding with the matrix.

Oxygen plasma provides highly electronegative and polar surface groups, which will likely affect fiber/matrix wettability and bonding. However, nitric acid treatment is believed to impart higher quantities of oxygen surface groups with less (although

significant) fiber tensile strength degradation. An acid treatment is also more feasible than a plasma treatment when considering the need for special equipment.

As discussed previously, polymers absorb water in part because of their polar constituents. There now seems to be opposing effects. Is it better to reduce the overall polarity of the interface so less water is attracted, but there is also a lower propensity for fiber/matrix chemical bonding? Or is it better to increase the polarity of the interface so there is likely to be more fiber/matrix bonding before water intrusion ever occurs, but at the cost of a more hydrophilic fiber surface? Also, how vulnerable are the bonds formed to hydrolysis? Nitrogen and ammonia plasmas provide the opportunity for bonding through reactive surface groups and a comparatively lower polarity, whereas oxygen plasma and acid oxidation provide highly reactive and polar surface groups, which likely affect both matrix wettability and fiber/matrix chemical bonding more strongly. Chemical bonding of the vinyl ester structure may occur from the unsaturated carbon points on the molecular chain ends or through hydrogen bonding of the hydroxyl moieties along the chain length. The hydroxyls likely offer the vinyl ester molecule the ability to adhere to polar bodies along its entire length, such as fibers, even though the only unsaturated reactive points are at the ends.

Hydrogen bonding, as the name implies, always involves a hydrogen atom. It exists between an electronegative atom and a hydrogen atom bonded to another electronegative atom.¹⁰⁴ It now becomes apparent why hydroxyl (OH) moieties on the vinyl ester chain would likely hydrogen bond with electronegative surface groups deposited on a carbon fiber surface. A hydrogen atom is bonded to an electronegative atom by a conventional covalent bond, and is loosely bonded to the second

electronegative atom by electrostatic (dipole-dipole) forces.¹⁰³ Hydrogen bonds are stronger than van der Waals forces, but weaker than ionic or covalent bonds. A hydrogen atom attached to a relatively electronegative atom is a “hydrogen bond donor”. This electronegative atom is usually fluorine, oxygen or nitrogen.^{103,104}

Water is prone to hydrogen bonding, and in fact, it determines many of its properties. The relatively high boiling point and apparent skin of water is due to the strong hydrogen bonding between water molecules. The oxygen of one water molecule has two lone pairs of electrons, each of which can form a hydrogen bond with hydrogens on two other water molecules. This can be repeated so that every water molecule is hydrogen bonded with up to four other molecules.¹⁰⁴ Ammonia (NH₃) forms even stronger hydrogen bonds with water than other water molecules do, resulting in an almost explosive solubility in water.¹⁰³ Ammonia does not form strong hydrogen bonds with itself, as evidenced by the fact that it boils at -33° C, while water boils at 100° C.

In planning this research, one must weigh the potential benefits of improved wettability, improved chemical bonding, fiber strength improvement, and fiber surface morphology changes, against fiber strength losses, reductions in wettability and the resultant attractiveness of the interface to water. Rather than focus on a treatment that will make the fiber/matrix interface less polar (and less attractive to water), this research takes the other route and focuses on a fiber surface treatment that makes the surface more polar and implanted with more reactive surface groups. This improves the chance of chemical bonding between the fiber and matrix (primary and hydrogen) before water exposure. The vinyl ester molecule has unsaturated reactive sites and numerous hydrogen bonding sites that may be utilized. Additionally, styrene acts as a cross-linker

in the vinyl ester system and may also serve to link the vinyl ester molecules to the reactive carbon fiber surfaces.

The formation of these bonds not only improves the fiber/matrix interfacial strength, but it may serve to occupy some of the vinyl ester bonding sites near the interface. Some of the numerous hydrogen bonding sites along vinyl ester molecules that would normally be attractive to water may be “tied up” and made less attractive to water. Matching polar, electronegative groups in the vinyl ester resin with those on the fiber surface may satisfy the strong polarities to some extent, resulting in a more balanced, less polar link connecting them, which would be less attractive to water molecules.

The potential drawback of making the fiber surface polar and reactive is that if the vinyl ester doesn't utilize all of this reactivity or interfacial voids exist, the fiber surface may draw water molecules to the interface and keep them there. If a significant amount of water is accumulated at the interface, debonding may occur as a result of matrix swelling and hydrolysis. Hydrolysis is a nucleophilic substitution in which water serves as the attacking nucleophile.¹⁰³ This is interpreted to mean that this substitution will only occur if water is more strongly charged than a particular chemical group that has formed a link across the fiber/matrix interface. If this is the case, water, or hydroxyl, will break the link and replace the lesser-charged compound. Because many of the possible surface groups deposited by nitric acid treatment are similar or greater in polarity than water (judging by electronegativity comparisons of the constituent atoms), water is unlikely to hydrolyze these groups and their bonds to the matrix. Of the possible surface groups identified, ester may be the most vulnerable to hydrolysis, as ester groups within vinyl ester can be hydrolyzed.³⁰

3.1.2 Carbon Fiber Surface Treatment and Silane Application to Improve Fiber/matrix Adhesion and Hydrolytic Stability

Silane coupling agents are used extensively in bonding glass fibers with numerous polymeric resins to improve composite performance, as well as hydrolytic stability. Unlike carbon fibers, glass fibers are vulnerable to degradation by water, and the usage of silane layers on glass fiber surfaces has been shown to protect them from attack by water. It is not clear how this occurs and several theories exist, but a well-accepted theory (chemical bonding theory) suggests that silanes go through hydrolysis and condensation reactions to ultimately form covalent bonds with the glass substrate. In this theory, it is believed that the silane molecule initially reacts with the hydroxyl moiety of the Si-OH groups on the glass surface. If this is indeed the case, it may be possible for the silane molecules to react with hydroxyl groups (or other hydroxyl-containing groups like carboxylic acid) that have been implanted on carbon fiber surfaces through oxidation. Silane coupling agents normally do not bond with untreated carbon fiber surfaces.^{105, 106}

Because nitric acid has been found to produce a high concentration of oxygen-containing surface groups, it is used as the initial surface treatment on the carbon fiber, prior to silane coupling agent application. As discussed previously, there are numerous types of silane coupling agents and a choice must be made regarding the type and functionality of the hydrolysable group, as well as the type of nonhydrolysable, organofunctional group. For this research 3-(trimethoxysilyl)propyl methacrylate has been chosen as the silane coupling agent. Tri-functional silane compounds, such as this, have been shown to provide the highest degree of hydrolytic stability in glass-fiber

composite systems.⁶⁵ Additionally, methacrylate silane types are frequently used to bond with vinyl ester resins.¹⁰⁷ Figure 25 depicts the 3-(trimethoxysilyl)propyl methacrylate molecule.

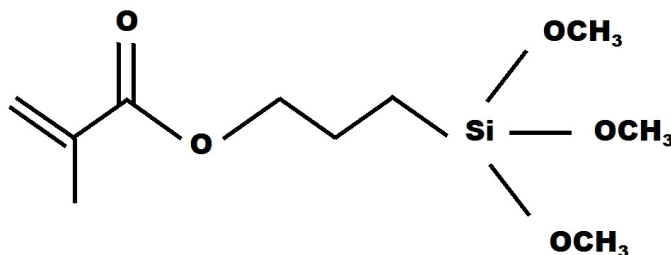


Figure 25 – 3-(trimethoxysilyl)propyl methacrylate

3.2 Experimental Methods and Results

To evaluate the nitric acid and nitric acid/silane surface modifications, information should be recovered for several parameters. First the post-treatment fiber and its surface should be evaluated before implementation into a composite. Next the resultant composite should be evaluated. The post-treatment fibers were evaluated by measuring their physical properties, such as tensile strength, modulus, and surface morphology, as well as their chemical surface properties, including amount and type of functional groups, surface energy, and fiber cohesion. Composites containing multiple fibers were evaluated by examining wetting, void content, transverse tensile strength, seawater weight gain and swelling, and damage induced by curing and exposure to seawater.

3.2.1 Fiber Treatment

Fiber surface oxidation was conducted on individual fiber tows, as well as fiber mat, using 70% concentrated nitric acid. The acid used was NF grade, indicating that it had met the limits for purity and testing specified by the National Formulary. The fiber treatment process was as follows:

1. Wash the fiber in distilled water for two hours.
2. Dry the fiber in an oven at 120° C for two hours.
3. Treat the fiber in boiling acid for varying periods time, ranging from 2.5 to 160 minutes. Boiling conditions were used to accelerate the treatments and to maintain a constant temperature (since the acid has a constant boiling temperature). In all treatments, the acid temperature was measured to be 120° C.
4. Wash the treated fiber in several changes of distilled water until the pH of the treatment water is close to that of the distilled water supply. pH was measured with a handheld pH meter.
5. Dry the treated fiber at 120° C for two hours.
6. Store the treated fiber in a vacuum with silica gel desiccant until use.

The carbon fiber tows were supported during treatment by wrapping them around glass rods that had been bent into frames with the aid of heat. The tow ends were secured with Teflon tape and the assembly was submerged into boiling acid for various time periods. The acid was brought to reflux using a water-cooled condenser (Figure 26).



Figure 26 – Carbon fiber nitric acid treatment configuration

Figure 27 shows an example of the glass rod frame that was used to treat the fiber tows. The frame size was designed to give spans of fiber in between supports that were of sufficient length for follow-up tests, such as the single fiber tensile and composite transverse tensile tests. The points where the fiber contacted the glass frame were easily identified for most treated fiber by a kink in the tow.



Figure 27 – Fiber bundle treatment glass rod frame

Fiber mat was treated by securing an individual 15.25 cm x 15.25 cm (6 in. x 6 in.) section of mat between a glass plate and a 316L stainless steel screen. 316L stainless steel wire was wrapped around the assembly ends and tightened by twisting to hold the assembly together. This type of stainless steel was chosen because of its resistance to nitric acid. Figure 28 describes the fiber mat treatment assembly and Figure 29 provides a photograph. In addition to sized fiber, the mats are woven together with other materials, whose nature is not disclosed. There are long, continuous fibers that run transverse to the carbon fiber directions that are believed to be glass fibers, put in place to provide transverse composite strength. Ramirez showed that the removal of these fibers significantly degraded composite transverse tensile strength.⁹⁷ The carbon fiber bundles are also woven together with a type of soft, flexible plastic. The glass-like fibers were removed prior to implementation into composites, and the flexible plastic weaving immediately dissolved in nitric acid. The soft, plastic weaving represented a very small amount of material and could not be physically removed without damaging the fiber mat. Because it was a small amount and readily dissolved, its effects on the resultant composites were assumed to be negligible.

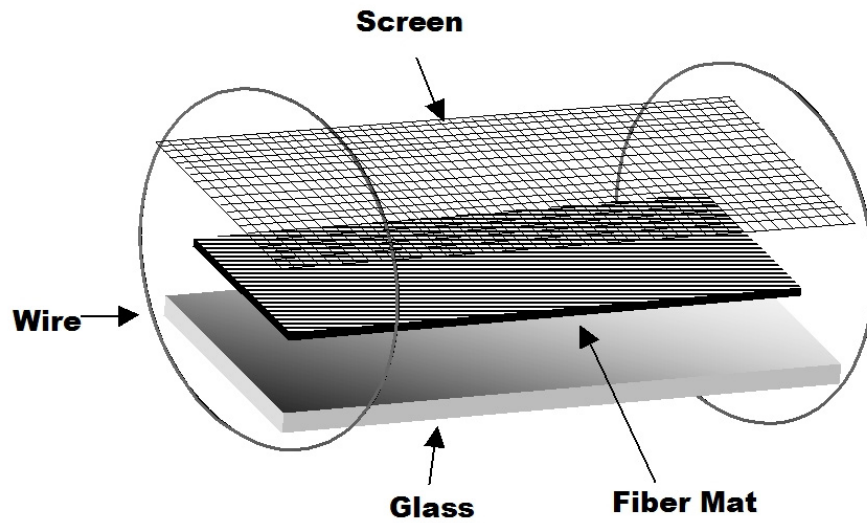


Figure 28 – Fiber mat treatment assembly diagram

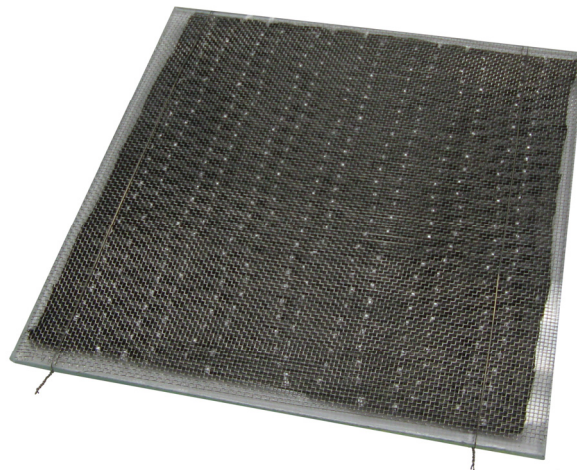


Figure 29 – Fiber mat treatment assembly photograph

Silane application was conducted on untreated fiber, as well as fiber that had been previously treated with nitric acid in both the single tow and woven mat forms. The silane application process was as follows:

1. Immerse the fiber in a solution of 15% silane in acetone for 1.5 hours at 50° C.
2. Wash the fiber in three changes of fresh acetone, for 10 minutes each.
3. Dry the fiber in an oven at 110° C for seven minutes.

Acetone was chosen as the solvent for silane treatment because it is polar and was expected to easily dissolve the 3-(trimethoxysilyl)propyl methacrylate silane. Acetone also evaporates quickly; assuring that the solvent is removed within the short drying period. The reaction temperature of the silane/acetone mixture (50° C) was chosen simply because it was about the highest temperature that could be used without reaching the boiling point of acetone (56.5° C). The higher treatment temperature was expected to aid the reaction between the silanes and the substrate. The short drying time at 110° C was used because others have described an optimum temperature and drying time to complete the silane surface reaction, while minimizing damage to the sensitive methacrylate groups. Vidic et al. found that drying a methacrylate silane at one hour above 100° C caused loss of most of the methacrylate double bonds, while brief drying at 110° C produced better results than room temperature drying. Vidic studied methacrylate silanes and glass surfaces.¹⁰⁸

3.2.2 Fiber Surface Morphology and Diameter

A magnified view of the fiber surface after treatment provides insight into the surface morphology and diameter changes that result. An understanding of the physical surface condition is beneficial in evaluating the extent of fiber/matrix mechanical interlocking and matrix wetting that is likely to result when the fiber is incorporated into a composite. Surface irregularities allow for fiber/matrix interlocking if good wetting is achieved, but fiber roughness also increases the possibility that small voids may exist at the fiber surface after resin infusion. If a composite strength change is observed, it is important to know if it can be attributed to mechanical interlocking, chemical bonding, or some degree of both. Additionally, surface flaws have an impact on fiber tensile strength and fiber diameter is important information to have when assessing fiber strength and the affect of the treatment on the fibers. Scanning electron microscopy (SEM) offers the capability to analyze the fibers under close magnification, so these factors can be evaluated.

Scanning electron microscopy requires that the surface of the scanned object be conductive, which usually means coating it with a conductive material, such as gold/palladium, or conducting analysis in an environmental scanning electron microscope where moisture assures conductivity.¹⁰⁹ Carbon fibers, however, are electrically conductive themselves and no further surface treatment or environmental control is required. In a SEM, electrons are emitted towards the sample, either thermionically from a tungsten or lanthanum hexaboride cathode, or via field emission. This electron beam is focused by one or two condenser lenses and then passes through pairs of scanning coils, which deflect the beam in a raster fashion over a rectangular area on the sample surface.

Interactions between the sample and the electron beam in this region lead to the subsequent emission of electrons, which are then detected to produce an image. Depending on the instrument, the resolution of a SEM can fall between 1 and 20 nm.¹¹⁰ The specific SEM used in this research was the Quanta 200 by FEI company (Figure 30).

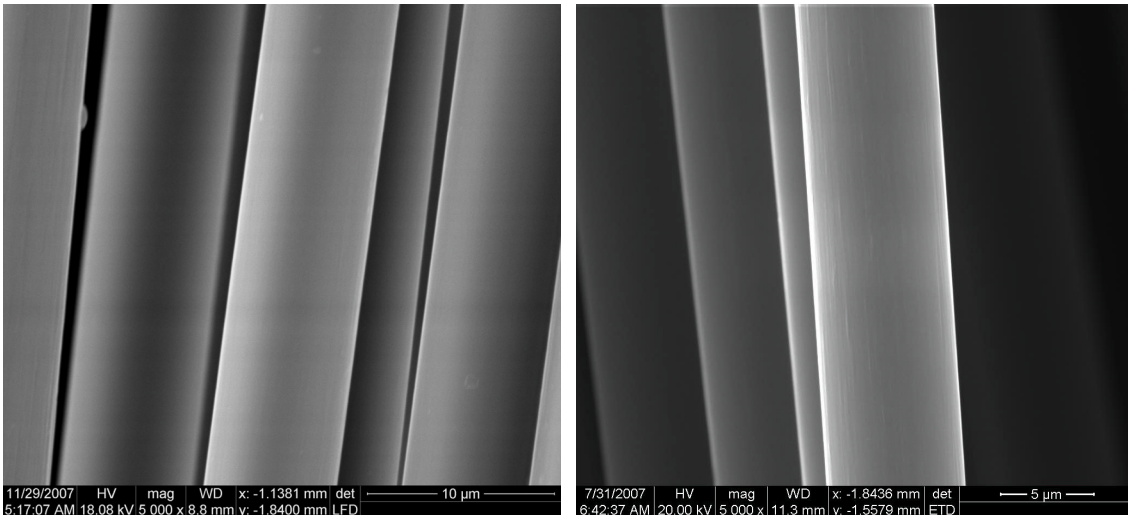


Figure 30 – Quanta 200 ESEM used in this research

Fiber surface morphology and diameter were evaluated by viewing fiber samples at 5000 times magnification. An average of at least 10 samples was used to determine fiber diameter for each different treatment type. Images were acquired through SEM and then measured with Scandium® SEM image analysis software. Because fiber surface defects were not common, the fibers analyzed for surface defects were not chosen at random. For each separate treatment sample, a search was conducted through a group of

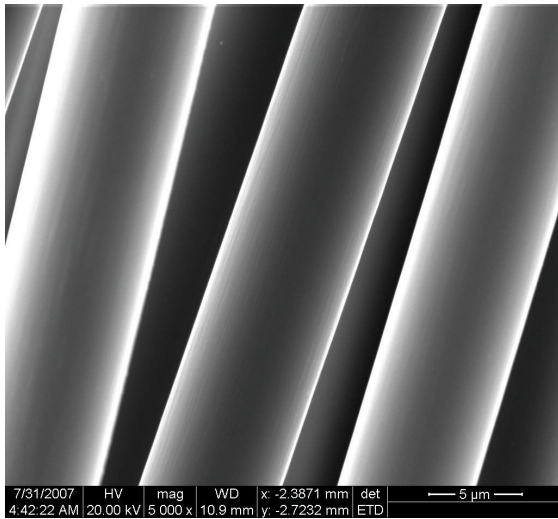
fibers to find surface flaws. This approach was taken so that the severity of the defects could be evaluated. Even though the defects are not common, they play an important role in fiber tensile strength. More importance was placed on reviewing the severity of the few defects that result from treatment than to take a random approach, in which defects may or may not be found. The importance of surface flaws on fiber tensile strength becomes evident when comparing the tensile strength at different test gage lengths. The longer the test gage length, the weaker the fiber apparently becomes. This is shown later on herein in the fiber tensile strength testing section. This phenomenon is presumably due to the increased probability of weak points in longer lengths of fiber, due to the presence of more flaws.

Most of the nitric acid treatments resulted in very little change in fiber surface morphology, but a significant decrease in fiber diameter with treatment time was observed. Figure 31, (a-h) shows the unsized (AS4) fibers at different stages of nitric acid treatment and Figure 32 (a-h) shows the sized (T700) fibers.

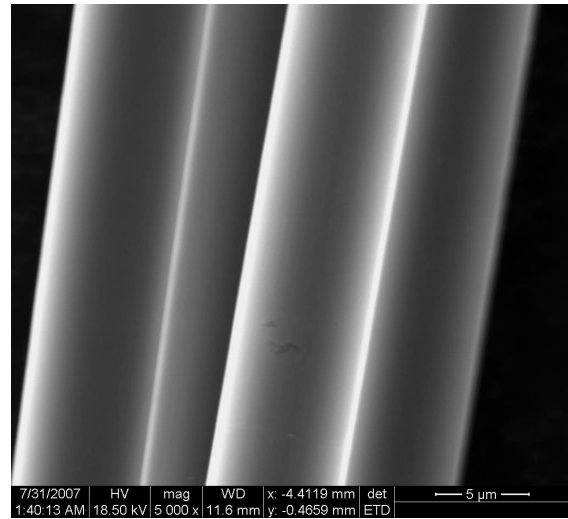


(a) Unsized, untreated fiber

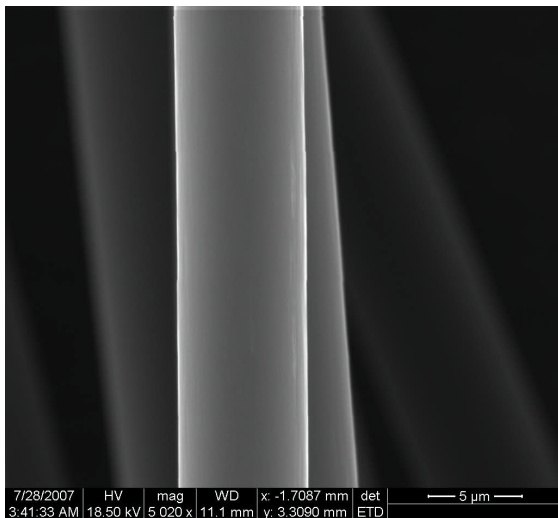
(b) Unsized, 5-minute acid treated fiber



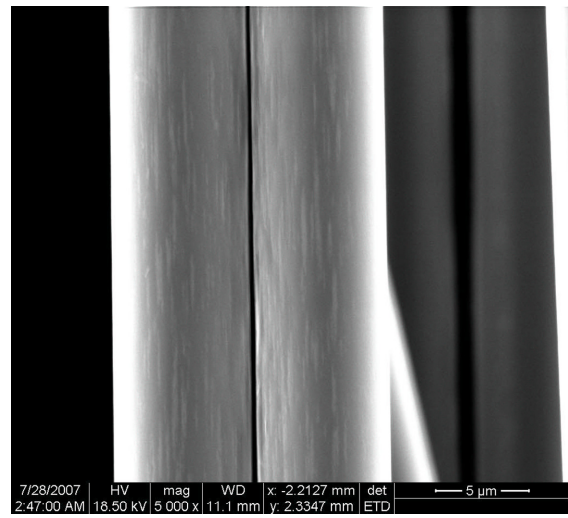
(c) Unsized, 10-minute acid-treated fiber



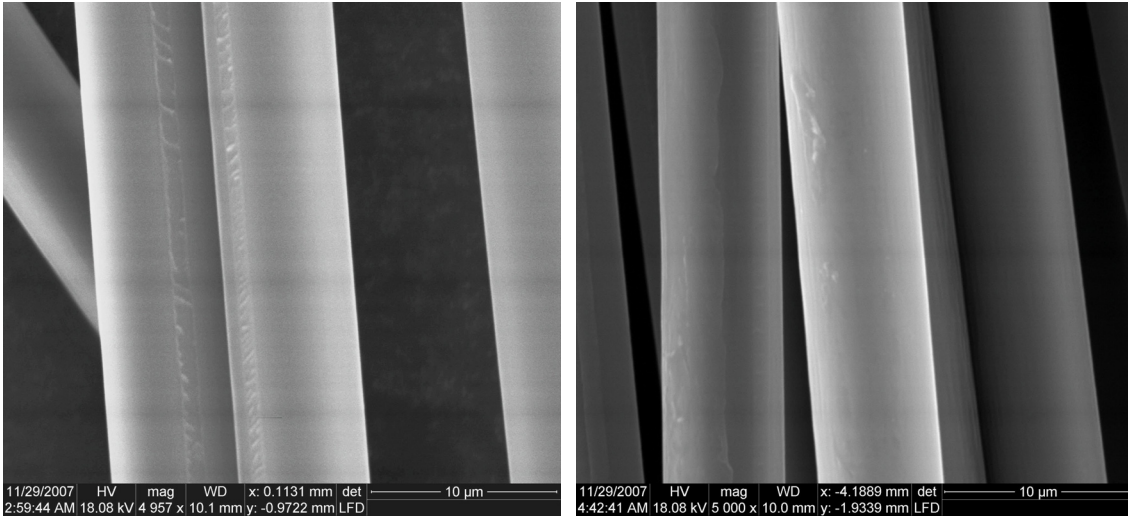
(d) Unsized, 20-minute acid-treated fiber



(e) Unsized, 40-minute acid-treated fiber



(f) Unsized, 80-minute acid-treated fiber

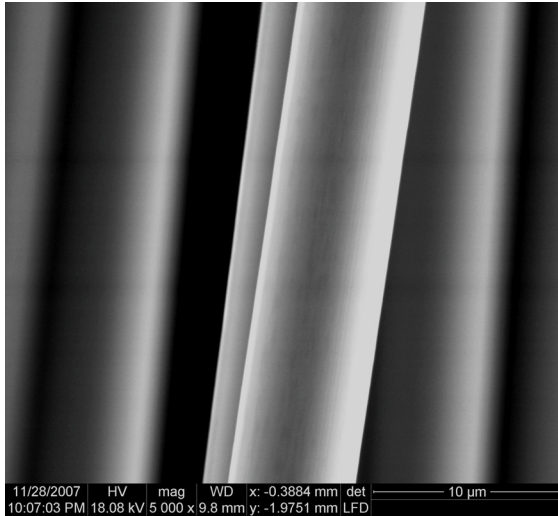


(g) Unsized, 120-minute acid-treated fiber

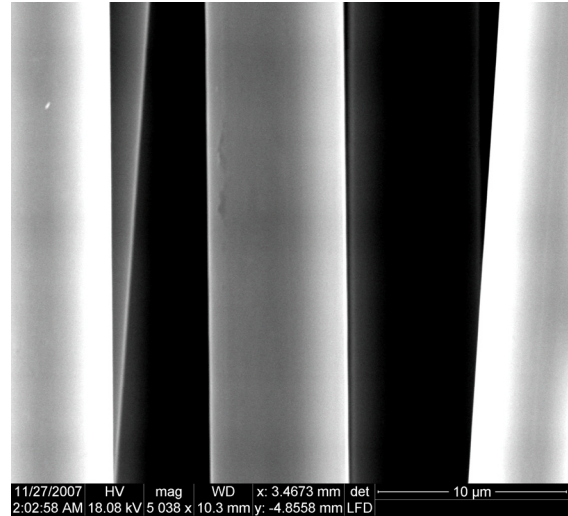
(h) Unsized, 160-minute acid-treated fiber

Figure 31 - Unsized fiber acid-treated SEM images

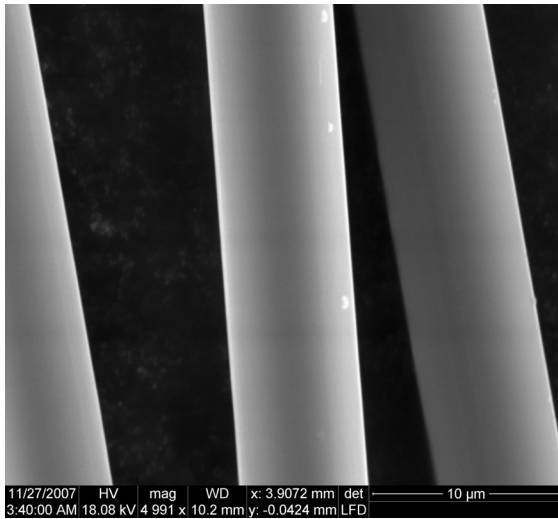
The unsized AS4 fibers remained smooth through most of the treatments. Striations showed up at the 5 and 10-minute treatments (Figure 31, (b) and (c)), but localized defects began to occasionally occur at 20 and 40 minutes (Figure 31, (d) and (e)). At 80 minutes, severe surface change was found in the form of longitudinal channels (Figure 31, (f)). Large, distinct defects and irregularities could be seen at 120 and 160 minutes (Figure 31, (g) and (h)), but the bulk of the fiber remained smooth. The unusual feature found on the 120-minute treated fibers will be discussed in the fiber cohesion section.



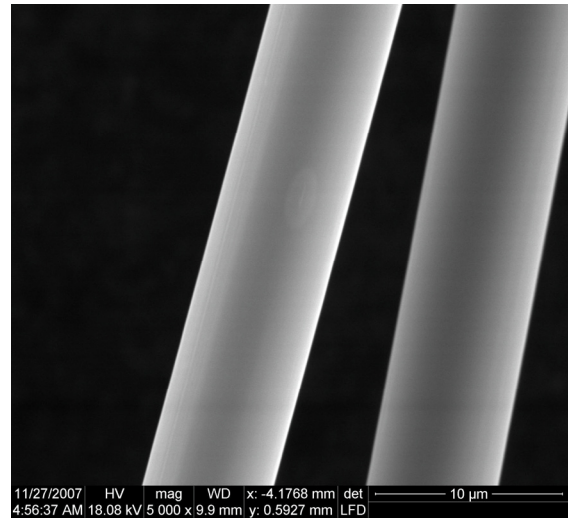
(a) Sized, untreated fiber



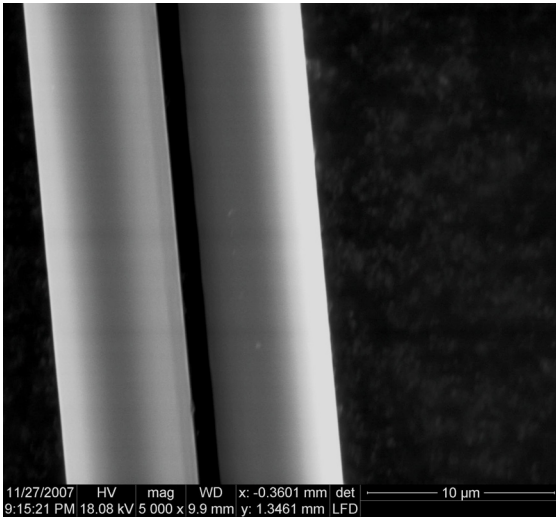
(b) Sized, 5-minute acid treated fiber



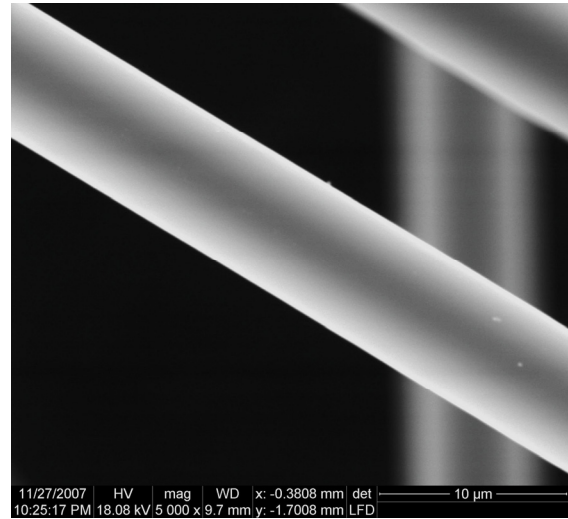
(c) Sized, 10-minute acid-treated fiber



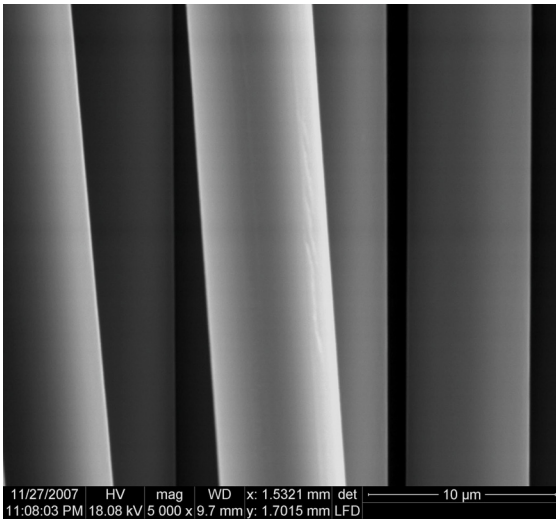
(d) Sized, 20-minute acid-treated fiber



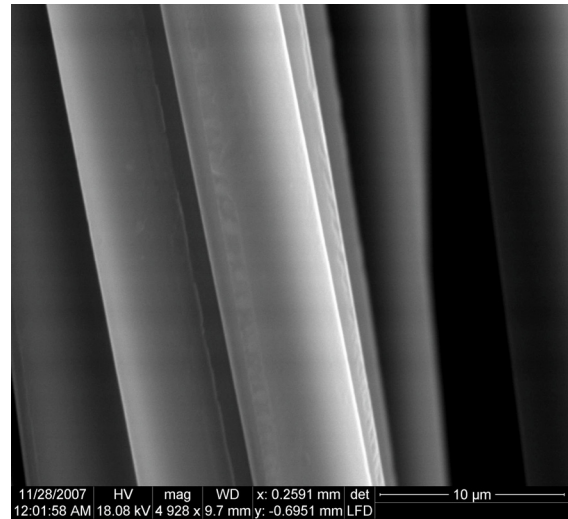
(e) Sized, 40-minute acid-treated fiber



(f) Sized, 80-minute acid-treated fiber



(g) Sized, 120-minute acid-treated fiber



(h) Sized, 160-minute acid-treated fiber

Figure 32 - Sized fiber acid-treated SEM images

The sized T700 fibers also remained smooth, with minor defects through 80 minutes of acid treatment, until slightly larger defects began to become evident at 120 minutes. Minor striations can be seen in the as-received (sized) (Figure 32, (a)). The

fiber surface was very smooth. Only minor flaws could be found at 5, 10, 20, 40 and 80 minute treatment times (Figure 32, (b) through (f)), but at 120 and 160 minutes, longitudinal channels can be seen (Figure 32, (g) and (h)). The 160-minute treated fibers also exhibit a similar feature as that found on the 120-minute treated unsized fiber, which will be discussed in the fiber cohesion section.

Although defects could be found on most treatment types, they were not easy to find and the bulk of the fibers remained generally smooth throughout all of the treatments. Therefore, mechanical interlocking is not expected to play a significant role in any composite strength changes that may be observed. Composite strength changes are therefore attributed to chemical bonding and wetting changes.

While the SEM images reveal only minor changes in the fiber surfaces, significant differences in fiber diameter were found, especially at longer treatment times, indicating that the overall fiber volume was being burned off. Figure 33 shows a plot of the AS4 (unsized) and T700 (sized) fiber diameters as a function of nitric acid treatment time. A significant diameter reduction can be seen in both fiber types with progressing treatment times, most notably at 160 minutes.

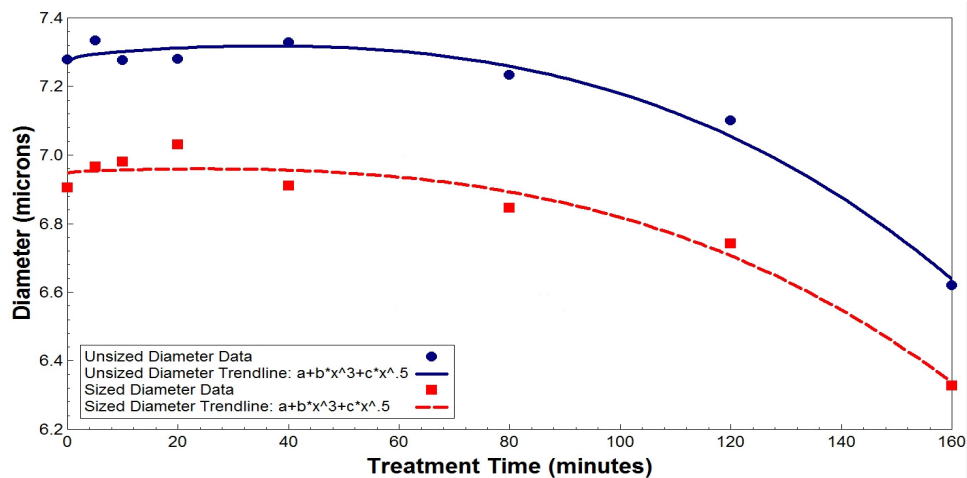


Figure 33 – Fiber diameter as a function of acid treatment time

Both sized and unsized fiber diameter changes with acid treatment can be described by the equation:

$$a + bx^3 + cx^{0.5} \quad (1)$$

, which was solved by nonlinear regression. The constants were found to be:

	FIBER DIAMETER CHANGE EQUATION CONSTANTS		
	a	b	c
Unsized	7.27	-1.82	8.70
Sized	6.95	-1.58	2.89

Table 5 - Fiber diameter change equation constants

Table 6 and Table 7 provide the standard deviation and median values of the sized (T700) and unsized (AS4) fiber diameter measurements, respectively. The entirety of the fiber diameter measurements can be found in Appendix A1. The average measurements obtained for the untreated fibers deviated from the manufacturer's values by 1.3% and 2.5% for the sized (T700) and unsized (AS4) fibers, respectively.

	SIZED (T700) FIBER DIAMETER (microns)							
	Untreated	5 Minute Treatment	10 Minute Treatment	20 Minute Treatment	40 Minute Treatment	80 Minute Treatment	120 Minute Treatment	160 Minute Treatment
Ave.	6.91	6.97	6.98	7.03	6.91	6.85	6.74	6.33
Std. Dev.	0.25	0.20	0.19	0.19	0.31	0.19	0.16	0.20

Table 6 – Sized fiber (T700) average diameter

	UNSIZE (AS4) FIBER DIAMETER (microns)							
	Untreated	5 Minute Treatment	10 Minute Treatment	20 Minute Treatment	40 Minute Treatment	80 Minute Treatment	120 Minute Treatment	160 Minute Treatment
Ave.	7.28	7.33	7.28	7.28	7.33	7.23	7.10	6.62
Std. Dev.	0.24	0.35	0.13	0.23	0.25	0.18	0.27	0.28

Table 7 – Unsize (AS4) fiber average diameter

In addition to diameter reductions, fiber weight was also found to decrease. Fiber weight loss due to acid exposure is addressed later in the section related to the evaluation of composite void content through nitric acid digestion.

3.2.3 Fiber Tensile Properties

Tensile Strength

Following surface treatment and prior to implementation into a composite for testing, the treated carbon fiber strength should be tested to account for changes. ASTM standard D 3379-75 provides standardized instructions for testing the tensile strength of high-modulus, single-filament materials. This specification identifies several requirements, including the fiber gauge length and crosshead speed to be used with a tensile testing machine. The fibers are glued onto a paper test fixture, similar to that depicted in Figure 34. Cyanoacrylate (super) glue was used, which quickly formed a strong bond and did not allow for fiber pullout. To aid in the proper alignment of the fiber and test grips, additional markings were included on the paper test fixtures, which are shown in Figure 34. Fibers were randomly pulled from a bundle, inspected for visible

damage, and each end of the fiber was aligned with the centerline that was printed down the length of the fixture before applying glue.

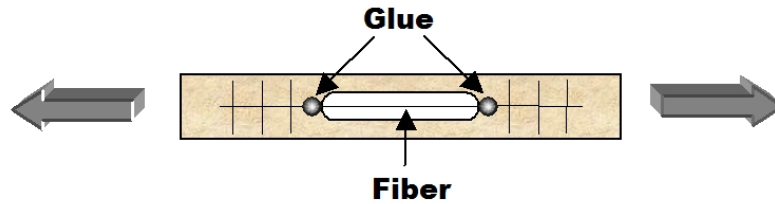


Figure 34 – Single fiber tensile test fixture

After allowing the glue to dry, the fixture was then placed into the grips of a tensile-testing machine (aligning the grip ends with the cross-hatched markings to assure alignment) and the sides of the paper fixture were cut away so that only the fiber was stressed during testing. A MTS 2N load cell, mounted on a MTS Insight 1kN test stand was used at a crosshead speed of 0.5 mm/min, which resulted in a test time of approximately one minute (as recommended by ASTM D 3379-75). The MTS test stand is shown in Figure 35, setup in the fiber tensile-testing configuration.



Figure 35 - MTS Insight 1kN test machine in the fiber tensile testing configuration

ASTM D 3379-75 allows for gage lengths from 20-30 mm. A 20 mm gage length was chosen because tests at this length provided the closest agreement between untreated fiber tested strength and the fiber manufacturers' reported strength. It is also expected that the fiber manufacturer would test their fibers in lengths that give the greatest strength values (the shortest lengths). Toray company reports that its T700 fiber has a strength of 4900 Pa (711 ksi), and Hexcel corporation lists 4692 Pa (680 ksi) for its AS4D fiber. At least 20 fibers were tested for each treatment condition, but after testing, any tensile strength data point that fell outside of two standard deviations from the mean was removed from the sample group. This did not remove a significant amount of data points, anywhere from zero to two from each test group. And the points that were removed usually deviated from the group significantly. Typically, the force versus displacement curves for the fibers were very straight, indicating a completely elastic material response. A typical fiber tensile test plot can be viewed in Figure 36. A curve such as this exhibits no plastic deformation, leading to a material that often fails prematurely in a brittle manner. Similar tensile test plots for all of the fibers tested can be found in Appendix A2. The average results obtained for the maximum fiber loads and stresses for each treatment time are shown in Figure 37 and Figure 38.

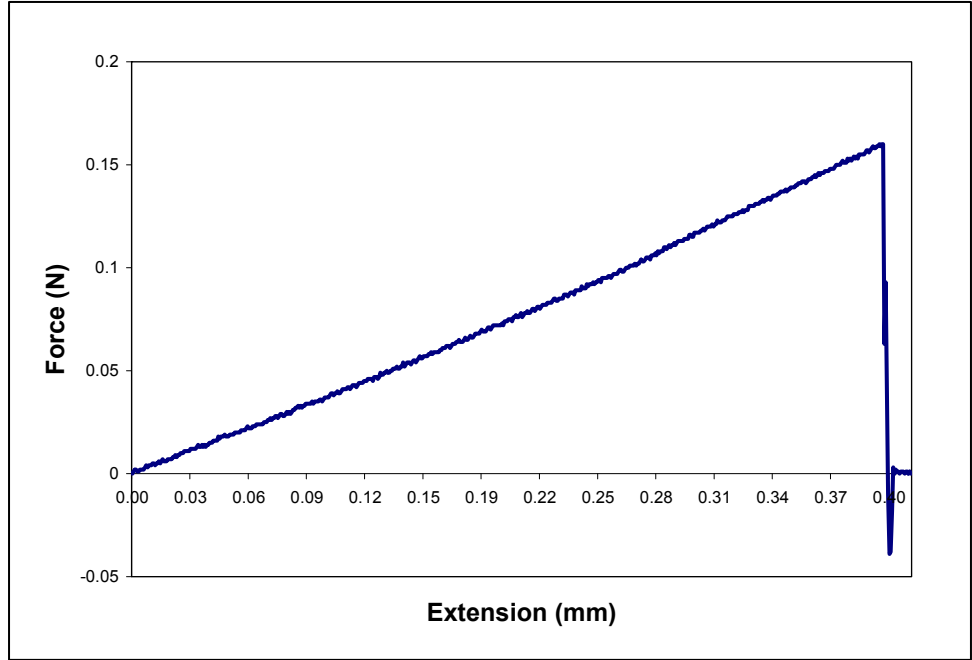


Figure 36 - Typical fiber tensile test plot (sized(T700) untreated)

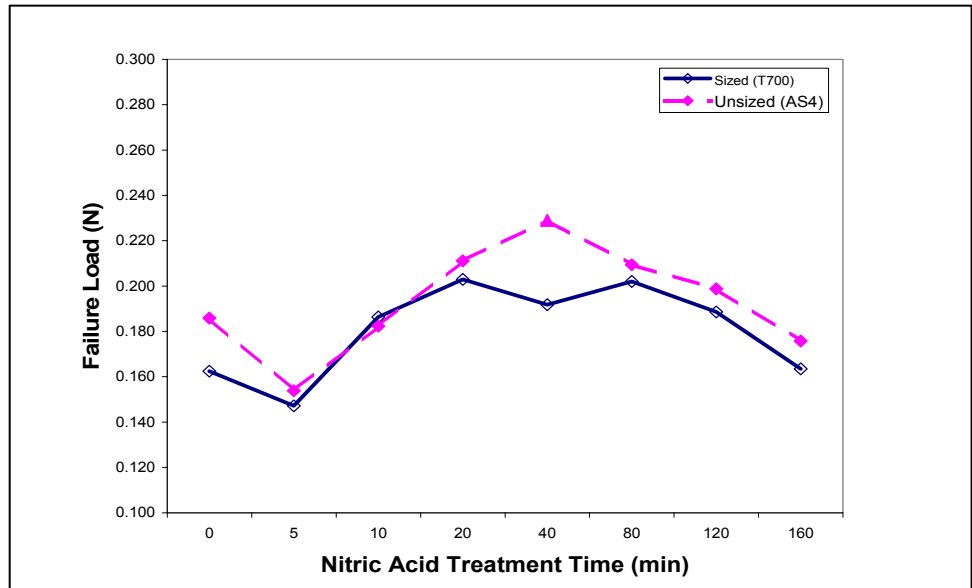


Figure 37 - Fiber load at break

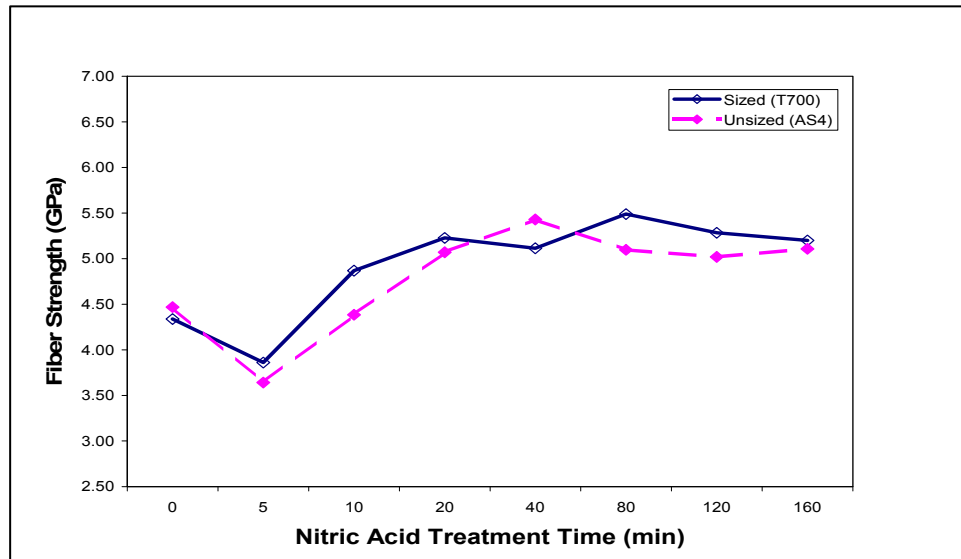


Figure 38 - Fiber strength

From Figure 37, it can be seen that in both fiber types, there is an increase in the maximum fiber load that results from nitric acid treatment, but that improvement is eventually lost at longer treatment times as the load decreases. Further clarification of this phenomenon is found by examining Figure 38. In Figure 38, the fiber strength is divided by the average fiber diameter measured for each treatment time to arrive at the average fiber stress at break. The fiber diameters were measured by SEM and are reported in the Fiber Surface Morphology and Diameter section herein. It becomes clear that the fibers don't actually lose strength with extended treatments, but they just lose cross-sectional area. After a short dip in the maximum fiber stress at 5-minute treatments, both fiber types achieve a failure stress that is greater than the untreated condition and remains constant. The apparent loss in fiber strength at extended treatment times is just a result of the reduction in fiber diameter. The fact that the fibers show an improved stress at failure that remains fairly constant with acid treatment, strongly

supports the theory that the mechanism of fiber strength improvement is the mitigation of surface flaws. Early treatments smooth the surface, but after the surface is smoothed, longer treatments only cause an even removal of carbon material.

While both fiber types generally showed an improvement in stress at break after treatment, they also showed an immediate decline in strength at 5-minute treatments, before the increase was realized. It is believed that this is because the outer layer of the as-received carbon fibers is imperfect and nonuniform, leading to an initial acid attack that is uneven, making the existing flaws more severe at short treatment times. Once this outer layer is removed and the surface flaws are minimized, there is a more even reduction in surface material, resulting in a smoother surface at longer treatment times. This is supported by the SEM micrographs that showed surface irregularities in the fibers at 5-minute treatment times (Fiber Surface Morphology and Diameter Section). Both fiber types behaved very similarly in both maximum load and maximum stress, including the initial drop at short treatment, followed by the increased load and stress profiles seen with extended treatment.

Measured fiber strength is strongly dependent on the length of the filament that is tested. To compensate for this, methods of extrapolating measured fiber strengths to lengths other than those tested have been developed. A commonly used method is weak link scaling.¹¹¹ Carbon fiber is a strong material, but it is also very brittle, which leads to its ultimate strength being determined by the flaws that exist within the tested lengths. The main idea of weak link scaling is that carbon fibers are only as strong as the weakest point along their length (the worst flaw), similar to the weakest length in a chain. As a longer length of fiber is tested, there exists a higher probability of more severe flaws,

which should lead to a lower value of tensile strength. Indeed, this has been observed in testing by others, as well as within this research. Lengths of 20, 25 and 30 mm carbon fibers were tested and as expected, the value of measured strength declined as the test gage length was increased. The strength values obtained for the different gage lengths can be seen in Figure 39. At least 10 fibers were tested for each gage length, and then averaged.

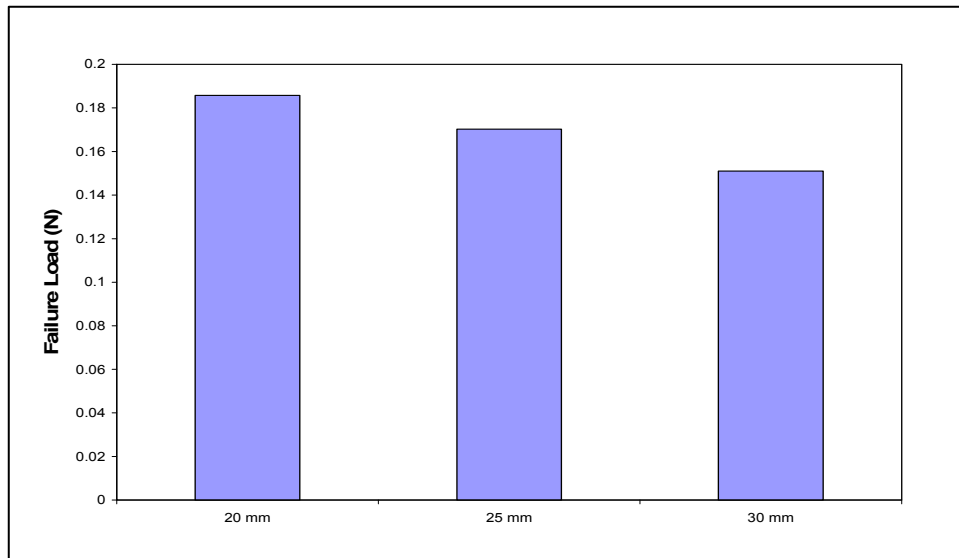


Figure 39 - Sized (T700) fiber failure load as a function of test gage length

Weak link scaling offers a way to analyze the statistical distribution of fiber tensile strengths at one gage length and predict tensile strengths at other gage lengths. The statistical distribution of carbon fiber tensile tests can be described by the two-parameter Weibull equation, which is of the form,^{111, 112}

$$P_{f(L)} = 1 - \exp \left[-L \left(\frac{\sigma}{\sigma_o} \right)^w \right] \quad (2)$$

where $P_{f(L)}$ is the probability of failure of a fiber of length L at a stress less than or equal to σ , σ_0 is the Weibull scale parameter (characteristic stress) and w is the shape parameter (Weibull modulus). The shape parameter describes the variability of the failure strength. Rearrangement of equation (2) gives the following equation:^{111, 112}

$$\ln \ln \left(\frac{1}{1 - P_{f(L)}} \right) = w \ln \sigma - w \ln \sigma_0 + \ln L \quad (3)$$

Using equation (3), the Weibull scale and shape parameters can be retrieved from a plot of $\ln \ln(1/1 - P_{f(L)})$ versus $\ln \sigma$. This is known as a Weibull plot and should produce a straight line, with gradient w and x-intercept, σ_0 , at $\ln \ln(1/1 - P_{f(L)}) = 0$, if the data can be subjected to this type of analysis. If this plot does not resemble a line, this type of analysis is not appropriate. After determining w and σ_0 from the plot, the strength of a fiber at a different length can be predicted by scaling the strength obtained from the tested length, as follows:^{111, 112}

$$\sigma_{0(2)} = \sigma_{0(1)} \left(\frac{L_1}{L_2} \right)^{\frac{1}{w}} \quad (4)$$

where $\sigma_{0(2)}$ and $\sigma_{0(1)}$ are the strengths for lengths L_2 and L_1 , respectively.

As noted before, any data points that were outside of two standard deviations from the mean were not included in the analysis. This only resulted in the removal of zero, one or two points from each data set of 20 or more, but it made a significant difference in the weak link analysis. Before removing these outlying data points, the Weibull plots did not always produce straight lines, indicating that a Weibull analysis may not be appropriate. However, after removing these outliers, the Weibull plots produced acceptable straight lines. The Weibull plots are shown in Figure 40 and Figure

41. Also on the plots, are the best-fit straight-line equations and the Weibull scale and shape parameters found from them.

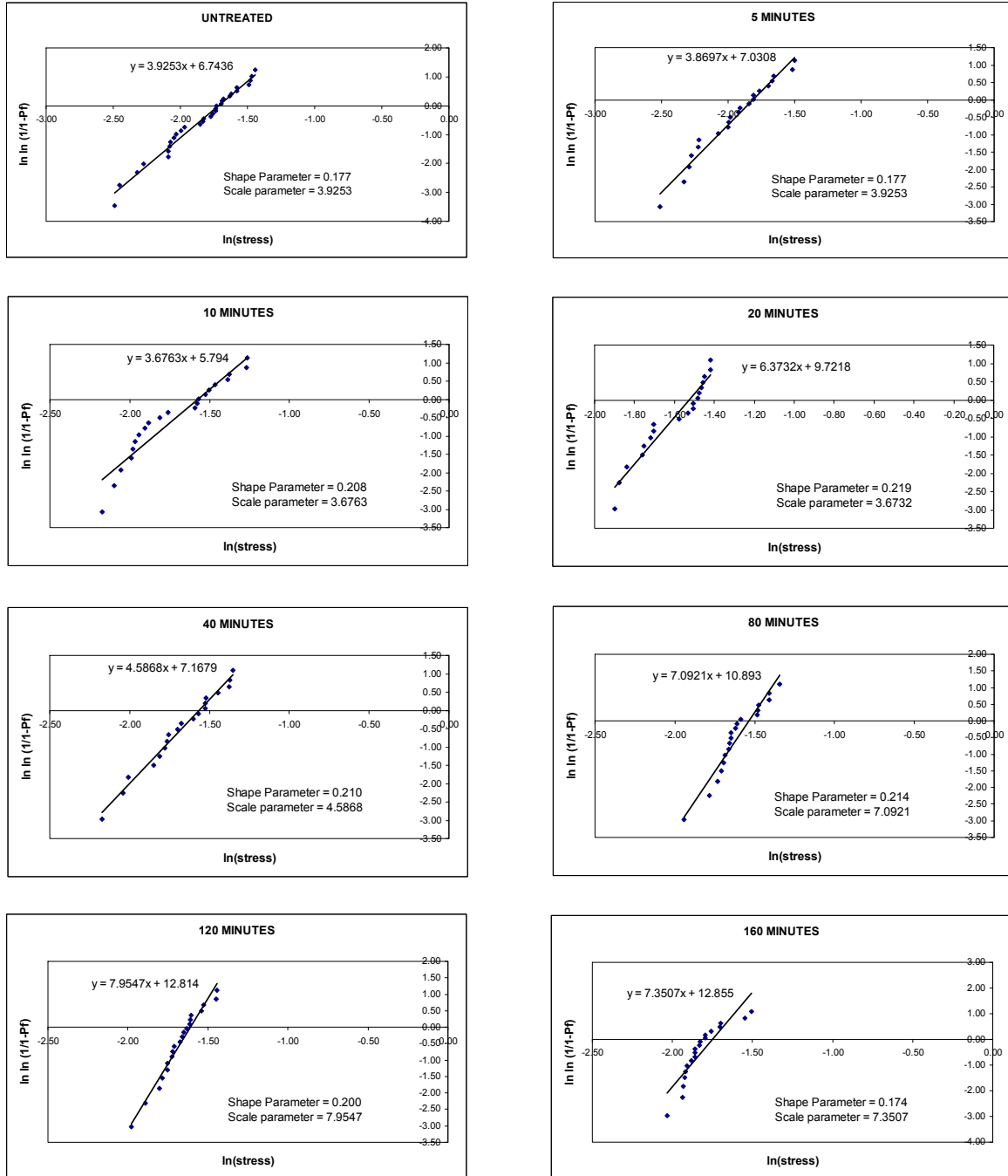


Figure 40 - Sized (T700) fiber Weibull plots, scale parameters and shape parameters

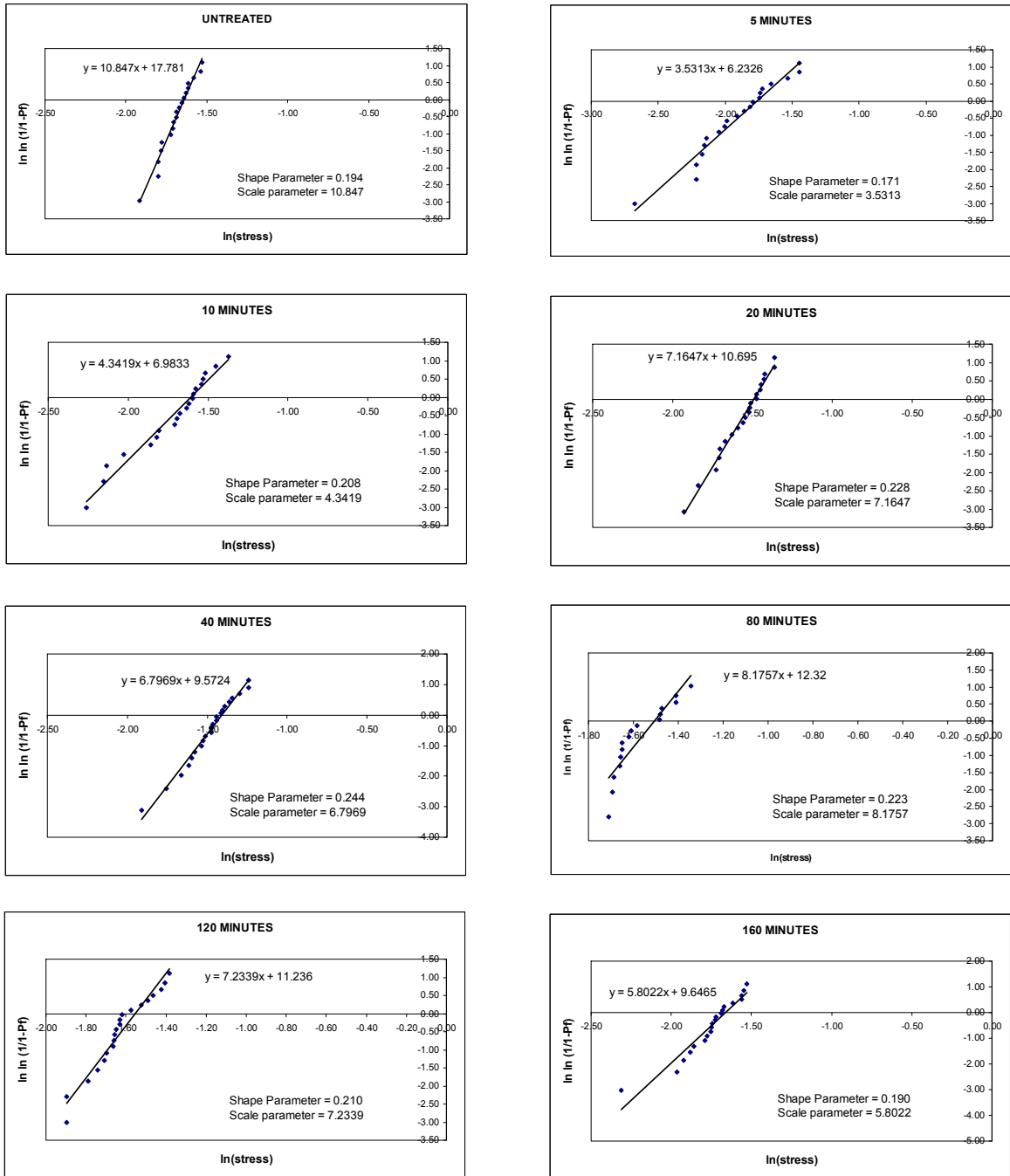


Figure 41 - Unsized (AS4) fiber Weibull plots, scale parameters and shape parameters

The predicted strengths for the different fiber treatments, using weak link scaling, can be observed in Figure 42 and Figure 43 for the sized (T700) and unsized (AS4) fibers, respectively.

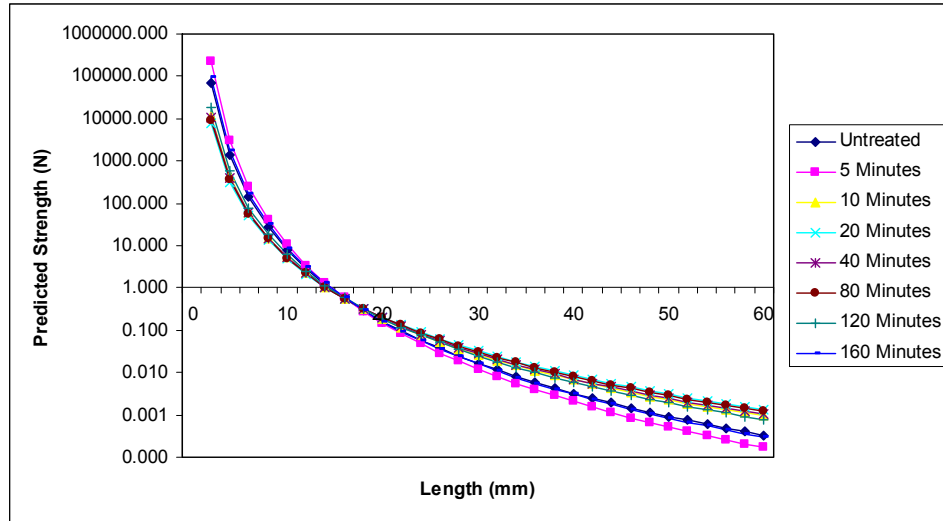


Figure 42 - Sized (T700) fiber predicted strength as a function of length

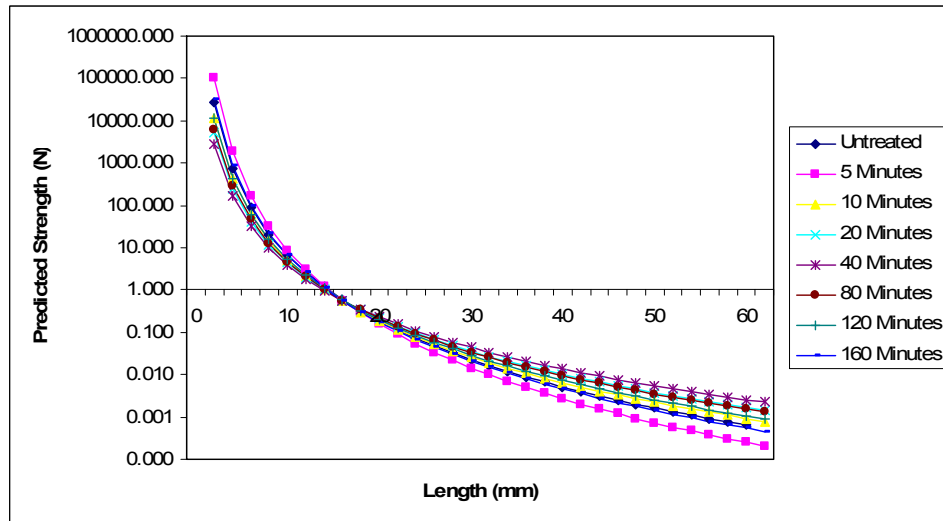


Figure 43 - Unsized (AS4) fiber predicted strength as a function of length

What is immediately apparent from the predicted strength plots is that the curves are not linear. Theory requires that a plot of the natural logarithm of characteristic strength versus the logarithm of length should give a straight line. Figure 42 and Figure 43 do not show a natural log length scale, but the curve shape does not change if the scale is converted to natural log. This suggests that this type of fiber strength scaling can only serve to give a basic idea of how strength varies with test gage length. Others have observed this type of behavior. Pickering et al. suggested that a parabolic curve fit is more appropriate for high-strength carbon fiber after evaluating weak link scaling on several different test gage lengths.¹¹¹ Elsewhere, others have attributed this nonlinearity found with brittle fibers to the potential for multiple types of defects within the population, such as interior and surface flaws.¹¹³

Young's Modulus

To further compare and evaluate the two types of as-received fibers (Toray T700 and Hexcel AS4), the moduli of the untreated fibers were determined from the tensile testing data. A higher-modulus fiber would be expected to have a more organized carbon structure and be more resistant to acid attack. Only the untreated fibers were considered because it was not expected that the modulus would change with acid treatment. This follows from the conclusion made herein that the tensile strength changes result from fiber surface modifications only (changes in diameter and mitigation of surface flaws). No bulk material property changes are expected. In order to determine modulus, ASTM D 3379-75 requires that the testing system compliance be determined because the test

system (grips, fixture, etc.) can contribute significantly to a very small measurement such as this. The fiber Young's Moduli were determined from the following equation:

$$Y_m = \frac{L}{CA} \quad (5)$$

Where Y_m is the Young's modulus (Pa), L is the specimen gage length (mm), C is the true compliance (mm/N) and A is the average fiber area (m²). The true compliance is calculated from the indicated compliance (C_a) and the system compliance (C_s), described in ASTM D 3379-75.

$$C = C_a - C_s \quad (6)$$

Furthermore, the indicated compliance (C_a) is:

$$C_a = \frac{I}{P} \times \frac{H}{S} \quad (7)$$

Where I is the total extension for a straight-line section on the load-time curve, extrapolated across the full chart scale (mm). P is the full-scale force (N), H is the test machine crosshead speed (mm/s) and S is the chart speed (mm/s).

Once the indicated compliance has been determined for three or more different gage lengths, a plot of indicated compliance versus gage length can be made for all specimens. A straight line is drawn to connect the specimens on this chart and the y-intercept (compliance axis) can be taken as the system compliance. Sized (T700) fiber was tested at three gage lengths (20, 25 and 30 mm), so that system compliance could be determined. At least 10 specimens were tested for each gage length. This resulted in average indicated compliances of 2.59, 3.25 and 3.75 mm/N for the 20, 25 and 30 mm gage lengths, respectively. By connecting these values with a line and reading the value

of the y-intercept, the system compliance (C_s) was found to be 0.27 mm/N. Figure 44 shows the system compliance chart.

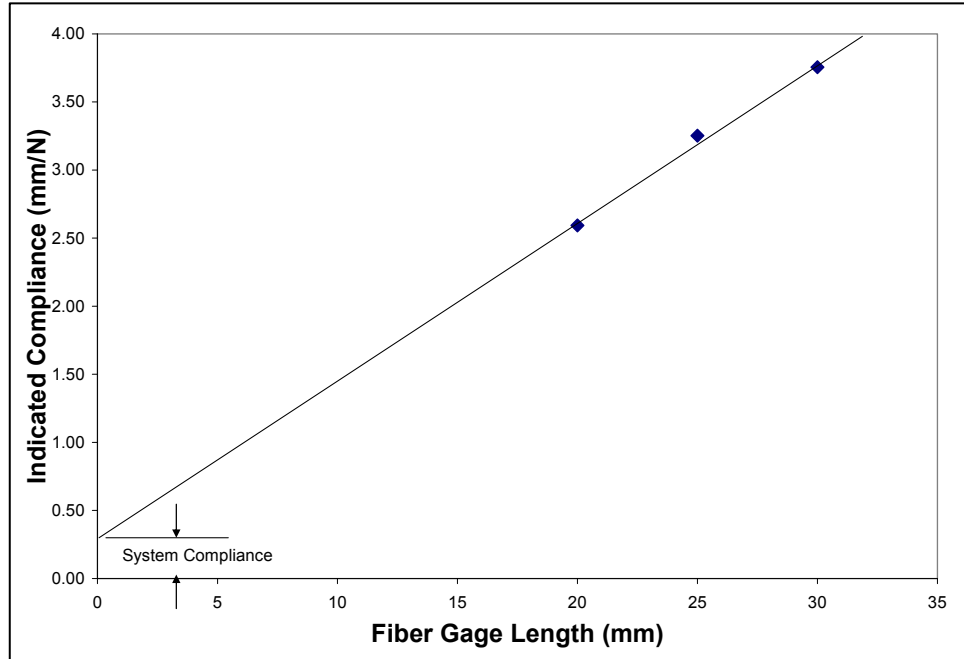


Figure 44 - System compliance chart

Returning to the 20 mm gage length case, it follows:

	FIBER COMPLIANCE AND YOUNG'S MODULUS	
	Sized (T700) Fiber	Unsize (AS4) Fiber
Average Indicated Compliance	2.59 mm/N	2.23 mm/N
True Compliance	2.32 mm/N	1.96 mm/N
Young's Modulus	230.5 GPa	245.3 GPa

Table 8 - Fiber compliance and Young's modulus results

The measured and calculated values for moduli are very close to the manufacturer's specifications in both fiber cases. Toray Co. lists 230 GPa for the T700 fiber and Hexcel Corp. lists its AS4D fiber as having a modulus of 245 GPa.

3.2.4 Resin Tensile Properties

Understanding fiber tensile properties are important for understanding composite behavior, but resin properties are also important. Specifically, it is important to understand resin tensile strength and elongation. Based on the tests conducted herein, resin compressive properties were not considered pertinent.

The manufacturer of the 411-350 Momentum resin puts forth certain typical properties, as shown in Table 9

	DERAKANE 411-350 MOMENTUM TENSILE PROPERTIES AS REPORTED BY MANUFACTURER
Tensile Strength	86 MPa
Modulus	3.2 GPa
Elongation, Yield	5-6%

Table 9 - Derakane 411-350 manufacturer-reported tensile properties

While composites rely on fibers (reinforcements) for the majority of their strength, the matrix also plays a very important structural role and its properties are also important. It was initially discovered that the resin properties were seriously lacking in comparison to the manufacturer's typical properties. However, this problem was

evaluated before any composites were made. The problem was found to be the method of mixing. It is necessary to allow time after mixing the promoter into the resin before it is catalyzed. One hour was found to be sufficient. When the catalyst was added immediately after mixing the resin and promoter, both the tensile strength and elongation suffered. Cobalt naphthenate was used as the promoter, MEKP was used as the catalyst, and no retarder was used. After casting the test specimens, they were allowed to cure for 24 hours at room temperature and then were postcured for two hours at 120° C. They were allowed to cool in the oven.

Tensile strength and elongation were measured by following the procedures outlined in ASTM D 638 (Standard Test Method for Tensile Properties of Plastics). This standard outlines the specimen size and testing speeds required. The specimen size used was the Type I size, which is the preferred one in the standard. The dimensions are specified below in Figure 45 in millimeters, followed by inches in parentheses.

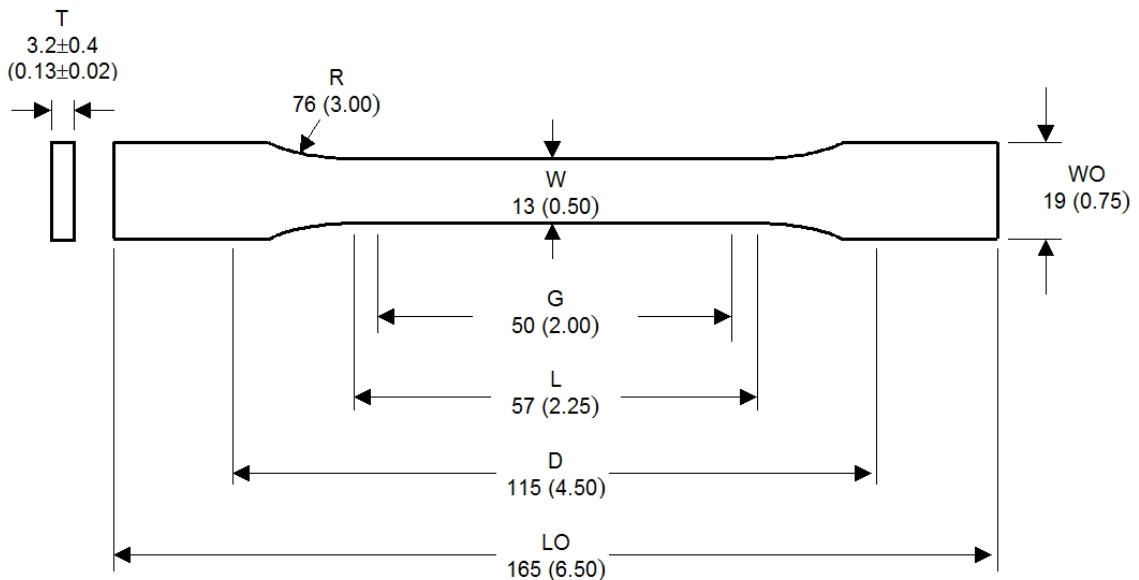


Figure 45 – Resin tensile test coupon dimensions

where, W = width of narrow section, G = gage length, L = length of narrow section, D = distance between grips, LO = overall length, WO = overall width, R = radius of fillet, and T = thickness.

The specimens were produced by first casting the resin in a RTV silicone mold, machining them to thickness with an end mill, and then sanding them with 80, 120, 220 and 400 grit sandpaper to remove any surface flaws. A relatively high machining pass-over speed was used, because it was found that the specimens would warp due to residual stresses forming from the heat created when the end mill slowly passed over the specimen. The pass-over speed was optimized with the spindle rotation speed to minimize heat build-up and avoid chipping. Figure 46 shows the silicone mold that was used to cast the test specimens.

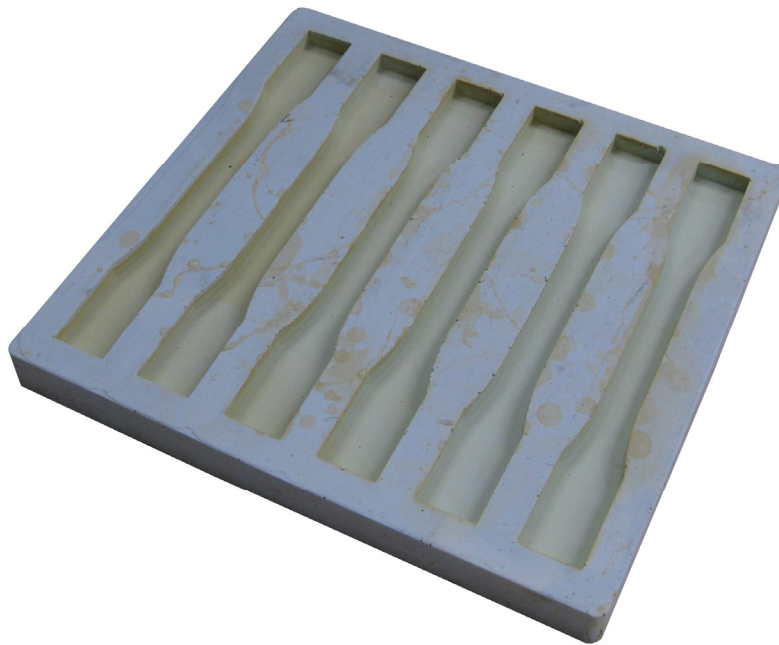


Figure 46 - Mold for resin tensile test specimens

Five specimens were tested for each resin type and the gage length, width and thickness was measured with a micrometer, accurate to three digits. They were tested on a MTS Insight 50 test stand at 5 mm/min. Additionally, a MTS extensometer was used to directly measure the material strain within the test gage length during testing, instead of relying on the displacement of the test stand. Displacement of the test stand measures elongation of both the gage length and the wider areas near the grips of the specimen. It also includes any compliance that may be innate to the machine configuration. Figure 47 shows the MTS Insight 50 in the configuration used and Figure 48 shows the extensometer.



Figure 47 - MTS 50 Insight test machine configured for resin tensile-testing

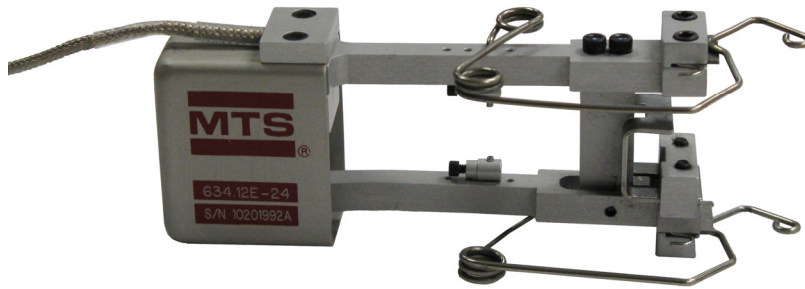


Figure 48 - MTS extensometer used for resin tensile-testing

After allowing the additional promoter-resin mixing time, the measured tensile strength and elongation became closer to that reported by the manufacturer. The modulus remained near the manufacturer’s published value either way. The averaged results are tabulated in Table 10 and each curve for the both resin mixing methods are shown in Figure 49 and Figure 50. The entirety of the data can be found in Appendix A3.

	DERAKANE 411-350 MOMENTUM TENSILE PROPERTIES (MEASURED vs. MANUFACTURER REPORTED)		
	Catalyzed immediately after mixing resin and promoter	Catalyzed 1 hour after mixing resin and promoter	Manufacturer reported typical properties
Tensile Strength	64.9 MPa	76.8	86 MPa
Modulus	3.2 GPa	3.1 GPa	3.2 GPa
Elongation, Yield	2.8%	4.7%	5-6%

Table 10 - Measured tensile properties of Derakane 411-350 Momentum

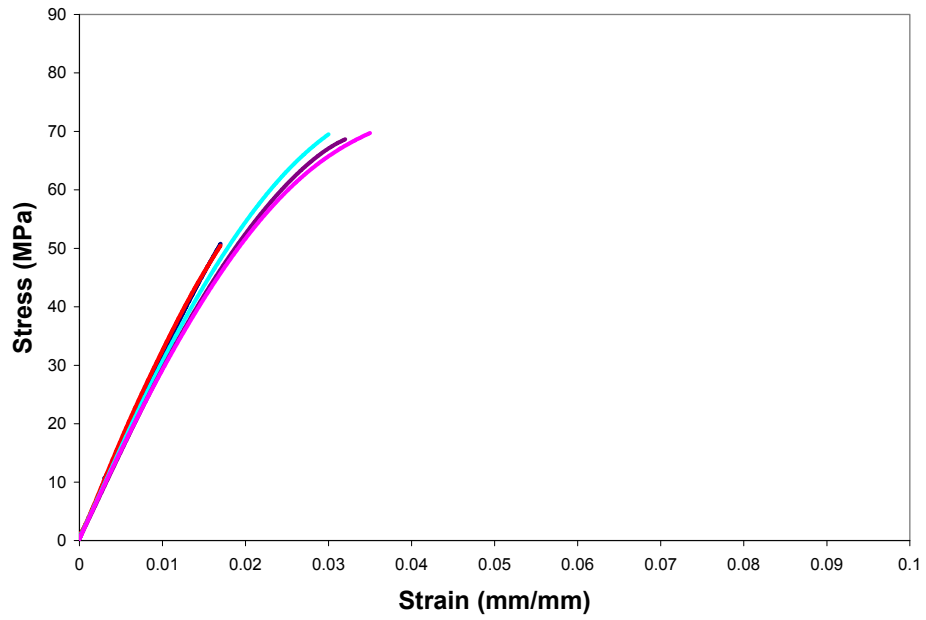


Figure 49 - 411-350 catalyzed immediately after mixing resin and promoter

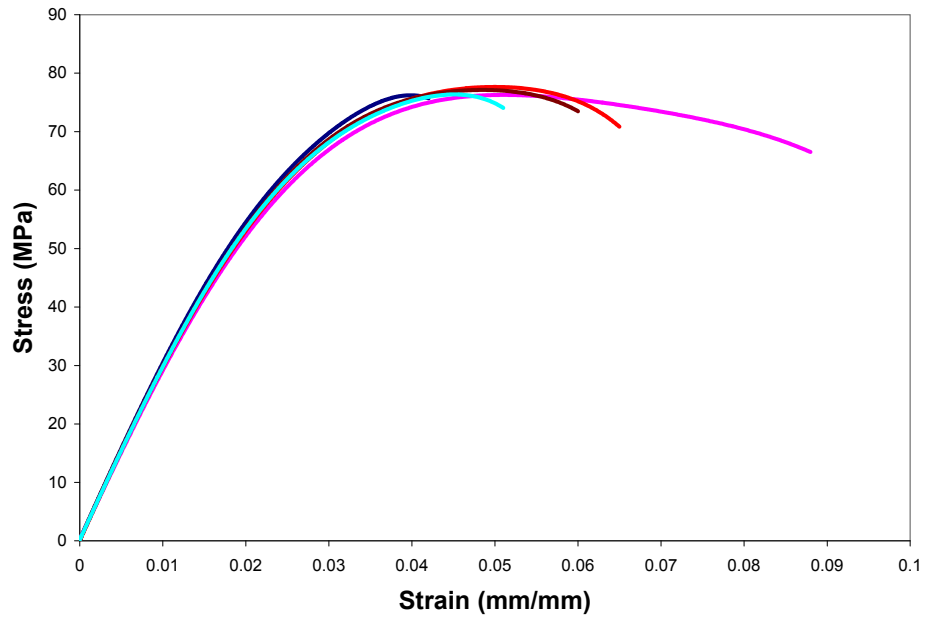


Figure 50 - 411-350 catalyzed one hour after mixing resin and promoter

By viewing Figure 49 and Figure 50, it can be seen that the modulus resulting from both mixing methods is similar, but all of the specimens that were catalyzed immediately after mixing resin and promoter fail before reaching their peak stress or elongation. This indicates that by allowing the resin and promoter to mix thoroughly for one hour, the toughness of the resin is improved. It can actually reach its peak values. It is thus necessary to include the waiting time into the resin preparation and when included, acceptable resin tensile properties are achieved.

As a comparison, two other vinyl ester resin types were also tested: Derakane 8084 by Ashland, Inc. and General Purpose VE-1110 by Fibre Glast Co. The Derakane 8084 is an elastomer-modified resin and the VE-1110 is a pre-promoted vinyl ester (with cobalt naphthenate). Typical curves of the 411-350 Momentum, 1110 and 8084 can be found in Figure 51.

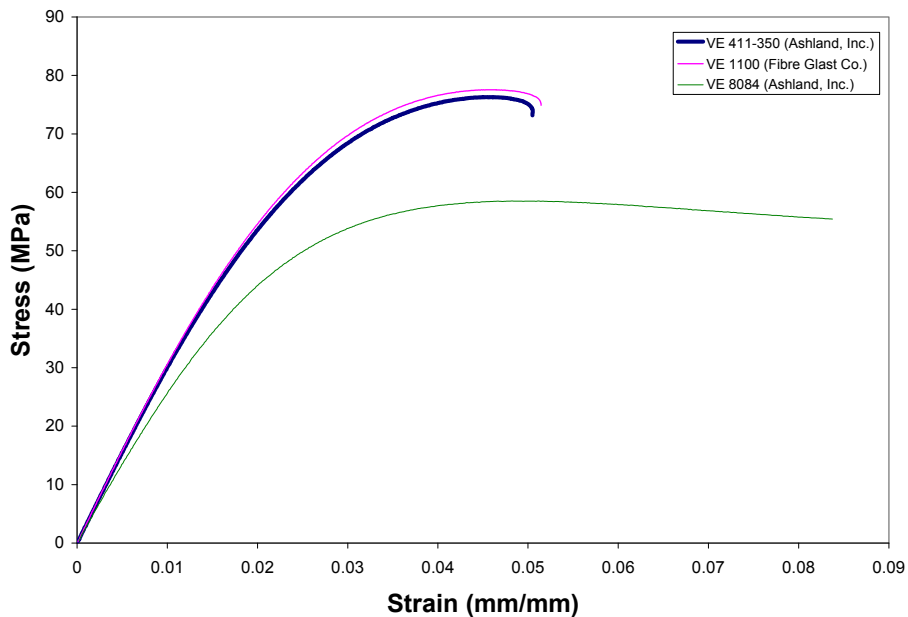


Figure 51 - Vinyl ester type comparison

It can be seen that the 411-350 and the VE-1110 are very similar. In fact, after discussions with Fibre Glast Co., it is suspected that the VE-1110 is also made by Ashland, Inc. (Hetrion 922L), but is sold to Fibre Glast and repackaged. As expected, the elastomer-modified resin (8084) had much more elongation, but less tensile strength.

3.2.5 Fiber Surface Functional Chemistry

Functional groups implanted on the fiber surface through treatment are a very important part of this research, providing insight into the physical results observed, such as bonding, wettability and ultimately, composite strength. Therefore, it is imperative to determine what chemical groups are present and to what extent. The overall amount of surface oxidation can be readily quantified using X-ray photoelectron spectroscopy (XPS), but deciphering which specific oxides comprise the overall total is a much more difficult task. Several methods are available to characterize the oxides on carbon fibers, such as infrared spectroscopy (IR),^{114, 115, 116, 117, 118, 119, 120, 121} temperature-programmed desorption (TPD),^{117, 122, 123, 124, 125} Boehm titrations and XPS,^{117, 126, 127} but only limited quantitative information can be ascertained with these techniques. The IR technique is limited by difficulties in accurately assigning IR bands and the inability to obtain quantitative information on oxide concentrations. TPD data is difficult to interpret because multiple oxides decompose at similar temperatures and produce similar decomposition products, such as carbon monoxide, carbon dioxide and water. Boehm titrations do not provide information on the concentration of different surface oxides. Using XPS, it is theoretically possible to discriminate between different surface oxides, but this method is often plagued with difficulty and requires high-resolution XPS

spectrometers.¹²⁸ Typical XP spectrometers are unable to resolve the individual components associated with different oxides because of the linewidth of the incident X-ray beam, the limited resolution of most electron energy analyzers, and the close proximity of individual peak components. Some oxides are also peak fit into the same component, such as hydroxyl and ether functionalities.¹²⁹ This results in most surface chemistry reports grouping oxides together, providing only an estimate of which functional groups are actually present.

In this research, chemical derivatization is employed in conjunction with XPS to quantify concentrations of hydroxyl, carbonyl and carboxylic acid groups on the treated fiber surfaces. Sized (T700) and unsized (AS4) fiber types, as well as five different treatment times (5, 20, 40, 80 and 160 minutes) of unsized fiber were analyzed. By first applying chemical derivatization, these three functional group types can be tagged with distinct chemicals, which are more easily identified and quantified with XPS. The indicator compounds make use of fluorine atoms (CF₃ groups), which are easily detected because fluorine is absent from native carbon surfaces and has a high XPS detectability.¹²⁸ XPS operates by irradiating a material with a beam of X-rays while simultaneously measuring the kinetic energy and number of electrons that escape from the top 1 to 10 nm of the material being analyzed.¹³⁰ The specific derivatization groups used are trifluoroacetic anhydride (TFAA) for hydroxyl, trifluoroethyl hydrazine (TFH) for carbonyl, and trifluoroethanol (TFE) for carboxylic acid. These compounds have been previously shown to bond with their respective target groups.^{131, 132, 133, 134, 135, 136, 137} The derivatization reactions are shown in Figure 52.

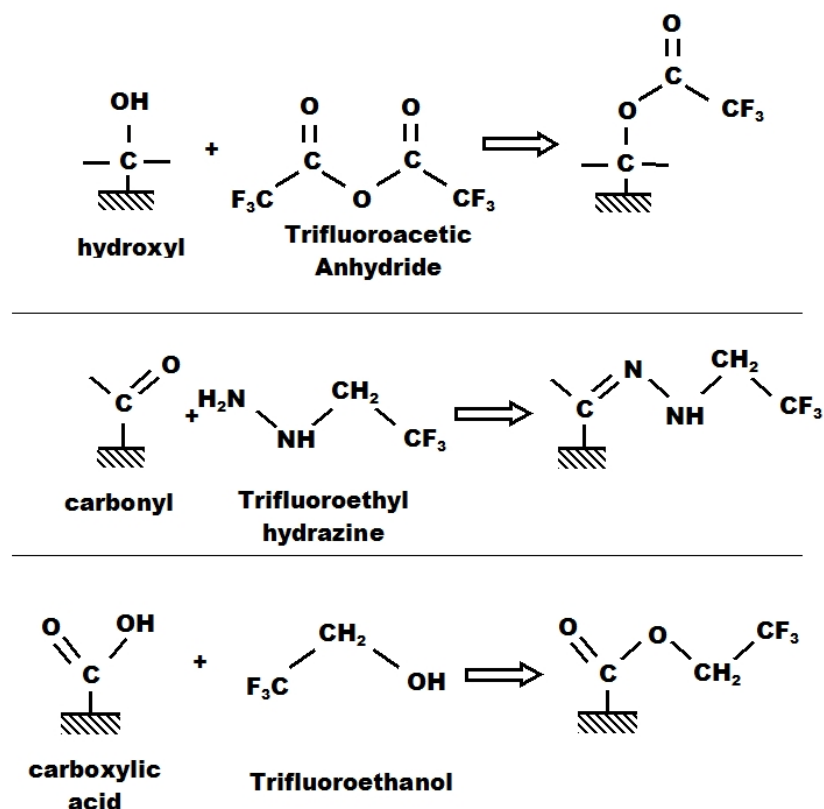


Figure 52 - Chemical derivatization reactions

The Fairbrother group in the Department of Chemistry at Johns Hopkins University conducted the chemical derivatization and XPS work on the differently treated fiber types that were provided to them. The different fiber types were numbered and no information was provided, so that the experiments were conducted in a blind study manner. Vapor-phase chemical derivatization was conducted by first placing the sample and derivatizing agent in a glass reaction vessel, keeping them within two inches of each other. The derivatizing agent was frozen with liquid nitrogen and the pressure of the reaction vessel was reduced to approximately 50 mTorr. The sealed reaction vessel was then allowed to return to room temperature under vacuum, resulting in a vapor phase reaction between the derivatization agent and the fiber samples. Derivatization reactions

were assumed to have reached completion when additional reaction time did result in an increase in the fluorine F(1s) signal measured by XPS. The stability of these fluorine-containing surface groups under X-ray radiation has been assessed by prolonged exposure (2 hours), where it was found that the concentration of fluorine did not change.¹²⁸ Using the derivatization reactions shown in Figure 52, the relationships between the surface oxide concentrations (hydroxyl, carbonyl and carboxyl) and the F(1s) signal acquired by XPS were established. This allows the use of the measured F(1s) signal to calculate the hydroxyl, carbonyl and carboxylic acid concentrations on the derivatized fibers, using equations (8) through (10).

$$\%[O_0]_{C-OH} = \frac{([F][C_0] + [F][O_0])}{(3\varepsilon - 6\varepsilon[F])} \times 100 \quad (8)$$

$$\%[O_0]_{C=O} = \frac{([F][C_0] + [F][O_0])}{(3\varepsilon - 6\varepsilon[F])} \times 100 \quad (9)$$

$$\%[O_0]_{COOH} = \frac{([F][C_0] + [F][O_0])}{(3/2\varepsilon - 5/2\varepsilon[F])} \times 100 \quad (10)$$

Where $\%[O_0]_x$ is the concentration of the surface oxide (hydroxyl, carbonyl or carboxylic acid), $[C_0]$ and $[O_0]$ are the initial concentrations of carbon and oxygen on the fibers before derivatization (as measured by XPS), $[F]$ is the fluorine F(1s) signal measured after derivatization, and ε is the efficiency of the derivatization reaction. It has been previously established that $\varepsilon \approx 1$ for equations (8) through (10) by comparing the predicted and measured values of fluorine on different polymers after derivatization with

these chemicals.¹²⁸ These polymers are well-characterized and known to have specific surface concentration of hydroxyl, carbonyl or carboxylic acid groups.

Before conducting chemical derivatization, the C(1s) and O(1s) regions of the different fiber treatment conditions were captured by XPS (Figure 53). To facilitate comparison between the different treatment times, the areas in the carbon regions were normalized to each other. So that the oxygen signal intensity between different samples could be compared directly, the signal intensity in the oxygen region was scaled to the C(1s) areas for each sample.

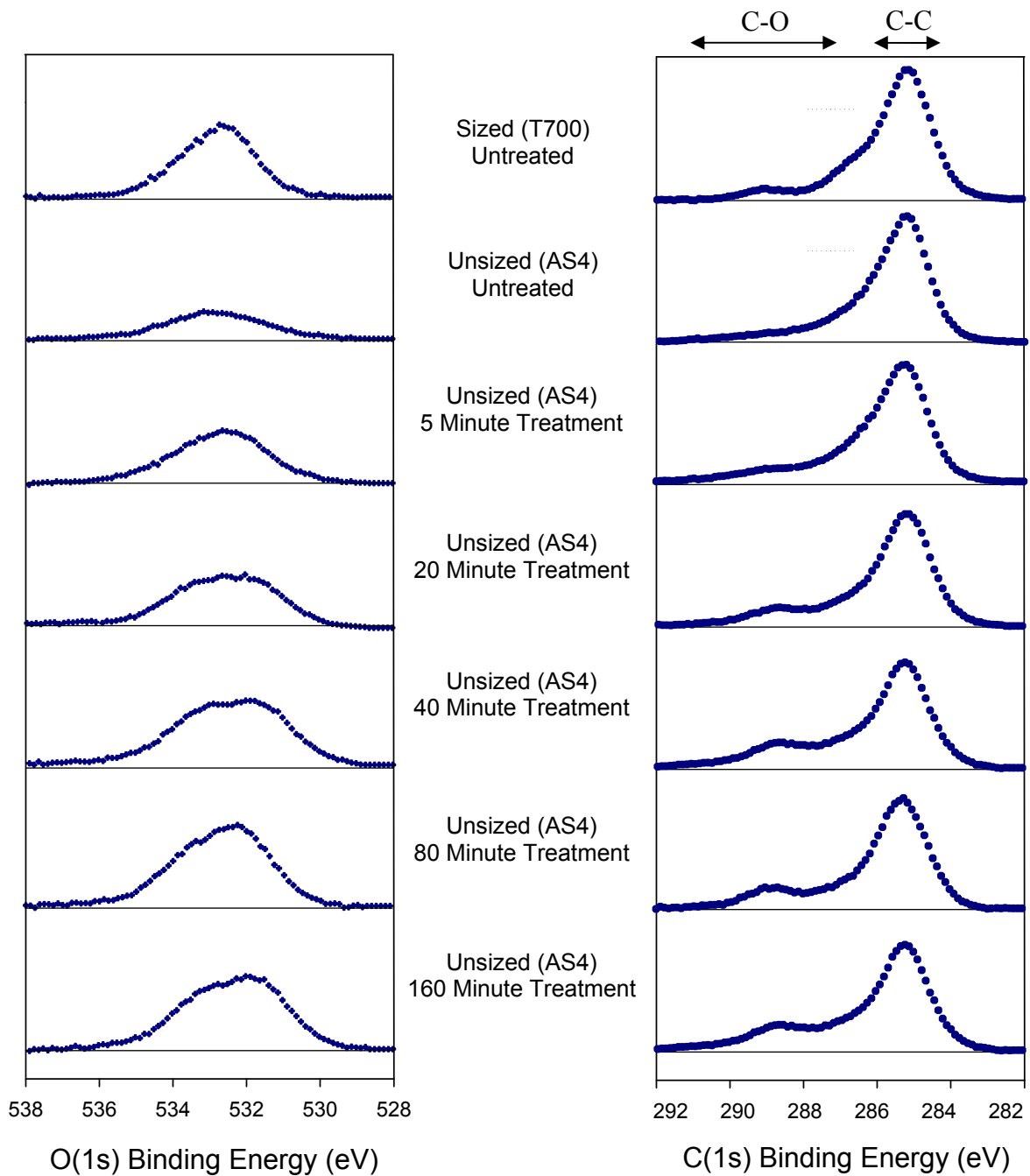


Figure 53 - C(1s) and O(1s) XPS measurements on Sized (T700) fiber and various treatments of unsized (AS4) fiber

Viewing the information provided in Figure 53 indicates that changes occur in both the oxygen and carbon-oxygen signals, but deciphering this information is a difficult

task that usually ends up in estimates of oxidation types that include several different possibilities. Referring to the O(1s) data, it can be identified that the sized (T700) fiber has a significant oxygen concentration in the untreated condition, and that nitric acid treatment contributes to a growing oxygen concentration on the untreated (AS4) fiber with extended treatment. The unsized (AS4) fiber has a relatively low oxidation level in its untreated condition. Examination of the C(1s) region of the XPS data indicates that the sized fiber has a significant amount of C-O type groups in the untreated condition (the hump to the left of the C-C peak). Additionally, the unsized (AS4) fiber shows an appreciable signal in the C-O region that increases with extended treatments.

Obtaining more information from the XPS data of the O(1s) and C(1s) regions is difficult. Because different oxygen-carbon states result in slight shifts of the peaks in the O(1s) and C(1s) regions, peak fitting is usually attempted. However, the different peaks that are sought are often very close together, causing them to be fit into the same peak. Combine this with the limited resolution of most XPS spectrometers, and the results are usually nothing more than educated estimates. By reacting derivatization chemicals with the treated fiber surfaces and then searching for the derivatization chemical fluorine tags, more detail about oxidation surface group types becomes available. Figure 54 shows the results of the chemical derivatization and XPS.

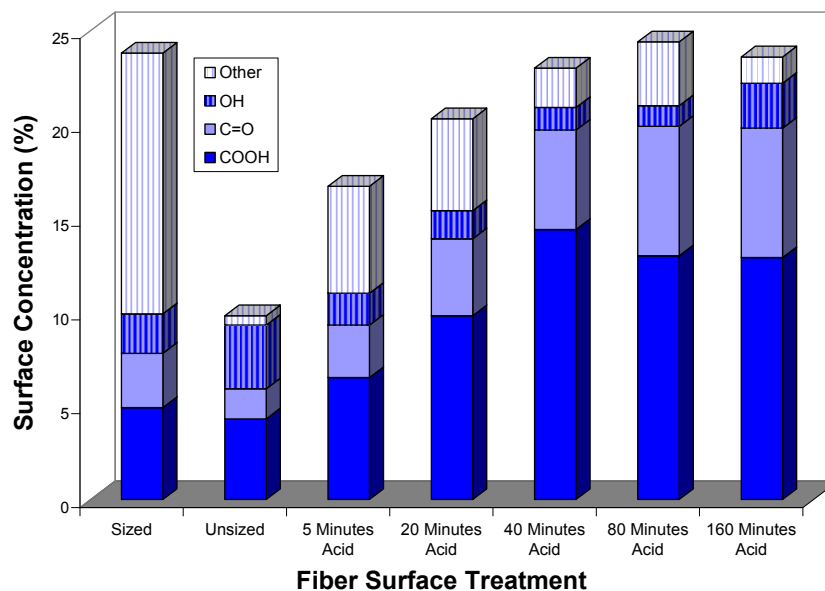


Figure 54 - Surface functional group type distribution from chemical derivatization and XPS (percentage of total surface concentration)

The exact values of the oxygen group percentages are shown in Table 11.

	FIBER SURFACE OXIDATION BY TYPE (%)						
	Sized	Unsized	5 Min Acid	20 Min Acid	40 Min Acid	80 Min Acid	160 Min Acid
OH	2.1	3.4	1.7	1.5	1.2	1.1	2.4
C=O	2.9	1.6	2.8	4.1	5.3	6.9	6.9
COOH	4.9	4.3	6.5	9.8	14.4	13	12.9
OTHER	13.9	0.5	5.7	4.9	2.1	3.4	1.4
TOTAL OXYGEN	23.8	9.8	16.7	20.3	23.0	24.4	23.6

Table 11 - Fiber surface functional oxygen percentages

By combining chemical derivatization with XPS, more information about the fiber surfaces has become clear. The relative concentrations of hydroxyl, carbonyl and

carboxylic groups can be specified. Nitric acid treatment causes a gradual increase in both carboxylic acid (COOH) and carbonyl (C=O) groups up to a point, at which the concentration levels off to a steady value. This indicates a maximum level of these groups that can be implanted with this oxidizing treatment. The carboxylic acid groups increased up to 235% over the untreated value, and carbonyl groups increased up to 331%. While carboxyl and carbonyl surface types increased with treatment, hydroxyl groups did not. The only fiber type that possessed a significant proportion of hydroxyl groups was the untreated, unsized (AS4) fiber. Nitric acid treatment caused a reduction in hydroxyl concentration when compared with the untreated fiber. The untreated, sized (T700) fiber is similar to the untreated, unsized (AS4) fiber with respect to the three groups tested, but is very different in the overall amount of surface oxidation. The majority of the sized fiber falls into the “other” types of surface oxidation, and is not well characterized by this method. It can only be concluded that the majority of the surface oxidation on the sized fiber is not hydroxyl, carbonyl or carboxyl. This is not a surprise, as the sized fiber is likely coated with a polymeric material and should be very different from the unsized and treated fibers. The untreated, unsized (AS4) fiber is very well characterized by this method, leaving very little to the “other” oxidation types. Its surface composition consists almost entirely of hydroxyl, carbonyl and carboxylic species. Nitric acid treatment introduces more unidentified surface oxidation with initial treatment, but that amount is reduced with extended treatments. The “other” category has several possibilities. It is believed that it may contain pyrones, lactones, anhydrides, esters and ethers.^{90, 114, 116, 117, 126, 138, 139} And in this case, where nitric acid is used as the oxidizing media, nitrates are also possible. However, the level of nitrogen identified via

XPS did not increase with lengthening treatment times. Nitrogen was found on the surfaces of both untreated and treated fibers, as shown in Figure 55. Therefore, the amount of nitrates created on the fiber surfaces with treatment is considered minimal.

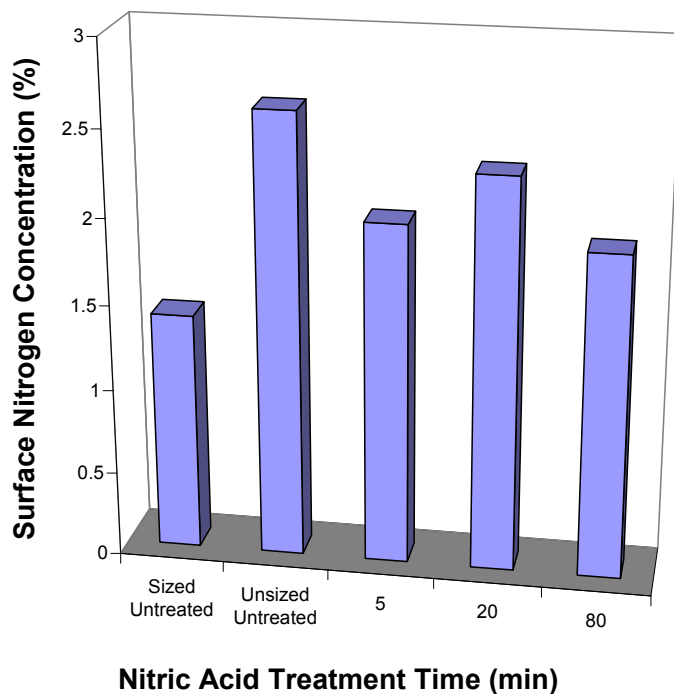


Figure 55 - Nitrogen percentage of total surface concentration from XPS

Overall, the most important information provided by chemical derivitization and XPS was that the surface concentration of both carboxylic and carbonyl groups increased significantly with nitric acid treatment time, and then reached a maximum level. Additionally, hydroxyl groups did not increase at all with treatment, and seemed to actually decrease. The sized fiber was confirmed to be very different than the unsize and treated fibers, and is poorly characterized with this method. The unsize and treated fibers, however, were well characterized by using chemical derivitization in conjunction with XPS.

3.2.6 Fiber-fiber Interaction

After modification of the fiber surface chemistry, interaction between adjacent fibers should be considered. The surface functional groups on one fiber may react with those on another fiber, as well as with the matrix resin. In order to evaluate this effect, fiber cohesion was evaluated by measuring the irreversible work required to separate a 25 mm (1 in.) long bundle of fiber along its length. This was quantified by calculating the area under the force-displacement curve. These tests were accomplished by gluing a tab on the end of the bundle, separating the tab into two halves with a razor-blade and pulling it apart, using a 2N load cell on a MTS Insight 1kN electromechanical test machine at 5 mm/min. Sized (T700) and unsized (AS4) fiber bundles, as well as six different nitric acid treatment times (10, 20, 40, 80, 120 and 160 minutes) of unsized fiber were analyzed. Additionally, unsized and acid-treated fiber bundles (2.5, 20 and 40 minutes) were subsequently treated with silane and subjected to the same cohesion tests. At least 5 samples of each were tested. Figure 56 describes this test and Figure 57 shows a photograph of this test in progress. The paper seen in the photograph was used to prevent any unglued fiber in the center of the bundle from pulling away from the gripping tabs.

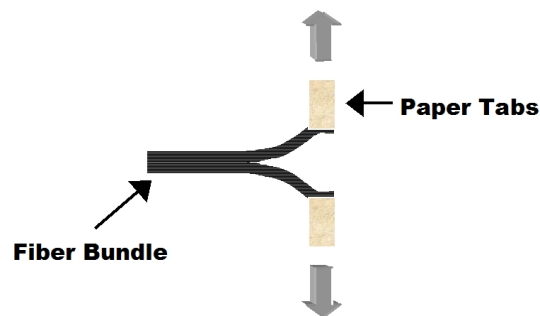


Figure 56 – Fiber cohesion test depiction

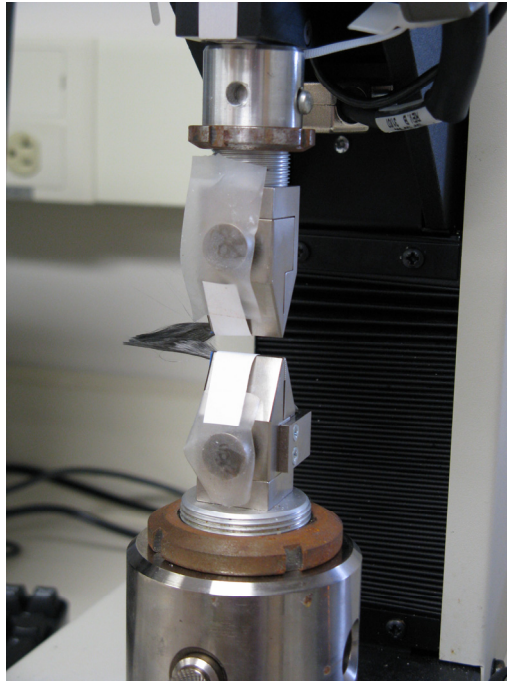


Figure 57 – In-progress fiber cohesion test

Because fiber entanglement could also contribute resistance to bundle separation, a set of tests was also conducted on an unsized (AS4) bundle that had been treated for 10 and 160 minutes in boiling distilled water. This provided a way to evaluate the contribution of increased entanglement alone (due to boiling), because water was not expected to alter the fiber surface chemistry of the unsized fiber, as the nitric acid does. To be consistent, the water-boiled fiber was subjected to the same procedure as the acid-treated fibers. It was washed for two hours in distilled water, dried for two hours at 120° C, treated in boiling water, and then dried again for two hours at 120° C. Five samples were tested. Figure 58 shows the results of the untreated and acid-treated fibers. Figure 59 shows the results of the distilled water boil. To arrive at a final value for the work of separation, the test was continued for at least 5 mm after complete bundle separation and the level recorded was used as the baseline. It was necessary to subtract the baseline

because the weight of the upper half of the bundle produced a significant non-zero bias into the force-distance curve.

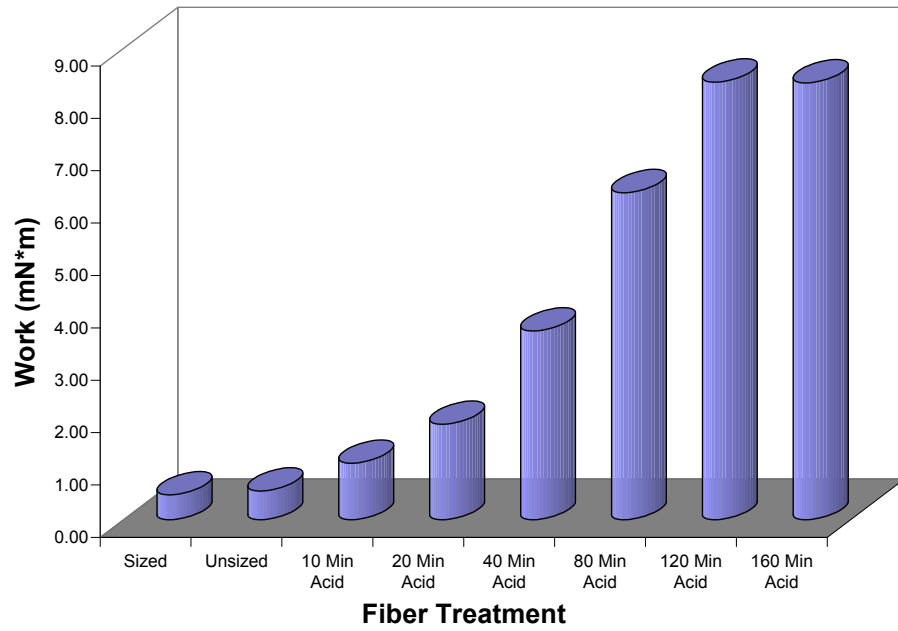


Figure 58 - Work of separation required for acid-treated fiber bundles

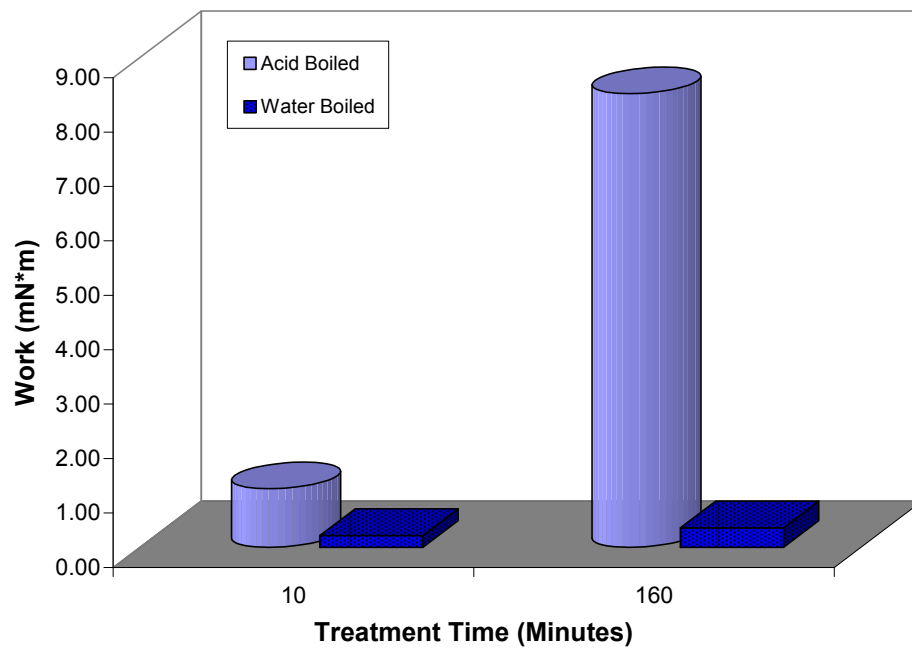


Figure 59 - Work of separation (acid-treated vs. water-treated)

Figure 58 illustrates a significant effect of fiber cohesion that increases with treatment time. When the abscissa (x-axis) is made to be linear, it shows that the increase in work is a linear function of acid treatment time, until 120 minutes of treatment is reached, at which time it appears to plateau. This can be seen in Figure 60.

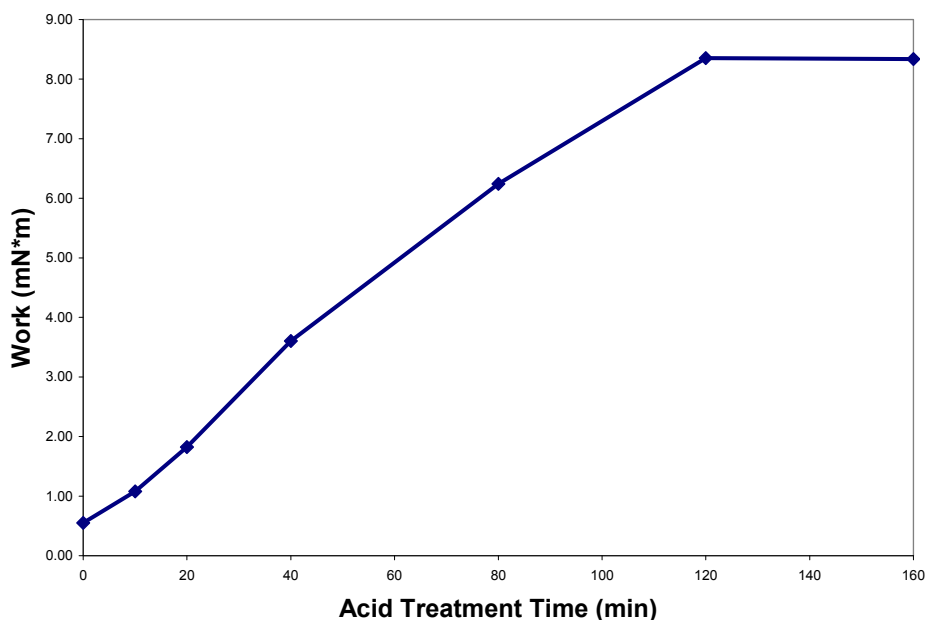


Figure 60 - Work of separation plotted against a linear time scale

This plateau may indicate a maximum level of oxidation that is reached. In fact, as determined by XPS and chemical derivatization herein, the levels of carbonyl and carboxylic groups were also observed to reach a stable value after extended treatment, although their stabilization occurred at an earlier treatment time. It is postulated that the fiber-fiber cohesion is a result of hydrogen bonding between functional groups on adjacent fibers, and as the functional group concentration is increased (carboxyl and carbonyl), so does the fiber-fiber cohesion. A similar example where spontaneous fiber-fiber hydrogen bonding is believed to occur can be found in paper, where this effect is believed to contribute a significant amount of strength.¹⁴⁰ As will be discussed in the

following sections, single fiber surface wettability is shown to improve, while fiber bundle wettability in resin is shown to decline with fiber acid treatment. This observed cohesion goes a long way towards explaining this, as the attraction between the fibers prevents the infusion of resin during composite formation.

Figure 59 shows that very little of the observed fiber bundle cohesion can be attributed to entanglement during boiling. The water-boiled bundles required much less work to separate than the equivalently acid-boiled bundles of 10 and 160 minutes.

In addition to the measurement of the work of separation, evidence of fiber cohesion can be seen in SEM views of the acid treated fiber bundles.

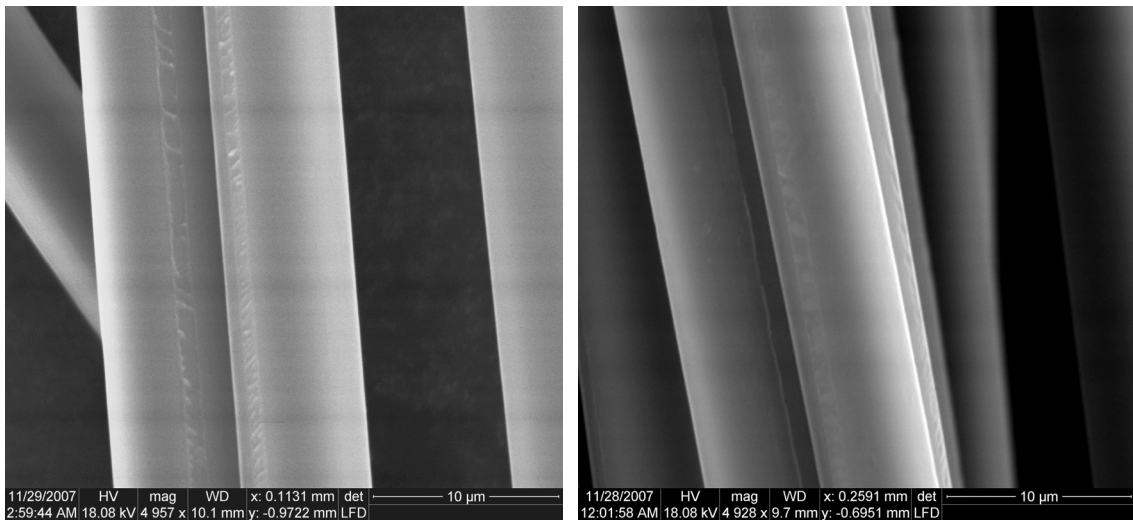


Figure 61 - Fiber cohesion markings on acid treated fibers: (a) 120-minute treated unsized fiber, and (b) 160-minute treated sized fiber

Viewing the fibers in Figure 61 reveals markings that show where the fibers had been cohering together. Both examples show fibers with longitudinal markings that match similar markings on the adjacent fibers. It appears that the fibers were pulled apart

during preparation for viewing in the SEM and markings were left in the areas of cohesion.

In addition to measuring the bundle cohesion of acid-only treated fibers, the bundle cohesion was measured for bundles that were treated with silane after nitric acid treatment. Silane was applied after 0, 2.5, 20 and 40 minute acid treatments on unsized fiber. Figure 62 shows the acid/silane treated fibers, alongside the acid-only treated fibers.

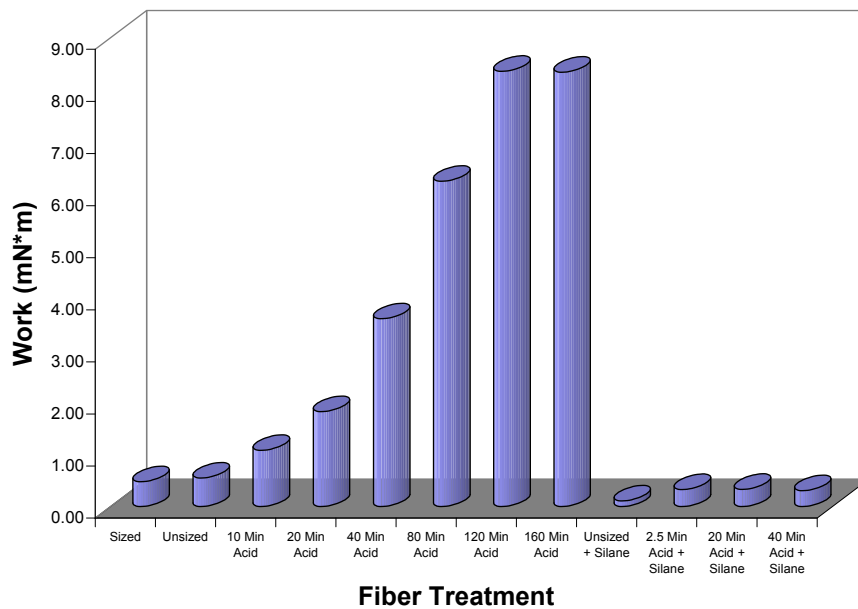


Figure 62 - Work of separation for acid treated and acid/silane treated fiber bundles

As can be seen in Figure 62, the application of silane to acid-treated fibers dramatically reduced the fiber bundle cohesion, providing evidence that the silane affected the surface of the acid-treated fibers. Moreover, the fiber cohesion remained constant for the acid/silane treated fibers, even though they had different levels of acid treatment (2.5, 20 and 40 minutes). The unsized, untreated fiber that was treated with

silane showed a reduced amount of cohesion, both over the untreated unsized fiber and the acid/silane treated fibers. This suggests that some degree of silane actually bonded to the bare unsized fiber. This is likely a result of the proprietary surface treatment that the manufacturer applies to the unsized fibers. As shown in the XPS fiber surface chemistry section herein, the unsized fiber does contain a limited amount of surface oxidation, although less than the nitric acid-treated fibers.

Overall, an increasing nitric acid oxidation time resulted in increasing fiber bundle cohesion up to 120 minutes, where the work of bundle separation stabilized. The addition of silane dramatically reduced the work of separation to untreated levels, which remained constant, regardless of acid treatment time before silane treatment.

This fiber cohesion test is not a standardized test and was created as a way to quantify the cohesion observed with the treated carbon fibers. Hence, this test deserves some explanation. The closest test method found to quantifying this type of phenomenon was ASTM D 2612 (Standard Test Method for Fiber Cohesion in Sliver and Top in Static Tests). At first, the title of this standard sounds very promising, but it is not applicable and cannot be used to test fiber cohesion in long, continuous fibers, such as carbon fibers. ASTM D 2612 arises from the textile industry and is used to measure the cohesion between non-continuous, irregular fibers, such as cotton and wool. In this test, a sliver of fibers is taped on the ends pulled apart, resulting in some fiber breakage, but mostly longitudinal slippage among adjacent fibers. See Figure 63.

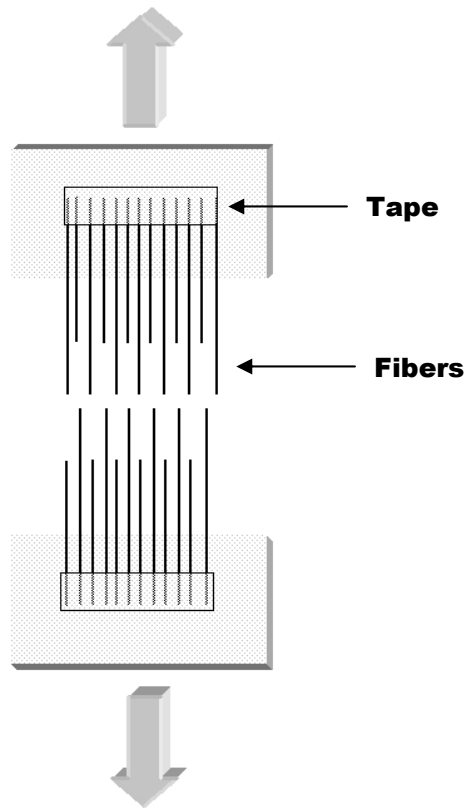


Figure 63 – Textile fiber cohesion test from ASTM D 2612

This test is not applicable to continuous fibers, such as carbon because the fibers cannot pull apart in the center of the test sample. They will just pull free at the ends, resulting in measurement of the resistance between the fibers and tape, the fibers and grips, or between fibers that are compressed together within the tape and grip area. If the ends are gripped tight enough, some fibers may break, and the fiber tensile strength is so strong that if an appropriate load cell was used, it would not be sensitive enough to measure the cohesive forces.

In ASTM D 2612, an equation is presented to standardize the results obtained for fiber cohesion:

$$DT = \frac{F \cdot L}{1000 \cdot M} \quad (11)$$

where, DT = drafting tenacity (mgf/tex), F = cohesive force (gf), L = specimen length (mm), and M = specimen mass (g).

This equation is nothing more than a way to combine the maximum force obtained with the linear density of the specimen. This is important with textiles, because linear density can vary significantly. This is not true with carbon fibers. They are relatively uniform and the bundle density does not vary significantly with length.

It was decided that the best way to quantify the treated carbon fiber cohesion was to measure the work required to separate the bundles laterally. No method could be envisioned to separate the bundles longitudinally, similar to that of ASTM D2612. The method was designed so that no fiber was gripped by both grips, meaning that no tensile breakage would occur. The complication of this method arises when one considers the angle of fiber separation. It varies from a minimum to a maximum. See Figure 64.

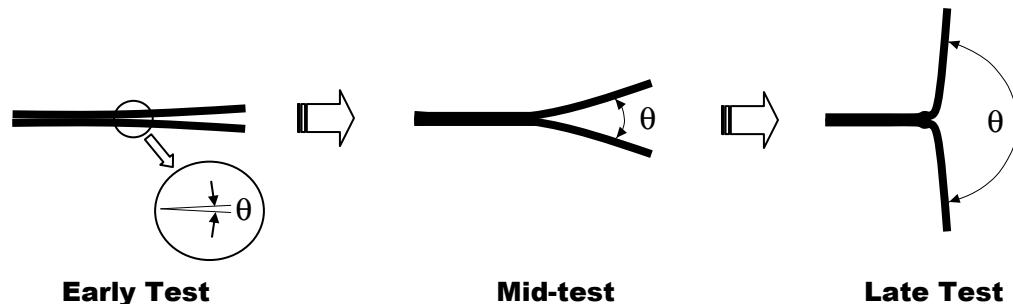


Figure 64 - Separation angle during fiber cohesion test

When the fiber separation initiates, the angle between the fibers is very small, but as the ends are separated, the angle continues to grow, until it reaches a maximum value. The question becomes, “What angle should be used?” Should a measurement only be taken after the angle has stabilized (large angle), or should a range of angles be used? It was chosen to measure the cohesion through the full range of angles and end the test

shortly after the angle reached its maximum. A 25.4 mm (1inch) fiber specimen served this purpose. This choice was made because it represented the entire spectrum of cohesion at different angles, instead of one scenario at the maximum angle. As a result, the force-displacement profile exhibited a slowly increasing force up to the point where the bundle reached its maximum separation angle. This was followed shortly by a decreasing force as the bundle end was reached and fibers came loose from each other. Figure 65 shows a typical fiber bundle force-displacement curve. The fiber cohesion data can be found in Appendix A4.

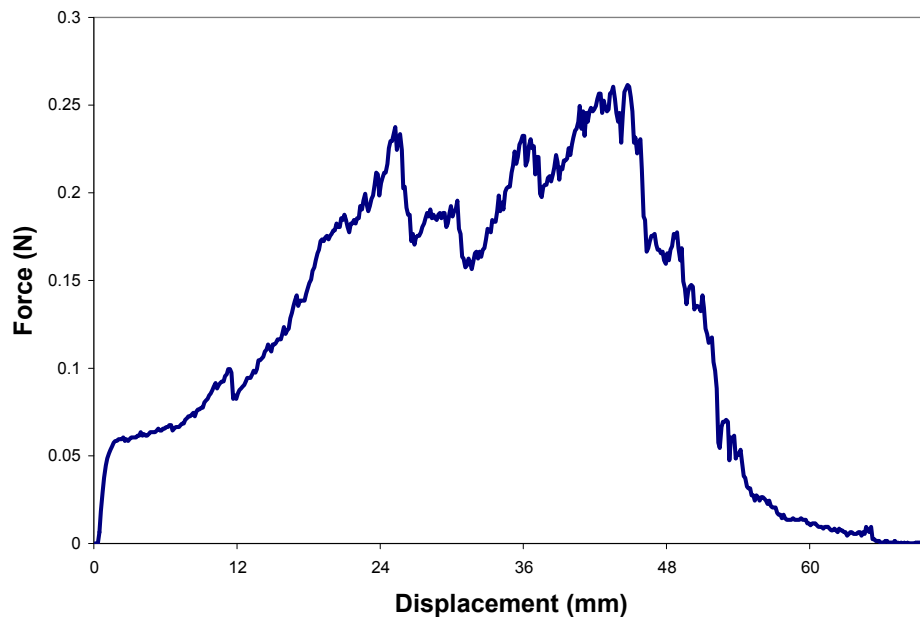


Figure 65 - Typical fiber bundle force-displacement curve

3.2.7 Fiber Surface Wettability

In order to form a robust adhesive bond between a fiber and matrix, the resin must easily wet the surface of the fiber. Without successful wetting, voids can exist at the interface and the composite will suffer. It is possible to develop an understanding of the engineering variables of adhesion and wettability through knowledge of the chemistry variables of liquid surface tension and solid surface energy. “Adhesion” describes the attraction that molecules of one material have towards those of another material. “Cohesion” describes the attraction molecules of a material feel towards other molecules of the same material. The surface tension of a liquid is a result of its cohesion. The similar term for solid materials is referred to as “surface energy”. Surface tension and surface energy result from imbalanced forces between molecules on the surface. In both liquids and solids, molecules within the interior of the material experience equal attractive forces in all directions. However, the forces affecting the surface molecules are imbalanced. Figure 66 describes how imbalanced forces cause surface tension in liquids.

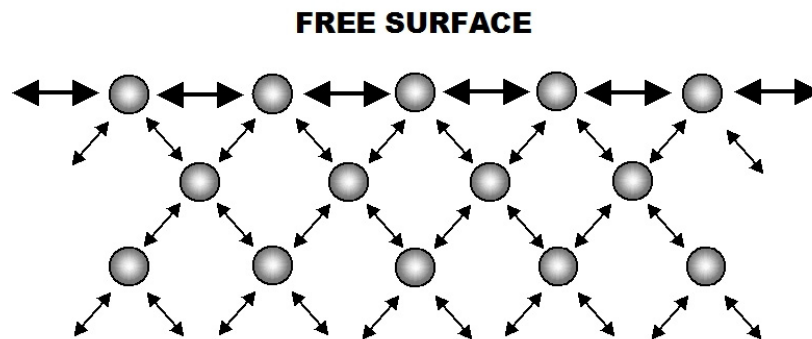


Figure 66 - Surface tension and surface energy

The surface tension of liquids is measurable by passing probes through the surface and recording the resulting changes in force. The surface energy of solids, however, cannot be directly measured. Therefore it is necessary to calculate solid surface energy

by relating the interactions of solids and liquids of known surface tension. A method that is commonly used to accomplish this involves applying a drop of liquid to a surface and measuring the angle of contact between the solid, liquid and vapor interface. This is a simple method and provides a good representation of the fundamental idea behind this approach. Figure 67 shows a liquid drop on a solid surface and identifies the contact angle.

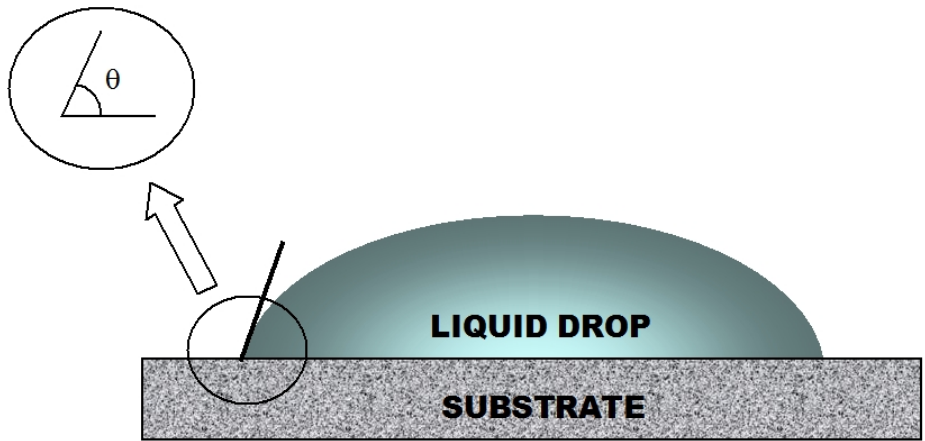


Figure 67 – Contact angle of a liquid drop on a solid surface

At equilibrium, the force balance on the liquid drop at the liquid-vapor-solid three-phase intersection can be represented by Young's equation:^{141, 142}

$$\gamma_{LV} \cos \theta = \gamma_{SV} - \gamma_{SL} \quad (12)$$

Where γ_{LV} , γ_{SV} and γ_{SL} are the surface tensions at the liquid-vapor, solid-vapor and solid-liquid interfaces and θ is the contact angle.^{141, 142} An appropriate liquid must be chosen for this method so that it doesn't completely wet out the surface, making it impossible to measure a contact angle. The quantity desired in determining a solid

material's surface energy is the solid-vapor surface tension. The liquid-vapor surface tension and the contact angle can be measured, but the solid-vapor and solid-liquid surface tension cannot. Therefore, it is only possible to calculate the magnitude of difference on the right-hand side of Young's equation.¹⁴¹ To determine the specific values, another equation is needed. In 1869, Dupre provided an equation for the work of adhesion between a liquid and solid:^{40, 141, 142}

$$W_a = \gamma_{SV} + \gamma_{LV} - \gamma_{SL} \quad (13)$$

Where W_a identifies the reversible work of adhesion. The work of adhesion is the decrease in Gibbs free energy per unit area when an interface is formed from two individual surfaces. The greater the work of adhesion, the greater the interfacial attraction.⁷⁶ Combining this equation with Young's equation (equation (12)) produces the Young-Dupre equation:^{76, 90}

$$W_a = \gamma_{LV}(1 + \cos \theta) \quad (14)$$

The Young-Dupre equation provides the adhesion work in terms of the measurable liquid-vapor surface tension and contact angle parameters. When the liquid wets the solid completely ($\theta = 0^\circ$), the work reaches the highest possible value, which is equal to twice the value of the liquid-vapor surface tension, γ_{LV} . And if it were possible that no attraction between the liquid and solid occurred ($\theta = 180^\circ$), the work, W_a , would

be equal to zero. The lower the contact angle (and higher the work of adhesion) between the solid and liquid indicates that better wetting of the solid can be expected.

The surface energies of solids and liquids are comprised of dispersive (London-d) and polar (Keesom-p) contributions. Therefore, the surface energies can be split as follows:¹⁴³

$$\gamma_{LV} = \gamma_{LV}^d + \gamma_{LV}^p = a_L^2 + b_L^2 \quad (15)$$

$$\gamma_{SV} = \gamma_{SV}^d + \gamma_{SV}^p = a_S^2 + b_S^2 \quad (16)$$

Where a_L and b_L are the square roots of the respective dispersive and polar constituents of the liquid-vapor surface energy, and a_S and b_S are the square roots of the respective dispersive and polar constituents of the solid-vapor surface energy. Relating the Young-Dupree equation and equations (15) and (16), the work of adhesion can be expressed as:¹⁴³

$$W_a = 2(a_L a_S + b_L b_S) \quad (17)$$

Which can be rearranged to give:

$$\frac{W_a}{2a_L} = a_S + b_S \left(\frac{b_L}{a_L} \right) \quad (18)$$

By using at least two different liquids, a plot of $(W_a/2a_L)$ versus (b_L/a_L) will give a straight line, with its slope and intercept defining the values of b_S and a_S , respectively, for the solid of interest.¹⁴³ Thus, the dispersive and polar components of surface energy, γ_{SV}^d and γ_{SV}^p , can be determined by squaring a_S and b_S , respectively.

While the classical droplet method provides an intuitive, visual indication of wetting and surface energy through the observed contact angle, it is not feasible to apply it to single fibers with diameters as small as carbon fibers (approximately 7 micrometers). Another method is available for this special case that allows the interpretation of the fiber surface energy, using the same equations used for the sessile drop method. Instead of measuring the contact angle by optical inspection of a droplet on a flat, solid surface, the force experienced when inserting and extracting a fiber from a liquid is measured and the contact angle is calculated. Once the contact angle is calculated, the same equations apply that were described above. Because the fiber is moving, the force measurement is a dynamic process, which is averaged over the entire length of fiber penetration. Also, because the fiber is dry upon insertion and wet upon extraction, the measured forces will differ. The contact angle calculated from the insertion forces is known as the *advancing* contact angle and the analogous angle determined during extraction is deemed the *receding* contact angle. An electrobalance tensiometer is used to measure the forces. The technique is known as the Wilhelmy plate technique because it utilizes the same methodology as the Wilhelmy plate method of determining liquid surface tension, which consists of dipping a flat plate into a liquid and measuring the forces. The Wilhelmy plate technique of measuring fiber-liquid contact forces is depicted in Figure 68.

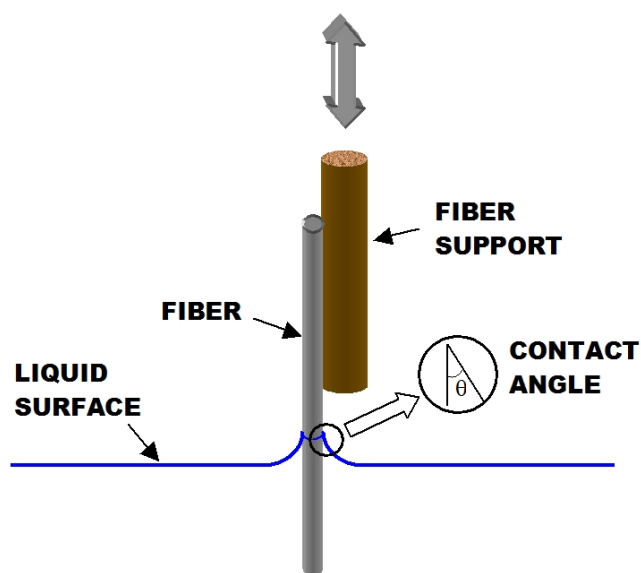


Figure 68 – Fiber contact angle measurement through tensiometry

Using the Wilhelmy plate technique, the contact force, M (micrograms), between a single fiber of circumference C and a liquid of surface tension γ_{LV} is described by the following equation:¹⁴³

$$M = \frac{C\gamma_{LV} \cos \theta}{g} \quad (19)$$

Where θ represents the *advancing* liquid/solid contact angle and $g = 980.6$ dyn/gm. This equation is useful in determining the solid-liquid contact angle. In order to use this equation, the advancing contact force, circumference of the fiber and the surface tension of the liquid must be known. In this research the contact force was measured using a CAHN DCA-322 Dynamic Contact Angle Analyzer with WinDCA32 software. Five to ten separate fibers were analyzed for each fiber tested and each fluid used. The CAHN DCA-322 electrobalance has a sensitivity of ± 0.1 μgm . The fiber circumference was determined by measuring the diameter of each fiber before tensiometry analysis. The

diameter was measured using a Mitutoyo LSM-6200 Laser Scan Micrometer, averaging 2 to 3 measurements along the immersion length of each fiber. The tensiometer and laser scan micrometer are shown in Figure 69 and Figure 70, respectively.



Figure 69 - Cahn DCA-322 dynamic contact angle analyzer



Figure 70 - Mitutoyo LSM-6200 Laser Scan Micrometer

Two fluids were used in the analysis: water and diiodomethane. These two particular fluids were chosen because they represent a broad range in polarity, which leads to a

comfortable separation between the reactions of the fluids and the solid surface. Kaelble et al. determined that the surface tension properties of these two fluids are as follows:

SURFACE TENSION PROPERTIES OF TENSIOMETRY TEST LIQUIDS AT 20° C		
	WATER	DIIDOMETHANE
γ_{LV}^p (dyn/cm)	51.0	2.3
γ_{LV}^d (dyn/cm)	21.8	48.5
γ_{LV} (dyn/cm)	72.8	50.8

Table 12 - Surface tension properties of water and diiodomethane

Using the above surface tension properties, along with equations (12) through (19), the contact angles and surface energies of the fibers can be calculated. Figure 71 through Figure 73 provide the advancing and receding contact angles, as well as the surface energies calculated. The contact angles are provided for both fluids, and the surface energy is shown as polar, dispersive and total energy.

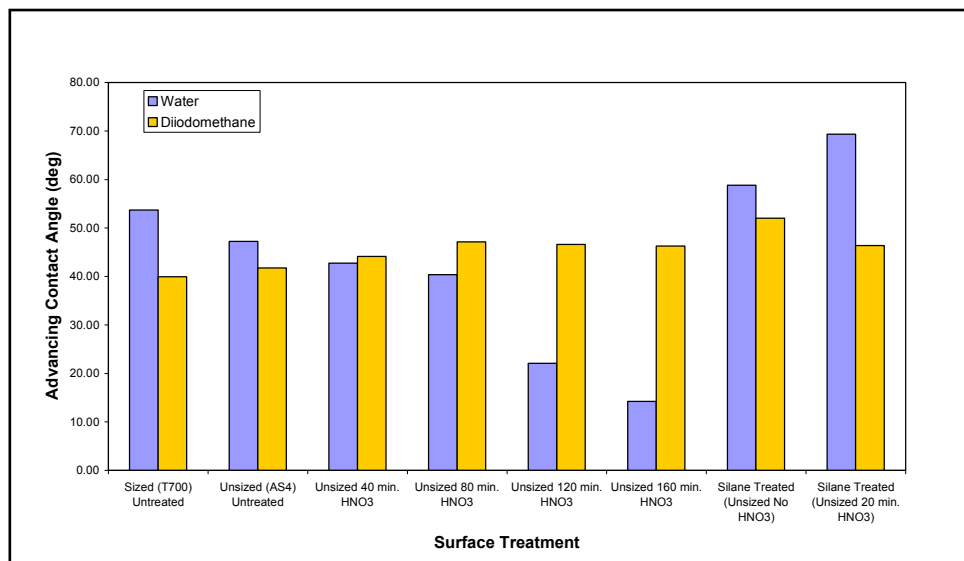


Figure 71 - Advancing contact angles with water and diiodomethane

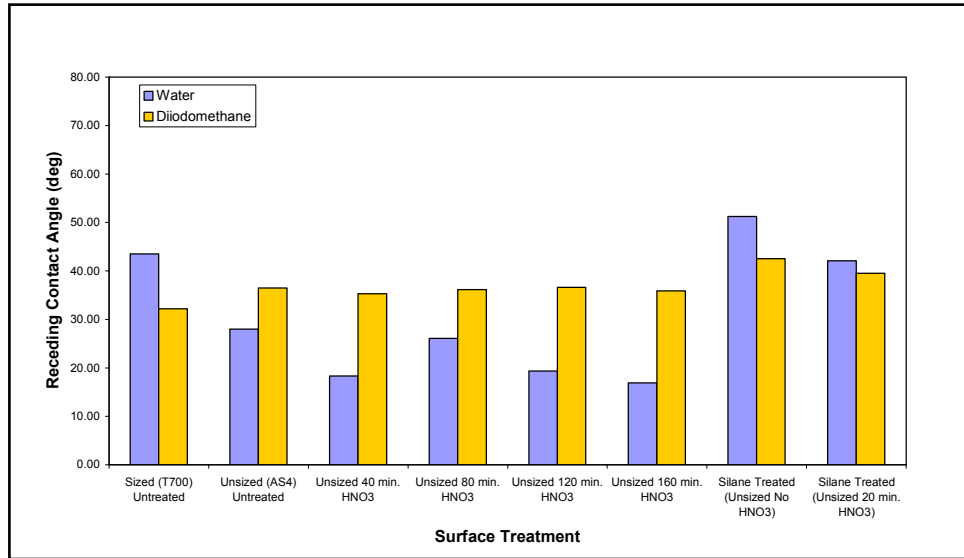


Figure 72 - Receding contact angles with water and diiodomethane

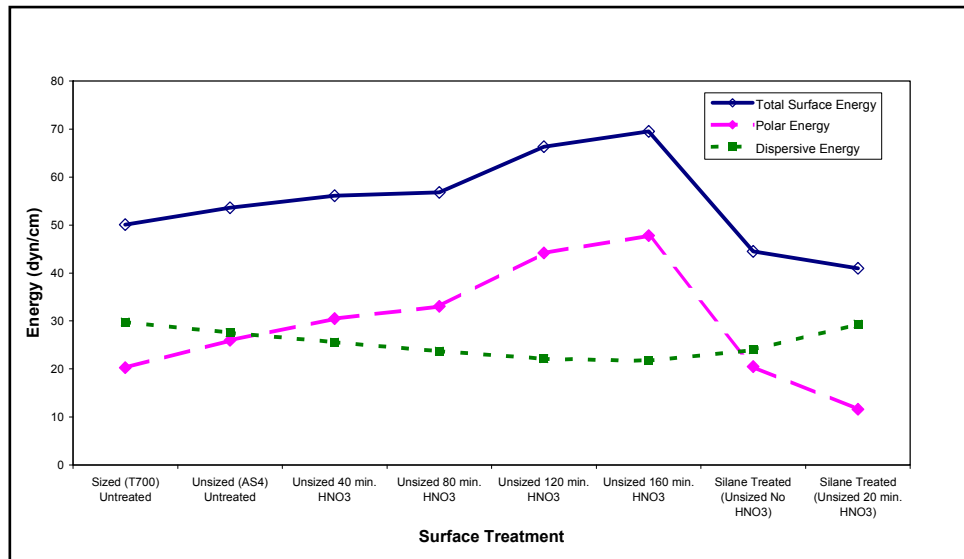


Figure 73 - Total, polar, and dispersive fiber surface energies

The entirety of the data can be found in Appendix A5.

Review of Figure 71 through Figure 73 elucidates several trends. When using water as the test media, an increase in nitric acid treatment time results in a reducing

advancing contact angle. This is indicative of increased wettability with treatment time. When considering the fiber types that have been treated with silane (with and without previous nitric acid treatment), a sudden increase in advancing contact angle is observed, corresponding to decreased wettability. Silane treatment has been reported to have no effect on carbon fibers,^{105, 106} but Figure 73 makes it clear that the silane treatment has changed the wettability of the fibers. Water is very polar, but the other test media used (diiodomethane) is not. Testing with diiodomethane resulted in only minor changes in advancing contact angle over any of the samples. Nitric acid treatment resulted in a slight increase in advancing contact angle with diiodomethane, up to 80 minutes treatment time, when it stabilized. The silane-treated fibers showed similar advancing contact angles with diiodomethane as the nitric acid-treated fibers. The receding contact angle data showed similar trends as the advancing contact angle data, as expected.

To focus on a surface energy standpoint, we turn to Figure 73. From Figure 73, it can be seen that the polar component of fiber surface energy, γ_{sv}^p , increases steadily with nitric acid treatment, but drops considerably with silane treatment. The slope of the acid-treated fiber types increases linearly with acid treatment time. The carbon fiber that had not been acid treated, but had been silane treated showed a similar polarity to the untreated fiber, but the fiber that had been treated in acid before silane treatment showed a reduced polarity, much less than any of the fiber types, including the untreated fiber. It appears that the silane was able to bond to the surface chemical groups present on the fiber, and longer acid treatment resulted in more functional groups, resulting in more silane bonding, as evidenced by lower polarity.

The dispersive energy, γ_{sv}^d , showed the opposite trend of the polar energy. It decreased linearly with nitric acid treatment and increased with silane treatment.

The total fiber surface energy is just the summation of the polar and dispersive components and in this case is largely dominated by the polar component. Like the polar component, the total fiber surface energy increased with nitric acid treatment and fell with silane treatment. The nitric acid treatment results were in accordance with results reported elsewhere.^{74, 76} Increased acid treatment results in increased surface oxidation, which, in theory, should result in increased fiber wettability. The total energy of the silane treated fiber (no acid treatment) was less than the untreated fiber and the energy of the silane treated fiber (previous acid treatment) was less than that. It is clear that preceding silane treatment with nitric acid treatment resulted in increased bonding of silane to the surface, but what about the untreated fiber that showed decreased surface energy with silane treatment? The answer to this lies in the surface condition of the “untreated” fiber. While the fiber was untreated in this research and unsized by the manufacturer, it had still undergone a proprietary surface treatment by the manufacturer. As can be reviewed in the XPS analysis herein, the untreated fiber has a small amount of surface oxidation. This preexisting surface oxidation probably serves to allow a certain amount of silane bonding, but further surface oxidation with nitric acid resulted in more.

3.2.8 Fiber Bundle Wettability

Single-fiber analysis with non-resin fluids may indicate increased polarity and wettability for oxidizing surface treatments, but it does not necessarily follow that a bundle of fibers will show the same increased wettability in resin. Single-fiber

wettability analysis is usually the method of choice when predicting how a given fiber surface treatment will improve or decrease fiber wetting in a composite,⁷⁶ but there are additional variables that affect a composite material that may drastically affect the perceived wettability. Fiber-fiber interaction is ignored, as well as the significant viscosity of most resins. Resin viscosity may hinder its ability to pervade small spaces in between fibers, especially if there is significant attraction between neighboring fibers. Fluids are typically chosen for their polarity in single-fiber wettability tests and usually, they are low viscosity. Water is commonly used.

Thus, to extend the single-fiber wettability results to a composite material, multiple fibers and resin were used. A single fiber bundle (treated or untreated) was immersed in catalyzed resin and allowed to cure. After post-curing, the single-bundle composite was then cross-sectioned, polished and viewed in a SEM to evaluate the degree of wetting that occurred before matrix hardening. If complete wetting did not occur, an area of unwetted fiber was found in the interior of the bundle. Figure 74 depicts this test.

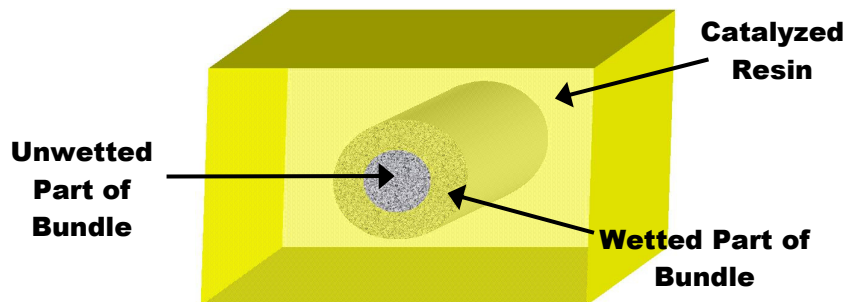


Figure 74 - Bundle wettability test

The results of the fiber bundle wettability test are shown in Figure 75. This test was conducted for sized (T700) and unsized (AS4) fiber, six different nitric acid treatment times, and for silane treatment with three different prior nitric acid treatment

times. The nitric acid treatments were conducted on unsized fiber bundles for periods of 2.5, 5, 10, 20, 40 and 80 minutes. The silane treatment was carried out on untreated, unsized bundles, as well as unsized bundles that had been treated in nitric acid for periods of 2.5, 20 and 40 minutes.

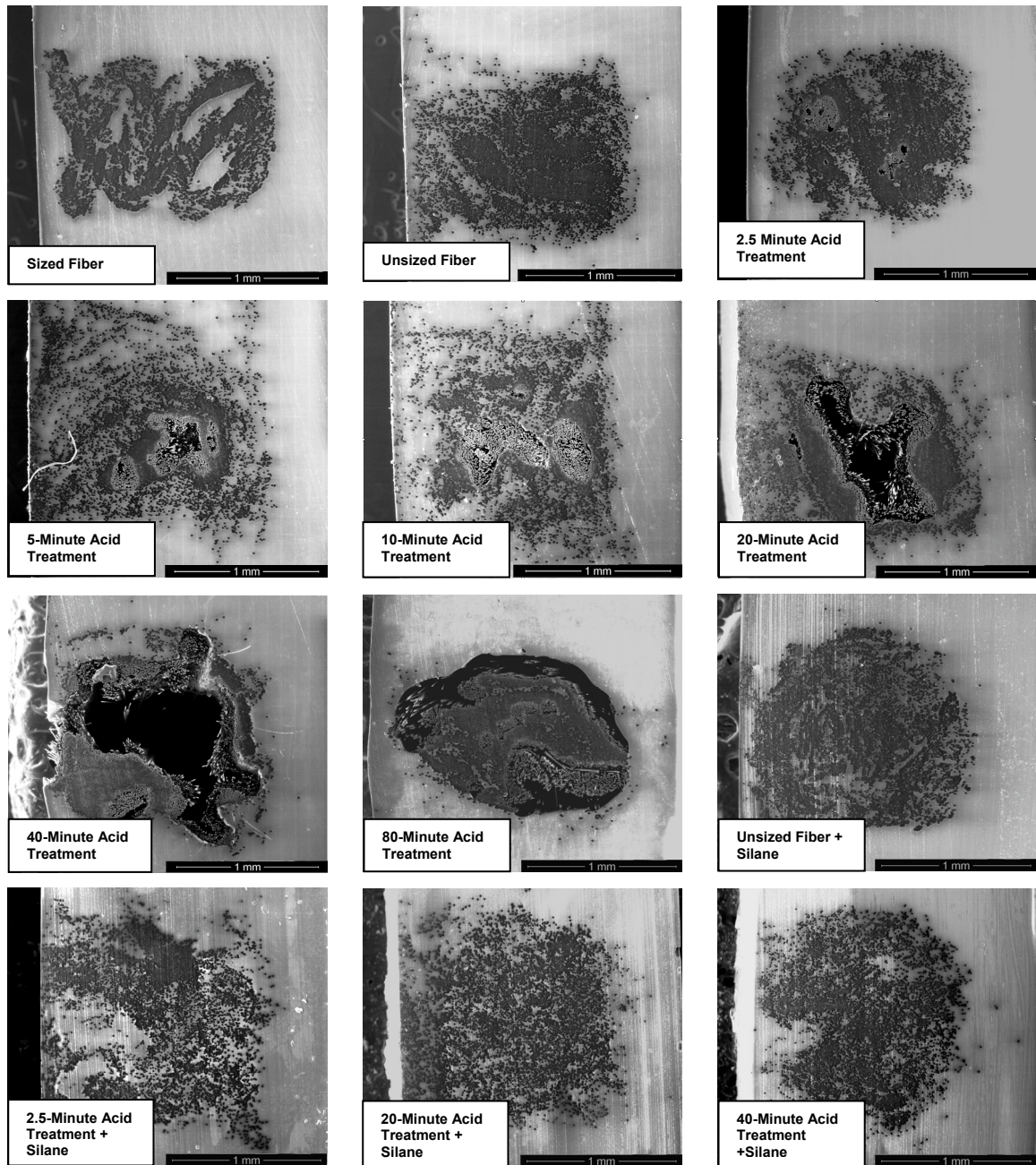


Figure 75 - Fiber bundle wettability test in resin

Figure 75 brings an interesting result to light. The wettability results obtained by wetting bundles in resin was opposite the results predicted through single fiber tensiometry measurements. Based on the total energy and polar energy calculated from the tensiometry contact angle tests, an increase in wettability would be expected with increasing nitric acid treatment time and the silane-treated fibers should be the least wettable. But as nitric acid treatment time increased, there were increasingly large areas of unwetted fiber within the bundles. And the silane-treated bundles completely wetted out, regardless of how long they were treated in nitric acid prior to silane application.

While a single fiber may be more wettable with an oxidizing nitric acid treatment and less wettable with a silane treatment, a group of fibers behaves differently. It is likely that the fiber cohesion discussed and measured herein plays an important role, as well as the resin viscosity. Fiber cohesion holds the fibers together, making areas of the fiber bundle difficult for the high-viscosity resin to pervade. Thus, the oxidizing treatment is making the fiber groups less wettable, instead of more wettable as commonly believed. The less polar silane treatments and untreated fibers allow complete wetting to occur.

It should also be noted that the result obtained with the silane treated fibers further supports the idea that the silane has bonded to the carbon fibers.

3.2.9 Composite Fiber Volume Fraction and Void Content

The relative proportion of fiber, matrix and void volume is useful information to help understand the overall quality of a composite. It also helps to understand how well the resin wetted the fiber during formation. Typically, a high fiber/matrix ratio and low

void content is desired. Reinforcements (fibers) provide the majority of the composite strength and one of the major purposes of the matrix is to maintain the position of the fibers so that their strength can be utilized. Thus, it is desirable to minimize the amount of matrix so that excess weight and volume is kept to a minimum. Voids are undesirable for obvious reasons. They provide stress concentrations, reduce fiber/matrix interfacial area and allow water diffusion into the composite, among other things. ASTM D 3171 (Standard Test Methods for Constituent Content of Composite Materials) outlines several procedures that can be used to evaluate the relative fiber, matrix and void ratios of composites. In this standard, the composite is weighed and the density is determined, the matrix is burned away (chemically or pyrolytically), and the remaining reinforcement is weighed. For this experiment, composite panels were made with sized and unsized fiber, as well as three acid treatment times (2.5, 5 and 10 minutes) and one acid treatment (5 minutes) followed by silane treatment. All of the acid treated fibers were of the sized variety because it was available in woven mat form. The process for making the composite panels is described earlier herein.

ASTM D 3171 allows the density of the composites to be determined by one of two methods. The first way calculates the density based on the weight of composite specimens in air and in a liquid, such as water (ASTM D 792). The second method measures the density by sinking composites in a column of fluids that vary in density (ASTM D 1505). ASTM D 792 (Density and Specific Gravity (Relative Density) of Plastics by Displacement) was chosen and used herein. The composite specimens were sized so that each one weighed near 1 gram, as specified, and at least two samples were used per composite type.

Each specimen was weighed both dry and wet on a scale, accurate to the ten-thousandths digit. Wet weight was obtained by suspending the specimen from a wire over a cup of water that was fixed to a support not on the scale. Distilled water at a temperature of 21° C was used, which is within the temperature requirements of the standard. Figure 76 shows the setup used to weigh the composite specimens in water.

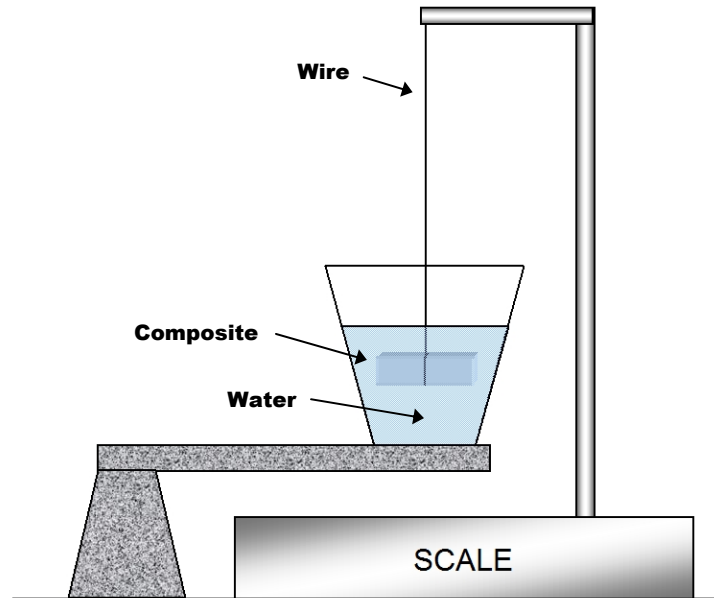


Figure 76 - Setup used to weigh composites in water

When weighing the specimens in water, an additional small wire was used to remove all bubbles before the weight was recorded. The weight of the suspension wire alone in water was also recorded so that its buoyancy could be factored into the equations. The density of the composite was found with the following:

$$D = SG \times 997.6 \text{ (kg/m}^3\text{)} \quad (20)$$

Where SG equals specific gravity and is calculated by:

$$SG = \frac{a}{(a + w - b)} \quad (21)$$

a = Mass of specimen in air

b = mass of specimen immersed in water and mass of partially immersed wire

w = mass of partially immersed wire

The density of the different specimens determined in this way is shown in Figure 77 and tabulated in Table 13.

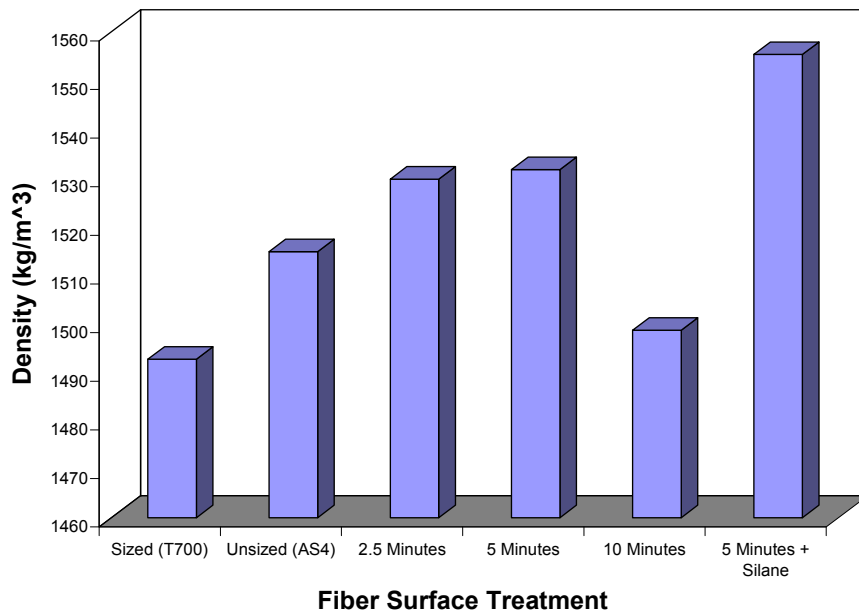


Figure 77 - Composite densities as determined by water displacement

COMPOSITE DENSITY (kg/m ³)					
Sized (T700)	Unsize (AS4)	2.5 Minutes Acid	5 Minutes Acid	10 Minutes Acid	5 Minutes Acid + Silane
1492.6	1514.7	1529.7	1531.6	1498.5	1555.3

Table 13 - Density of composite specimens determined by ASTM D 792

In most homogeneous materials, density is a good indicator of void percent. However, the different constituents of composite materials usually have different densities and the total density depends on fiber/matrix ratio, as well as void percent. Therefore, it is necessary to continue to determine the fiber/matrix ratios in order to understand why the composite densities are different. As previously mentioned ASTM D 3171 was followed and nitric acid was used to digest the matrix from the composite. Each composite was digested in 40 ml of 70% nitric acid for six hours at 100° C, and then the contents were filtered through sintered glass crucibles so that only the fiber remained. The fiber was then weighed to determine how much it contributed to the total composite weight. A vacuum pump was used to aid the filtering process. Figure 78 shows the filtering apparatus used.



Figure 78 - Filter setup for matrix acid digestion

Vinyl ester is a chemically resistant resin, which leads to the requirement of such a long exposure time in a high temperature of nitric acid. Because of the rigorous acid exposure, fiber volume loss can also be expected. This effect was shown previously herein, where the carbon fiber diameters were found to decrease with extended acid exposure times. To account for fiber mass change, a blank of only fiber that was equivalent to the amount of fiber in the composites was exposed to the same digestion procedure. One gram of unsized fiber was used. It was shown herein in the fiber diameter section that the diameter loss of both types of fiber in nitric acid is similar. The composite fiber weights were then compensated to account for the amount of fiber mass

loss found in the blank fiber test. After the composites were digested and filtered, the fiber was rinsed three times in distilled water, followed by three rinses in acetone. The acetone rinse was not prescribed by the standard, but it was found that some matrix solid material would coagulate and remain after the water rinses. The acetone successfully dissolved the remaining solid material. Then the fiber-containing crucible was dried in an oven for one hour at 100° C, all residues were wiped off, and it was then weighed. The difference between the fiber-containing crucible and the empty crucible produced the fiber weight.

The following equations were used to arrive at the composite properties. The fiber and matrix densities used for computation were provided by the manufacturers.

Fiber Weight Percent

$$W_r = \frac{M_f}{M_i} \times 100 \quad (22)$$

Where,

M_i = initial mass of the specimen (grams)

M_f = final mass of the specimen after digestion (grams)

Fiber Volume Percent

$$V_r = \frac{M_f}{M_i} \times 100 \times \frac{\rho_c}{\rho_r} \quad (23)$$

Where,

ρ_r = density of the fiber

ρ_c = density of the composite specimen

Matrix Weight Percent

$$W_m = \frac{M_i - M_f}{M_i} \times 100 \quad (24)$$

Matrix Volume Percent

$$V_m = \frac{M_i - M_f}{M_i} \times 100 \times \frac{\rho_c}{\rho_m} \quad (25)$$

Where,

ρ_m = density of the matrix

Void Volume Percent

$$V_v = 100 - (V_r + V_m) \quad (26)$$

Through equations (22) through (26), the following results were obtained for fiber and matrix weight percent, fiber and matrix volume percent, and void volume percent, shown in Figure 79, Figure 80 and Figure 81, respectively.

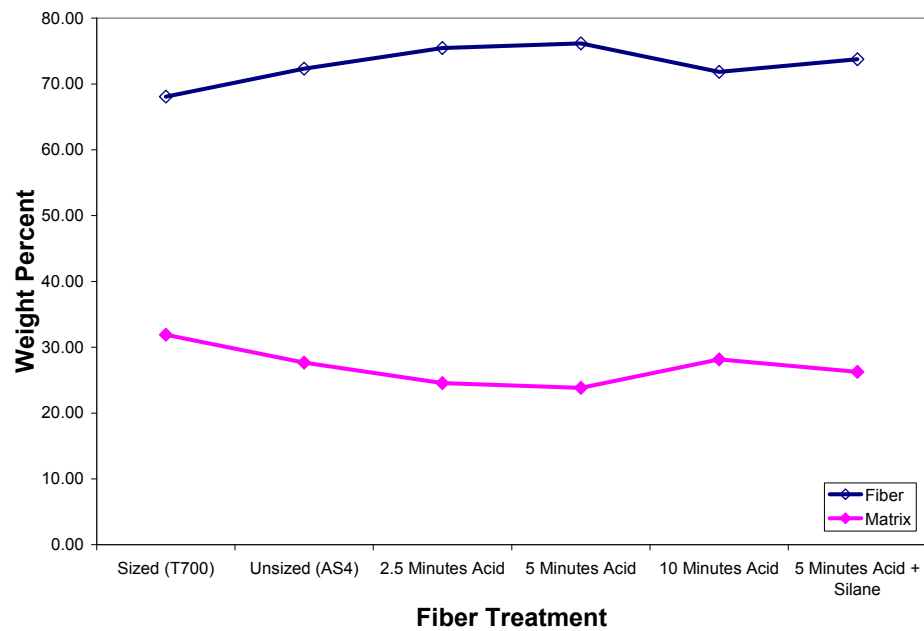


Figure 79 - Composite fiber and matrix weight percents

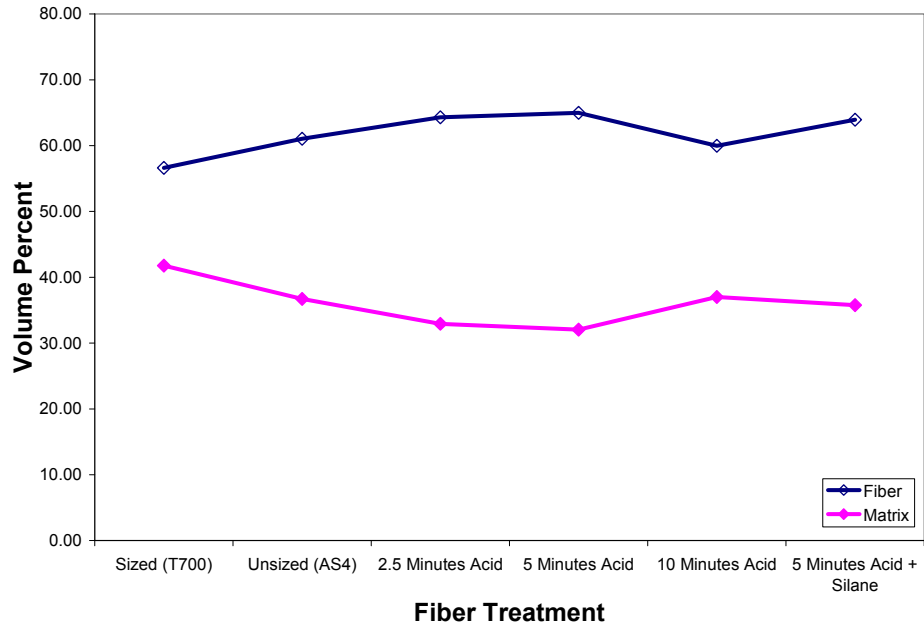


Figure 80 - Composite fiber and matrix volume percents

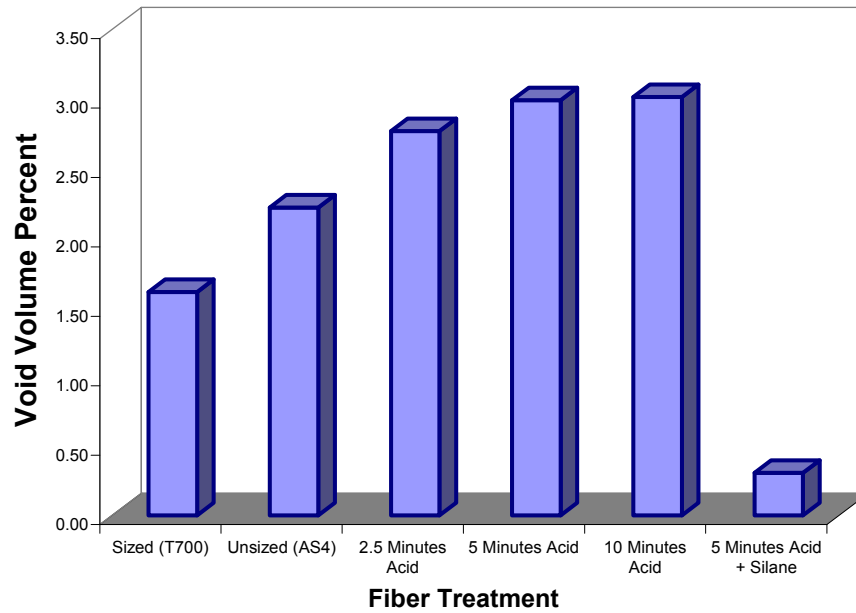


Figure 81 - Composite void volume percents

For clarification, the weight and volume percents are tabulated in Table 14.

COMPOSITE FIBER SURFACE TREATMENT	WEIGHT PERCENT		VOLUME PERCENT		
	Fiber	Matrix	Fiber	Matrix	Voids
Sized (T700)	68.08	31.92	56.63	41.76	1.61
Unsize (AS4)	72.34	27.66	61.06	36.72	2.22
2.5 Minutes Acid	75.47	24.53	64.30	32.93	2.77
5 Minutes Acid	76.16	23.84	64.99	32.02	2.99
10 Minutes Acid	71.85	28.15	59.98	37.01	3.01
5 Minutes Acid + Silane	73.75	26.25	63.93	35.76	0.31

Table 14 - Composite weight and volume percents

Review of Figure 79 through Figure 81 immediately yields that the composite treated with acid and then silane had a very low void percent and a relatively high fiber/matrix ratio; both desirable composite properties. The void content of the acid-only treated fiber composites increased in correlation with increasing acid treatment time. This supports the results seen herein in the bundle wettability tests, but unlike the bundle wettability tests, the composites were formed with the aid of compression. Increasing void content is a result of nitric acid fiber treatment with or without compression molding. It should also be noted that these composites were made in a very tedious way, to try to avoid void content. Each layer was agitated, thoroughly saturated with resin and rolled out with a steel bar before stacking into the four-ply composite. Compression was then applied as described earlier. Also, the VARTM process resulted in even poorer

results with acid treated fiber, as no composites could be formed due to poor wetting, even at low fiber treatment times.

The fiber/matrix ratio also increased with fiber treatment time, except for the 10-minute treatment. A high fiber/matrix ratio is usually desirable, but in this case, it appears to be due to poor wetting, making it undesirable. The fiber bundles did not separate enough to allow sufficient resin infusion, resulting in a low-resin composite. While the 10-minute acid treated composite followed the expected trend with overall void content, it had a lower than expected fiber/matrix ratio. It appeared to contain more resin than the other acid-treated types. It would be expected that as fiber treatment lengthened, wetting would decrease and the fiber/matrix ratio would increase. This difference may have been due to variation in the labor-intensive compression molding process. Commercial compression-molding equipment was not available and this was done in a makeshift way. The 10-minute treated fibers could have been better agitated to better separate them, or the entire lay-up process could have been completed faster, leaving a less viscous resin available when compression started. The high matrix content in combination with the high void content of the 10-minute treated composite explains the low density observed. In contrast, the low void content and relatively low matrix content of the acid and silane treated composite explain its high density. Notably, the sized commercial fiber displayed the second-lowest void content and the highest resin content.

From the standpoint of void content and fiber/matrix ratio, the acid and silane treated composite was by far the best quality and the acid-only treated composites were the poorest, with the untreated (sized and unsized) fibers falling in between.

3.2.10 Composite Transverse Tensile Strength

The ultimate goal of most fiber treatments is to improve composite properties, and strength is usually high on the list. There are several ways to measure composite strength, but the strength in the direction opposite the fiber direction is most indicative of the quality of the fiber/matrix interface. This is because failure does not occur by breakage of the fibers in their strong (longitudinal) directions. Instead, failure occurs either by failure of the bond between the fiber and matrix or, in cases of a well-bonded interface, failure of the matrix in between the fibers. Two common methods used to measure transverse composite properties are the transverse tensile test and the transverse flexure test. The flexure test is often preferred because failure occurs along a line near the center of the span that is subjected to bending. There is only a small chance that a significant material flaw will exist in this small failure area. The transverse tensile test, however, subjects the entire length of the composite to the same stress, and failure usually occurs at a flaw that is distributed somewhere along the specimen length, leading to lower strength values than those found with transverse flexure tests. Most of the fiber used in this research was in the form of single tows, which had not been woven into a mat. This presented a challenge when it came to producing composite specimens. It was not practical to weave a mat of out of treated fiber for every different type of treatment. This would be extremely time consuming and wasteful, as fiber mat treatment required significant amounts of acid and silane. Therefore, a transverse composite property test was chosen that required only one fiber bundle. A single-bundle transverse tensile test was used, which was similar to that described by Ageorges et al.¹⁴⁴ In this method, a

fiber bundle was cast in the transverse direction across the center of a dog-bone shaped resin specimen. The specimen geometry is depicted in Figure 82.

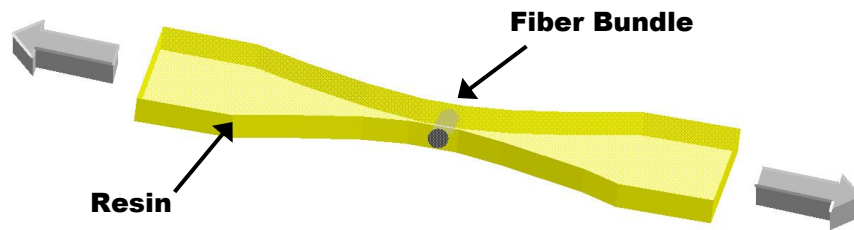


Figure 82 - Single-bundle transverse tensile test

This geometry assures that the highest stress occurs in the narrower region where the fibers are located. In addition, a specimen of this shape eliminates one of the main concerns expressed with the transverse tensile test. The transverse tensile test is often criticized because it is flaw-sensitive. A constant-width transverse tensile specimen will likely fail at a major flaw along its length or at the test grips, leading to a low strength prediction. This also makes this test susceptible to changes with test gage length. A dog-bone specimen with a radius of curvature along its length assures that the highest stress occurs only in the center and eliminates failure at distributed flaws. The dimensions are similar to those used by Ageorges et al.¹⁴⁴, with the exception that the bundle was held in place by 1mm x 1 mm channels on each side of the mold cavity, instead of placed flat between an upper and lower mold surface. Glass strips were also placed over the open mold to assure consistent thickness in the fiber and grip areas. Figure 83 shows a photograph of the RTV silicone mold used.

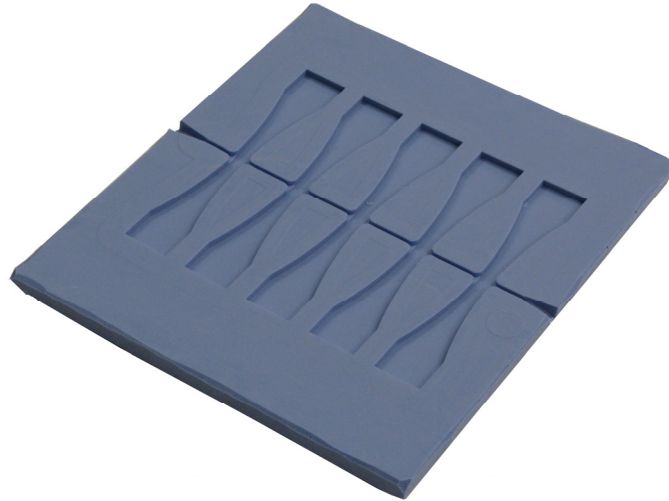


Figure 83 - Single-bundle transverse tensile silicone mold

Sized and unsized fiber bundles, as well as five nitric acid treatment times (2.5, 5, 10, 20, 40 minutes) of unsized fiber were analyzed. Beyond 40-minute treatments, the specimen quality was so poor that it became difficult to handle or test them. Additionally, silane-treated specimens were made using sized and unsized bundles, as well as 2.5, 20 and 40 minute acid treatment times. A set of at least 10 samples was tested for each treatment in the dry condition as well as after immersion in 40° C seawater. The transverse tensile specimens made with untreated and nitric acid-treated fiber were tested after one, two and three months of seawater exposure. The silane-treated fibers were tested after three months of seawater immersion. All specimens were cured for 24 hours at room temperature, followed by a two-hour post-cure at 120°C before testing or seawater immersion.

The transverse tensile specimens were tested on a MTS Insight 1kN test machine at 0.2 mm/min, which is shown in Figure 84, setup in the configuration used.



Figure 84 - MTS Insight 1kN test machine in the transverse tensile testing configuration

Untreated and Nitric Acid-treated

The transverse tensile test results for the untreated and nitric acid-treated fiber types can be seen in Figure 85. The acid treatment was applied equally to both types of fiber to determine if they responded differently.

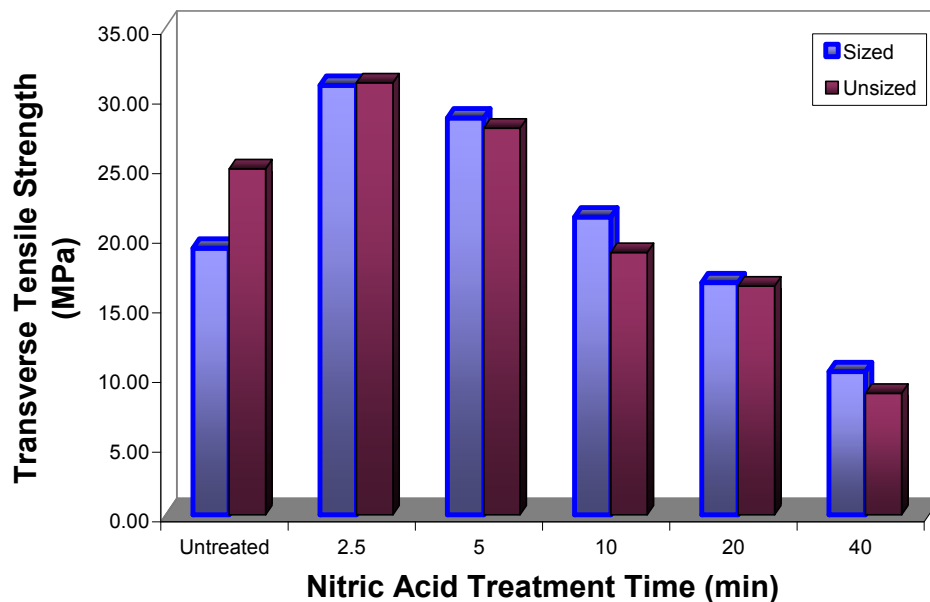


Figure 85 - Transverse tensile strength of the untreated and acid-treated fiber types

With the exception of the untreated condition, both fiber types (sized and unsized) behaved similarly after acid treatment. This is another indication that these two types of fiber (Toray T700 and Hexcel AS4) can be treated equally after acid treatment. As pointed out previously, these two fiber types also behaved similarly in terms of tensile strength, modulus and surface geometry before and after acid treatment. It is interesting to note that the sized fiber performed poorer than the bare unsized fiber did. The unsized fiber is not a completely virgin surface, as it has a proprietary surface treatment that was applied by the manufacturer. This treatment was previously found to be oxidative in nature herein, but showed a lesser amount of surface oxidation than the acid-treated fibers. This information was discussed previously in the XPS and chemical derivatization section.

A very interesting feature that is clearly visible in Figure 85 is that although the acid treatment initially increases the transverse tensile strength, it is followed by a steady decline in both fiber types. The initial strength increase is 61% for the sized fiber and 25% for the unsized fiber. The fact that the two fiber types become equal after acid exposure, even though they start out different, indicates that the acid has removed the sizing and it is no longer acting as a factor in the transverse tensile strength. It's presence in the acid after removal apparently does not affect the fiber surface groups that are implanted. The strength decline that occurs with increasing acid treatment time is most likely explained by viewing the bundle wettability results presented earlier herein. It was shown that the wettability of the fiber bundle decreased significantly as fiber treatment time in acid was lengthened.

Furthermore, there is clearly an improvement in fiber/matrix adhesion, because the 2.5-minute treated type showed much more strength than the untreated (unsized) type, even though it was shown to have poorer wetting than the unsized, untreated type. In the bundle wettability tests, both untreated fiber types showed excellent wetting, while all acid treatment types (including the 2.5 minute treatment) showed unwetted areas. Therefore, there is a trade-off between the improved fiber/matrix surface adhesion and the decreased multiple fiber wetting.

To evaluate the seawater durability of the nitric acid surface treatments, transverse tensile specimens were tested after one, two and three months of exposure to 40° C seawater. The results are shown in Figure 86.

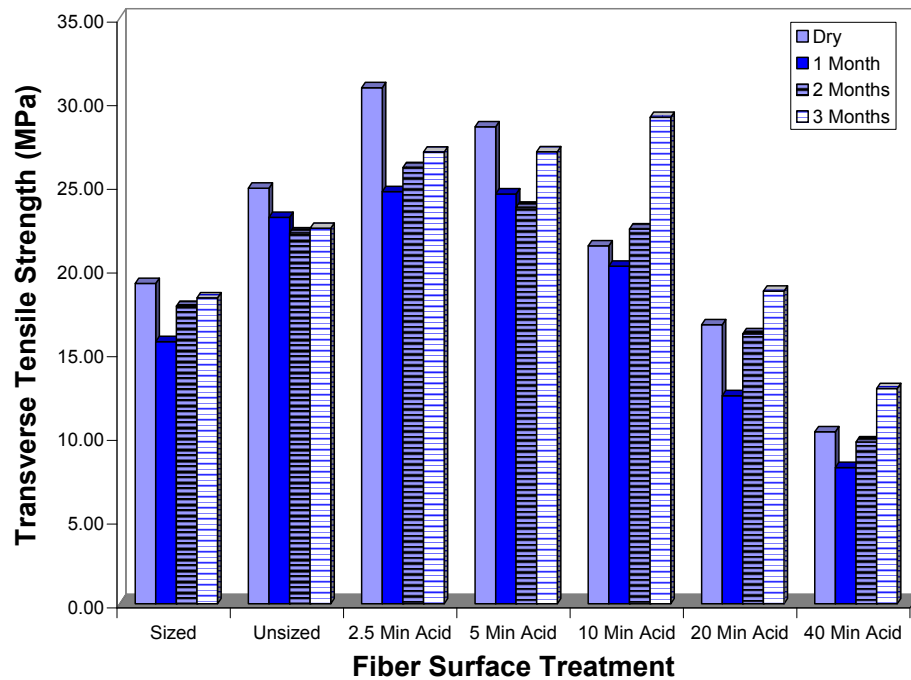


Figure 86 - Nitric acid-treated transverse tensile strength before and after seawater exposure

From Figure 86, it can be seen that all of the fiber surface types experienced a drop in transverse tensile strength at one month. However, for most of the types, the strength change reversed and the composites showed more strength at longer seawater exposure times. This can be attributed to two possibilities. The first is that the nitric acid surface treatment is durable with seawater exposure. The second possibility raises an issue with this type of transverse tensile test. This test results in a high percentage of resin within the fracture zone in comparison to composites that are prepared with the aid of pressure or vacuum. In this test the fiber bundle is placed within a fixed-size region of resin. It is well known that water plasticizes plastic resins and it has been shown that this plasticizing increases the resin fracture toughness.²⁰ Therefore, the resin in these high-

resin proportion samples may plasticize and toughen, leading to an increase in test strength.

Acid/silane treated

Transverse tensile testing was also conducted on specimens made with fibers that had undergone either silane treatment alone, or silane treatment after varying levels of acid treatment (2.5, 20 and 40 minutes). The results are shown in Figure 87.

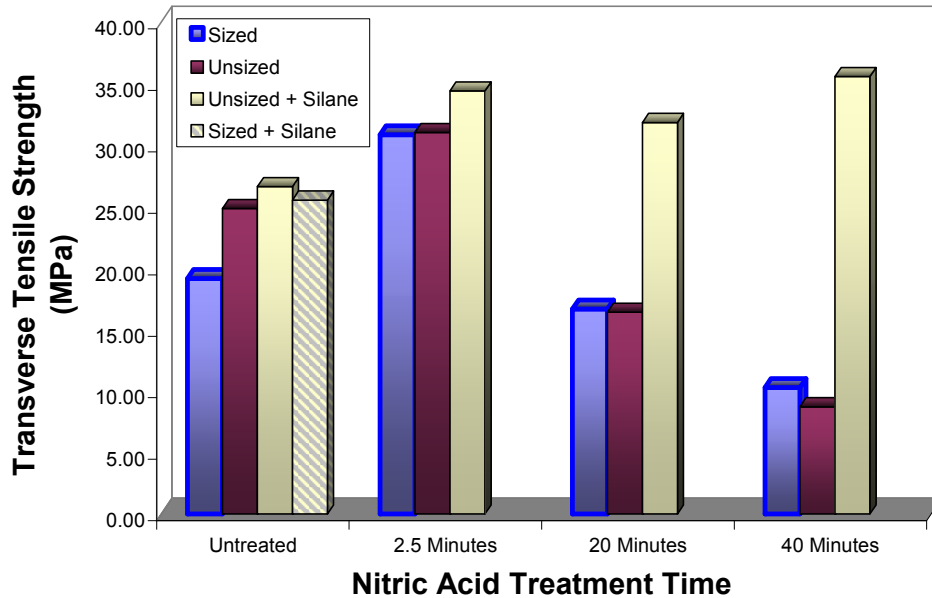


Figure 87 - Acid/Silane-treated transverse tensile strength

Review of Figure 87 indicates that the application of silane to the acid-treated fibers resulted in a very significant increase in transverse tensile strength, especially when compared to the highly acid-treated types. The acid/silane treated fibers produced the strongest composites overall and did not exhibit the strength decline that the acid-only treated types did with extended treatment. Instead, the silane-treated types maintained a constant high strength. The acid/silane treated fibers produced transverse tensile strength

improvements of 86% and 56% over the untreated sized and unsized fiber types, respectively. It appears that the silane was able to bond to the surface functional groups on the fibers that were introduced by nitric acid treatment. Providing even more evidence for this is the fact that the acid/silane-treated fibers showed higher strength than the silane-only treated fibers.

Another notable point is that both types of silane-only treated fibers produced approximately equal strengths, while the untreated fibers differed. It is likely that the acetone-based silane solution that was used to treat the fibers dissolved the sizing on the sized fibers, making them similar in surface condition as the unsized fibers.

The silane-treated fibers were also tested after three months of seawater exposure. The results are shown in Figure 88.

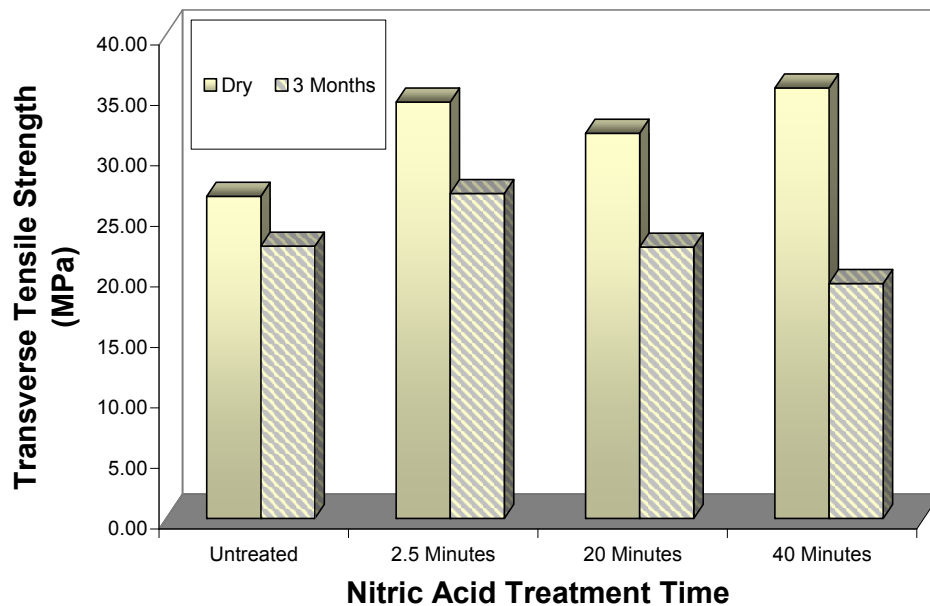


Figure 88 - Silane-treated transverse tensile strength before and after seawater exposure

The silane-treated fibers produced composites that lost transverse tensile strength with seawater exposure. This strength loss seemed to increase with the nitric acid

treatment time that was used as a preparation for silane treatment. The increased polarity of the fibers that were treated to a higher degree in acid, may continue to attract water and damage the interface, even after silane has been applied. The silane may not be able to satisfy the polarity of the more highly acid-treated fibers through bonding. The most resilient acid/silane type was the 2.5-minute treatment, or the one with the least acid treatment. This low level of acid treatment also produced the best acid-only composites, which were stronger than the untreated ones.

It is difficult to explain and compare the strength changes observed in the acid-only and silane-treated types. The silane-treated types all exhibited excellent wetting, regardless of acid treatment time, while the acid-only treated types showed wetting problems. Poor wetting changes the diffusion process significantly, and may make this transverse tensile test unreliable for the acid-only treated types. There are also numerous methods that can be used to apply silanes that result in different water durability results. Chua et al. reported that silanes on glass fibers protected them against water attack, but only when applied in thin chemisorbed layers.¹⁴⁵ Excess (physisorbed) layers were found to reduce the composites' ability to resist water attack. And as discussed earlier, physisorbed silane is likely to change the properties of the matrix interphase through interdiffusion. While the silane was applied in a method to achieve a thin-chemisorbed layer in the current experiment, the type of silane distribution was not verified. Hence, it may be unwise to compare the silane results with the acid-only results, and the durability of the silane treated fibers may change if the silane application method is altered.

3.2.11 Transverse Tensile Failure Analysis

In addition to measuring composite strength to evaluate changes caused by fiber surface treatment, much can be learned about fiber/matrix adhesion, wetting and failure types with SEM analysis. While scanning electron microscopy cannot quantify adhesion or strength, it can indicate how the composite failed. When reviewing composite failure surfaces, three types of information were considered: wetting, resin failure type, and interface failure mode.

Wetting – A cross-sectional view of a failed composite specimen provides a general indication of the degree of resin wetting that occurred.

Resin Failure Type – Analyzing the fracture surface of resin areas provides an indication of how the resin failed. Ductile failures indicate possible plasticizing of the resin. Brittle failures were identified as areas that exhibited smooth cleavage fracture surfaces, while ductile failures were associated with areas that lacked smooth cleavage surfaces and showed considerable local deformation. These types of fracture surfaces have been described in the brittle and ductile fracture of other polymer types.¹⁴⁶

Interface Failure Type – Clean fibers and cylindrical depressions in the matrix indicate debonding failure due to poor adhesion, whereas fibers that have fractured resin attached to them indicate that the fiber/matrix bond was stronger than the resin during failure. Figure 89 graphically describes these two failure types.

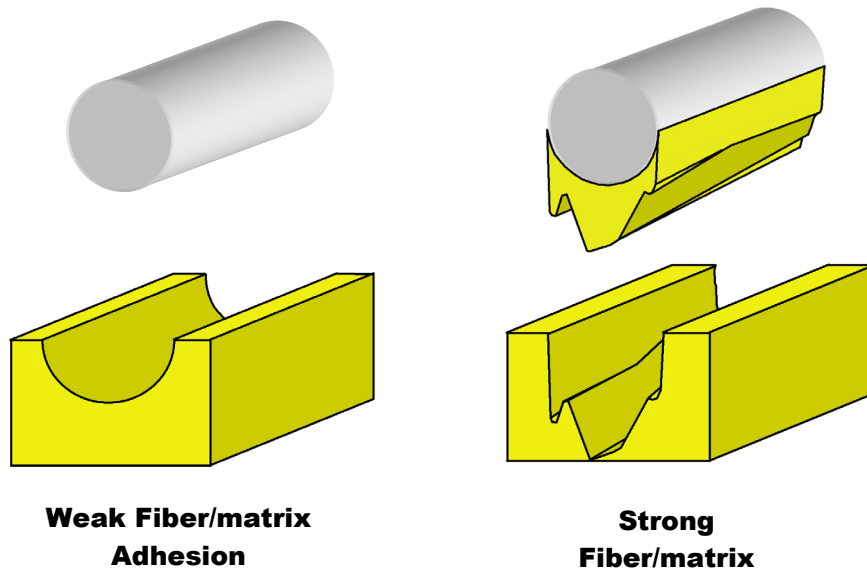


Figure 89 - Interfacial fiber/matrix failure types

In order to compare composite failures before and after seawater exposure, SEM analysis was conducted on dry specimens as well as specimens that were transverse tensile tested after two months of exposure to seawater at 40° C. These results are shown in Figure 90 through Figure 101, with the dry views shown in the left column and the corresponding seawater exposed views alongside in the right columns. Three magnifications are shown for each failure surface: 50x, 150x and 500x because different information can be obtained from different magnifications. To make evaluation of the images as straightforward as possible, noteworthy features are marked directly on the images and a general discussion follows at the end.

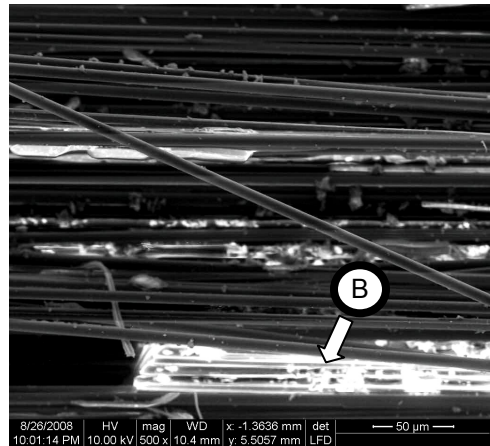
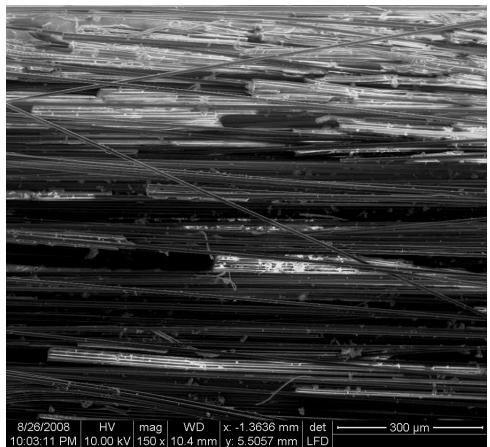
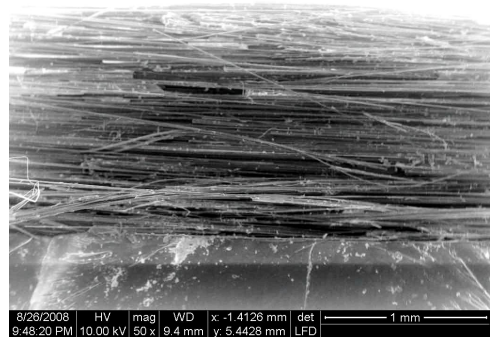
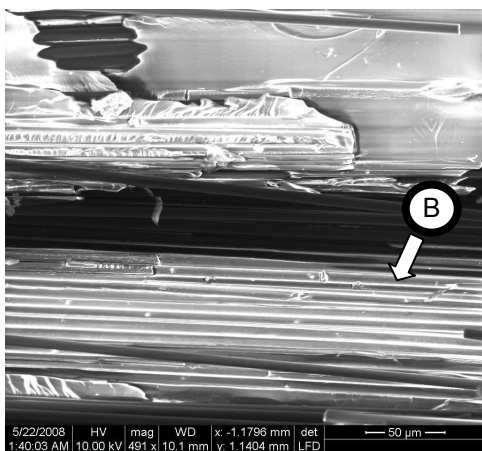
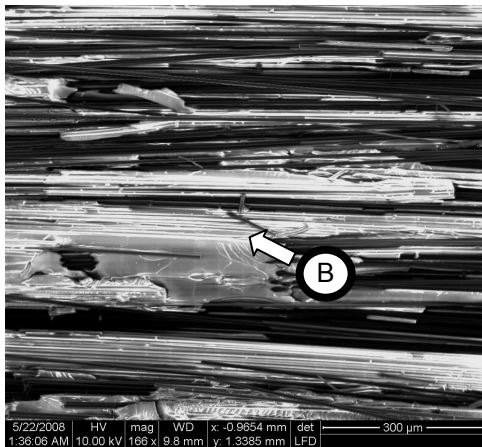
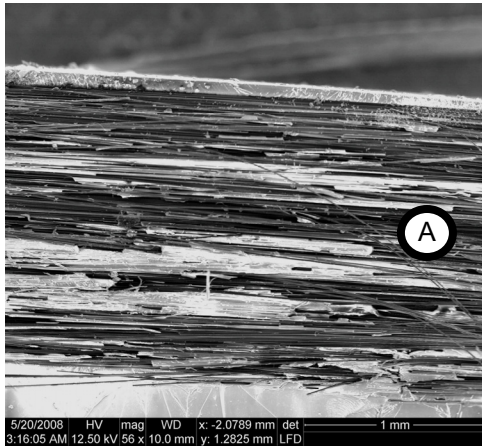


Figure 90 - Sized (T700) transverse tensile failure dry (L) and 2 months seawater exposure (R)

NOTES: (A) This surface condition allows good overall wetting, (B) Both dry and seawater-exposed specimens exhibit cylindrical channels and bare fibers, indicative of fiber/matrix debonding failure.

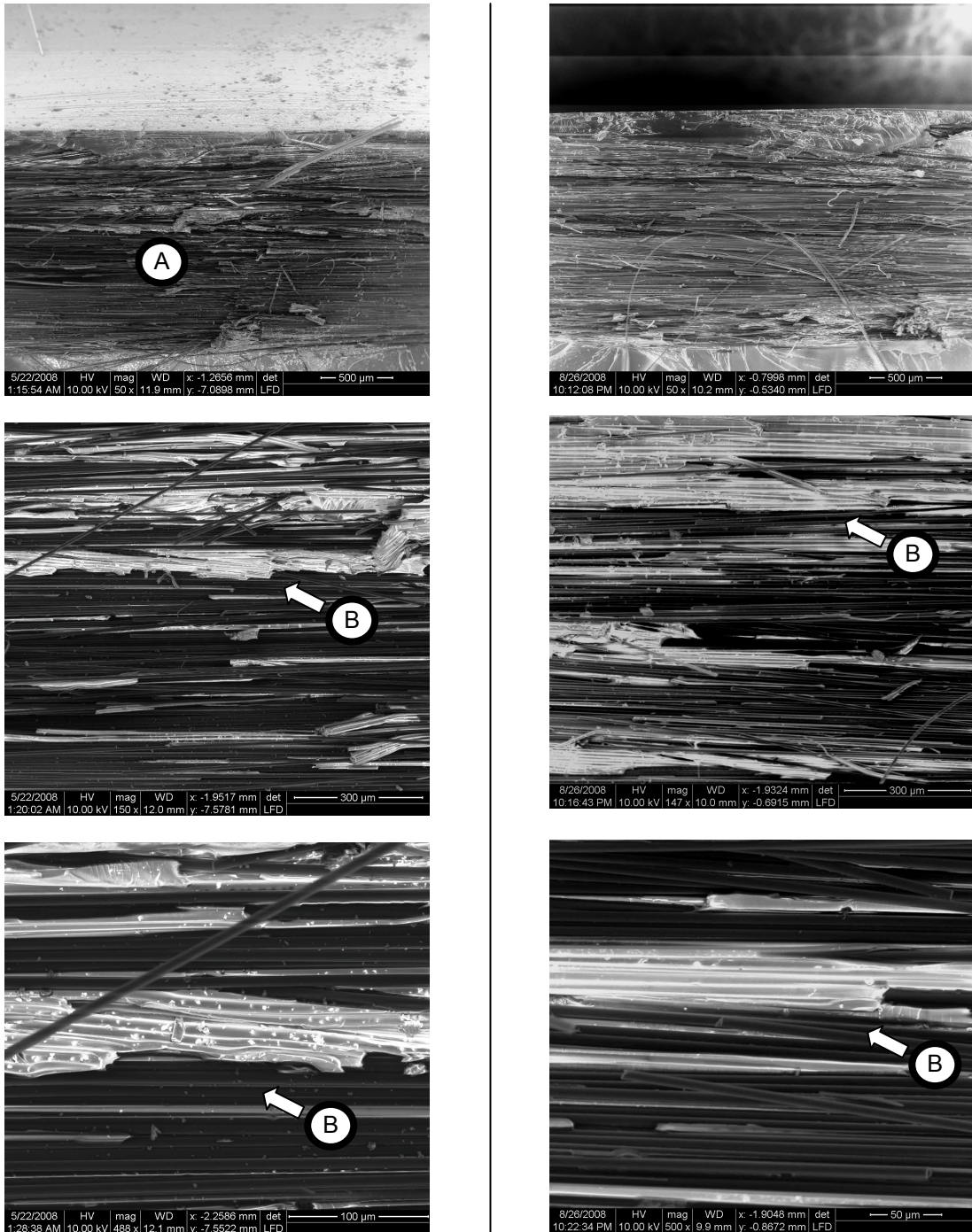


Figure 91 - Unsized (AS4) fiber transverse tensile failure dry (L) and after seawater exposure (R)

NOTES: (A) This surface condition allows good overall wetting, (B) Both dry and seawater-exposed specimens exhibit cylindrical channels and bare fibers, indicative of fiber/matrix debonding failure.

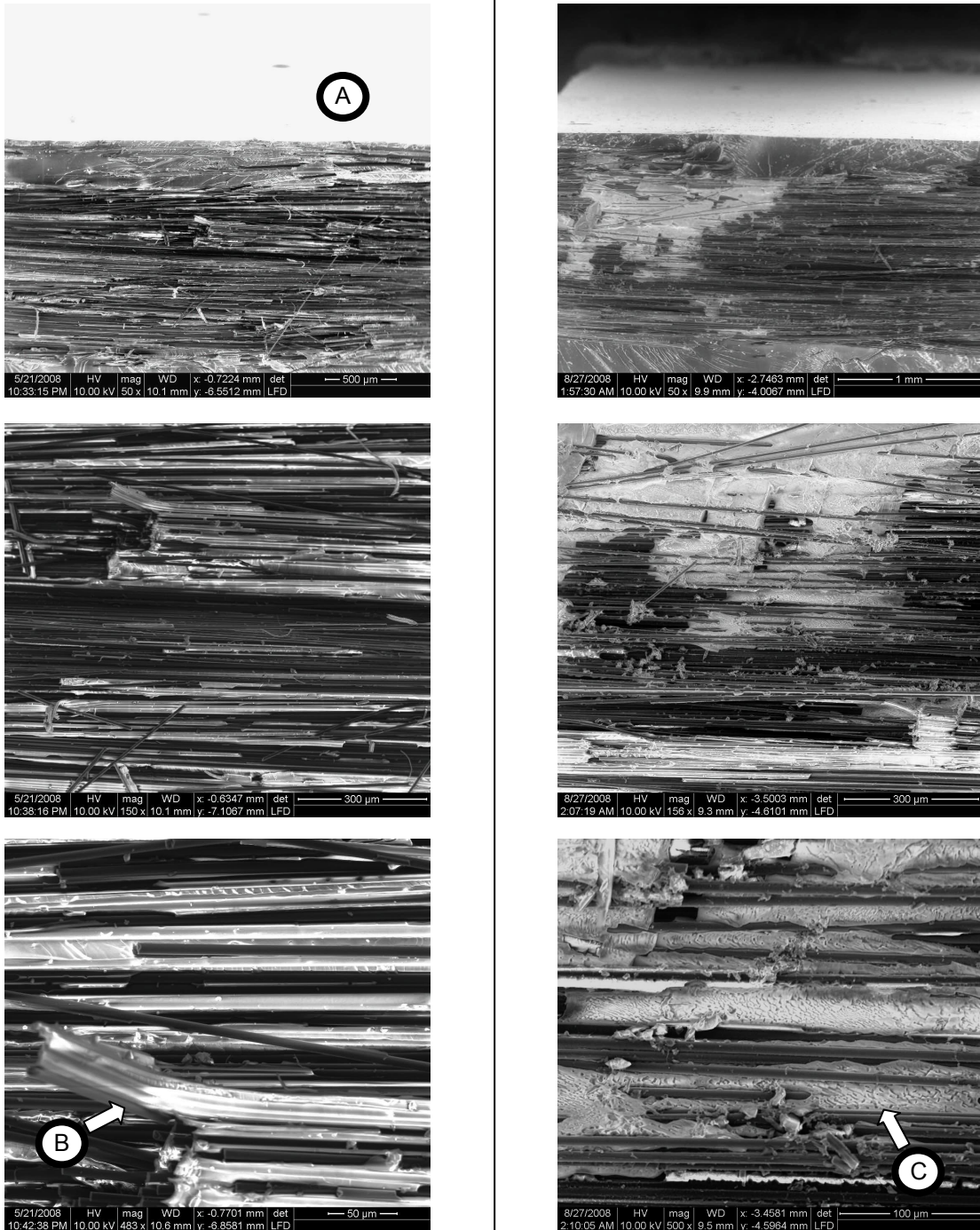


Figure 92 - 2.5 minute treated unsized fiber transverse tensile failure dry (L) and after seawater exposure (R)

NOTES: (A) This surface condition allows good overall wetting, (B) Dry specimens exhibit cylindrical channels and bare fibers, indicative of fiber/matrix debonding failure, (C) Seawater exposed specimens exhibited a change to a ductile matrix failure mode, suggesting resin plasticization.

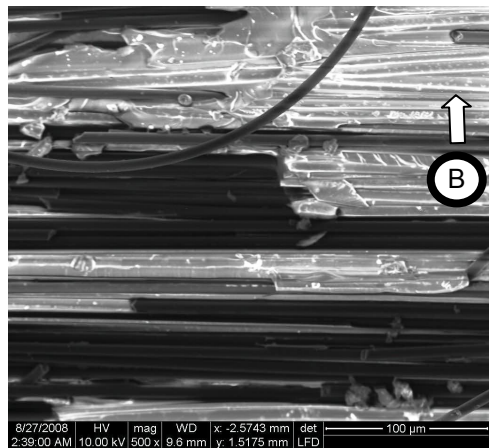
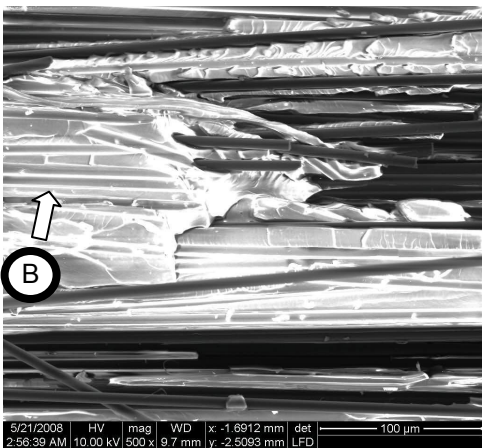
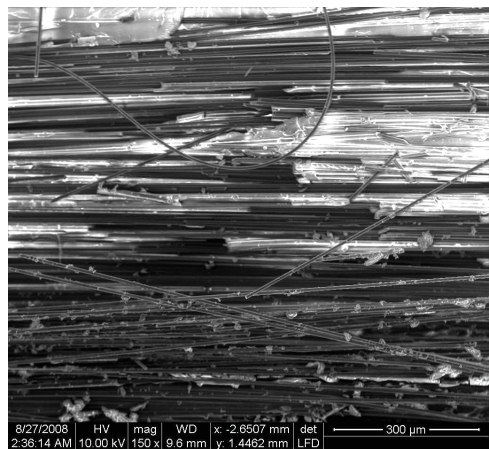
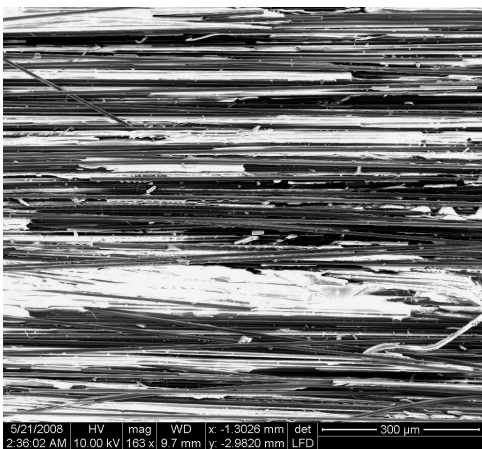
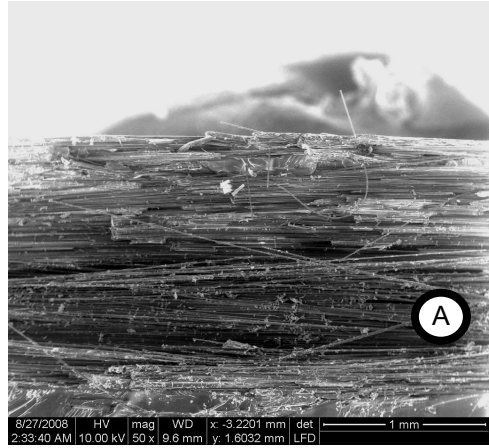
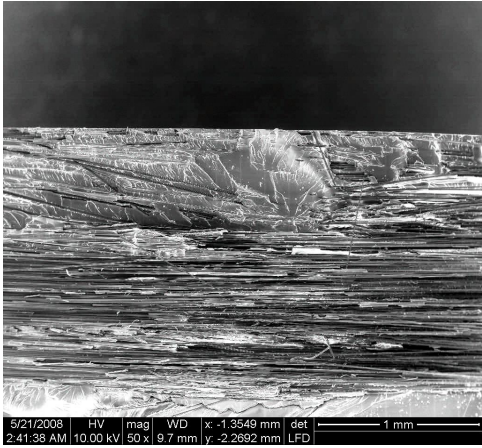


Figure 93 – 5 minute treated unsized fiber transverse tensile failure dry (L) and after seawater exposure (R)

NOTES: (A) This surface condition shows unwetted areas, (B) Both dry and wet specimens exhibit cylindrical channels and bare fibers, indicative of fiber/matrix debonding failure.

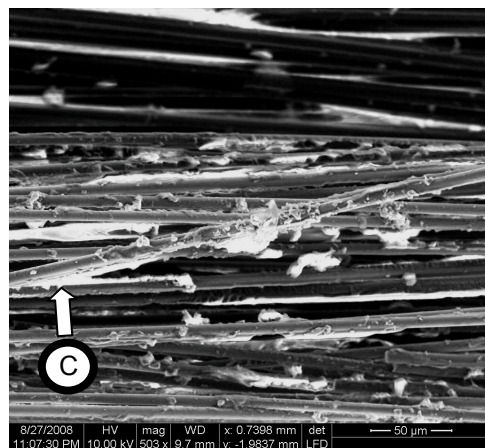
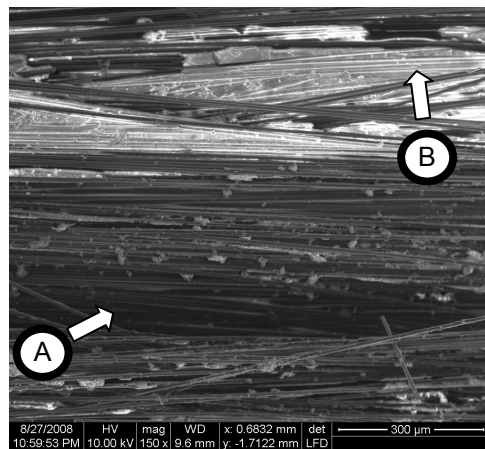
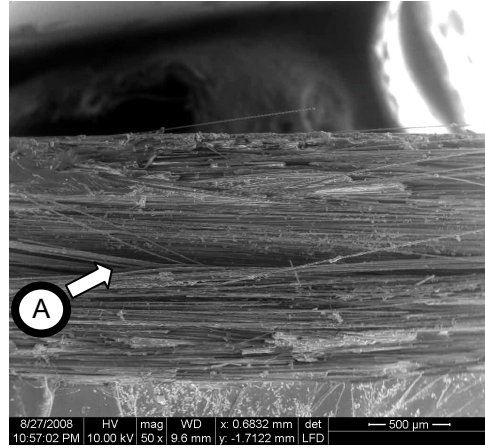
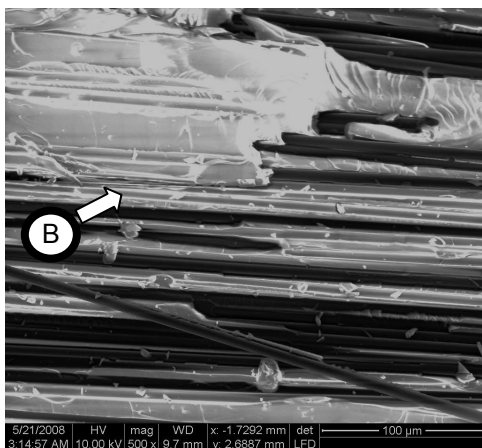
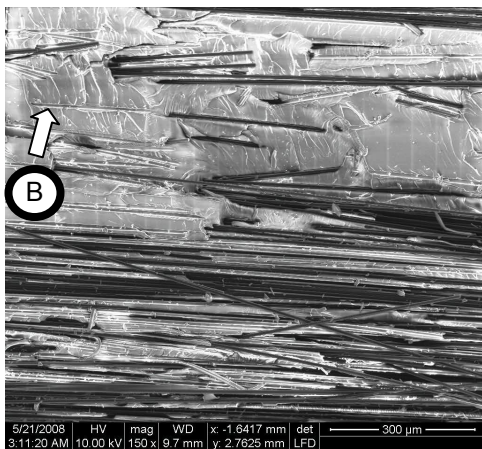
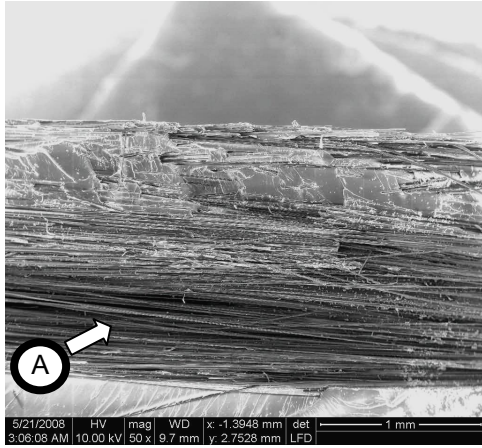


Figure 94 - 10 minute treated unsized fiber transverse tensile failure dry (L) and after seawater exposure (R)

NOTES: (A) This surface condition shows unwetted areas, (B) Both dry and wet specimens exhibit cylindrical channels and bare fibers, indicative of fiber/matrix debonding failure, (C) Seawater exposed specimens also exhibited some areas where fractured resin remained attached to the fibers, indicative of good fiber/matrix adhesion.

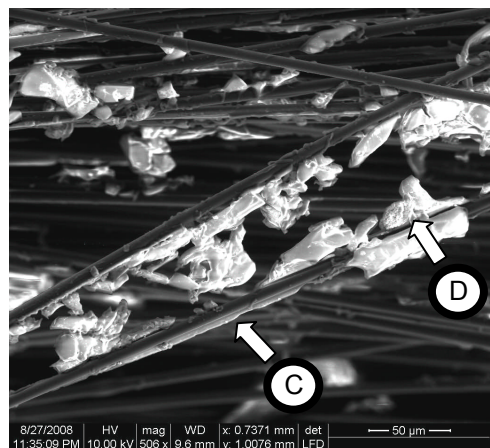
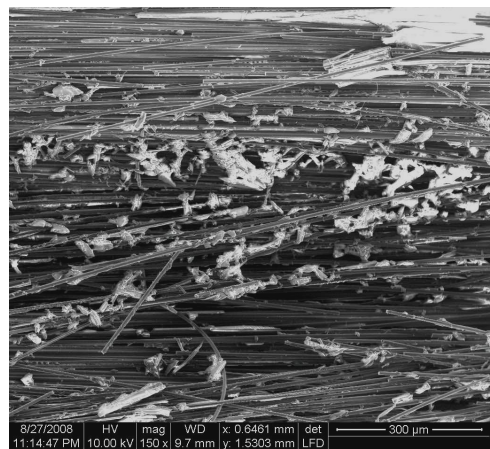
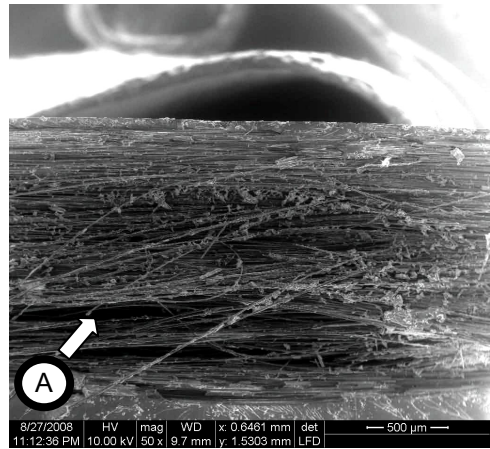
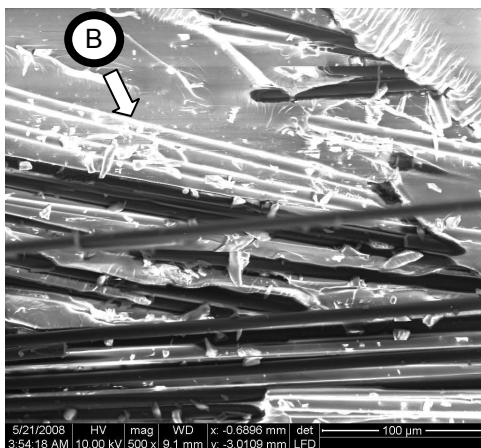
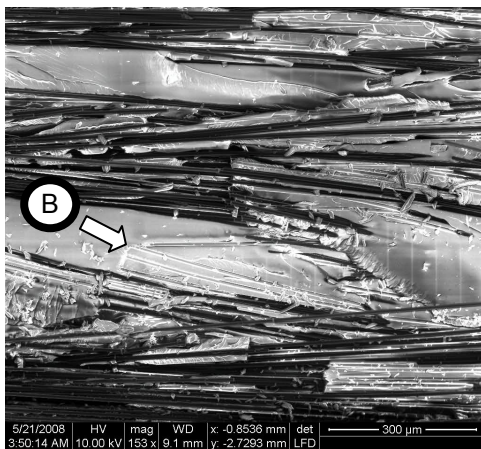
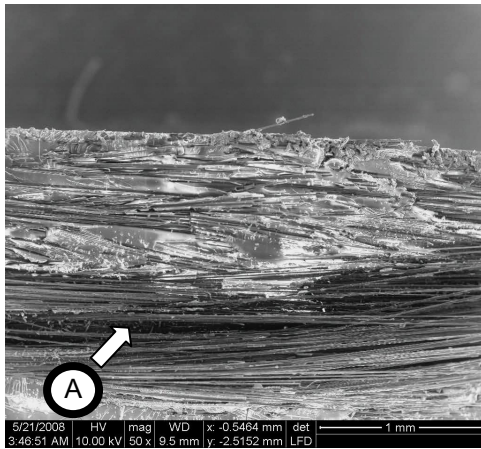


Figure 95 - 20 minute treated unsized fiber transverse tensile failure dry (L) and after seawater exposure (R)

NOTES: (A) This surface condition shows unwetted areas, (B) The dry specimen exhibited cylindrical channels and bare fibers, indicative of fiber/matrix debonding failure, (C) Seawater exposed specimens exhibited regions where fractured resin remained attached to the fibers, indicative of good fiber/matrix adhesion, (D) The wet specimen resin showed areas of ductile failure.

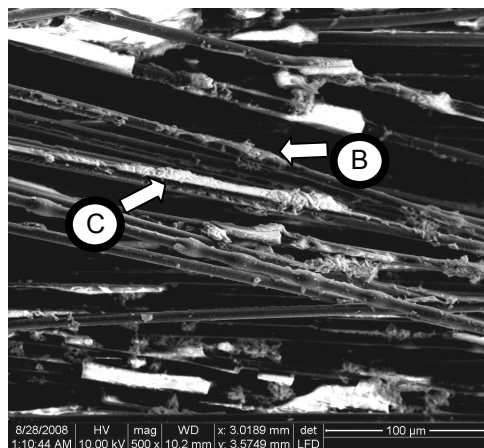
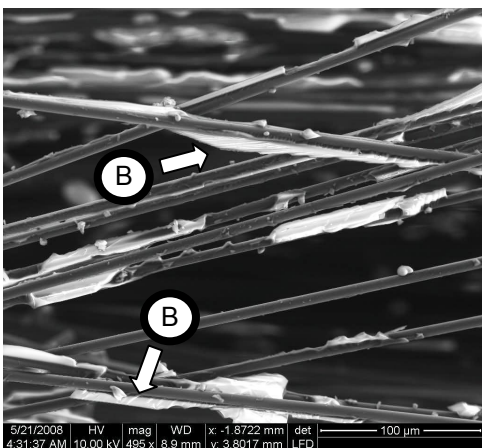
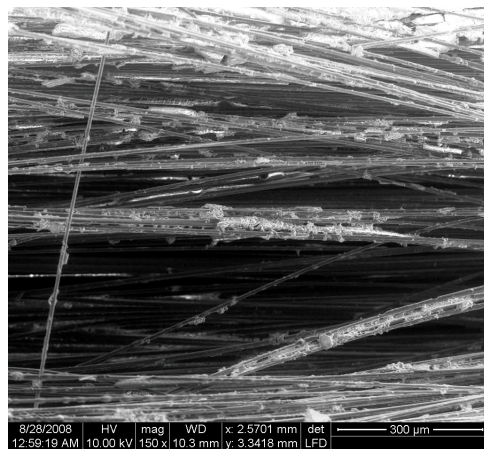
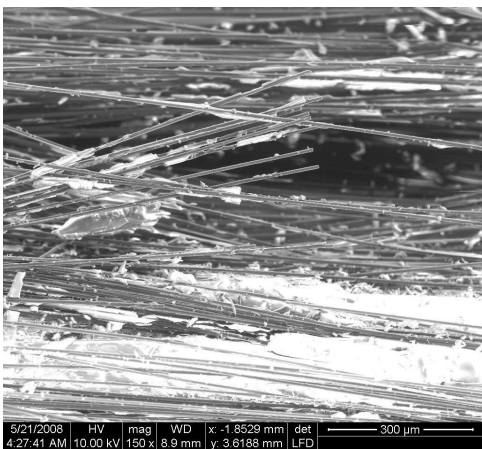
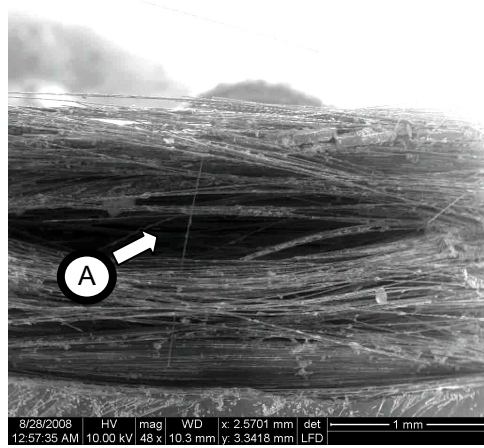
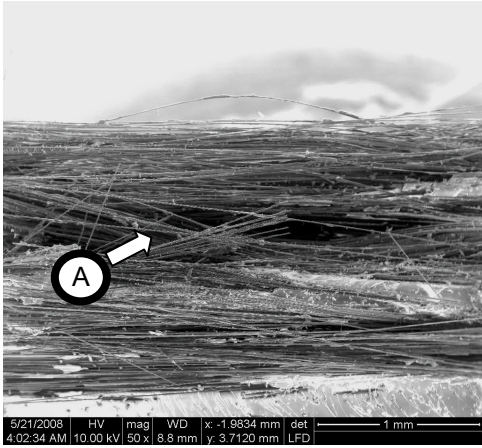


Figure 96 - 40 minute treated unsized fiber transverse tensile failure dry (L) and after seawater exposure (R)

NOTES: (A) This surface condition shows unwetted areas, (B) Both dry and seawater exposed specimens exhibited areas where fractured resin remained attached to the fibers, indicative of good fiber/matrix adhesion, (C) The wet specimen resin showed areas of ductile failure.

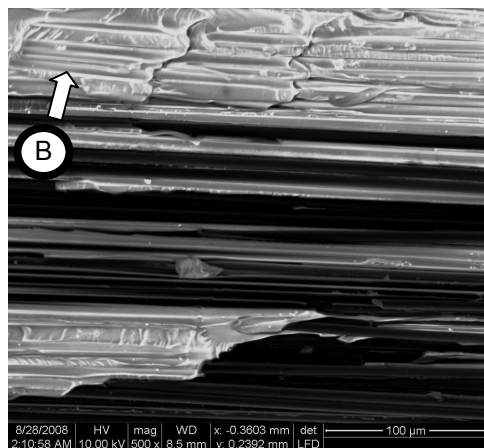
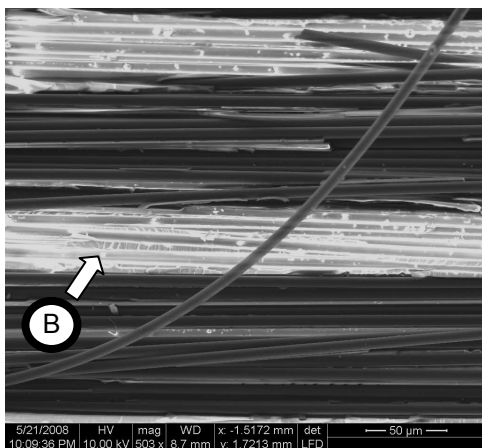
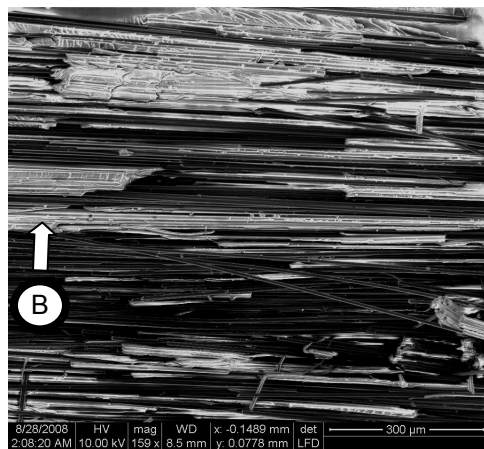
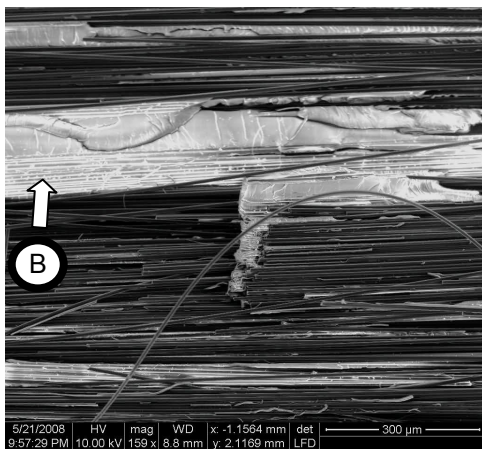
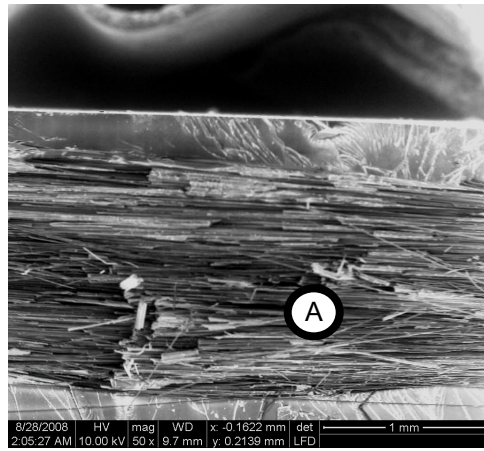
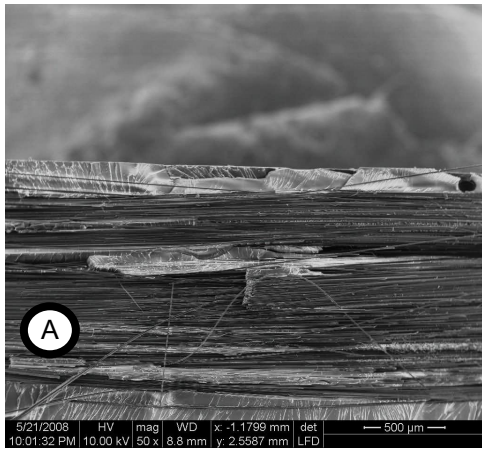


Figure 97 – Silane-treated sized fiber (no acid treatment) transverse tensile failure dry (L) and after seawater exposure (R)

NOTES: (A) This surface condition allows good overall wetting, (B) Both dry and wet specimens exhibit cylindrical channels and bare fibers, indicative of fiber/matrix debonding failure.

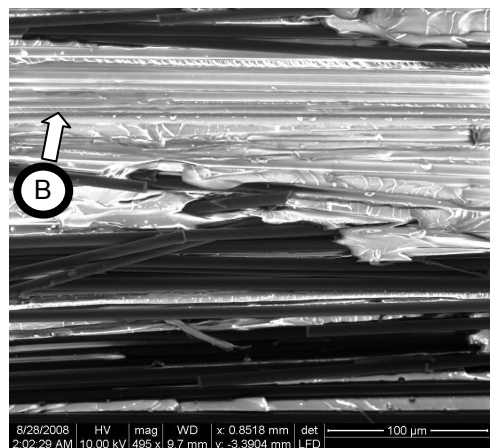
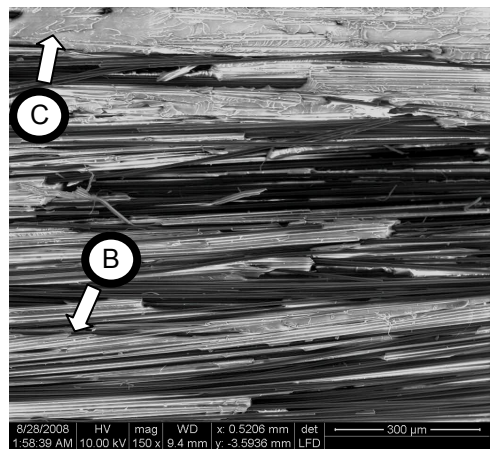
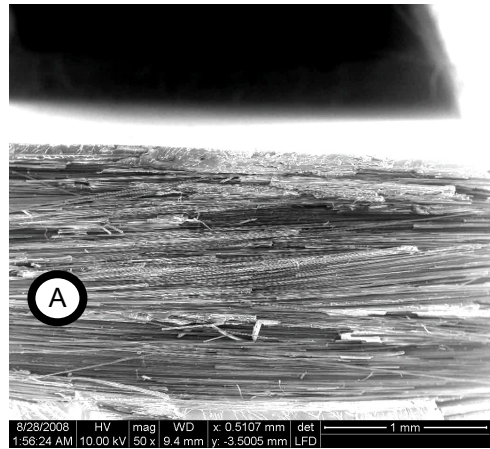
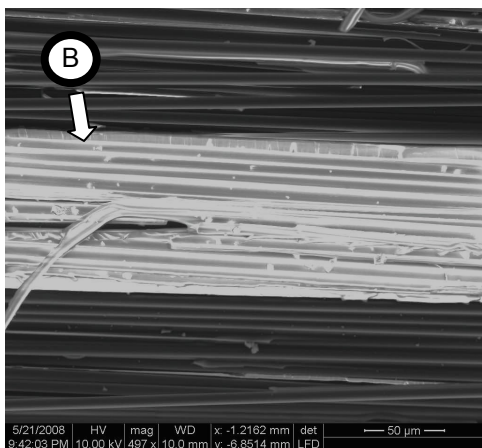
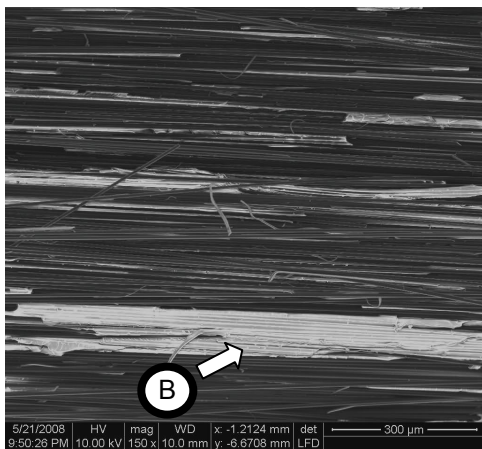
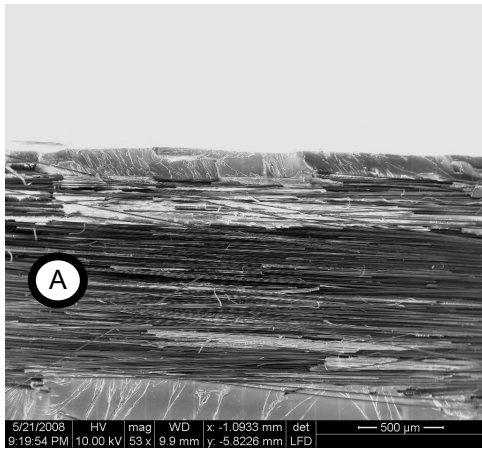


Figure 98 – Silane-treated unsized fiber (no acid treatment) transverse tensile failure dry (L) and after seawater exposure (R)

NOTES: (A) This surface condition allows good overall wetting, (B) Both dry and wet specimens exhibit cylindrical channels and bare fibers, indicative of fiber/matrix debonding failure, (C) The wet specimen showed some areas of ductile fracture.

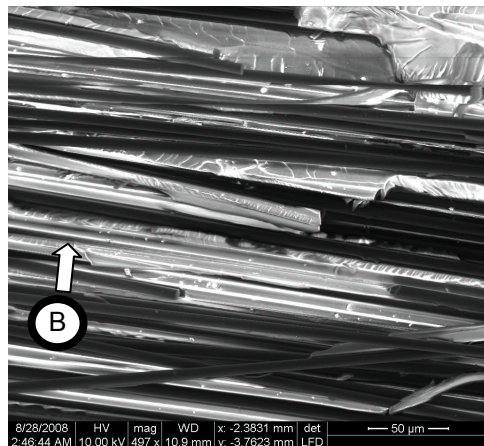
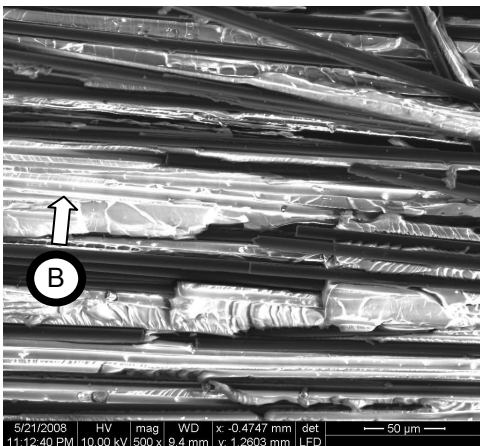
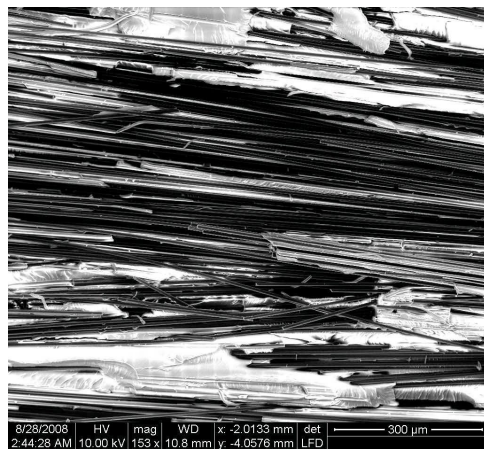
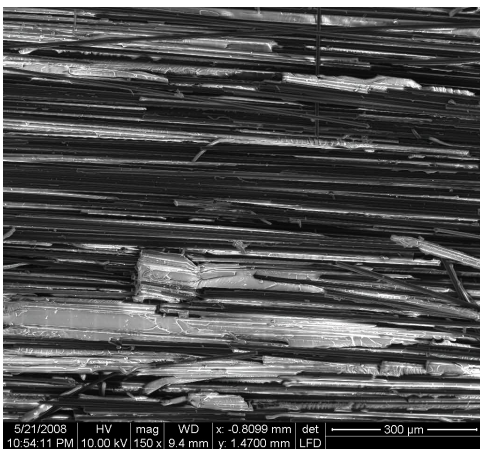
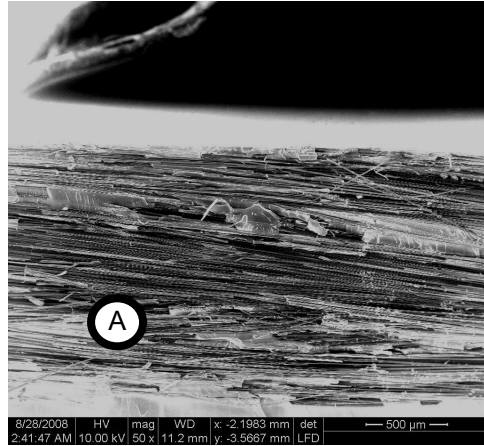
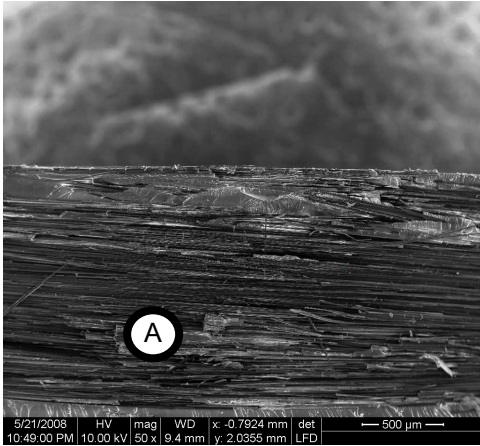


Figure 99 – Silane-treated unsized fiber (2.5 minute acid treatment) transverse tensile failure dry (L) and after seawater exposure (R)

NOTES: (A) This surface condition allows good overall wetting, (B) Both dry and wet specimens exhibit cylindrical channels and bare fibers, indicative of fiber/matrix debonding failure.

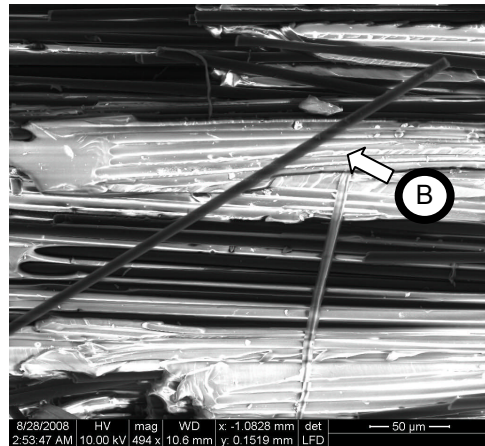
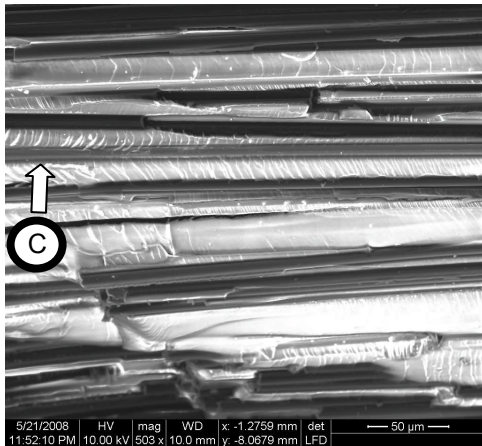
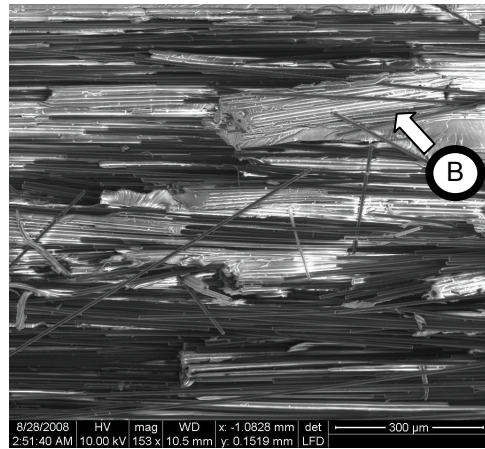
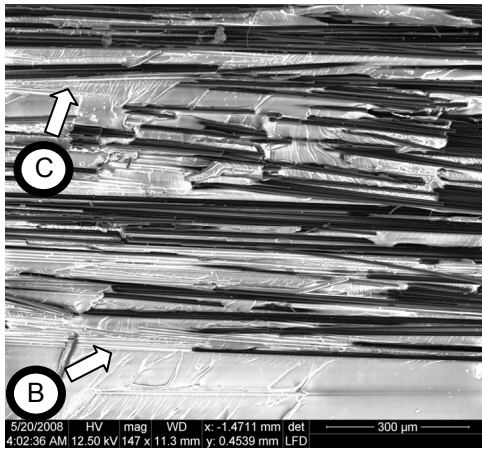
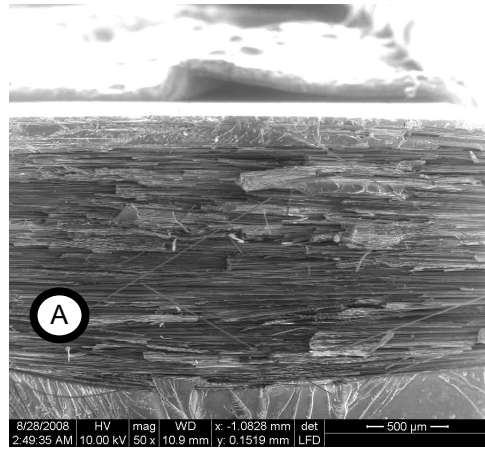
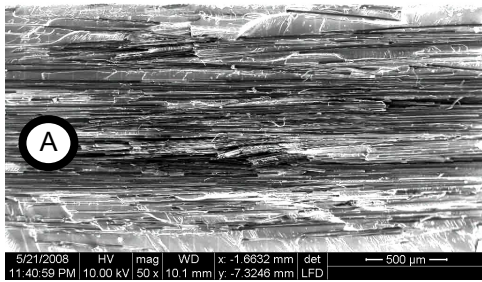


Figure 100 – Silane-treated unsized fiber (20 minute acid treatment) transverse tensile failure dry (L) and after seawater exposure (R)

NOTES: (A) This surface condition allows good overall wetting, (B) Both dry and wet specimens exhibit cylindrical channels and bare fibers, indicative of fiber/matrix debonding failure, (C) The dry specimens showed areas where the matrix failed, instead of the interface. The failure path followed the fiber contour, but did not travel along the interface.

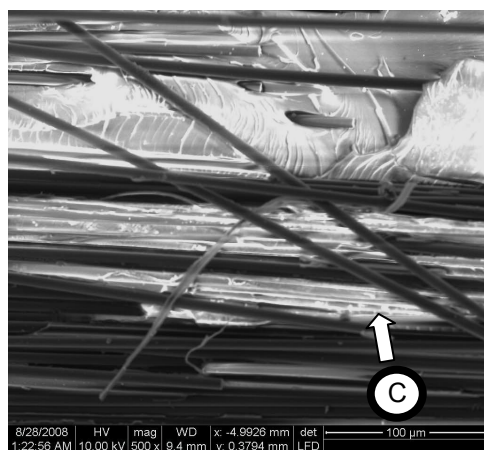
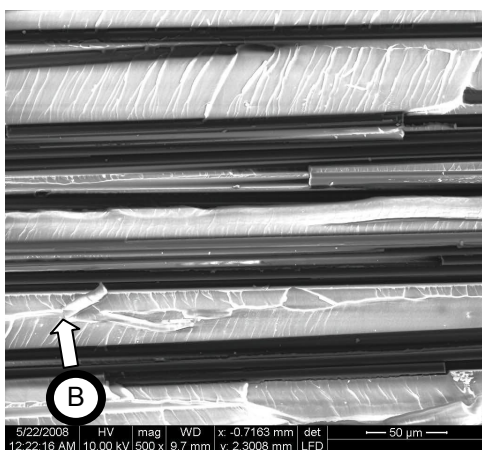
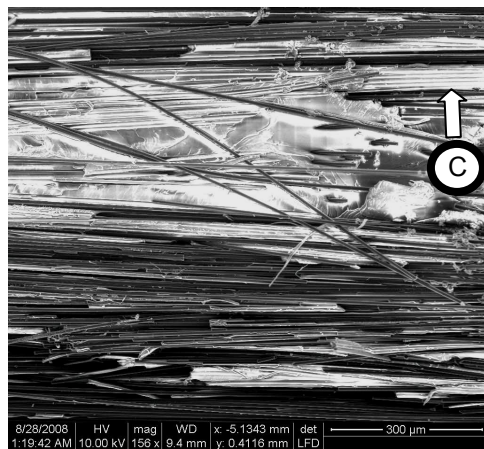
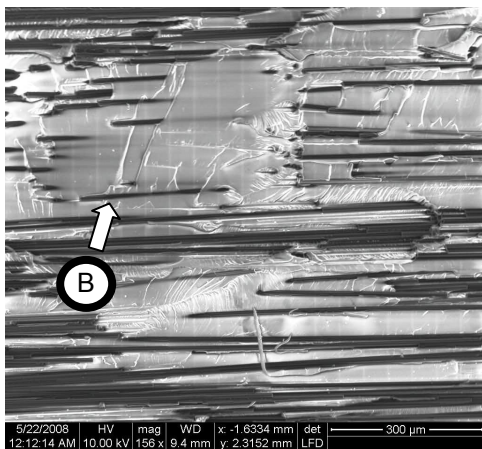
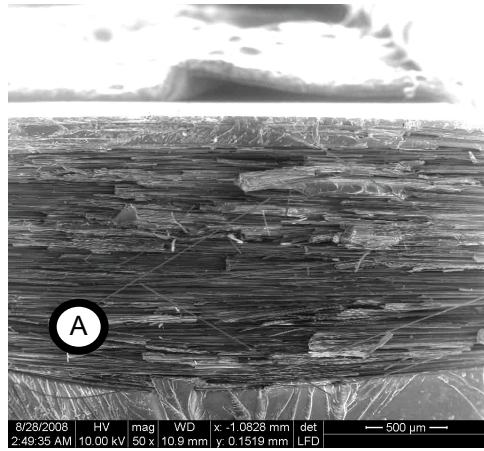
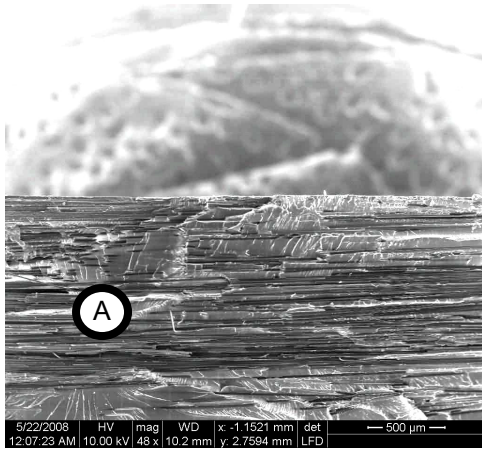


Figure 101 – Silane-treated unsized fiber (40 minute acid treatment) transverse tensile failure dry (L) and after seawater exposure (R)

NOTES: (A) This surface condition allows good overall wetting, (B) The dry specimen showed some fiber debonding, but the matrix failure followed an independent path (not along fiber/matrix interfacial boundaries), (C) The wet specimen showed significant fiber/matrix debonding.

Much information has become available by viewing the failed cross-sections of the transverse tensile specimens. General cross-sectional wetting has been determined, as well as the types of failures. Table 15 and Table 16 summarize the observations found.

PROBLEM TYPE	ACID FIBER TREATMENT TYPE													
	Sized Untreated Fiber		Unsize Untreated Fiber		2.5 Minute Acid Treatment		5 Minute Acid Treatment		10 Minute Acid Treatment		20 Minute Acid Treatment		40 Minute Acid Treatment	
	Dry	Wet	Dry	Wet	Dry	Wet	Dry	Wet	Dry	Wet	Dry	Wet	Dry	Wet
Unwetted Areas								√	√	√	√	√	√	√
Fiber/matrix Debonding	√	√	√	√	√		√	√	√	√	√			
Resin Interfacial Failures (Instead of Debonding)										√		√	√	√
Ductile Resin Failure Mode						√						√		√

Table 15 - Untreated and acid-treated fiber transverse tensile specimen failure types

PROBLEM TYPE	ACID/SILANE FIBER TREATMENT TYPE									
	Sized Untreated Fiber		Unsize Untreated Fiber		2.5 Minute Acid Treatment		20 Minute Acid Treatment		40 Minute Acid Treatment	
	Dry	Wet	Dry	Wet	Dry	Wet	Dry	Wet	Dry	Wet
Unwetted Areas										
Fiber/matrix Debonding	√	√	√	√	√	√	√	√		√
Resin Interfacial Failures (Instead of Debonding)							√		√	
Ductile Resin Failure Mode				√						

Table 16 - Silane-treated transverse tensile specimen failure types

The unwetted areas were identified by looking for fiber areas that had no resin within them. This information is somewhat redundant, but supportive of the results seen in the fiber bundle wettability tests. In the fiber bundle wettability tests, all of the acid-only treated fiber bundles showed unwetted areas. The untreated and silane-treated types showed complete wetting.

Fiber/matrix debonding was observed in all of the fiber treatment types, with a few exceptions. No debonding was seen in the 2.5-minute acid-treated specimen, but it presented with a significant change to ductile resin fracture. Figure 102 shows an enlarged example from above of fiber/matrix debonding. The clean fibers and depressions left in the mating resin are obvious. This example was from the sized, untreated fiber in the dry condition.

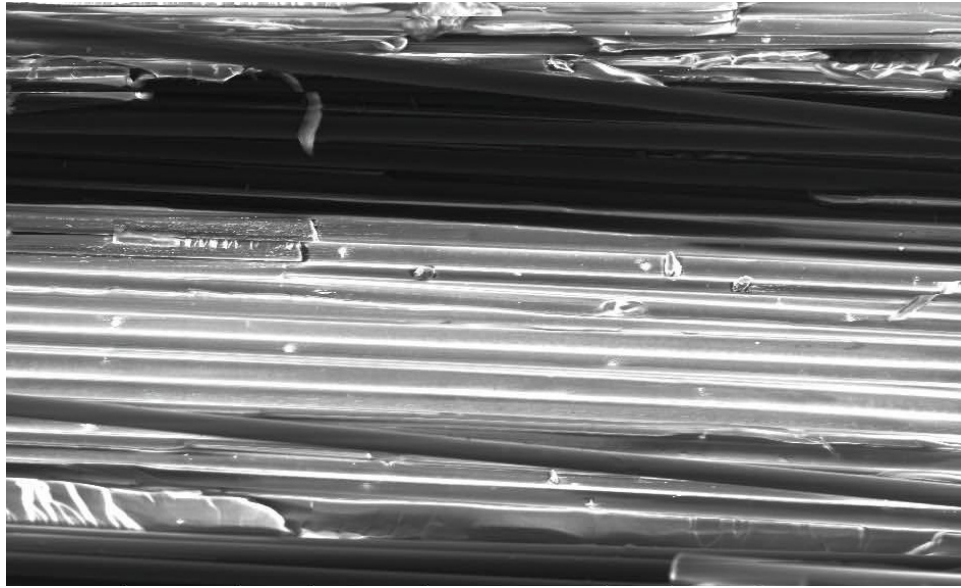


Figure 102 - Example of fiber/matrix debonding observed

Interestingly, the 20-minute acid-only treatment resulted in fiber/matrix debonding when dry, but showed some interfacial resin failure after seawater exposure. This indicates that after seawater exposure, the fiber/matrix bond may have been stronger than the resin, causing the matrix to fail. The 40-minute acid-only treatment presented this type of interfacial resin failure in both the wet and dry conditions. Figure 103 shows an enlarged view of this failure type when dry (40-minute acid treatment), and Figure 104 shows an enlarged view of this after seawater exposure (20-minute acid treatment).

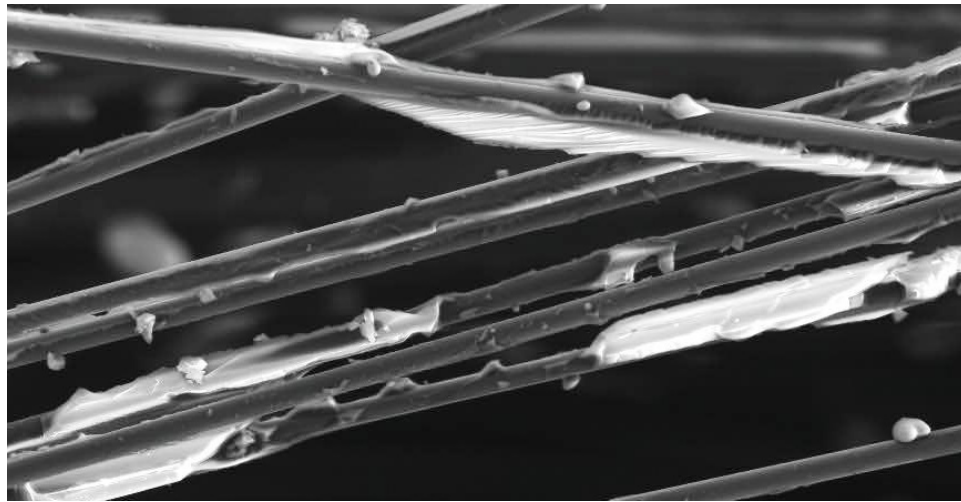


Figure 103 - Example of resin interfacial failure in dry acid-treated composite

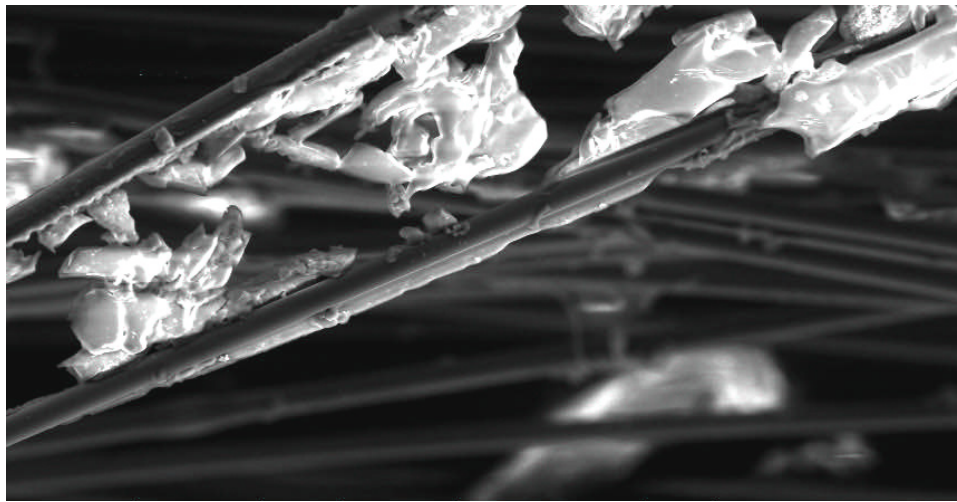


Figure 104 - Example of resin interfacial failure in seawater-exposed acid-treated composite

While the extended acid treatments resulted in poor wetting of the fiber bundles, it appears that they also resulted in strong fiber/matrix adhesion that persisted through seawater exposure. In the dry condition, it can be seen from Figure 103 that the resin attached to the fiber is actually fractured, and not just a bit of resin that was stuck to only

that fiber and no others. This means that the resin was forced to break, rather than debond. The seawater-exposed resin was likely plasticized, which could have reduced the strength of the fiber/matrix bond necessary to break it, but the resin was definitely weaker than the bond.

Plasticization of the resin after water exposure is known to occur and has become evident through failure mode analysis on the resin failure surfaces of the transverse tensile specimens. Before seawater exposure, the fracture surfaces displayed brittle behavior, with smooth cleavage planes and definite regions of crack propagation. See Figure 105, which is enlarged from Figure 93.



Figure 105 - Brittle fracture seen in dry specimens

But after seawater exposure, some specimens exhibited characteristics of ductile failure. They did not show large, smooth cleavage planes and displayed considerable local deformation. Figure 106 shows this failure type, which is an enlarged area of the 2.5-minute treated specimen.

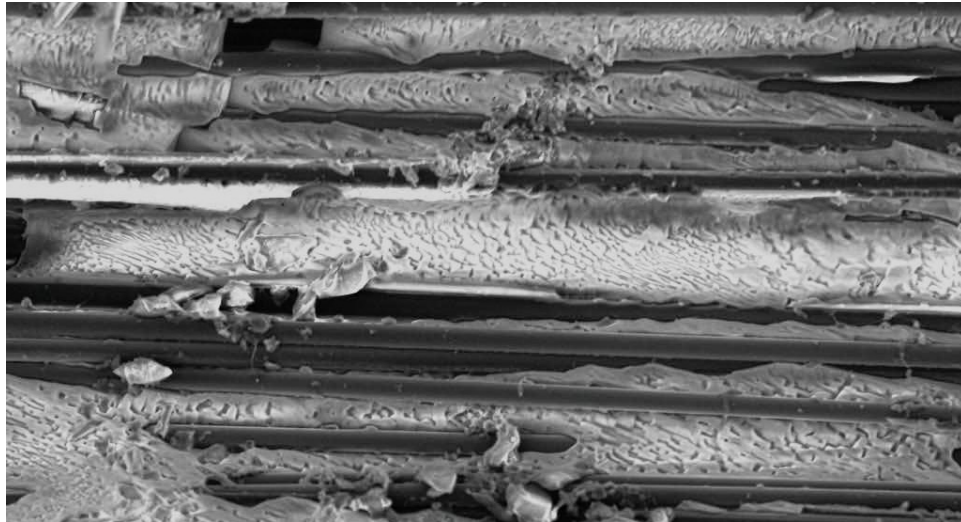


Figure 106 - Ductile fracture seen in seawater-exposed specimens

This can be seen in other seawater-exposed specimens, such as the 20-minute acid-treated specimen (Figure 107).

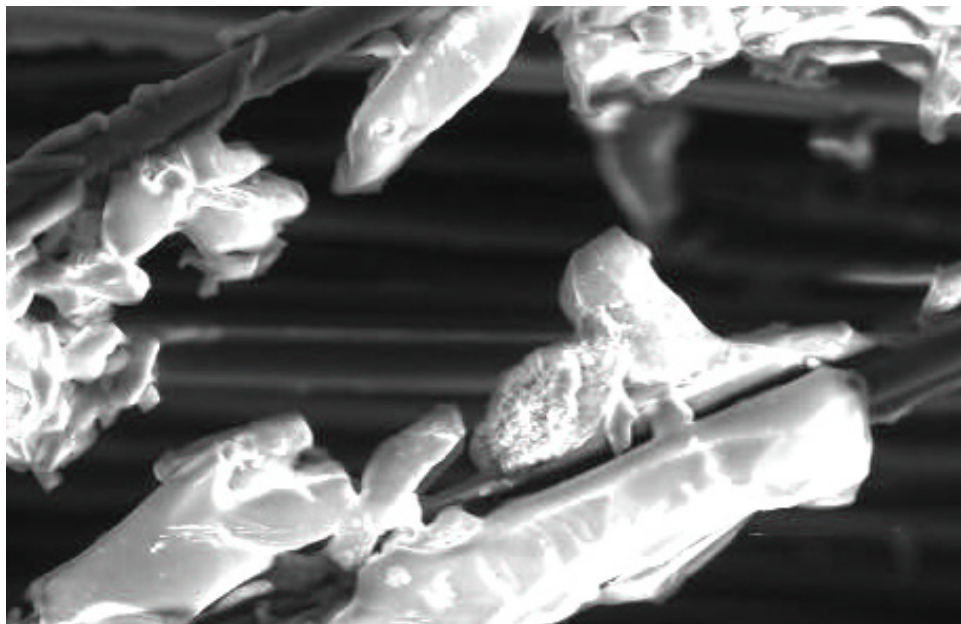


Figure 107 - Ductile fracture seen in seawater-exposed specimens

The dry acid/silane-treated specimens also exhibited matrix failure (instead of debonding) in some areas, but these areas appeared different because of the excellent wetting that was achieved in the silane-treated specimens. Figure 108 shows an enlarged image of this type of failure observed in the 20-minute acid/silane treated specimen.

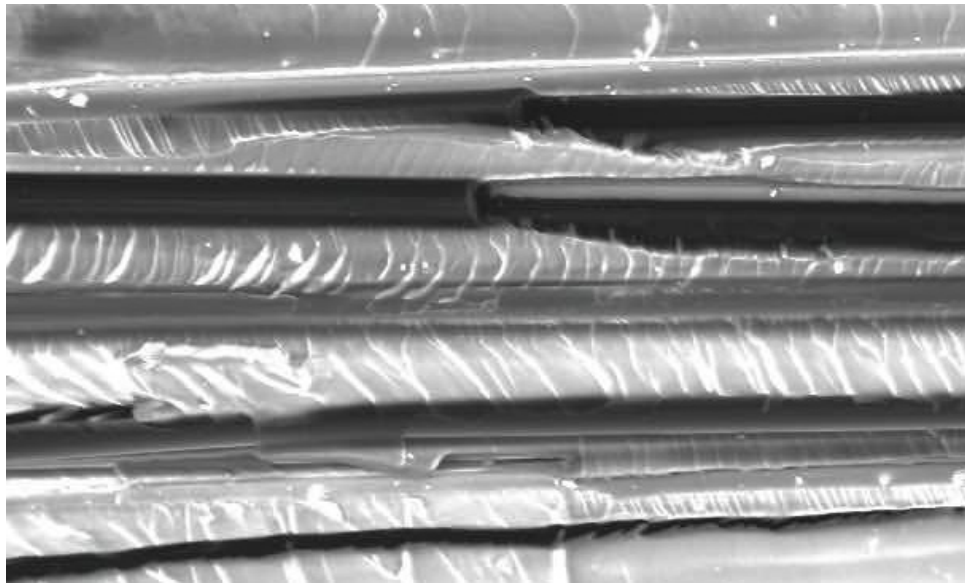


Figure 108 - Example of resin interfacial failure in a silane-treated composite

The dry silane-treated composites also exhibited another type of matrix failure, as shown in Figure 109, which is taken from the dry images of the 40-minute acid/silane treated specimen.

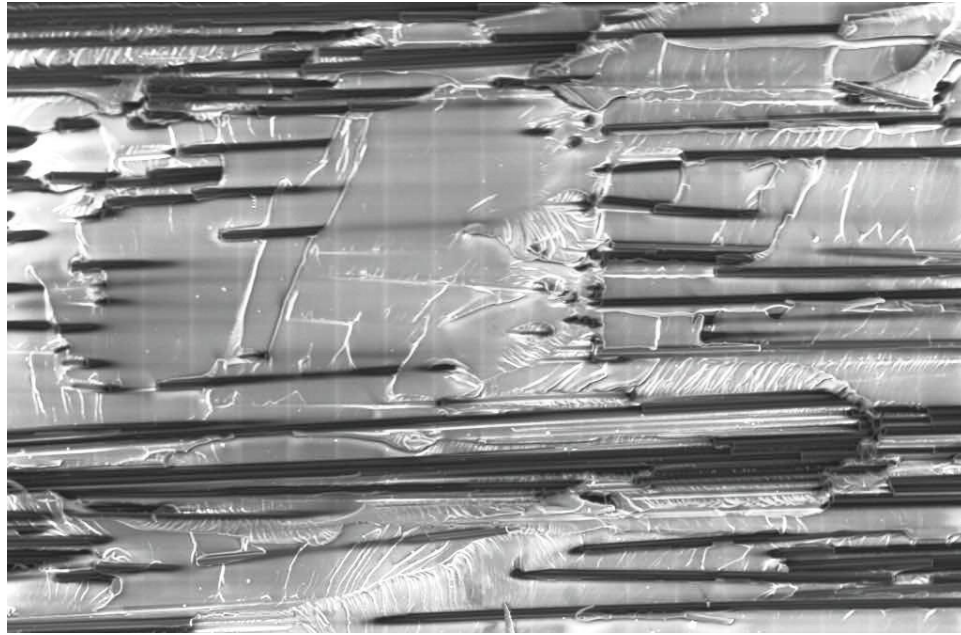


Figure 109 - Example of resin interfacial failure in a silane-treated composite

In this failure type, the matrix failed with apparently no tendency to follow the fiber/matrix interfacial boundaries. There is a straight fracture, and the fibers are only exposed where they interrupted the crack path. Very few channels in the resin from debonding can be found. This possibly indicates that the silane-treated interfacial bond has improved fracture toughness because the cracks do not follow that boundary.

In summary, the acid-only treated fiber bundles resulted in poor wetting in the transverse tensile specimens, which supports the fiber bundle wettability data presented earlier. However, the composites made with fibers that had undergone extended acid treatment showed improved fiber/matrix adhesion, even after seawater exposure, as evidence by resin fracture, instead of debonding. The acid/silane treated fibers resulted in excellent wetting and good adhesion in the dry condition. They also showed resin failure, instead of debonding in some cases. But after seawater exposure, the silane-

treated fiber bundles failed primarily through fiber/matrix debonding. A brittle resin failure mode was observed in dry specimens, but the resin of some specimens failed in a ductile manner after seawater exposure, providing evidence of resin plasticization.

3.2.12 Composite Seawater Weight Gain and Swelling

As mentioned previously, composites are known to absorb a considerable amount of water. Carbon fiber in itself does not absorb water,⁹⁷ but vinyl ester is very absorbent due to the polarity of the polymer chains and free volume (voids), when present. In order to measure composite weight gain and swelling, the need for a macro-composite material with a high fiber fraction was inescapable. If a specimen was used that consisted of a large proportion of resin, such as those containing only a single fiber or bundle, the majority of the weight gain and swelling observed would be due to the neat resin and it would be very difficult to discern any contribution from different fiber surface treatments.

To make macro-composites from treated fiber, it was necessary to treat pre-woven fiber mats. This was done with the method formerly described herein in the Fiber Treatment section. The composites were produced by placing 4 plies of fiber mat (treated or untreated) in between two 15.24 cm x 15.24 cm (6 in. x 6 in.) steel plates with catalyzed and promoted resin, taping the transverse edges with cellophane (packing) tape to prevent fiber extrusion, and compressing the soaked mats with a MTS Insight 50 Electromechanical testing machine. The steel plates were polished to a mirror-like finish and coated with a silicone-based mold release agent. The unsized fiber was not available in the woven mat form, so it was necessary to first wrap the tow around a frame several

times to simulate a fiber mat before introduction into the composite. The tow was wrapped so that there was the same number of bundles per width as the sized fiber mat that was used. Compression was necessary to form the composites because there was a significant difference in wettability between some of the different fiber treatments. All composite panels were made with the fiber layers oriented in a unidirectional direction. It should be noted that the Vacuum Assisted Resin Transfer Molding (VARTM) process was initially attempted, but no composites could be made with the acid-treated treated fiber, due to extremely poor wetting. VARTM was not attempted with acid-treated fibers that had also been treated with silane. The composites were prepared by first using a hand lay-up method and then compressing, first to 344 kPa (50 psi) and then to 688 kPa (100 psi), and left under pressure overnight to cure. After removal and post-cure (24 hours at room temperature followed by 2 hours at 120°C), the composite panels were then cut into 63.5 mm (2.5 in.) x 12.7 mm (.5 in.) specimens with the fiber ends exposed along the long direction of the specimen. The panels were approximately 1 mm thick. See Figure 110. Panels were made with sized and unsized fiber, as well as three acid treatment times (2.5, 5 and 10 minutes) and one acid treatment (5 minutes) followed by silane treatment. No attempts were made to form composites with fiber treated for more than 10 minutes, due to the increasingly poor wetting observed in the lower treatment times.

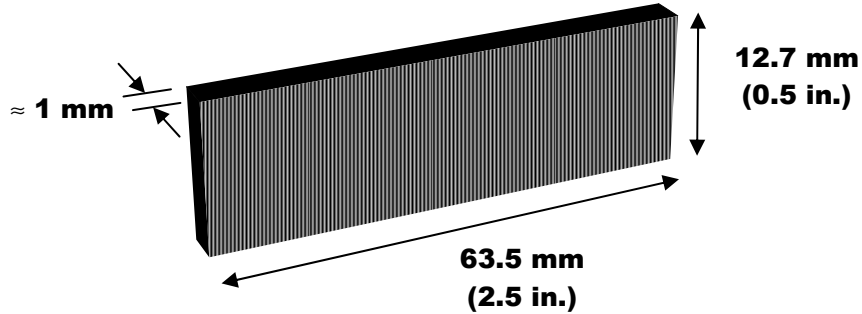


Figure 110 - Composite weight gain and swelling specimen

The composite specimens were immersed in 40°C seawater, and periodically removed, wiped dry, weighed and measured. There were ten samples of each composite type. The specimens were always dried in exactly the same way and left in open air for the same amount of time before weighing. They were each removed from the seawater bath, dried with paper towels (including edges), dried again with a fresh paper towel, measured for swelling, and then dried again with another fresh paper towel before weighing. Length was measured during the drying process to allow more drying time before weight measurement. Only the longitudinal direction was measured. The thickness was too small to accurately measure small dimensional changes and little swelling was expected in the fiber direction, due to fiber resistance to elongation. The weight gain and swelling of the various composites was carried out for a period of 134 days, when it was decided that all of the data sets had reached stable values.

Figure 111 and Figure 112 show the weight gain and swelling data, respectively, expressed as percent changes.

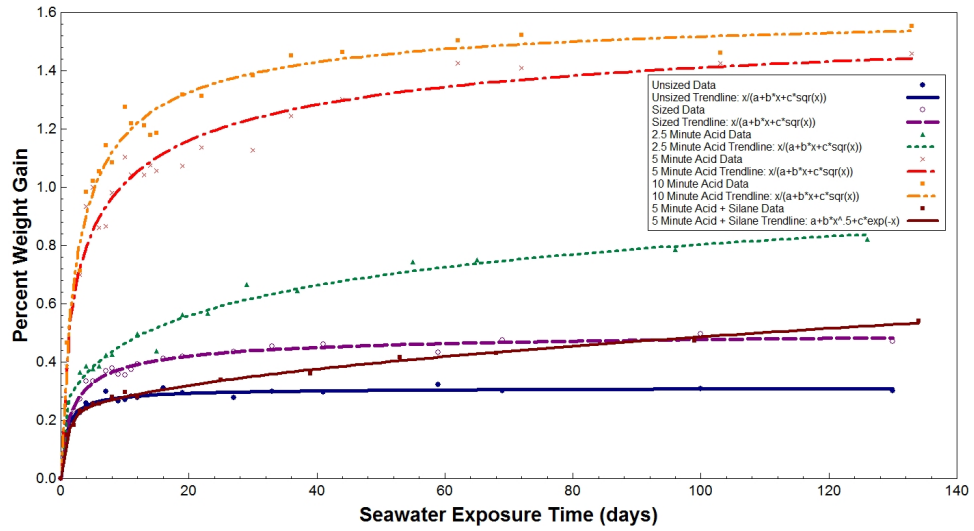


Figure 111 - Percentage weight gain of composites in seawater with different fiber surface treatments

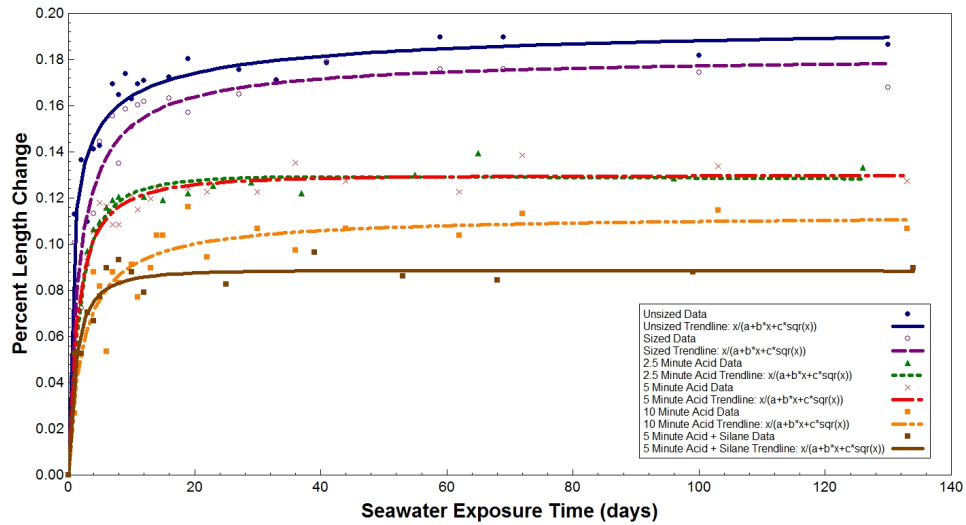


Figure 112 - Percentage length change of composites in seawater with different fiber surface treatments

All of the weight gain and swelling change curves could be represented by the same equation, except for the weight gain of the acid/silane treated specimen. The common equation was:

$$\frac{x}{(a + bx + c\sqrt{x})} \quad (27)$$

And the best-fit equation for the acid/silane specimen weight gain was:

$$a + bx^{0.5} + c \cdot \exp(-x) \quad (28)$$

Both equations were solved by nonlinear regression. The constants for the weight gain equations were found to be:

	COMPOSITE WEIGHT GAIN EQUATION CONSTANTS		
	a	b	c
Unsize	1.71	3.15	0.82
Sized	1.83	1.91	1.72
2.5 Minute Acid Treated	-2.14	0.76	5.09
5 Minute Acid Treated	0.44	0.60	1.09
10 Minute Acid Treated	1.15	0.61	0.40
5 Min Acid + Silane	0.19	0.03	-0.19

Table 17 - Constants for composite weight gain equations

The constants for the length change equations were found to be:

	COMPOSITE LENGTH CHANGE EQUATION CONSTANTS		
	a	b	c
Unsize	1.39	5.00	3.02
Sized	8.27	5.46	1.05
2.5 Minute Acid Treated	16.28	8.09	-4.76
5 Minute Acid Treated	12.23	7.80	-2.06
10 Minute Acid Treated	19.33	8.82	0.93
5 Min Acid + Silane	14.37	11.52	-3.65

Table 18 - Constants for composite length change equations

Comparing the weight gain data with the geometric swelling of the seawater-immersed composites provides interesting information. The composite specimens with

more extensively acid-treated fibers gained more weight. However the order of increasing swelling was the opposite. Less swelling occurred with longer treatment time, with the exception of the 2.5 and 5-minute treatments, which were approximately equal. While more weight was gained by composites with longer fiber acid-treatments, less dimensional swelling occurred. The order of weight gain and swelling for the composites made with nitric acid-treated fiber was as follows:

	DESCENDING ORDER OF WEIGHT GAIN AND SWELLING OF ACID-TREATED FIBER COMPOSITES	
	WEIGHT GAIN	SWELLING
1	10 Minute Acid Treatment	Unsize Untreated Fiber
2	5 Minute Acid Treatment	Sized Untreated Fiber
3	2.5 Minute Acid Treatment	2.5 Minute Acid Treatment
4	Sized Untreated Fiber	5 Minute Acid Treatment
5	Unsize Untreated Fiber	10 Minute Acid Treatment

Table 19 - Weight gain and length change order rankings

There are two likely explanations as to why the composites with more extensively acid-treated fibers gained more weight. The increasing water absorption with treatment time could indicate that the increased polarity at the interface attracts more water and/or there are more voids to contain water in the more highly treated specimens. It is likely a combination of both, but the inverse weight gain and swelling behavior strongly suggests the presence of more voids associated with longer treatments. The composite doesn't have to swell as much because as water enters, it already has space for it (voids). This is supported by the poor wetting observed with treatment in the bundle wettability test

described previously herein, and upon SEM examination, it was found that voids were more easily identified in the composite specimens made with treated fibers. This is presented in the following section.

It was shown in the fiber surface wettability section through tensiometry measurements that the longer the fibers were treated in acid, the more attractive they became to water (as evidenced by the lower contact angle). It is possible that some of the available polar bonding sites of the treated fiber surfaces are satisfied through bonding to the resin, but there may also be some degree of fiber polarity that is not satisfied through bonding that serves to attract more water into the composite. All types of bonds (ionic, covalent and hydrogen) involve only a limited number of interaction partners. When there are relatively fewer reactive sites on the fiber surface when compared to that of the resin, there is less available reactivity left after composite formation to attract water. However, when the fiber surface contains a relatively high amount of reactive sites in comparison to the surrounding resin, there is an excess amount of fiber surface reactive sites that are not consumed and likely attract water.

The composite formed with fiber that had been silane treated after acid treatment behaved differently (and favorably) when compared to the other types. The composite made with acid/silane treated fibers showed very little weight gain and very little swelling. The acid/silane composite type gained less weight than all of the acid-treated fiber composites, as well as the sized, untreated fiber composite. Only the unsized fiber composite type gained less weight. The acid/silane composite type also showed the least swelling of all the composite types. As shown through tensiometry measurements in the fiber wettability section herein, acid-treated fibers that are treated with silane show a

large reduction in polar surface energy. Additionally, the single bundle wettability tests showed that the acid/silane treated fibers are easily wetted by the vinyl ester resin. These two factors lead to a composite that has a nonpolar fiber/matrix interface and very little free volume. The reduced polarity of the acid/silane fiber surface was also verified through tensiometry measurements and the improved wettability and low void content was verified through single bundle wettability tests and void content measurement through acid digestion.

Both the increased fiber surface polarity and decreased wettability with longer nitric acid treatment explain the increasing seawater weight gain with increasing fiber acid-treatment times. However, the reciprocal effect of less swelling with more weight gain can only be described by the presence of larger quantities of free volume within the composites with longer acid treatment times. The composites made with acid and silane treated fibers showed very little weight gain and swelling, presumably due to the minimal fiber surface polarity and excellent wettability, which results in low void content.

3.2.13 Composite Cross-sectional Analysis and Seawater Damage

A question that arises with an increase in polarity of the fiber/matrix interface is whether that polarity serves to attract even more water. Fiber surface treatments may help to form chemical bonds between the fiber and matrix, but if more water is drawn to the interface, or within the composite in general, any benefit may be lost. Composite damage after seawater exposure was investigated by cross-sectioning unstressed specimens, before and after three months of seawater exposure. The composites that were evaluated were the same ones that were used to measure weight gain and swelling.

The fiber surface conditions consisted of sized and unsized fiber, as well as three acid treatment times (2.5, 5 and 10 minutes) and one acid treatment (5 minutes) followed by silane treatment. Fiber/matrix debonding and localized composite cracking were searched for by cross-sectioning the composites, polishing the surfaces and examining them in a SEM. Polishing was conducted by first cutting the composite specimen near its center with a diamond-tipped blade on a low-speed saw. The cut surface was then wet-sanded with 400, 600, and 800-grit sandpaper. Finally, the surfaces were polished with 3 μ m and 1 μ m particulate pastes. Magnifications of 200x, 500x, 1000x and 3000x were used for SEM analysis of each treatment. In addition, magnifications of 100x and 7000x were also sometimes used to view interesting features that were found. Using several different magnifications provides different information for the same material. For example, the distribution uniformity of the fibers and resin can be more easily seen at lower magnifications, but higher magnifications are required to see areas of fiber/matrix debonding. The primary features that were sought out in the micrographs were (1) the uniformity of fiber/resin distribution, (2) areas of poor wetting, (3) fiber/matrix debonding and (4) cracking. The dry condition cross-sections are shown below in Figure 113 through Figure 118, with the corresponding seawater-exposed cross-sections shown in Figure 119 through Figure 124. Interesting features are marked on the micrographs and a short explanation follows each figure, with a general discussion at the end.

Dry Condition

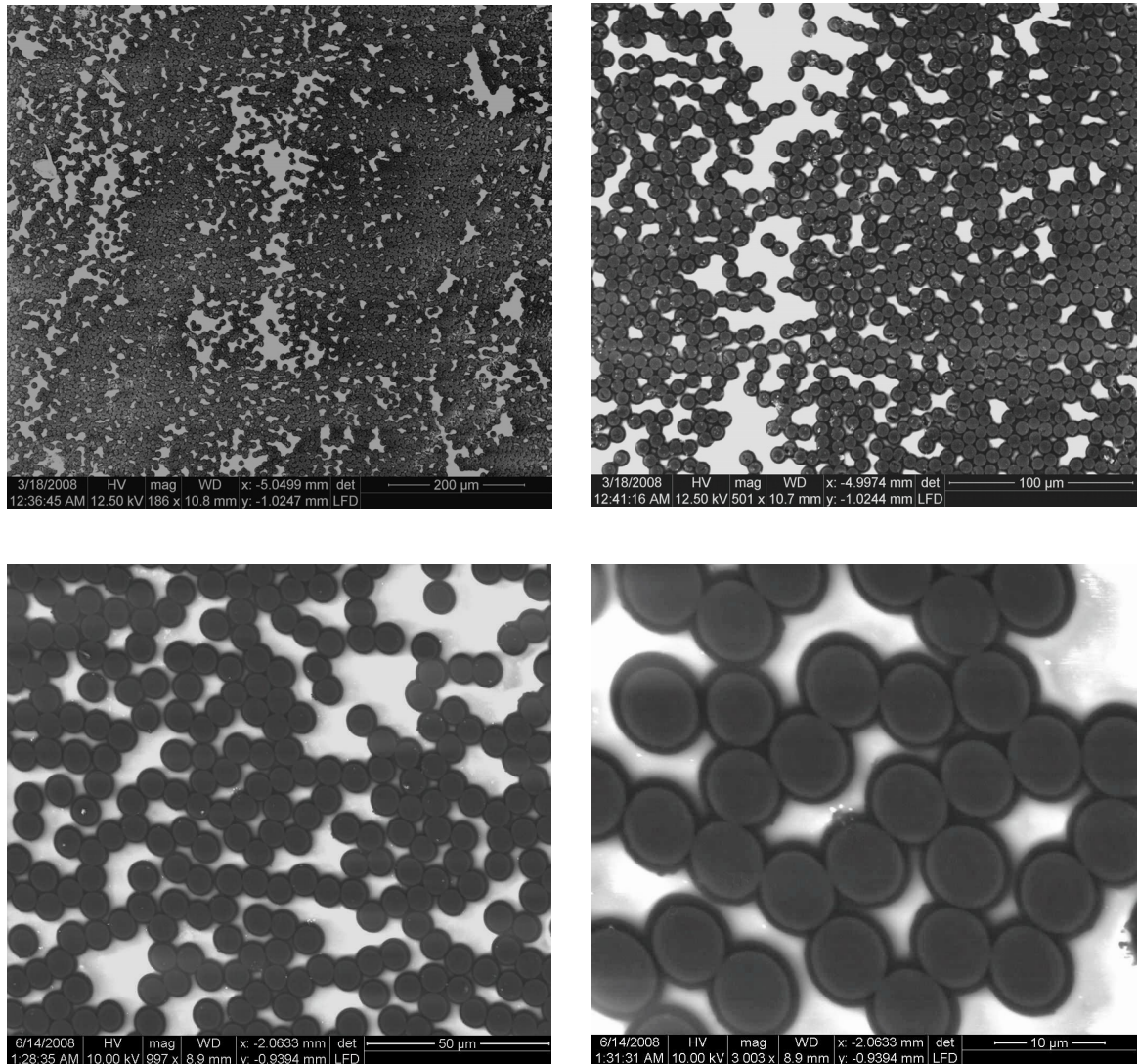


Figure 113 – Dry, sized fiber composite cross-sectional views

Examination of the dry sized (T700) fiber composite reveals that the fibers are uniformly distributed and wetting is complete. No cracks or debonds are found.

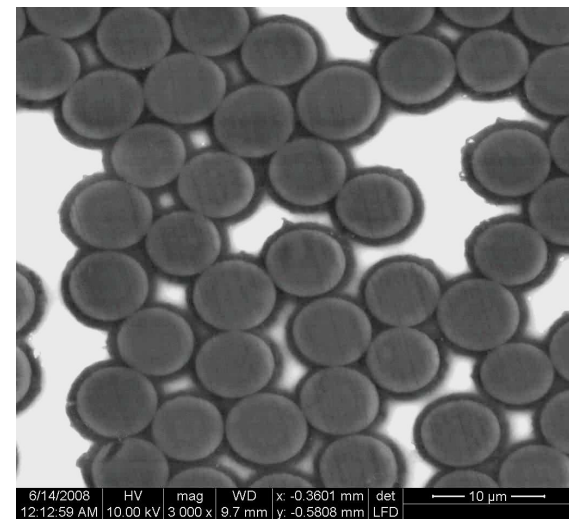
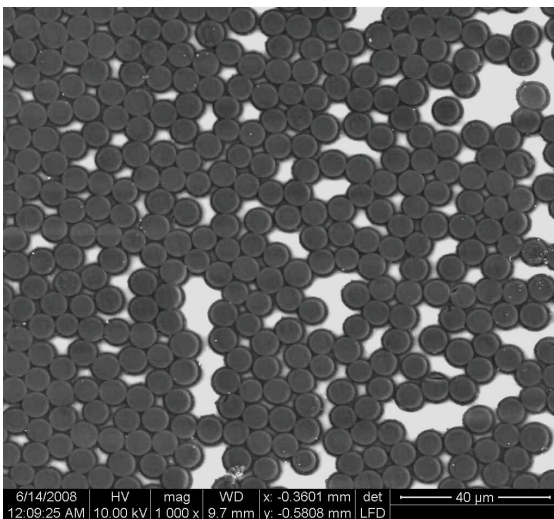
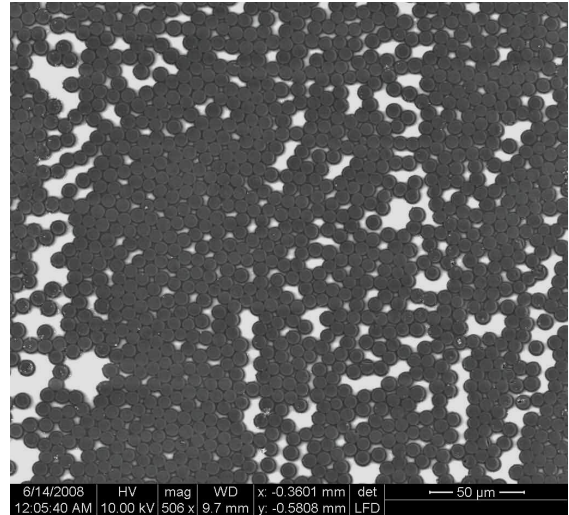
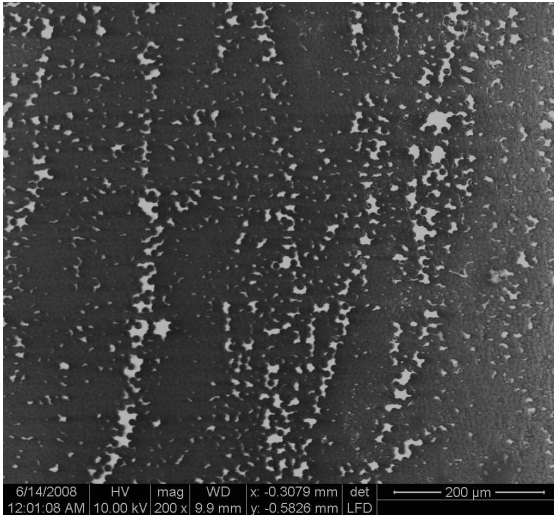


Figure 114 – Dry, unsized fiber composite cross-sectional views

Like the dry sized (T700) fiber composite, the dry unsized (AS4) fiber composite contains an even distribution of fibers and resin, complete wetting, with no cracks or debonding.

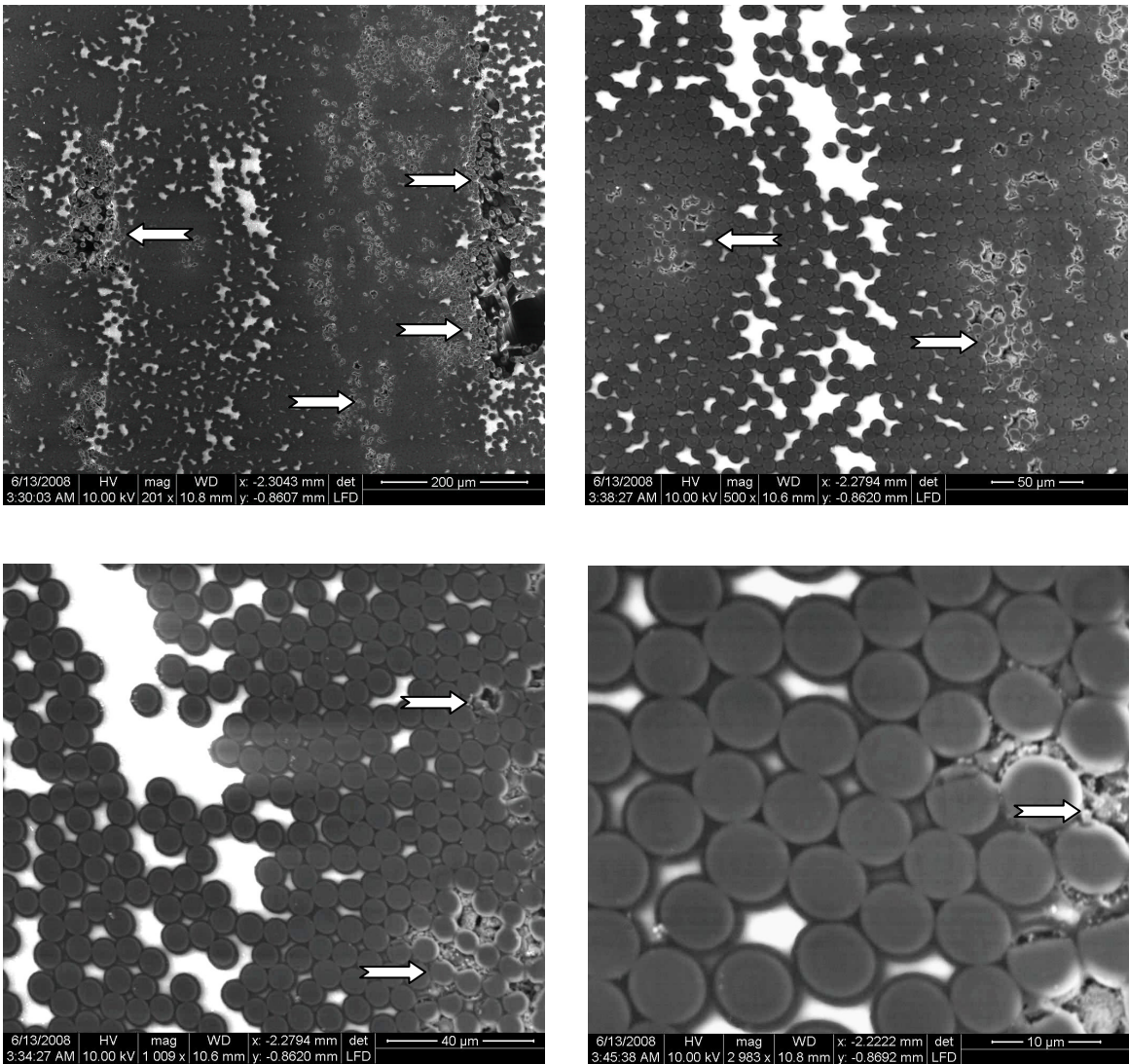


Figure 115 – Dry, 2.5-minute acid-treated sized fiber composite cross-sectional views

The dry composite made with 2.5-minute acid-treated fiber shows areas of non-uniform fiber distribution and areas that did not wet completely. These are marked on the figures.

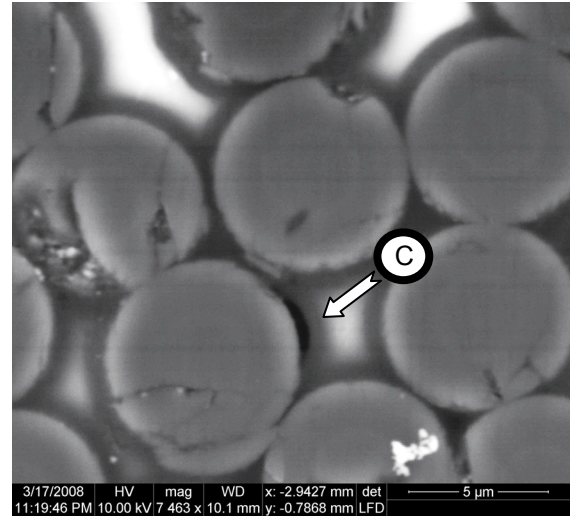
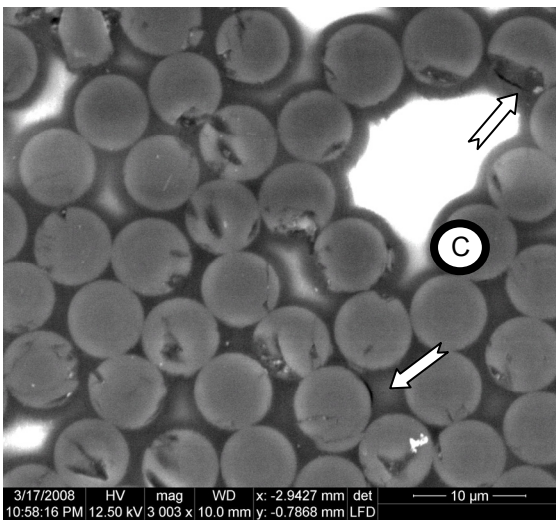
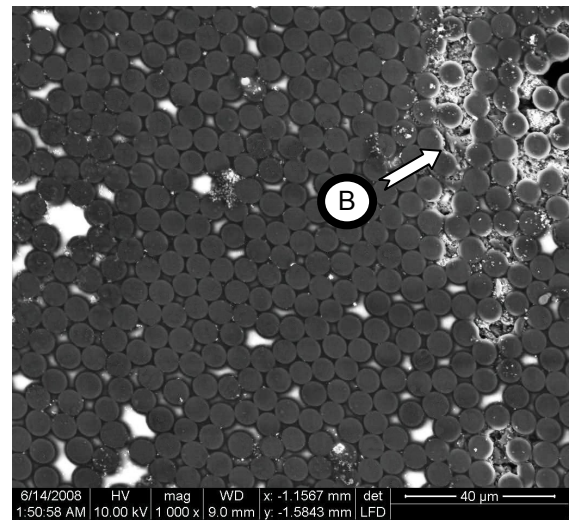
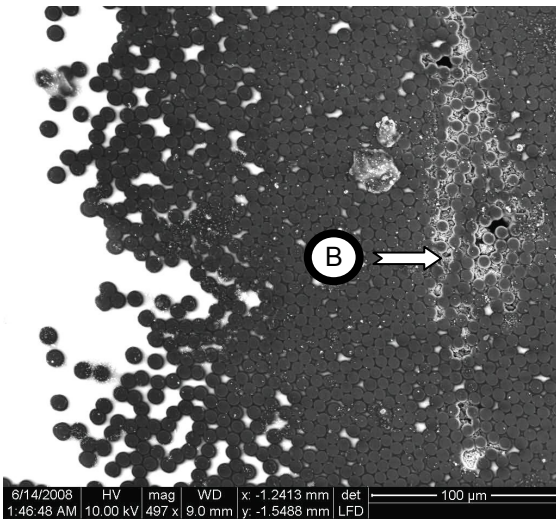
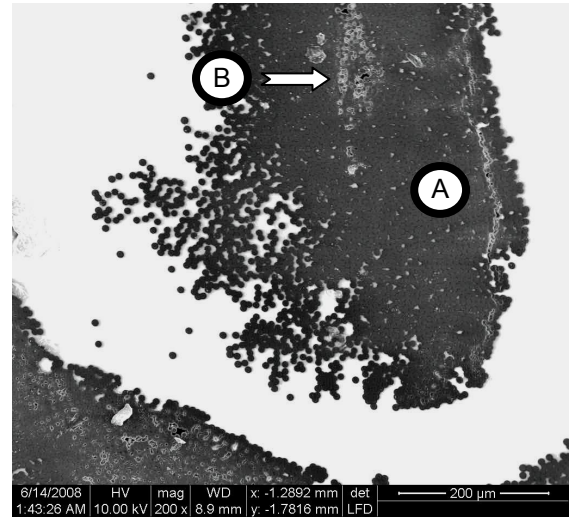


Figure 116 – Dry, 5-minute acid-treated sized fiber composite cross-sectional views

The dry composite made with fibers that had been acid-treated for 5 minutes shows: (A) Areas of extremely uneven fiber/matrix distribution. It appears as though the fiber bundles cohered together and channels of resin flowed in between. (B) Areas of incomplete wetting. (C) Fiber/matrix debonding.

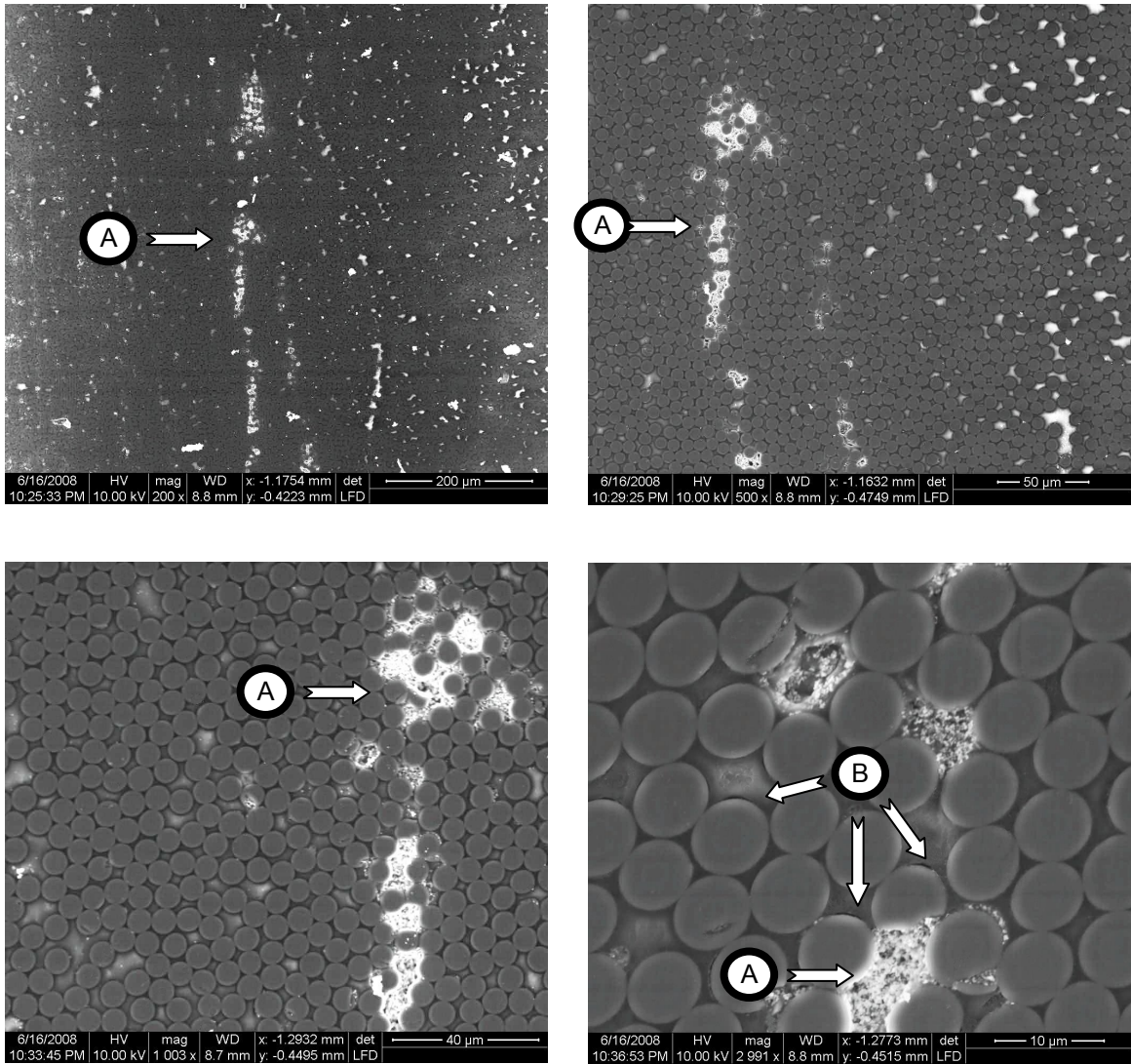


Figure 117 – Dry, 10-minute acid-treated sized fiber composite cross-sectional views

The dry composite made with fibers that had been acid-treated for 10 minutes shows: (A) Areas of incomplete wetting, and (B) Fiber/matrix debonding.

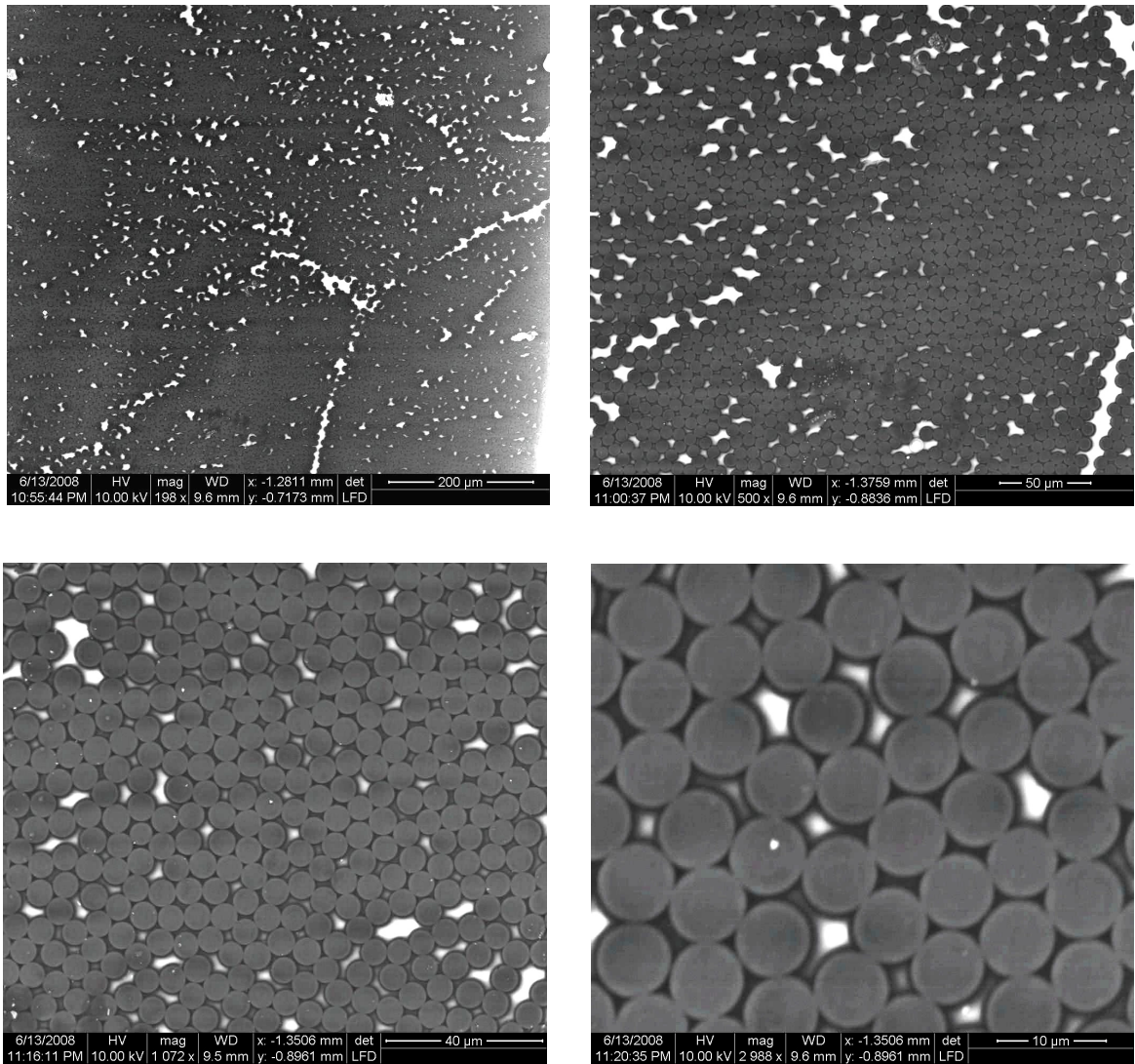


Figure 118 – Dry, 5-minute acid-treated and silane-treated sized fiber composite cross-sectional views

Although 5-minute acid treatment alone results in a dry composite with non-uniform fiber/resin distribution, areas of unwetted fiber and fiber/matrix debonding, following the 5-minute acid treatment with silane treatment resulted in a composite with uniform fiber/resin distribution, complete wetting, and no cracks or debonds.

Wet Condition

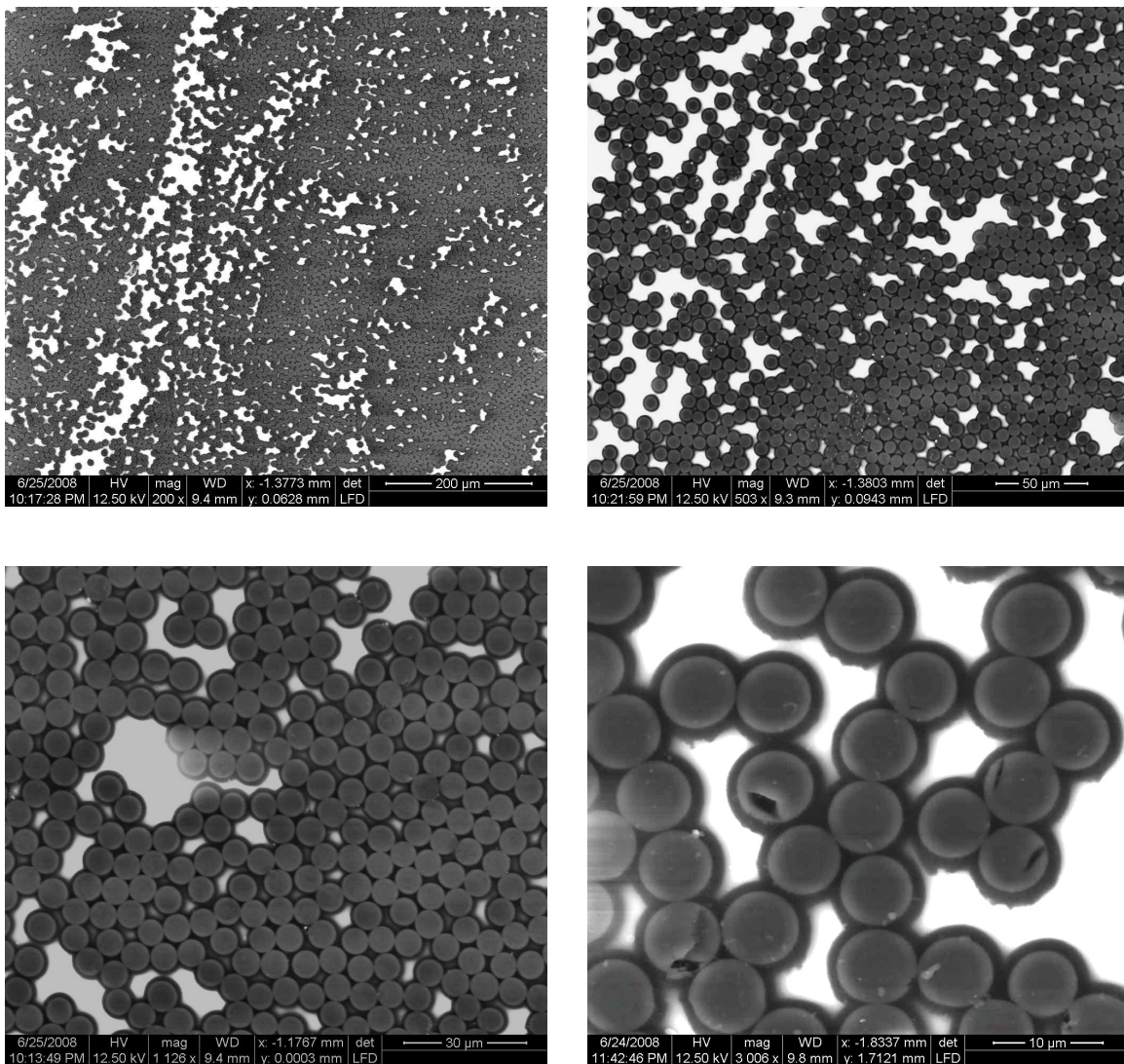


Figure 119 – Seawater-exposed, sized fiber composite cross-sectional views

After three months of exposure to 40° C seawater, the composites made with sized (T700) fiber showed no cracking or debonding.

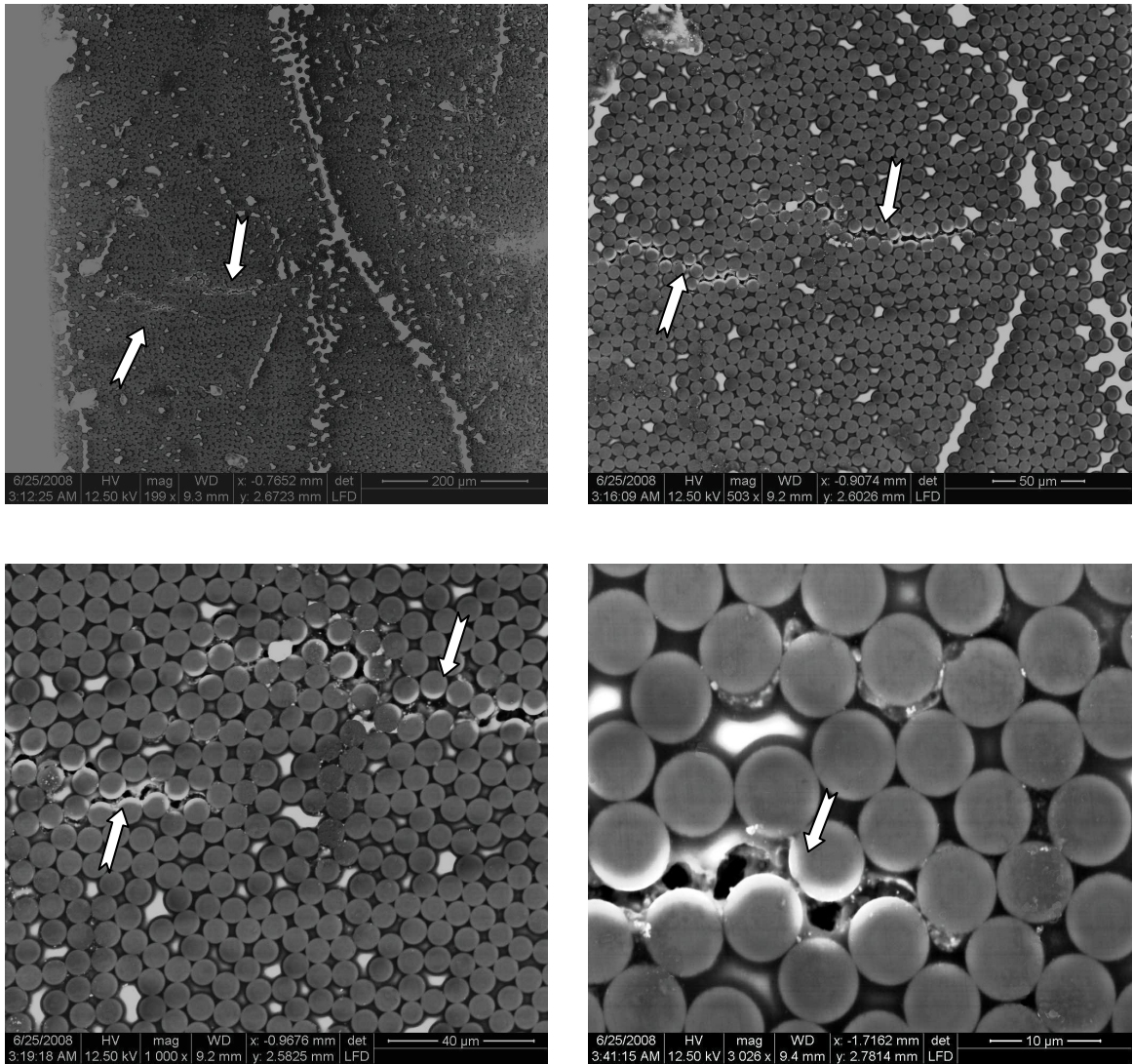


Figure 120 – Seawater-exposed, unsized fiber composite cross-sectional views

After three months of exposure to 40° C seawater, the composites made with unsized (AS4) fiber some significant cracking, which followed the boundaries of the fiber/matrix interface. These areas are marked on the figure.

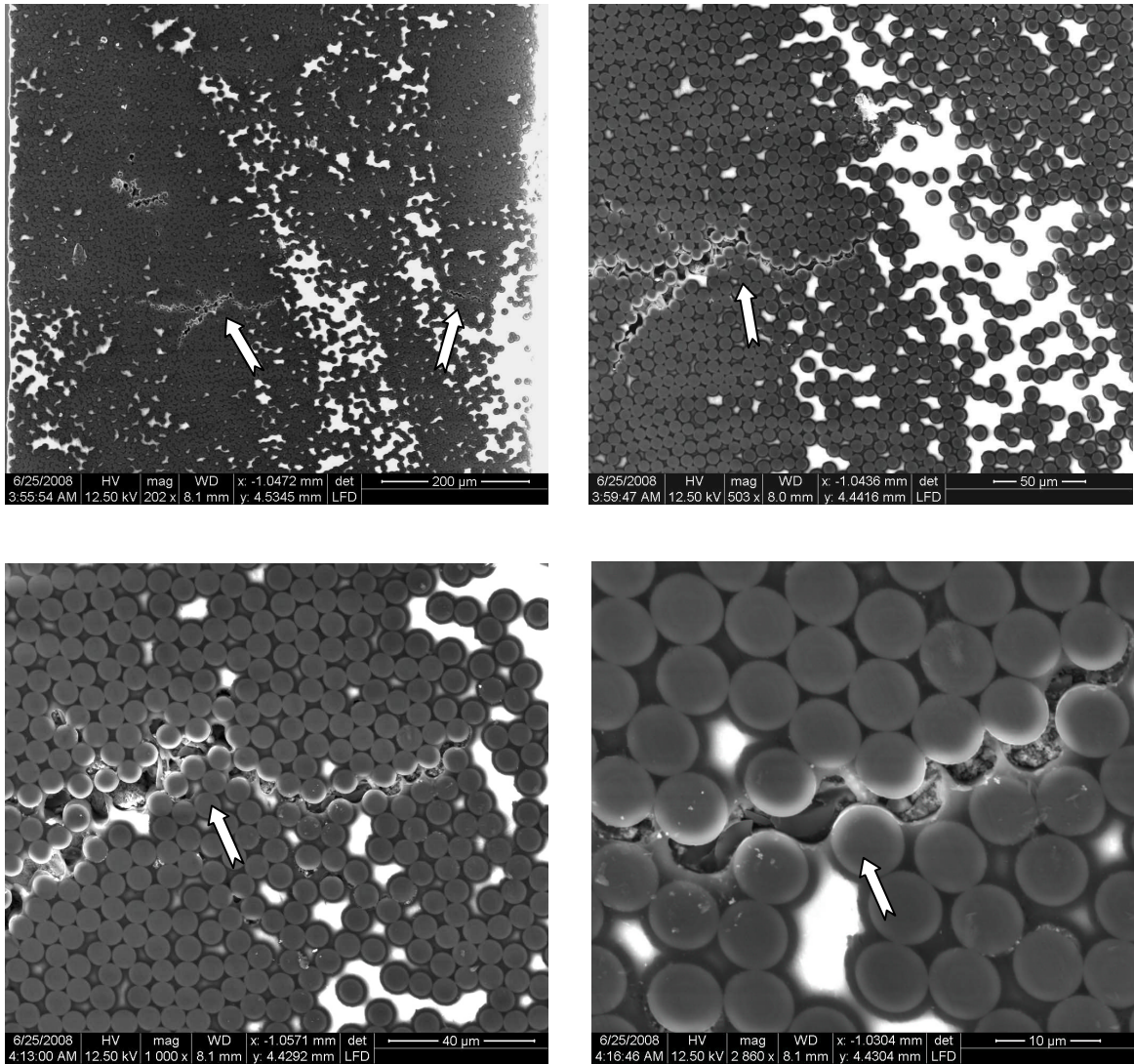


Figure 121 – Seawater-exposed, 2.5-minute acid-treated sized fiber composite cross-sectional views

After three months of exposure to 40° C seawater, the composites made with 2.5-minute acid-treated fiber showed some cracking, which followed the boundaries of the fiber/matrix interface. This cracking was similar to that seen with the unsized, untreated fiber, maybe slightly worse. These areas are marked on the figure.

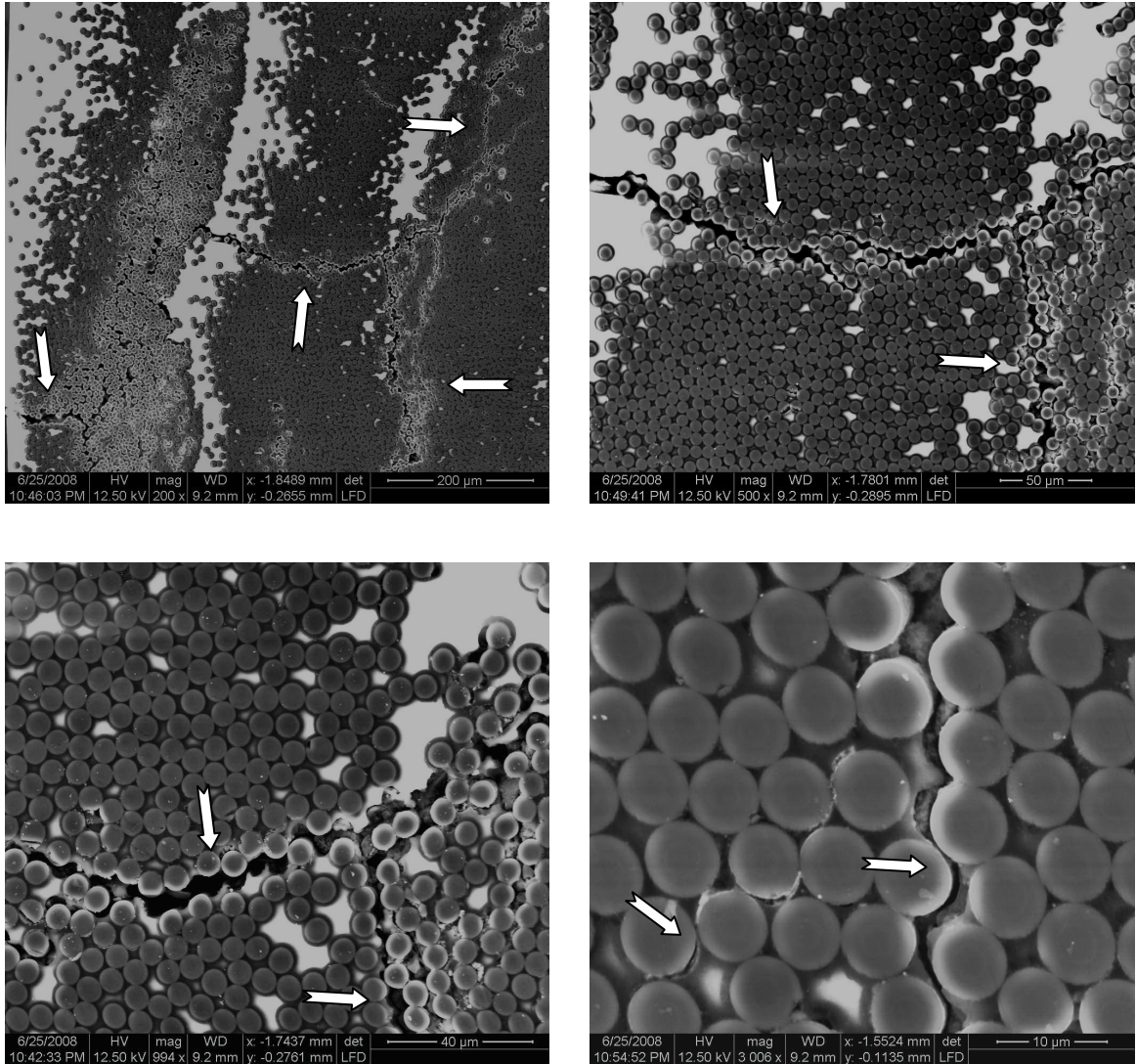


Figure 122 – Seawater-exposed, 5-minute acid-treated sized fiber composite cross-sectional views

After three months of exposure to 40° C seawater, the composites made with 5-minute acid-treated fiber showed extensive areas of cracking, which extended into wetted areas, as well as unwetted areas. This cracking followed the fiber/matrix interface, and

was worse than that seen at lesser treatment times. The areas of cracking are marked on the figure.

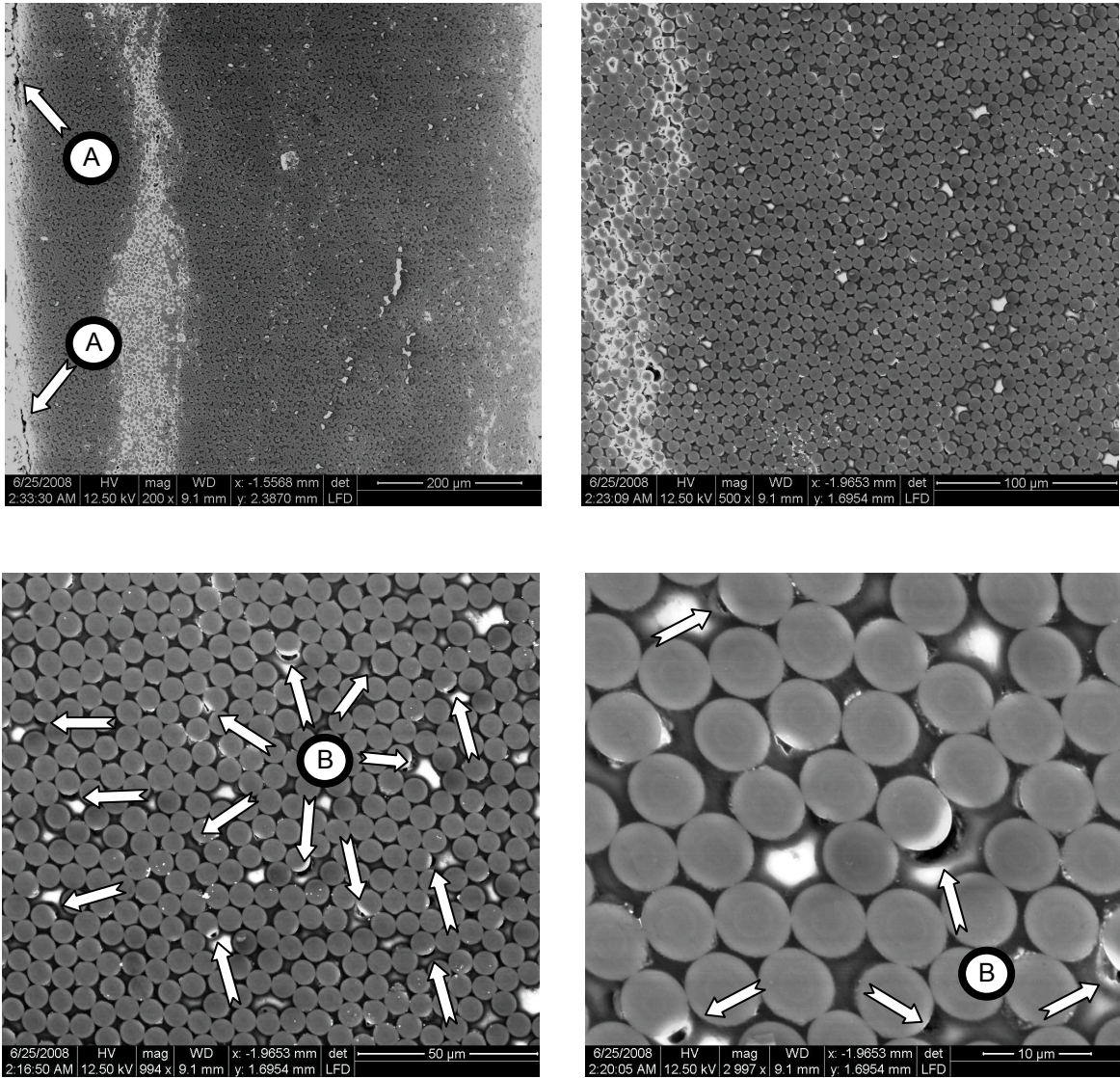


Figure 123 – Seawater-exposed, 10-minute acid-treated sized fiber composite cross-sectional views

After three months of exposure to 40° C seawater, some cracking was found within the composites made with 10-minute acid-treated fiber. However, the cracking was observed parallel and near the edge of the material, instead of within the bulk and perpendicular to the edge as seen with the untreated unsized, 2.5 minute treated, and 5

minute treated fiber composites. Additionally several individual fiber/matrix debonds were identified. These cracks (A) and debonds (B) are marked on the figure.

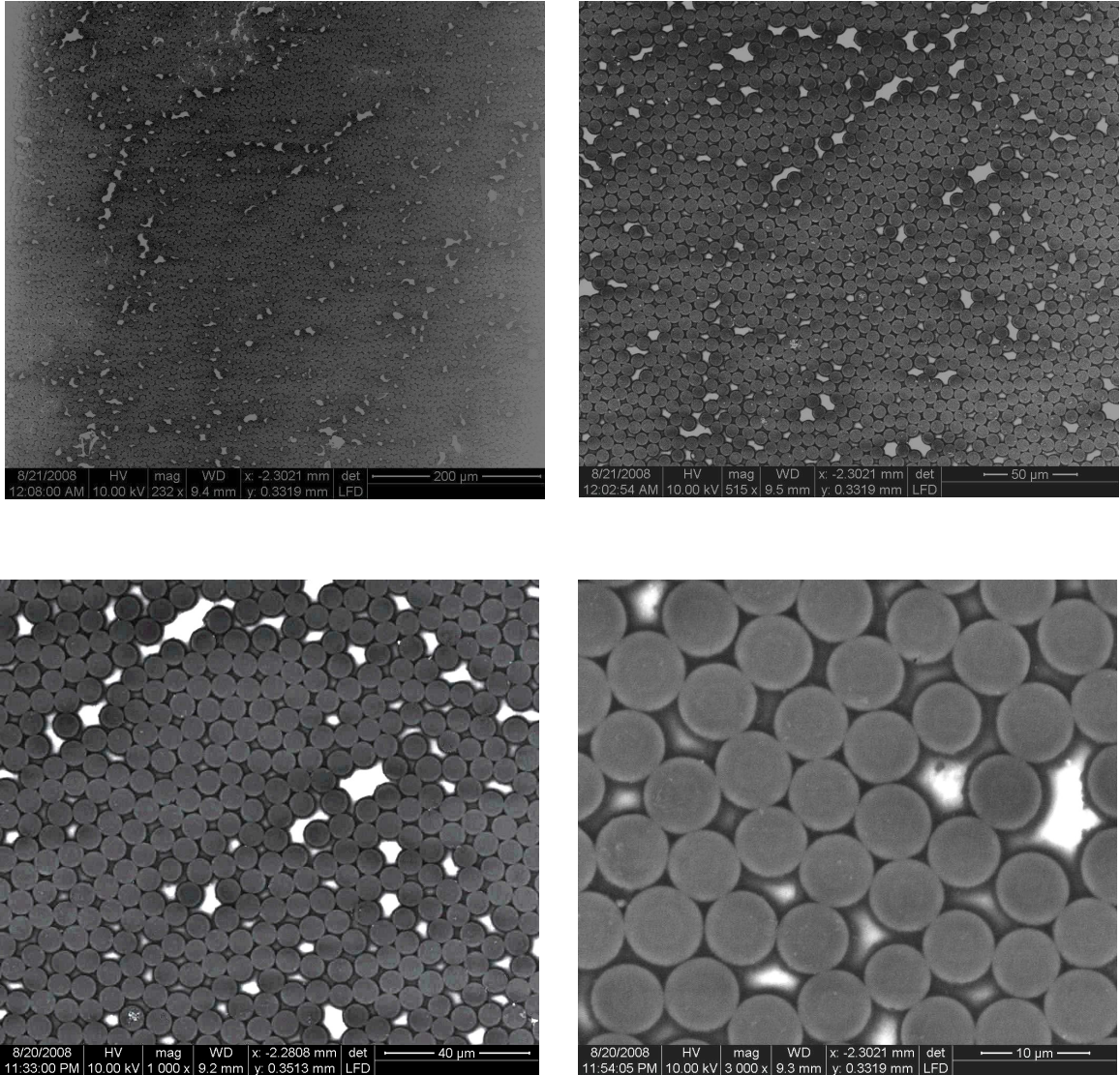


Figure 124 – Seawater-exposed, 5-minute acid-treated and silane-treated sized fiber composite cross-sectional views

After three months of exposure to 40° C seawater, the composites made with fiber that had been treated for 5 minutes in acid, followed by silane treatment very much resembled the dry condition. No cracking or debonding was observed after seawater exposure.

In the dry condition, three surface treatment types allowed the formation of quality composites as judged by cross-sectional examination. The as received sized and unsized fibers, as well as the acid/silane treated fibers all produced composites with good overall fiber/matrix distribution, complete wetting, and no visible debonding. All of the nitric acid-treated fiber types produced composites that displayed poor fiber/matrix distribution, poor wetting and fiber/matrix debonding.

Only two fiber surface conditions persevered through the seawater exposure period without visible damage. They were the as-received, sized (T700) and the acid/silane treatment. The as-received, unsized (AS4) fiber and the nitric acid-treated fiber types all displayed problems, including cracking, fiber/matrix debonding, or both. Table 20 lists the problems found for all conditions.

PROBLEM TYPE	FIBER TREATMENT TYPE											
	Sized Untreated Fiber		Unsize Untreated Fiber		2.5 Minute Acid Treatment		5 Minute Acid Treatment		10 Minute Acid Treatment		5 Minute Acid Treatment + Silane Treatment	
	Dry	Wet	Dry	Wet	Dry	Wet	Dry	Wet	Dry	Wet	Dry	Wet
Poor Distribution of Fiber and Resin					√	√	√	√				
Unwetted Areas of Fiber					√	√	√	√	√	√		
Fiber/Matrix Debonds							√	√	√	√		
Cracking				√		√		√		√		

Table 20 - Composite wet and dry problem table

The differences observed in the seawater perseverance of the different composite types may reflect the rates of water absorption and the relative toughness of the interphase regions. Chua et al.¹⁴⁵ proposed that void content plays a major role in composite water absorption and interface “wicking” plays a minimal role. The effect of composite void content surely had an opportunity to emerge in the case of the acid-treated composites, which were found to have larger void volume percentages. In addition, as it has been discussed previously, treating the fiber surfaces with nitric acid results in highly polar surfaces that are attractive to water. In combination, the increased void content and polar interfaces likely leads to an increased water absorption rate. The acid-treated composites gained the most weight upon seawater exposure, but showed less dimensional change, likely due to the available space for water within the voids. While less overall composite swelling occurred, the increased water absorption rate likely caused large localized differential swelling stresses, which contributed to cracking. This type of cracking behavior has been noted before by Weitsman et al.⁴³ Tsai and others¹⁴⁷ also discussed that a strong fiber/matrix bond results in a brittle and notch sensitive interface, while a weak bond results in a tough interface. This effect is also plausible, based on the review of the failed seawater-exposed composites that had been treated with nitric acid. They showed significant interfacial debonding and cracking that followed the interfacial boundary.

On the other hand, the acid/silane treated fibers produced composites that showed no signs of cracking or debonding. They also showed very little swelling and weight gain, as discussed earlier herein. There was less seawater absorption, which translates to less swelling stresses within the composite, but there may be more to the silane effect

than just that. The interface formed by the silane-treated fibers may be tougher and have a different modulus than without. Much research has been done on the interphase region formed with silane treated glass fibers. Physisorbed silane on the fiber surface may diffuse into the surrounding matrix materials and form a region of different properties. Drown et al.⁶⁹ conducted experiments on epoxy that had an epoxy-compatible silane mixed within it. They observed a reduction in the glass transition temperature of the material, indicating that the silane had reduced the cross-link density. This is understandable because the silane is designed to react with the matrix. Overall, they concluded that the epoxy mixed with silane, and hence the fiber interphase region, is stiffer, stronger and has a lower toughness than that without silane. Conversely, Chua et al.⁷⁰ conducted similar experiments by mixing silane with polyester and concluded that the resin became less stiff and tougher. They also performed coefficient of friction tests on fibers pulled from the matrix and found that there was less pressure on fibers when the resin was treated with silane, indicating that the matrix had been plasticized. The idea of the silane altering the interphase modulus is known as the “restrained layer” theory, or an “interpenetrating network”. There is also another theory that may apply in this scenario. It is called the “deformable layer” theory, and it is based on the idea that the silane, which connects the fiber and matrix can be deformed to allow for differential swelling between the two phases without failure. The deformable layer theory is not likely to provide enough flexibility to cope with the large interfacial stresses that likely result, but it may contribute to a smaller extent.

Thus, the low void content in the silane-treated composites led to less water absorption, swelling and internal stress. The hydrophobic nature of the silane-treated

fiber surfaces probably contributed to the low water absorption as well. And the silane presence likely toughened the interphase region by diffusion into and plasticization of the resin, as well as providing a deformable layer between the two phases. Together, these effects resulted in a composite that showed no cracking or debonding after seawater exposure.

Both the sized and unsized fibers formed good composites in the dry condition. Neither showed signs of poor wetting or debonding, but only the composite with sized fiber endured the seawater exposure period. The sizing likely introduces a toughening effect. The interface between the unsized fiber and resin is abrupt, but the sizing acts as a buffer zone, so that the transition between the fiber and resin is more gradual. The sizing may introduce a much more significant deformable layer, due to its thickness.

While the acid-treated and unsized fiber have no sizing or silane application, they may still induce interphase property changes within the surrounding resin, due to their reactive surfaces. Remember that even though the unsized fiber was not treated, it still maintained a lesser amount of surface oxidation from the manufacturers surface treatment. The reactive fiber surfaces may attract certain components (such as the curing agent, MEKP) of the uncured resin to their surface making a rich region immediately near the fiber and a depleted zone farther away. Williams et al.²² found supporting evidence of this with unsized carbon fiber and epoxy. Using fiber pullout studies and nano-indentation, they observed a region within 100 nm of the fiber to have increased stiffness and a region within 500 nm of the fiber to have decreased stiffness. They postulated that the increased stiffness area resulted from mechanical immobilization due

to the fiber, and that the decreased stiffness area was caused by depression of the local glass transition temperature, due to the attraction of amines within the resin to the fiber.

Upon review of the composite cross-sections before and after seawater exposure, only the silane-treated and sized fibers produced composites that endured. It is expected that there was less internal stress within the silane-treated composite to produce cracking, due to the lower weight gain and swelling observed. This probably helped significantly, but the sized fiber composite did swell significantly and likely had internal stresses, and also did not fail. Toughening of the interface likely plays an important role in the success of the sized and silane-treated fibers in resisting cracking. Mixing silane with resin has been found to plasticize it, resulting in increased toughness. The sizing may also interdiffuse with the resin and provides an intermediary zone to ease the transition from resin to fiber. Both surface finishes may provide a deformable layer between the fiber and matrix. The higher void content of the acid-treated fiber composites resulted in significant water absorption at high rates, which means that there were areas of great differential swelling that are conducive to cracking. Additionally, the interphase around the acid-treated fibers may not have been toughened as much as that around the silane-treated fibers, even though the fiber reactivity likely changes the matrix chemistry within the vicinity of the interface. And finally, stronger adhesion is known to result in brittle interfaces with low toughness, similar to those observed here. The high void content, the lack of significant interphase toughening and the possible improved fiber/matrix adhesion all contribute to the cracking and debonding observed in the acid-treated fiber composites after seawater exposure.

3.3 Discussion

This work can be viewed to consist of two parts: the effects of acid and acid/silane treatment on carbon fibers, and the effects of these fiber treatments on carbon/vinyl ester composites. It is important to first understand the fiber effects before an understanding of composite behavior can be developed. The fiber effects can be grouped into physical and chemical changes. For the physical type, fiber surface morphology, diameter, strength and modulus were considered. Chemically, the fiber surface energy, surface functional group type, and cohesion between fibers were investigated. For the composite evaluations, multiple fiber wetting, void content, fiber/matrix fractions, transverse tensile strength, weight gain and swelling, failure modes, and seawater-induced damage were investigated.

The experimentally determined fiber tensile strength and modulus of both fiber types were found to be close to that reported by the manufacturers before treatment. It is widely reported that oxidizing treatments weaken carbon fibers. When using nitric acid as the oxidizer, this can only be considered to be true when looking at the force required to break the fibers. Strength does not decrease with extended treatments, it actually increases to a stable value. The fiber diameter changes with acid treatment and this is crucial information to have when evaluating strength. This consistent level of improvement in failure stress supports the idea that the strength increase comes from the smoothing and/or removal of surface defects. Once the surface is smoothed, the strength does not change, regardless of how long the fiber is treated. This is also consistent with the surface morphology results presented herein. While surface defects could be found on fibers at extended treatment times, they were difficult to find and the bulk of the fibers

remained smooth. Further support for the strengthening by defect removal theory comes by pointing out that carbon fiber strength is largely dependent on surface flaws, due to their brittle nature. This was shown to be true when three different gage lengths of fiber were tested, showing a decrease in strength that was proportional to test gage length. There is a higher probability of flaws in longer test gage lengths. The consistently smooth fiber surface that was found also precludes mechanical interlocking from becoming a factor in any composite strength changes that were observed.

Nitric acid treatment also resulted in a substantial increase of carbonyl (331%) and carboxylic acid (235%) surface functional groups. This change has often been suspected, but the chemical derivatization/XPS method used herein has allowed quantification of these groups. Contrary to common belief, the hydroxyl groups did not increase with nitric acid treatment. The carbonyl and carboxylic acid groups increased up to a constant level, indicating that their maximum concentration had been reached. This happened at 80 minutes for the carbonyl types and 40 minutes for the carboxyl types. In addition to hydroxyl, carbonyl and carboxylic acid groups, there was also a portion of the fiber surface oxidation that was not identified. This “other” group proportion was not large for any of the fiber types, except the as-received, sized fiber, but it was expected that the sized fiber would be much different due to its polymeric coating.

Along with the increase in carboxyl and carbonyl groups, came a change in surface energy. The polar surface energy increased linearly with nitric acid treatment, and the dispersive energy decreased linearly. The total surface energy, which is a summation of the two, showed an increase. Acid-treated fibers that were subsequently treated with silane showed very low polar energy and high dispersive energy, opposite to

that found with acid-only treated fibers, indicating that the silane had bonded to the acid-treated surfaces. Increases in fiber polarity that are observed with nitric acid treatment are often used to assume that wettability will improve in composites, but this was not found to be the case in this research. Just because a single fiber is more wettable, it doesn't necessarily follow that a group of fibers will be.

Individual fiber surface characteristics are often considered, as well as fiber/matrix composite properties, but fiber-fiber interaction is usually ignored when evaluating fiber surface treatments. The fiber surface treatments applied herein had a significant affect on fiber-fiber interaction, which impacted composite properties. Fiber interaction was evaluated by measuring the cohesion between neighboring fibers within a bundle. The bundles were pulled apart slowly, starting at one end, measuring the work required to separate them. Significant fiber-fiber cohesion was found for acid treated fibers, which increased linearly with acid treatment, up to 120 minutes, where it reached a maximum level, similar to the maximum levels reached in the carbonyl and carboxylic acid group concentrations. In total, the work of separation increased by 1,418% over the untreated condition. It is believed that this cohesion effect is a direct result of the surface functional groups that are implanted on the fiber surfaces during treatment. The nitric acid treatment introduces highly polar surface groups (carbonyl and carboxylic acid) that are capable of hydrogen bonding with each other. This hydrogen bonding, as well as van der Waals forces, creates an attraction between neighboring fibers. The acid-treated fibers that were treated with silane, however, showed a very minimal amount of cohesion, regardless of their acid pretreatment time. The silane was able to bond to the surface groups on the fiber surface, creating a new surface that was much less polar and much

more dispersive, leading to less fiber-fiber attraction. The acid/silane treated fibers had the lowest surface polar energy (including the untreated types), and a high dispersive energy, roughly equal to that of the sized fiber.

The fiber cohesion emerged as a significant composite issue during the bundle wettability tests, where treated and untreated bundles were immersed in catalyzed vinyl ester resin, and the amount of wetting was judged in a SEM by viewing cross-sections of the cured composites. Both untreated fiber types (sized and unsized) showed complete wetting. However, all of the acid-treated types exhibited unwetted areas within the bundle, which grew larger as fiber acid treatment time was increased. The 2.5-minute treated bundle showed only small unwetted areas, whereas the longer-treated fibers resulted in very large areas of unwetted fiber that completely compromised the composites. Despite the prediction of increased wettability that is often made through tensiometry measurements on single fibers that have been oxidized, the reverse was actually true when using multiple fibers with catalyzed resin as the fluid. Single-fiber tensiometry is useful for characterizing the surface energy on single fibers, but caution should be exercised when making the leap to composite wettability. Surface energy tensiometry measurements utilize only individual fibers and fluids other than resin. There is no consideration for fiber-fiber interaction or fluid viscosity. It is true that a single fiber will wet easily with a nonviscous fluid, such as water, but when multiple fibers that cohere to each other are exposed to a viscous resin, wetting is not as straightforward.

The poor wetting of acid-treated fiber bundles was observed not only in single bundles immersed in unpressurized resin, but it was also found when pressure and

vacuum were used to make macro-composites. The four-layer composites that had been pressurized to 688 kPa (100 psi) showed unwetted areas when their fibers had been treated with acid, and no acid-treated fiber composites could be made using VARTM. With VARTM, only slight surface wetting was achieved on the outer edges of the fiber bundles, but the end result was more similar to the original fiber than a composite material. Similar to the single bundle wettability tests, full wetting was achieved on macro-composites formed with untreated fiber, both sized and unsized.

When acid-treated fiber was subsequently treated with silane, excellent wetting was observed in both single-bundle wettability tests (2.5, 20 and 40 minute acid pre-treatments) and in macro-composites (5-minute acid pre-treatment). Also, recall that the surface energy tensiometry measurements indicated that the acid/silane treated fibers had the lowest polar surface energy and nearly the highest dispersive energy. When a fiber has higher surface energy, the system will be driven to minimize the total energy by more complete wetting. According to established practice, this surface energy condition would indicate that the acid-silane treated fibers should be less wettable than the more polar, higher-energy acid-only treated fibers. But this is not the case in composites. The acid/silane treated fibers are much more wettable to resin than the acid-only treated fibers when multiple fibers are used. You may also recall that the acid/silane treated fiber bundles showed much less cohesion than the acid-only treated bundles did. It appears that the cohesion between fibers plays a large role in multiple-fiber wettability, regardless of the wettability predictions obtained with single fibers. As fiber-fiber cohesion is minimized, better wetting and less composite void content is achieved. It is extremely important to consider fiber-fiber cohesion when predicting wettability with a given fiber

surface treatment. A less polar fiber surface results in less fiber-fiber attraction, leading to easier penetration of the viscous resin.

In addition to direct observation of wetting with SE microscopy in the single-bundle and macro-composite specimens, the differences in wettability were also quantified by measuring the void content of macro-composite specimens. This also indicated larger void content associated with nitric acid fiber treatment and less with acid/silane treatment. The void content increased gradually, along with nitric acid fiber treatment time. The composites made with sized and unsized fiber had less void volume percent than the acid-treated fiber composites, but the acid/silane treated fiber composite had the least void volume overall. The sized and unsized fiber types produced composites with 1.61% and 2.22% void content, respectively, the acid-treated types reached up to 3.01%, and the acid/silane treated type dropped to 0.31%.

It should be expected that changes in matrix wetting would impact composite strength. The single-bundle transverse tensile tests conducted herein indicated that a short nitric-acid treatment caused a significant increase in transverse tensile strength, but longer treatments resulted in a steady decline to very poor strength. Even though unwetted areas were observed in all acid-treated fiber composite types, composite strength still improved for the 2.5-minute (shortest) treatment time by 61 and 25 percent over the sized and unsized fiber types, respectively. This indicates that either the fiber/matrix adhesion was improved, or the interphase region was toughened by the acid treatment. Evidence can be found for both, but improved adhesion is more likely the cause. Herein, examination of the failure surfaces yielded that specimens made with highly oxidized fibers showed resin failure, instead of fiber/matrix debonding. This is a

classic indicator that the fiber/matrix bond is stronger than the surrounding resin. Also, Williams et al.²² found a region of decreased stiffness around unsized fibers in epoxy resin, with a smaller region of increased stiffness immediately next to the fiber. Even though they used unsized, untreated fiber, it is likely that the fiber maintained an oxidative treatment that manufacturers supply to unsized fibers. It is possible that the reactive fiber surface attracted components of the uncured resin, such as the curing agent, leaving a high concentration immediately next to the fiber and a depleted zone outside of that boundary. It is possibly a combination of both improved adhesion and modification of the resin properties near the fiber that resulted in improved transverse tensile strength with the short (2.5 minute) acid treatment, but the improved adhesion is expected to play the larger role.

The declining strength observed with fibers that had been treated in nitric acid for longer time periods stems from the wettability issues that arise from the acid treatments. The transverse tensile strength is a give and take relationship between the improved adhesion and reduced wettability. Eventually, when the wetting becomes very poor, the composite strength seriously suffers, even if there is improved fiber/matrix adhesion.

In contrast to the acid-only treatment results, the acid/silane treatment produced very strong transverse tensile strength results, regardless of the length of nitric acid pretreatment. The acid/silane treatment produced transverse tensile specimens that were up to 86% stronger than the untreated sized fiber and 56% stronger than the untreated unsized fiber. This was the strongest result obtained for any surface treatment. When the sized and unsized fibers were treated in silane without acid pretreatment, both produced strengths only roughly equal to the untreated unsized fiber. This indicates a small

increase in sized fiber strength occurred to make it equal to the unsized fiber, but it is believed that the acetone in the silane solution just dissolved the sizing, essentially making it another unsized fiber. The full strength of the silane treatment was not realized until the fibers were pretreated with nitric acid, indicating that the silane needed to bond to the surface functional groups that were implanted through nitric acid treatment. 2.5, 20 and 40-minute acid pretreatments were used, but they all produced similar strength results with silane. There was no loss in wetting or strength as observed in the acid-only treatments with increasing acid treatment time. Furthermore, some of the acid/silane treated composites exhibited resin failure (instead of fiber/matrix debonding) that indicates that the fiber/matrix bond had become stronger than the surrounding matrix.

Composite strength in seawater depends on several aspects of the composite, such as the durability of the interfacial bond, amount of seawater that is absorbed, rate of absorption, void content, and the degree of resin plasticization. The transverse tensile specimens made with fiber that had been treated in only nitric acid exhibited a loss in transverse tensile strength after one month of exposure to 40° C seawater. This was not unexpected. However, at two and three months, the transverse tensile strength improved for all of the acid-treated transverse tensile types, with the more highly treated ones improving to a level above the dry condition. This could be due to a durable fiber/matrix bond and due to changes in the resin from water absorption. It is likely a combination of both. The only failed transverse tensile specimens that exhibited resin fracture (versus fiber/matrix debonding) after seawater exposure were the types that had undergone the longest acid treatments (20 and 40 minutes). None of the others showed this type of failure. In some areas of these specimens the resin was still attached to the fibers after

breakage, with the resin displaying a fractured surface. Because the resin fractured and remained attached to the fiber, it indicates that the bond was stronger than the matrix in that region. The 40-minute treatment type showed this failure mode in both wet and dry specimens, but the 20-minute treatment type showed this failure mode in only the wet specimen. Because the 20-minute treatment type showed this failure mode only after immersion, it indicates that either the bond became stronger or the matrix became weaker during seawater exposure. It was likely a reduction in resin strength, combined with a bond that remained durable. The idea of reduced resin strength is supported by observations that were made from some of the failure views. Some of the specimens exhibited a ductile fracture mode after seawater immersion, where the dry specimens always failed in a brittle cleavage-type manner. Ductile failure likely serves to increase the fracture toughness of the matrix, thereby improving the overall test strength of the transverse tensile specimens. The vinyl ester resin is very brittle in the dry state and it was shown herein that when the promoter and resin were allowed to sit before being catalyzed, toughness was significantly improved, which led to the achievement of improved strength and elongation for the resin alone. It is not unrealistic to assume that toughening of the matrix through seawater plasticizing could also improve transverse tensile test strength. It makes sense that this could explain the improvement of strength of the highly acid-treated specimens to a level above the dry state, because those specimens depended almost entirely on resin strength, due to poor wetting of the fibers.

The fibers that were treated with silane after nitric acid treatment displayed excellent transverse tensile strength when dry. However, they declined in strength after exposure to seawater. Furthermore, the acid/silane types that had undergone longer nitric

acid pretreatments lost more strength than those with less acid pretreatment. In the dry state, all of the acid/silane types produced a roughly equivalent improved transverse tensile strength. The strength was high, but there was no improvement with longer acid treatment time. It is possible that the silane only needs a slight acid treatment to provide an adequate amount of surface functional groups to bond to, and longer treatments only create unnecessary surface groups. These unnecessary surface groups only serve to increase fiber polarity (as seen in the surface energy experiments herein), which may attract additional water to the interface, resulting in more strength loss. Another indication that the acid/silane bond was degraded by seawater exposure was that all of the failure surfaces exhibited fiber/matrix debonding, even though they exhibited some resin failure in the dry condition, which is indicative of strong bonding. It was shown that the silane can be bonded to the treated fiber surfaces, but creating the ideal interface may require some optimization. Other researchers have discovered that the right amount of surface silane on glass fibers improves hydrolytic stability, but the wrong amount degrades it. Typically, a thin monolayer is desired.

Seawater absorption plays a huge role in the durability of composites. It changes both the size and weight of the composites. Swelling can induce differential stresses within the composite as some regions swell before others (edges versus interior), and some constituents swell more than others (matrix versus reinforcement). Voids play a role in water absorption, as they provide a clear path for fluid to travel and provide a place for it to reside without inducing swelling. Additionally, swelling is affected by the interface. A polar interface is likely to be more attractive to water than a nonpolar one and a damaged interface (debonding or cracking) provides a route for capillary influx.

The composites made with acid-treated fiber gained more weight than those made with untreated fiber (sized and unsized), and the weight gain increased with fiber treatment time. The swelling behavior, however, was inversely proportional to the weight gain behavior. The acid-treated fiber composites swelled less than the untreated fiber composites, and the degree of swelling decreased with fiber acid treatment time. The more highly acid-treated fiber composites gained more weight and swelled less, and vice versa. The explanation for this can be found in the void content of the composites. The composites made with fibers that had undergone longer acid treatments had higher void contents, so as seawater came in, excessive swelling was averted in two ways. First, as the composite swelled, it was able to expand into internal voids, instead of overall dimensional swelling. Second, some of the absorbed water filled the internal free volume and did not contribute to composite swelling. The idea of water filling free volume within composites can be traced back to the work of Marom and Broutman,⁶¹ Weitsman et. al,⁴³ and Apicella and Nicolais¹⁴⁸. Marom and Broutman used transverse tensile stress to show increased water absorption equilibrium, Weitsman et. al showed that internal cracking allowed increased water absorption, and Apicella and Nicolais have described the entrance of water into epoxy or polyester by using the theory of solvent diffusion, which provides that water is absorbed into the free volume spaces of the resin. The increased water absorption of the acid treated composites can be explained in part by the increased void content, but it is likely a result of the increased fiber surface polarity as well. As the fiber surface polarity is increased (with acid treatment), it becomes more attractive to water. This was shown during the single fiber tensiometry measurements herein, when the more acid-treated fibers met water with a lower contact angle.

In contrast to the acid-treated fiber composites, the acid/silane treated fiber composite had a nonpolar fiber surface, as well as low void content. This combination of beneficial attributes showed itself in the weight gain and swelling behavior. The acid/silane treated fiber composite swelled less than any other type, including the untreated fiber types (sized and unsized) and also had a very low weight gain, only slightly higher than the untreated, unsized fiber type. The nonpolar fiber surface and low void content significantly reduced seawater weight gain and swelling.

Due to poor wettability and fiber distribution, only three of the fiber types produced acceptable composites in the dry state, the sized, unsized and acid/silane treated fibers. Of these three, only two remained intact through the seawater exposure period, the sized and acid/silane treated. The durability of these two composite types is most likely attributed to tough interphase regions around the fibers. The polymeric sizing on the sized fibers provides a transition zone between the fiber and matrix that is less brittle and is likely to be more forgiving to differential swelling between the two phases. This can be classified as a deformable layer. The sized fiber also produced the weakest transverse tensile strength specimens of those that were completely wetted out. This indicates that the adhesion between the sized fibers and matrix is weak. It is well known that weak interfaces produce tough composites because the interfaces debond before the bulk composite cracks. The composite made with acid/silane treated fiber probably produced a tough interphase region by a combination of two means. There may have been a deformable layer that was formed through the silane link between the two phases, and there was likely an interpenetrating network of silane that changed the interphase modulus. Both of these theories have been proposed before as to the reasons why silane

improves the properties of glass fiber composites. It has been described by other researchers that silane changes resin properties when mixed with it during the curing process.^{69, 71} Because the silane is designed to bond with the resin, it is likely that any physisorbed silane on the fiber surface diffuses into the interphase region, bonds with the resin, thereby limiting the amount of cross-linking that takes place in the resin. Less cross-linking plasticizes the matrix, reducing the modulus. Additionally, it has been described by others working with glass fibers that the amount of silane applied is crucial for hydrolytic stability. A small monolayer produces hydrolytic stability with glass fibers, but too much silane decreases water resistance.¹⁴³ It is possible that excess silane was present in this case, causing vulnerability of the interfacial bond to water. While adhesion may be reduced, the loss of interfacial bonding during exposure may have toughened the composite to reduce cracking in the same way that the weak sized fiber/matrix bond likely does.

The unsized fiber produced a well-wetted composite in the dry state, but did not withstand seawater exposure like the sized and acid/silane treated fiber composites did. Again, this observation can most likely be attributed to interface/interphase toughness. The unsized fibers did not toughen the interphase to the extent the sized and acid/silane treated fibers did. With the unsized fibers, there is an abrupt transition between the fiber and matrix, with no flexibility for differential swelling and very little interphase plasticization. And while the slightly oxidized surface of the unsized fibers may serve to modify the interphase region by attracting resin components, such as curing agents, it is unlikely that it could toughen the interphase region to the extent that the interdiffusing silane does. Furthermore, it has been found previously that there is a high-modulus

region around oxidized fibers, just inside of the low-modulus region.⁶⁷ This high modulus region may make the interface brittle and negate any benefit from the lower modulus region. Therefore, the unsized fiber composite was left with an abrupt transition from fiber to matrix properties and a less tough interphase region, that could not endure swelling.

The acid-only treated fibers were compromised by limited wetting even before water exposure, and demonstrated extensive cracking afterwards. As observed in the failure views of the 20 and 40-minute acid-treated transverse tensile tests, there appeared to be good adhesion after water exposure, as evidenced by fractured matrix remaining attached to the fibers. Just as poor interfacial adhesion is known to produce tough bulk composites, strong interfacial adhesion is known to produce the opposite. Strong adhesion is not good for the composite when there is no interphase toughening mechanism to resist cracking. The acid-treated fibers probably influenced the interphase in a similar way as the unsized fibers, but to a greater extent. The acid treated surface may create a zone of increased modulus immediately around the fiber and a region of decreased modulus immediately outside of that due to the attraction of resin curing agents. This effect likely produced less toughening than the interdiffusion of silane, and in combination with the strong adhesion, resulted in a composite with poor toughness. The less tough, well-adhered interface of the acid-treated fibers fared much worse in seawater than the tougher, less well-adhered interface of the acid/silane treatment did. Figure 125 describes the types of interphase regions that are likely formed with the different fiber surface conditions studied.

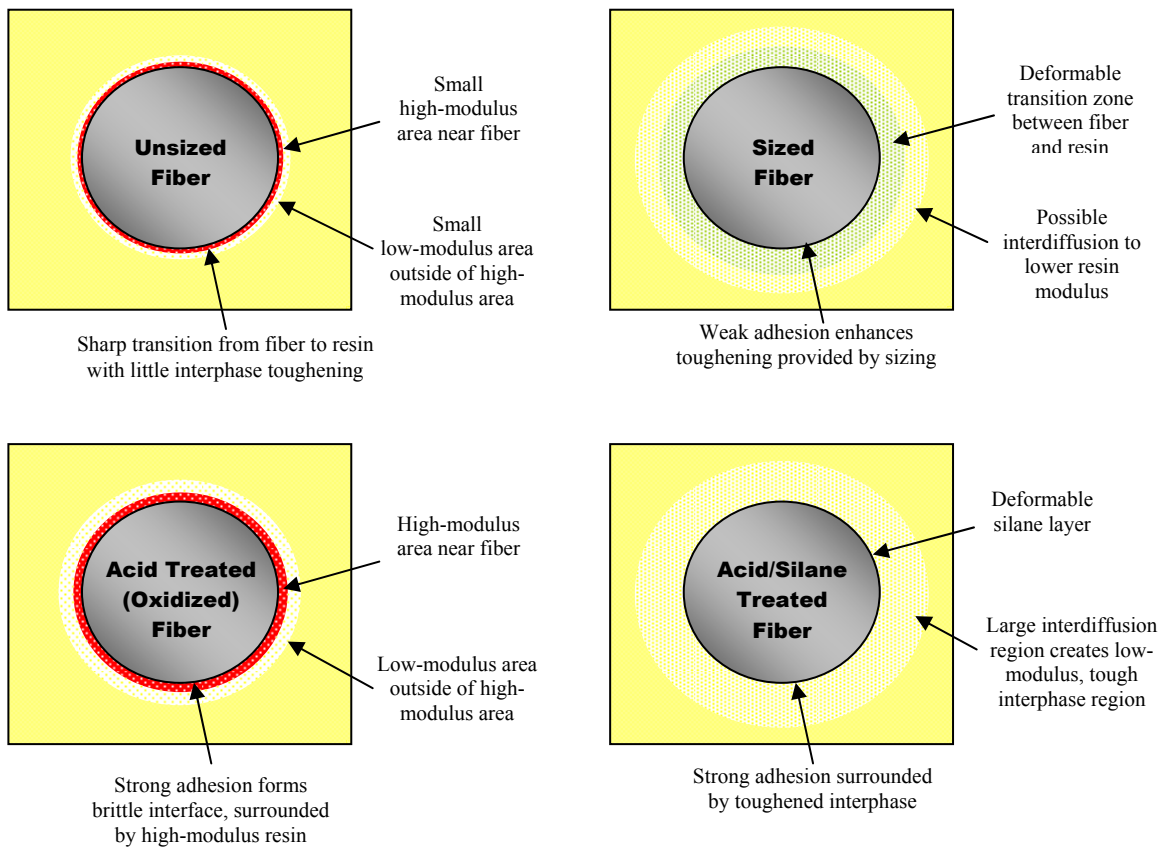


Figure 125 - Probable interphase characteristics

3.4 Conclusions

Carbon fiber surface modification with nitric acid and 3-(trimethoxysilyl)propyl methacrylate silane affected both fiber and composite properties. The nitric acid treatment physically affected the fiber surfaces by removing carbon material, and chemically affected them by implanting reactive functional groups. These fiber changes became evident through changes in fiber size and strength, surface chemistry, surface energy and fiber cohesion. Subsequently treating the nitric acid-treated fibers with silane

also caused the fiber surface energy and cohesion to change in ways that were quite different from nitric acid treatment alone.

Several carbon fiber changes were observed with nitric acid treatment:

- The high strength (type I) carbon fibers used in this research remained smooth during treatment, but their diameters decreased significantly. At the longest treatment time (160 minutes), the sized fiber diameter decreased by 8.4 percent and the unsized fiber diameter decreased by 9.1 percent.
- Fiber tensile strength decreased at the shortest treatment time (5 minutes), but then increased to a constant level. The decrease in strength after short treatment was 11.1 percent and 18.6 percent (sized and unsized fiber types, respectively), while the long term increase was observed to be 19.8 and 15.2 percent. These changes in strength are likely attributable to reductions in the severity and number of fiber surface defects, due to carbon fiber's sensitivity to flaws. At early treatment times, it is believed that the acid attacks fiber surface imperfections, weakening the fiber, but at longer treatment times, more of the surface material is evenly removed, resulting in a smoother, more perfect surface.
- The surface concentrations of carbonyl and carboxylic acid groups increased significantly with treatment, but then reached a constant level, indicating that maximum concentration levels had been reached. Hydroxyl concentrations did not significantly increase. The maximum increase in carbonyl concentration was found to be 331 percent, and the maximum increase observed for carboxylic acid was 234 percent.

- With nitric acid treatment, fiber polar surface energy increased linearly up to a maximum increase of 84 percent at 160 minutes of treatment. Fiber dispersive energy was seen to decrease linearly to a 21 percent reduction at 160 minutes. The total amount of surface energy increased significantly (30 percent), leading to predictions of improved fiber wettability.
- Fiber cohesion increased significantly with acid treatment (up to 1400 percent), until a maximum level was reached at 120 minutes.

Subsequent treatment of the nitric acid-treated fibers with 3-(trimethoxysilyl)propyl methacrylate silane resulted in different fiber surface properties:

- Contrary to acid-treated fibers, acid/silane treated fibers exhibited low polar and increased dispersive energy. The acid/silane treated fiber type represented a 71 percent decrease in polar energy, and a 6.5 percent increase in dispersive energy from the untreated fiber. The differences were much bigger when compared to the acid treated fibers. These changes brought about a significant reduction in the total surface energy (24 percent from the untreated fiber), leading to predictions of poorer wettability.
- Contrary to acid-treated fibers, acid/silane treated fibers showed minimal cohesion, even less than that found with untreated fibers.

The specific fiber property changes observed after surface treatment affected fiber/matrix composite properties as well. Both nitric acid and nitric acid/silane types of

fiber treatment caused changes in fiber/matrix wetting, transverse tensile strength and the composites' responses to seawater immersion.

For composites made with nitric acid-treated fibers:

- Transverse tensile specimens formed with fibers that had undergone short acid treatment times exhibited improved transverse tensile strength, suggesting improved fiber/matrix adhesion. The transverse tensile strength observed after a 2.5-minute acid treatment increased by 61 percent over the untreated, sized fiber, and 25 percent over the untreated, unsized fiber.
- Composites formed with fibers that were more extensively treated with nitric acid suffered from poor wetting that resulted in high void contents and declining transverse tensile strength. Very serious wetting problems were observed when immersing treated bundles in catalyzed resin, leading to large unwetted fiber areas. Compression-molded macro-composites also exhibited increased void contents. Fibers that had undergone 10 minutes of acid treatment resulted in an average composite void content of 3.0 percent, while untreated, sized and untreated, unsized fibers produced 1.6 and 2.2 percent composite void contents, respectively. Single-fiber contact angle measurements and surface energy calculations predicted that the acid-treated fibers would be more wettable, but the opposite was found to be true when using multiple fibers in resin. It is likely that the fiber cohesion observed after acid treatment, in combination with the high viscosity of the liquid resin, contributed to the poor wettability observed. Wettability prediction by surface energy calculation takes into account the thermodynamic properties of the surface, but it

doesn't consider other factors, such as fluid viscosity, fiber packing and fiber interaction. It may be difficult for the viscous resin to infiltrate fiber bundles that are held tightly together by inter-fiber cohesive forces.

- Upon seawater exposure, the acid-treated fiber composites tended to gain increased weight, but swell less. As fiber treatment time increased, more weight gain was observed, which can be explained by fiber surface polarity and composite void content. The more highly treated fibers had higher surface polarity (as shown in the surface energy calculations), making them more attractive to water, and the increased composite void contents seen with increased acid treatment times caused higher void contents, allowing increased diffusion rates and amounts. The inverse relationship observed with swelling behavior can also be attributed to increasing void content with acid treatment. Larger void contents provide room for absorbed water to reside within the composite without causing swelling, and when swelling does occur, the composite has room to swell internally (into the voids), in addition to overall external dimensional growth.
- Transverse tensile testing after exposure to seawater rendered minimal strength loss and fiber/matrix failure modes that suggest the existence of hydrolysis-resistant interfacial bonds. Untreated fibers and low acid treatment times yielded composite interfaces that failed exclusively by fiber/matrix debonding after seawater exposure. However, when longer acid treatment times were applied before seawater exposure, matrix cohesive failures could be observed, indicating that the matrix failed cohesively before the interface debonded.

- Nitric acid-treated fiber composites showed extensive cracking upon seawater exposure, indicating poor interfacial toughness. The creation of a strong fiber/matrix bond without any toughening mechanism results in an interface that is likely to crack during differential expansion of the fiber and matrix. There is an abrupt transition of material properties between the fiber and matrix. If adhesion is weak between these two phases, debonding is likely upon differential expansion, but if strong bonding exists, cracking will likely ensue. Treating the fibers to make the surfaces more polar may add to this effect by attracting certain components of the liquid resin (such as curing agent) to the fiber surfaces, leaving a concentrated region near the fiber and a depleted zone outside of that. Some evidence of this phenomenon has been put forth by Williams et al.,¹⁹ when they tested the modulus of epoxy resin around unsized graphite fibers. They found a small zone of increased modulus immediately near the fiber (100 nm), surrounded by a region of decreased modulus (500 nm). Combining increased fiber/matrix adhesion with a zone of increased modulus next to the fiber would result in an interface that is prone to brittle cracking failure when subjected to differential fiber/matrix swelling.

Acid/silane treated fiber composites yielded much different behavior than did the acid-treated fibers. All aspects of the acid/silane treated fiber composites were different, including transverse tensile strength, wetting and responses to seawater exposure:

- The acid/silane treated fibers produced exceptionally strong transverse tensile specimens, indicating the presence of strong fiber/matrix adhesion. The acid/silane treatment produced improvements of 86 and 43 percent over the untreated sized and

unsized fibers, respectively. This improvement was even greater than that seen with the short acid treatment times. However, unlike the acid treated fiber specimens, the acid/silane treated fiber transverse tensile specimens did not lose their strength with increased nitric acid pretreatment time. A short acid pretreatment (2.5 minutes), followed by silane application, produced transverse tensile strength similar to that observed with longer acid pretreatment (40 minutes), whereas acid-only treatment resulted in declining strength with increasing treatment time. The sustained strength improvement can be attributed to the fact that the acid/silane composites did not suffer from wetting problems like the acid treated fiber types did.

- Composites made with acid/silane treated fibers exhibited excellent wetting and low void content. While nitric acid treated fiber bundles showed serious wetting problems with increasing treatment times, the wetting problems disappeared when the fiber bundles were subsequently treated with silane. Compression-molded composites also showed improvement. The untreated sized and unsized fibers produced composites with void contents of 1.6 and 2.2 percent, respectively, and the acid-treated fibers resulted in up to 3.0 void percent, but the acid/silane treated composite had a low 0.3 percent void content. The acid-treated fibers had high surface energy, which predicted better wettability, and the acid/silane treated fibers had low surface energy, which predicted poor wettability, but the opposite was observed when applying liquid resin to treated fiber bundles. Although surface energy can provide an indication of material wettability, true composite wettability cannot be determined without considering multiple fibers and viscous resin. When

strong fiber cohesion is present, wetting by viscous resin is hampered, and vice versa.

- The acid/silane treated fiber composite exhibited both low weight gain and swelling after seawater exposure. This is likely due to the nonpolar nature of the fiber interface formed with silane, and the low void content observed with the acid/silane treated fiber composite, due to good wetting.
- The acid/silane treated fiber composite showed excellent composite quality both before and after seawater exposure. Evidence of good fiber/matrix distribution and wetting were found, and no cracking or debonding was identified after seawater exposure. This apparent composite durability probably resulted from low seawater absorption, combined with a tough fiber/matrix interface/interphase. It was pointed out earlier that the acid-treated fibers resulted in a condition of strong bonding, a high modulus interphase zone, and no toughening mechanisms, leading to an interface that was not fracture tough. Conversely, the acid/silane interface does have toughening mechanisms. Chua et al. have shown that silane plasticizes matrix resins, leading to improved fracture toughness.⁶³ If there was excess silane present on the acid/silane treated fibers, an interdiffused interphase region probably resulted, leading to a toughened zone around the fiber. In addition to the potentially lower modulus interphase region, the interface boundary may have also contributed to composite toughness. As long as the silane link remained connected between the fiber and matrix, it may have acted as a deformable layer to compensate for differential swelling between the fiber and matrix. Furthermore, if the silane link was hydrolyzed or otherwise broken, composite toughness would also be improved.

Faced with differential fiber/matrix swelling, the matrix could debond from the fiber, instead of forcing matrix cracking. Interphase plasticization through silane interdiffusion, in addition to a forgiving interface, most likely resulted in a fracture-resistant composite.

- The only drawback observed with the acid/silane treatment was that the fiber/matrix bond did not appear to be durable in seawater. Examination of both transverse tensile strength and fiber/matrix failure mode led to this conclusion. Some of the acid/silane treated fiber transverse tensile specimens failed by matrix cohesive failure before seawater exposure, but switched to fiber/matrix debonding after exposure, indicating a loss in fiber/matrix adhesion. Transverse tensile strength was seen to reduce by 22 percent after seawater exposure with the fibers that had been treated with nitric acid for 2.5 minutes before silane treatment. But the fibers that had been pretreated for 40 minutes in acid produced composites that lost 45 percent of their dry strength after seawater exposure. The amount of strength loss in seawater was proportional to acid pretreatment time, and it is believed that there is an optimum level of acid pretreatment. Only a specific amount of surface functional groups on the fibers can be made to bond with the silane. Any excess groups go unbonded to the silane and may continue to attract water to the interface, due to their polar nature. Additionally, the method of silane application may also impact whether or not the resulting fiber/matrix bond is durable to water. Chua et al. previously reported that silane application can cause seawater durability improvement, or degradation, with glass fibers, depending on how the silane is applied.¹²⁷ It may therefore be worthwhile to examine the method of silane

application in more detail, so that improved seawater durability may be attained in this application.

Treating high-strength carbon fibers with nitric acid, and acid followed with 3-(trimethoxysilyl)propyl methacrylate silane treatment produces notable, but different results. Composites made with nitric acid-treated fibers suffered from many ailments that worsened with acid treatment time. Despite the drawbacks seen with highly acid-treated fibers, short acid treatment times produced composites with strong transverse tensile strength and apparent seawater durability, without giving up too much in decreased wettability and increased seawater absorption. However, all of the acid treatments led to composites with poor interfacial toughness, and for this reason, acid treatment alone is not recommended for marine environments where differential swelling between the fiber and matrix is inevitable. Further research with surface oxidation without the addition of some sort of toughening mechanism is unlikely to change the susceptibility to cracking that these composites possess.

On the contrary, the acid/silane treated fibers produced composites that seemed to yield many desirable characteristics, such as excellent interfacial toughness, excellent wetting, low swelling and low weight gain in seawater. These improved properties bode well for marine use. But the acid/silane treated fiber composites did not produce perfect results. While they showed excellent fiber/matrix adhesion when dry, this was degraded after seawater exposure. But this may not preclude the use of this treatment. It may be that only a little adjustment is required. As discovered in glass fibers, how a silane is applied determines whether it improves or degrades composite water durability.¹²⁷ The

silane appeared to bond to the carbon fiber through the fiber surface oxidation. Optimization of the acid pretreatment time and silane application methods may well yield a more seawater durable fiber/matrix bond, leading to an excellent overall marine composite. Further research is recommended for the acid/silane case. In addition to analyzing the optimal methods of acid pretreatment and silane application, examination of fiber/matrix adhesion through single-fiber adhesion tests and examination of the interphase region properties by nano-indentation methods are recommended.

APPENDICES

A1 Fiber Diameter Measurements

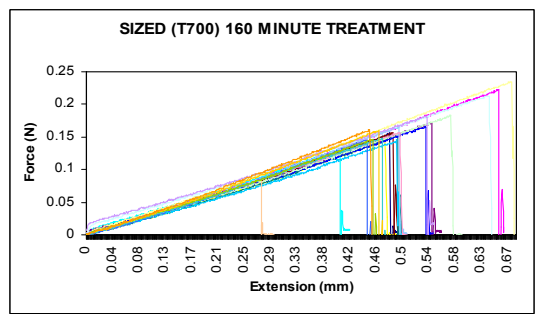
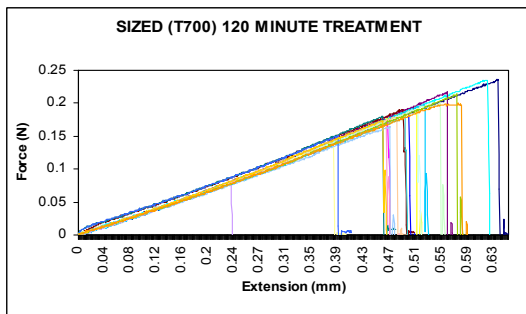
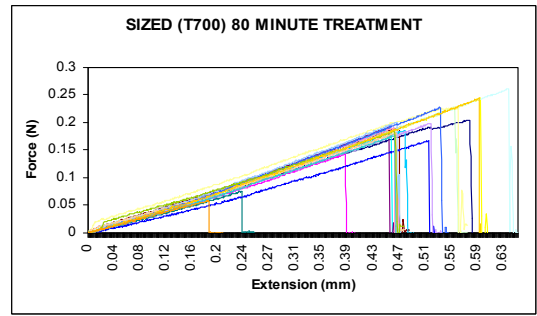
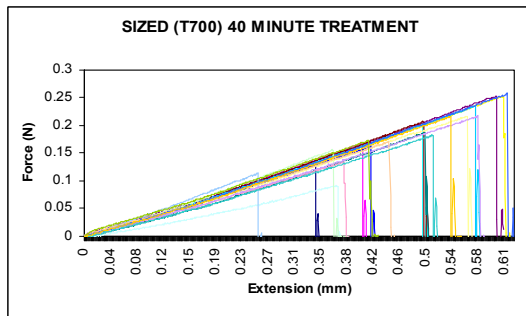
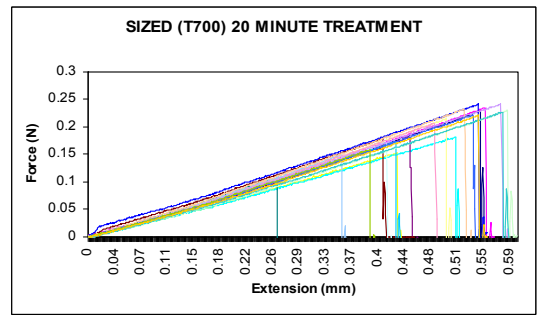
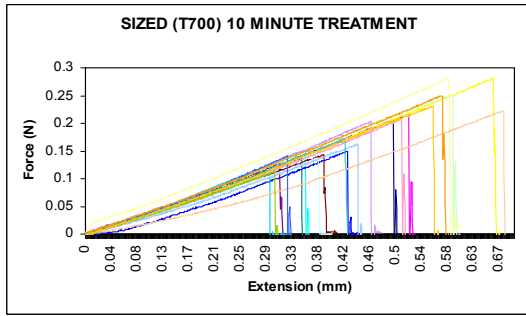
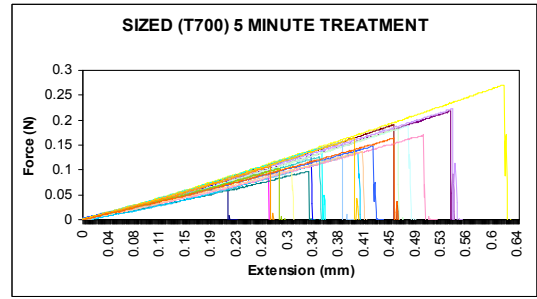
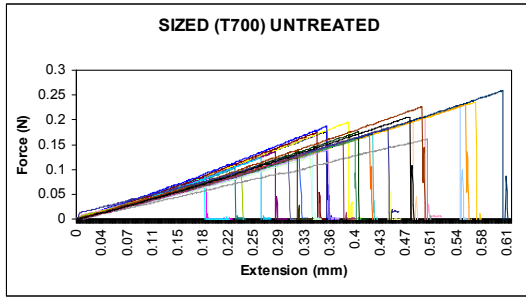
	SIZED (T700) FIBER DIAMETER (MICRONS)							
	Untreated	5 Minute Treatment	10 Minute Treatment	20 Minute Treatment	40 Minute Treatment	80 Minute Treatment	120 Minute Treatment	160 Minute Treatment
1	6.9420	7.3988	6.9428	7.3186	6.6338	6.8671	6.7254	6.3352
2	6.8209	6.8831	6.9525	6.8092	7.1374	6.6187	6.7262	6.2655
3	7.0090	6.9995	6.8692	7.0355	6.5047	6.9301	6.8441	6.3493
4	7.0793	7.0547	7.4247	7.1814	7.049	6.8017	6.8545	6.5568
5	6.8920	6.6631	7.1091	7.2224	7.1884	6.6701	6.7994	6.0509
6	6.4416	7.1039	7.0377	6.9855	7.4987	7.0541	6.6397	6.6703
7	6.5646	6.9816	6.9174	6.707	6.7804	6.7219	6.9046	6.5081
8	6.7847	6.7875	6.7034	6.9393	6.5528	7.2566	6.8937	6.2883
9	6.4002	6.9825	6.87	7.1239	6.8884	6.7594	6.3937	6.1356
10	6.9291	6.8134	6.9806	6.9824	6.8701	6.7803	6.6388	6.1147
11	6.942							
12	6.8209							
13	7.009							
14	7.0793							
15	6.892							
16	6.4416							
17	6.5646							
18	6.7847							
19	6.4002							
20	6.9291							
Ave.	6.91	6.97	6.98	7.03	6.91	6.85	6.74	6.33
Std. Dev.	0.25	0.20	0.19	0.19	0.31	0.19	0.16	0.20

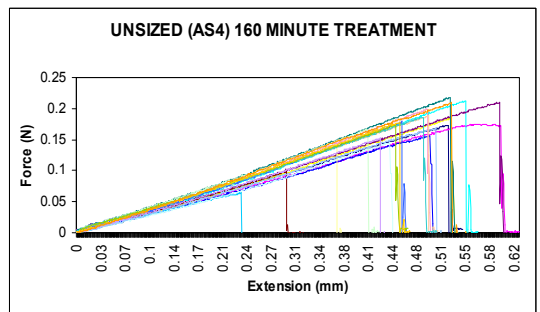
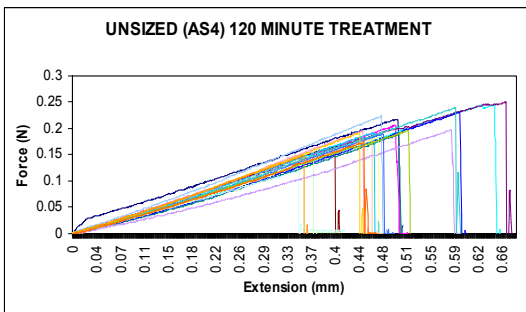
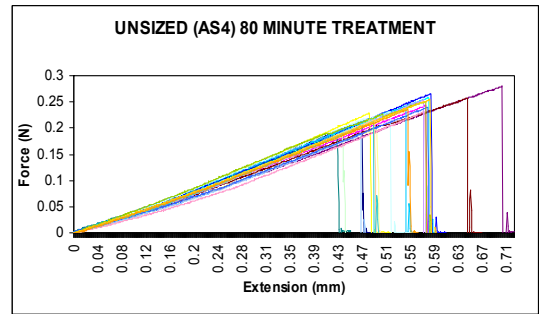
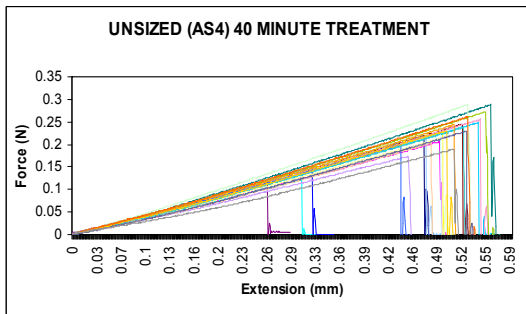
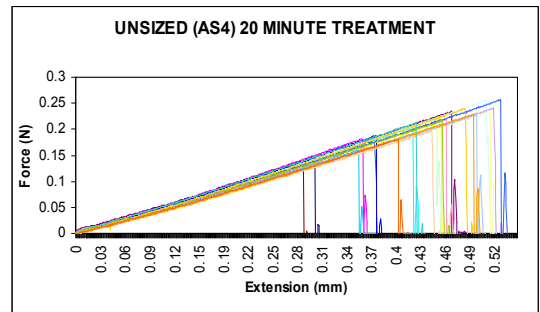
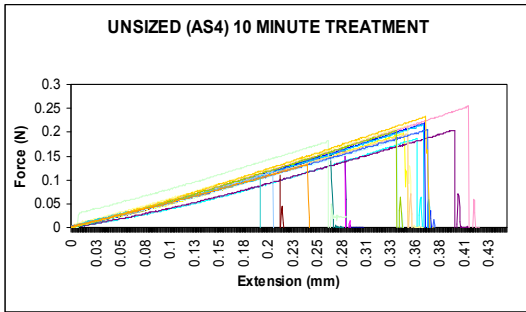
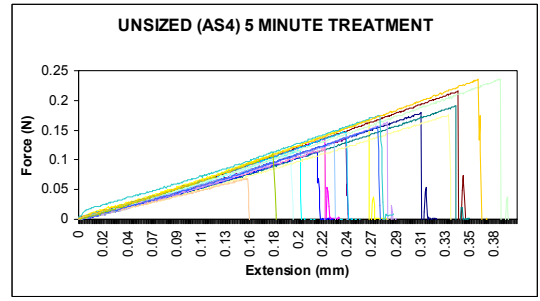
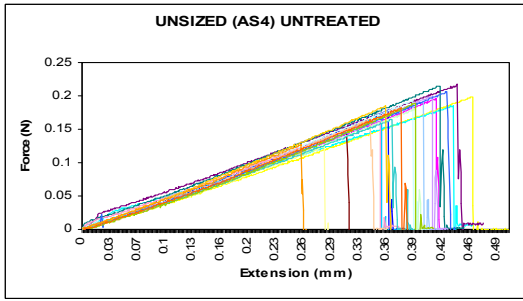
	UNSIZED (AS4) FIBER DIAMETER (MICRONS)							
	Untreated	5 Minute Treatment	10 Minute Treatment	20 Minute Treatment	40 Minute Treatment	80 Minute Treatment	120 Minute Treatment	160 Minute Treatment
1	7.3307	6.8742	7.1307	7.4275	6.936	7.2557	6.6657	6.5861
2	7.4297	6.5563	7.2744	7.1849	7.7424	7.1557	6.6993	6.6159
3	7.3073	7.5239	7.4153	7.1223	7.5454	7.1489	7.1064	6.4208
4	6.8571	7.4319	7.3383	7.0999	7.4324	7.0785	7.0161	6.5609
5	7.0466	7.3599	7.138	7.5014	7.0666	7.3277	7.0962	6.7496
6	7.7625	7.5694	7.2859	7.7669	7.4637	7.301	7.1867	6.1535
7	7.3815	7.624	7.3263	7.1056	7.0742	7.112	7.0572	6.9138
8	7.2071	7.6266	7.1504	7.0355	7.2661	7.6532	7.3074	6.7168
9	7.1525	7.388	7.5081	7.2701	7.3743	7.0302	7.4227	7.1259
10	7.2983	7.3891	7.1985	7.2907	7.3783	7.2652	7.4543	6.3609
Ave.	7.28	7.33	7.28	7.28	7.33	7.23	7.10	6.62
Std. Dev.	0.24	0.35	0.13	0.23	0.25	0.18	0.27	0.28

A2 Fiber Tensile Test Measurements

	SIZED (T700) FIBER TENSILE LOAD (N)							
	Untreated	5 Minute Treatment	10 Minute Treatment	20 Minute Treatment	40 Minute Treatment	80 Minute Treatment	120 Minute Treatment	160 Minute Treatment
1	0.083	0.081	0.114	0.107	0.091	0.059	0.079	0.084
2	0.086	0.097	0.123	0.15	0.114	0.076	0.138	0.131
3	0.098	0.101	0.128	0.153	0.13	0.143	0.151	0.144
4	0.103	0.103	0.137	0.159	0.134	0.168	0.165	0.145
5	0.124	0.108	0.138	0.172	0.157	0.177	0.168	0.146
6	0.124	0.109	0.14	0.173	0.163	0.181	0.173	0.147
7	0.125	0.126	0.143	0.179	0.169	0.184	0.173	0.148
8	0.126	0.135	0.149	0.182	0.171	0.185	0.178	0.152
9	0.129	0.136	0.152	0.182	0.173	0.19	0.179	0.156
10	0.131	0.138	0.163	0.207	0.183	0.191	0.181	0.156
11	0.136	0.146	0.172	0.216	0.187	0.192	0.187	0.156
12	0.14	0.148	0.204	0.222	0.202	0.192	0.19	0.16
13	0.157	0.158	0.206	0.222	0.208	0.198	0.192	0.161
14	0.16	0.164	0.208	0.227	0.217	0.2	0.195	0.166
15	0.161	0.164	0.217	0.229	0.217	0.205	0.199	0.166
16	0.17	0.171	0.223	0.231	0.218	0.227	0.2	0.172
17	0.172	0.183	0.231	0.233	0.235	0.228	0.201	0.182
18	0.176	0.189	0.25	0.235	0.253	0.229	0.214	0.183
19	0.176	0.191	0.252	0.242	0.254	0.244	0.217	0.213
20	0.177	0.219	0.281	0.242	0.259	0.244	0.235	0.222
21	0.184	0.223	0.282			0.261	0.236	0.235
22	0.185	0.271						
23	0.187							
24	0.196							
25	0.198							
26	0.206							
27	0.206							
28	0.226							
29	0.228							
30	0.23							
31	0.236							
32	0.259							
Ave.	0.162	0.147	0.186	0.203	0.192	0.202	0.189	0.163
Std. Dev.	0.05	0.05	0.05	0.04	0.05	0.05	0.03	0.03

	UNSIZE (AS4) FIBER TENSILE LOAD (N)							
	Untreated	5 Minute Treatment	10 Minute Treatment	20 Minute Treatment	40 Minute Treatment	80 Minute Treatment	120 Minute Treatment	160 Minute Treatment
1	0.125	0.069	0.104	0.132	0.114	0.059	0.119	0.064
2	0.127	0.109	0.116	0.145	0.122	0.076	0.15	0.099
3	0.147	0.109	0.118	0.159	0.148	0.143	0.15	0.14
4	0.165	0.114	0.132	0.178	0.173	0.168	0.167	0.146
5	0.165	0.116	0.156	0.181	0.19	0.177	0.175	0.152
6	0.168	0.118	0.162	0.182	0.199	0.181	0.181	0.156
7	0.169	0.129	0.164	0.188	0.203	0.184	0.183	0.167
8	0.179	0.135	0.181	0.196	0.206	0.185	0.189	0.169
9	0.181	0.137	0.184	0.204	0.215	0.19	0.19	0.173
10	0.182	0.148	0.187	0.21	0.217	0.191	0.191	0.174
11	0.185	0.156	0.195	0.213	0.22	0.192	0.192	0.175
12	0.185	0.163	0.198	0.218	0.229	0.192	0.196	0.178
13	0.188	0.167	0.203	0.219	0.229	0.198	0.196	0.179
14	0.191	0.175	0.204	0.22	0.231	0.2	0.198	0.185
15	0.194	0.176	0.206	0.229	0.236	0.205	0.207	0.186
16	0.196	0.179	0.214	0.229	0.237	0.227	0.218	0.188
17	0.199	0.191	0.216	0.234	0.243	0.228	0.225	0.199
18	0.199	0.216	0.219	0.235	0.245	0.229	0.231	0.21
19	0.206	0.235	0.234	0.24	0.249	0.244	0.241	0.21
20	0.215	0.235	0.254	0.241	0.256	0.244	0.245	0.213
21	0.217			0.256	0.261	0.261	0.251	0.217
22				0.256	0.273			
23					0.289			
24					0.289			
Ave.	0.186	0.154	0.182	0.211	0.229	0.209	0.199	0.176
Std. Dev.	0.02	0.04	0.04	0.03	0.05	0.05	0.03	0.04

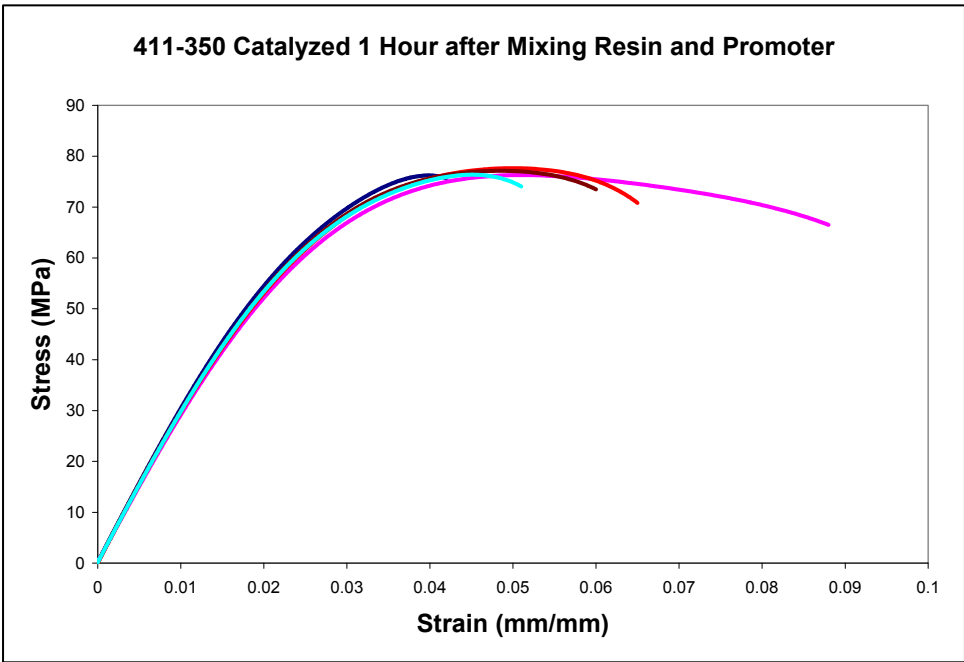
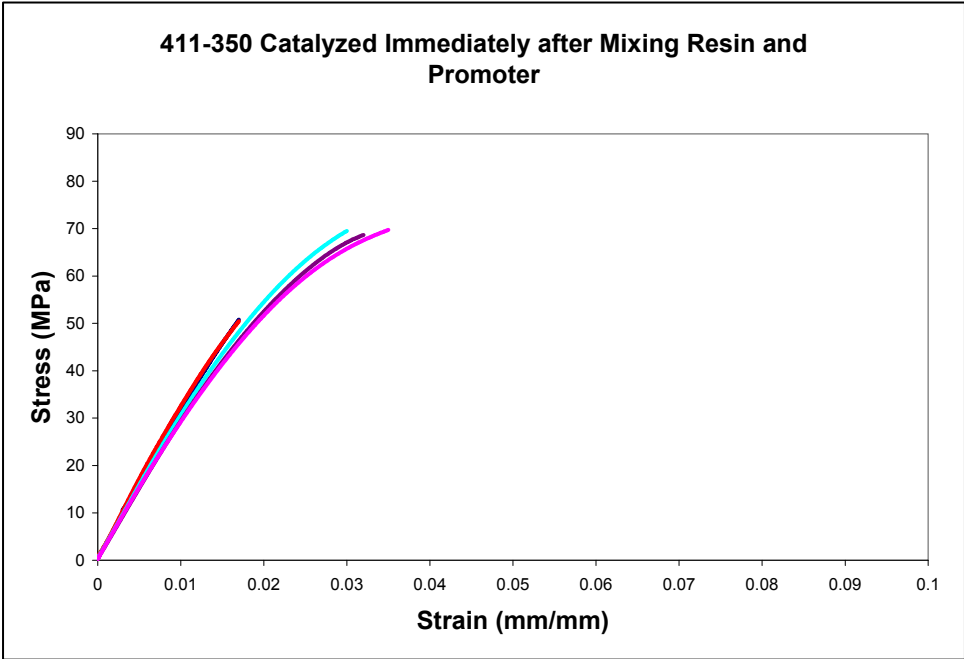




A3 Resin Tensile Test Measurements

VINYL ESTER 411-350 (CATALYZED IMMEDIATELY AFTER MIXING PROMOTER AND RESIN)						
	Width (mm)	Thickness (mm)	Peak Load (N)	Peak Stress (MPa)	Strain at Break (mm/mm)	Modulus (MPa)
1	12.250	4.585	2911.43	51.80	0.017	3240.26
2	11.948	5.178	3178.32	51.40	0.017	3508.29
3	12.110	4.875	4111.53	69.60	0.030	3216.96
4	12.330	4.910	4147.52	68.50	0.031	3084.27
5	12.125	5.398	4579.90	70.00	0.035	3127.85
Ave.	12.128	5.090	4004.32	64.88	0.028	3234.34
Std. Dev.	0.15	0.31	707.30	9.75	0.01	165.26

VINYL ESTER 411-350 (CATALYZED 1 HOUR AFTER MIXING PROMOTER AND RESIN)						
	Width (mm)	Thickness (mm)	Peak Load (N)	Peak Stress (MPa)	Strain at Break (mm/mm)	Modulus (MPa)
1	11.203	3.320	2855.53	76.80	0.041	3174.11
2	11.010	3.140	2635.86	76.20	0.050	3033.95
3	11.185	3.562	3092.69	77.60	0.049	3081.60
4	11.102	3.302	2797.74	76.30	0.046	3087.05
5	10.965	3.435	2903.43	77.10	0.048	3136.47
Ave.	11.093	3.352	2857.05	76.80	0.047	3102.64
Std. Dev.	0.098	0.181	191.59	0.67	0.002	41.92



A4 Fiber Bundle Cohesion Test Measurements

	FIBER BUNDLE WORK OF SEPARATION (N*mm)						
	Sample 1	Sample 2	Sample 3	Sample 4	Sample 5	Sample 6	Ave
Sized (T700)	0.48	0.74	0.31	0.45	0.39		0.48
Unsize	1.09	0.33	0.64	0.47	0.16	0.61	0.55
10 Minute Acid Treated	0.96	1.58	0.86	1.29	0.69		1.08
20 Minute Acid Treated	2.32	0.47	2.82	2.62	1.15	1.55	1.82
40 Minute Acid Treated	3.91	3.29	4.25	3.97	2.59		3.60
80 Minute Acid Treated	7.24	5.24	3.95	5.22	7.00	5.19	6.24
120 Minute Acid Treated	6.44	5.50	8.40	13.07			8.35
160 Minute Acid Treated	6.51	8.14	9.47	6.61	10.97		8.34
Unsize + Silane	0.11	0.15	0.11	0.06	0.38		0.11
2.5 Minute Acid Treated + Silane	0.13	0.28	0.57				0.33
20 Minute Acid Treated + Silane	0.40	0.25	0.31	0.35			0.33
40 Minute Acid Treated + Silane	0.22	0.35	0.22	0.12	0.61		0.30
10 Minute Water Boil	0.28	0.27	0.15	0.26	0.14	0.21	0.22
160 Minute Water Boil	0.14	0.52	0.35	0.44	0.35		0.36

A5 Fiber Surface Energy Measurements

SIZED UNTREATED FIBER SURFACE ENERGY DATA						
SAMPLE NO.	FIBER DIAMETER (MICRONS)				ADVANCING CONTACT ANGLE (DEG)	RECEDING CONTACT ANGLE (DEG)
	Sample 1	Sample 2	Sample 3	Ave.		
1	7.44	7.32	7.26	7.34	48.72	44.64
2	7.36	7.45	7.49	7.43	73.2	60.14
3	7.1	7.41	7.52	7.34	46.33	44.73
4	7.02	7.09	7.66	7.26	65.1	48.74
5	7.85	7.8	7.74	7.80	54.12	39.83
6	7.32	7.22	7.09	7.21	60.48	47.89
7	7.61	7.53	7.61	7.58	45.4	40.05
8	7.79	7.72	7.87	7.79		
9	7.69	7.63	7.61	7.64	51.96	37.02
10	7.1	7.17	7.18	7.15	53.3	38.7
11	7.39	7.6	7.18	7.39	38.48	33.54
AVE.				7.45	53.71	43.53

UNSIZE D UNTREATED FIBER SURFACE ENERGY DATA						
SAMPLE NO.	FIBER DIAMETER (MICRONS)				ADVANCING CONTACT ANGLE (DEG)	RECEDING CONTACT ANGLE (DEG)
	Sample 1	Sample 2	Sample 3	Ave.		
1	6.91	6.65	6.79	6.78	38.66	26.9
2	6.98	6.98	7.1	7.02	39.96	20.99
3	7.32	7.41	7.46	7.40	61.5	38
4	7.14	7.23	7.16	7.18	42.72	20.81
5	7.01	7.01	7.04	7.02	40.43	22.05
6	6.97	7.01	6.96	6.98	42.84	31.84
7	7.48	7.42	7.42	7.44	51.6	35.08
8	6.92	7.07	7.07	7.02	48.34	26.69
9	6.94	6.93	6.98	6.95	53.02	25.3
10	7.22	7.3	7.27	7.26	53.26	32.34
AVE.				7.11	47.23	28.00

A6 Transverse Tensile Strength Measurements

SIZED FIBER – NO TREATMENT NO SEAWATER IMMERSION											
Specimen	1	2	3	4	5	6	7	8	9	10	AVE
Width	3.88	3.9	4.06	3.86	4.06	3.94	3.76	3.92	3.85	3.73	3.90
Thickness	2.18	2.19	2.14	2.16	2.19	2.13	2.16	2.13	2.07	2.12	2.15
Load	183.01	130.01	168.52	180.36	225.49	185.42	102.97	172.76	130.11	129.70	160.83
Stress	21.64	15.22	19.40	21.63	25.36	22.09	12.68	20.69	16.33	16.40	19.14

SIZED FIBER – 2.5 MINUTE ACID TREATMENT NO SEAWATER IMMERSION											
Specimen	1	2	3	4	5	6	7	8	9	10	AVE
Width	3.50	3.71	3.79	3.76	3.69	3.75	3.63	3.85	3.76	3.75	3.72
Thickness	2.06	2.09	2.08	2.07	2.02	2.06	2.09	2.08	2.01	2.03	2.06
Load	146.51	269.71	197.14	272.49	239.52	261.71	262.74	210.13	238.89	265.69	236.45
Stress	20.32	34.78	25.01	35.01	32.13	33.88	34.63	26.24	31.61	34.90	30.85

SIZED FIBER –5 MINUTE ACID TREATMENT NO SEAWATER IMMERSION											
Specimen	1	2	3	4	5	6	7	8	9	10	AVE
Width	3.92	3.72	3.84	3.72	3.82	3.77	3.90	3.77	3.81	3.64	3.79
Thickness	2.16	2.14	2.17	2.13	2.12	2.14	2.15	2.13	2.08	2.09	2.13
Load	220.55	250.83	311.01	243.24	185.92	244.51	201.63	288.60	198.22	161.69	230.62
Stress	26.05	31.51	37.32	30.70	22.96	30.31	24.05	35.94	25.01	21.25	28.51

SIZED FIBER – 10 MINUTE ACID TREATMENT NO SEAWATER IMMERSION											
Specimen	1	2	3	4	5	6	7	8	9	10	AVE
Width	3.88	3.85	3.91	3.70	3.91	3.87	3.78	3.87	3.96	3.86	3.86
Thickness	2.15	2.13	2.09	2.11	2.15	2.15	2.14	2.16	2.17	2.24	2.15
Load	139.41	142.12	217.52	200.00	156.15	227.24	189.93	237.00	145.72	120.76	177.58
Stress	16.71	17.33	26.62	25.62	18.58	27.31	23.48	28.35	16.96	13.97	21.49

SIZED FIBER – 20 MINUTE ACID TREATMENT NO SEAWATER IMMERSION											
Specimen	1	2	3	4	5	6	7	8	9	10	AVE
Width	3.79	3.77	3.75	3.97	4.10	3.86	3.93	3.85	3.74	3.74	3.85
Thickness	2.13	2.15	2.08	2.10	2.17	2.13	2.13	2.23	2.16	2.13	2.14
Load	51.42	161.80	182.56	132.23	215.22	90.34	154.60	47.17	117.03	217.89	137.02
Stress	6.37	19.96	23.41	15.86	24.19	10.99	18.47	5.49	14.49	27.35	16.66

SIZED FIBER – 40 MINUTE ACID TREATMENT NO SEAWATER IMMERSION											
Specimen	1	2	3	4	5	6	7	8	9	10	AVE
Width	3.83	3.73	3.86	3.81	3.72	3.73	3.84	3.78	3.74	3.88	3.79
Thickness	2.17	2.17	2.18	2.13	2.14	2.12	2.09	2.10	2.13	2.04	2.13
Load	100.16	47.02	105.53	135.66	54.07	120.41	60.07	47.71	82.72	77.08	83.04
Stress	12.05	5.81	12.54	16.72	6.79	15.23	7.49	6.01	10.38	9.74	10.28

UNSIZED FIBER – NO TREATMENT NO SEAWATER IMMERSION											
Specimen	1	2	3	4	5	6	7	8	9	10	AVE
Width	3.84	3.91	3.83	3.77	3.79	3.86	3.77	3.84	3.67	3.72	3.80
Thickness	2.05	2.03	2.06	2.10	2.00	2.10	2.07	2.03	1.95	2.00	2.04
Load	221.60	206.59	205.23	197.98	173.38	183.34	220.84	157.63	164.13	196.56	192.73
Stress	28.15	26.03	26.01	25.01	22.87	22.62	28.30	20.22	22.93	26.42	24.86

UNSIZED FIBER – 2.5 MINUTE ACID TREATMENT NO SEAWATER IMMERSION											
Specimen	1	2	3	4	5	6	7	8	9	10	AVE
Width	3.76	3.75	3.8	3.58	3.84	3.79	3.72	3.93	3.82	3.78	3.78
Thickness	2.01	1.99	2.04	2.00	1.90	2.05	1.98	2.01	1.95	2.04	2.00
Load	206.79	205.00	197.36	275.38	249.47	233.60	247.23	244.77	228.01	245.49	233.31
Stress	27.36	27.47	25.46	38.46	34.19	30.07	33.57	30.99	30.61	31.84	31.00

UNSIZED FIBER – 5 MINUTE ACID TREATMENT NO SEAWATER IMMERSION											
Specimen	1	2	3	4	5	6	7	8	9	10	AVE
Width	3.79	3.62	3.67	3.8	3.77	3.89	3.85	3.81	3.76	3.98	3.79
Thickness	2.00	2.07	2.06	2.08	2.02	2.06	2.15	2.11	2.09	2.09	2.07
Load	212.07	220.88	235.71	236.79	205.06	193.00	178.43	227.42	163.53	248.91	212.18
Stress	27.98	29.48	31.18	29.96	26.93	24.08	21.56	28.29	20.81	29.92	27.02

UNSIZE FIBER – 10 MINUTE ACID TREATMENT NO SEAWATER IMMERSION											
Specimen	1	2	3	4	5	6	7	8	9	10	AVE
Width	3.72	3.67	3.76	3.81	3.83	3.98	3.82	3.94	3.69	3.77	3.80
Thickness	2.10	2.14	2.08	2.13	2.07	2.11	2.14	2.15	2.03	2.10	2.11
Load	98.88	154.94	177.54	156.81	142.74	153.91	139.41	165.84	173.13	141.56	150.48
Stress	12.66	19.73	22.70	19.32	18.00	18.33	17.05	19.58	23.11	17.88	18.84

UNSIZE FIBER – 20 MINUTE ACID TREATMENT NO SEAWATER IMMERSION											
Specimen	1	2	3	4	5	6	7	8	9	10	AVE
Width	3.77	3.74	3.59	3.64	3.81	3.72	3.92	3.64	3.68	3.55	3.71
Thickness	2.13	2.11	2.19	2.05	2.07	2.09	2.05	2.12	2.06	2.11	2.10
Load	51.87	121.50	84.96	146.96	168.44	152.26	133.67	146.21	75.48	188.66	127.00
Stress	6.46	15.40	10.81	19.69	21.36	19.58	16.63	18.95	9.96	25.19	16.40

UNSIZE FIBER – 40 MINUTE ACID TREATMENT NO SEAWATER IMMERSION											
Specimen	1	2	3	4	5	6	7	8	9	10	AVE
Width	3.80	3.72	3.83	3.72	3.84	3.91	3.86				3.81
Thickness	2.01	2.03	2.03	2.01	2.00	1.85	2.06				2.00
Load	89.12	70.27	89.72	69.71	87.49	44.17	13.43				66.27
Stress	11.67	9.31	11.54	9.32	11.39	6.11	1.69				8.72

UNSIZE FIBER – NO TREATMENT ONE MONTH SEAWATER IMMERSION											
Specimen	1	2	3	4	5	6	7	8	9	10	AVE
Width	3.95	4.01	3.86	4.03	3.86	4.00	4.04	4.04	4.02	4.06	3.99
Thickness	2.18	2.48	2.19	2.19	2.21	2.21	2.24	2.17	2.25	2.16	2.23
Load	171.92	247.64	96.33	89.74	102.20	123.03	163.34	129.92	163.67	117.05	140.49
Stress	19.97	24.90	11.40	10.17	11.98	13.92	18.05	14.82	18.09	13.35	15.66

UNSIZE FIBER – 2.5 MINUTE ACID TREATMENT ONE MONTH SEAWATER IMMERSION											
Specimen	1	2	3	4	5	6	7	8	9	10	AVE
Width	3.75	3.88	3.73	3.78	3.78	3.71	3.91	3.79	3.66	3.69	3.77
Thickness	2.09	2.12	2.12	2.14	2.04	2.19	2.14	2.14	2.17	2.10	2.13
Load	187.84	173.75	148.74	207.88	208.39	205.40	244.69	209.64	180.86	206.20	197.34
Stress	23.97	21.12	18.81	25.70	27.02	25.28	29.24	25.85	22.77	26.61	24.64

UNSIZE FIBER – 5 MINUTE ACID TREATMENT ONE MONTH SEAWATER IMMERSION											
Specimen	1	2	3	4	5	6	7	8	9	10	AVE
Width	3.86	3.97	3.96	4.03	4.01	3.93	3.77	3.97	3.94	3.86	3.93
Thickness	2.21	2.22	2.16	2.21	2.18	2.15	2.23	2.21	2.21	2.15	2.19
Load	216.48	228.62	249.08	233.15	205.81	140.63	209.55	247.63	235.02	150.20	211.62
Stress	25.38	25.94	29.12	26.18	23.54	16.64	24.93	28.22	26.99	18.10	24.50

UNSIZE FIBER – 10 MINUTE ACID TREATMENT ONE MONTH SEAWATER IMMERSION											
Specimen	1	2	3	4	5	6	7	8	9	10	AVE
Width	3.99	4.09	3.88	3.98	3.97	4.07	3.91	4.03	3.82	3.81	3.96
Thickness	2.09	2.18	2.24	2.26	2.17	2.2	2.24	2.19	2.18	2.25	2.20
Load	172.95	166.73	190.86	211.29	170.06	137.11	172.93	216.60	146.70	171.43	175.67
Stress	20.74	18.70	21.96	23.49	19.74	15.31	19.74	24.54	17.62	20.00	20.18

UNSIZE FIBER – 20 MINUTE ACID TREATMENT ONE MONTH SEAWATER IMMERSION											
Specimen	1	2	3	4	5	6	7	8	9	10	AVE
Width	3.84	3.70	3.94	3.91	3.90	4.04	3.81	3.93	3.91	3.93	3.89
Thickness	2.14	2.28	2.09	2.17	2.27	2.24	2.29	2.27	2.27	2.26	2.23
Load	111.42	87.37	184.30	42.25	233.12	72.42	46.24	69.24	98.73	128.17	107.33
Stress	13.56	10.36	22.38	4.98	26.33	8.00	5.30	7.76	11.12	14.43	12.42

UNSIZE FIBER – 40 MINUTE ACID TREATMENT ONE MONTH SEAWATER IMMERSION											
Specimen	1	2	3	4	5	6	7	8	9	10	AVE
Width	3.92	3.78	4.03	3.81	3.88	3.91	3.85	3.78	3.72	3.71	3.84
Thickness	2.11	2.16	2.17	2.12	2.09	2.11	2.16	2.17	2.04	2.05	2.12
Load	50.52	57.37	47.71	74.68	125.62	46.74	53.82	83.30	56.56	62.22	65.85
Stress	6.11	7.03	5.46	9.25	15.49	5.67	6.47	10.16	7.45	8.18	8.13

UNSIZE FIBER – NO TREATMENT TWO MONTHS SEAWATER IMMERSION											
Specimen	1	2	3	4	5	6	7	8	9	10	AVE
Width	3.93	3.71	3.97	3.89	3.84	4.05	3.89	3.77	3.93	4.03	3.90
Thickness	2.21	2.20	2.48	2.17	2.21	2.40	2.50	2.16	2.23	2.24	2.28
Load	133.98	127.58	251.27	115.90	124.25	167.71	218.14	187.95	140.09	128.12	159.50
Stress	15.43	15.63	25.52	13.73	14.64	17.25	22.43	23.08	15.98	14.19	17.79

UNSIZE FIBER – 2.5 MINUTE ACID TREATMENT TWO MONTHS SEAWATER IMMERSION											
Specimen	1	2	3	4	5	6	7	8	9	10	AVE
Width	3.64	3.81	3.85	3.79	3.95	3.79	3.78	3.8	3.81	3.80	3.80
Thickness	2.04	2.09	2.16	2.10	2.04	2.11	2.02	2.08	2.10	1.98	2.07
Load	181.18	245.96	178.07	230.50	184.21	229.06	171.34	206.73	230.24	195.78	205.31
Stress	24.40	30.89	21.41	28.96	22.86	28.64	22.44	26.15	28.78	26.02	26.06

UNSIZE FIBER – 5 MINUTE ACID TREATMENT TWO MONTHS SEAWATER IMMERSION											
Specimen	1	2	3	4	5	6	7	8	9	10	AVE
Width	3.93	3.81	3.98	3.91	3.98	3.83	3.64	3.85	3.80	3.95	3.87
Thickness	2.21	2.23	2.16	2.22	2.17	2.16	2.22	2.24	2.17	2.23	2.20
Load	253.13	192.36	221.64	227.04	115.27	184.32	229.76	167.98	207.46	216.58	201.55
Stress	29.14	22.64	25.78	26.16	13.35	22.28	28.43	19.48	25.16	24.59	23.70

UNSIZE FIBER – 10 MINUTE ACID TREATMENT TWO MONTHS SEAWATER IMMERSION											
Specimen	1	2	3	4	5	6	7	8	9	10	AVE
Width	3.89	3.96	3.83	4.00	3.9	3.72	3.92	3.86	4.06	3.84	3.90
Thickness	2.17	2.20	2.23	2.21	2.27	2.21	2.25	2.21	2.20	2.15	2.21
Load	204.61	127.98	184.23	238.09	181.92	227.26	207.06	245.02	161.33	150.54	192.80
Stress	24.24	14.69	21.57	26.93	20.55	27.64	23.48	28.72	18.06	18.23	22.41

UNSIZE FIBER – 20 MINUTE ACID TREATMENT TWO MONTHS SEAWATER IMMERSION											
Specimen	1	2	3	4	5	6	7	8	9	10	AVE
Width	4.03	3.76	3.92	3.92	3.87	3.87	3.88	3.75	3.87	3.75	3.86
Thickness	2.21	2.18	2.21	2.23	2.20	2.22	2.15	2.23	2.10	2.24	2.20
Load	146.79	209.01	86.67	65.14	182.57	74.39	99.20	114.88	201.02	180.02	135.97
Stress	16.48	25.50	10.00	7.45	21.44	8.66	11.89	13.74	24.74	21.43	16.13

UNSIZE FIBER – 40 MINUTE ACID TREATMENT TWO MONTHS SEAWATER IMMERSION											
Specimen	1	2	3	4	5	6	7	8	9	10	AVE
Width	3.89	3.68	3.90	3.96	3.65	3.80	3.78	3.59	3.57	3.79	3.76
Thickness	2.14	2.04	2.22	2.20	2.17	2.22	2.11	2.18	2.12	2.15	2.16
Load	45.53	68.28	125.60	43.02	34.44	47.71	42.61	229.33	46.77	97.02	78.03
Stress	5.47	9.10	14.51	4.94	4.35	5.66	5.34	29.30	6.18	11.91	9.67

UNSIZE FIBER – 10 MINUTE ACID TREATMENT THREE MONTHS SEAWATER IMMERSION											
Specimen	1	2	3	4	5	6	7	8	9	10	AVE
Width	3.89	3.74	3.57	3.85	3.6	3.52	3.71	3.81	3.82	3.74	3.73
Thickness	1.92	1.97	1.98	2.07	2.07	2.07	2.04	1.93	2.08	1.99	2.01
Load	258.80	233.41	220.33	129.28		215.31	212.67	203.54	244.51	220.63	215.39
Stress	34.65	31.68	31.17	16.22		29.55	28.10	27.68	30.77	29.64	28.83

UNSIZE FIBER – 2.5 MINUTE ACID TREATMENT THREE MONTHS SEAWATER IMMERSION											
Specimen	1	2	3	4	5	6	7	8	9	10	AVE
Width	3.63	3.72	3.74	3.85	3.74	3.86	3.66	3.78			3.75
Thickness	1.93	1.92	2.00	2.05	1.91	2.08	2.07	1.94			1.99
Load	172.12	200.51	234.37	205.32	173.45	213.94	169.19	239.44			201.04
Stress	24.57	28.07	31.33	26.01	24.28	26.65	22.33	32.65			26.99

UNSIZE FIBER – 5 MINUTE ACID TREATMENT THREE MONTHS SEAWATER IMMERSION											
Specimen	1	2	3	4	5	6	7	8	9	10	AVE
Width	3.63	3.66	3.63	3.66	3.86	3.64	3.61	3.65	3.66	3.66	3.67
Thickness	1.92	2.04	1.99	2.06	2.08	1.98	2.08	2.07	1.94	1.91	2.01
Load	222.63	228.68	226.37	236.61	230.79	61.73	217.97	174.94	181.11	209.25	199.01
Stress	31.94	30.63	31.34	31.38	28.75	8.56	29.03	23.15	25.51	29.93	27.02

UNSIZE FIBER – 20 MINUTE ACID TREATMENT THREE MONTHS SEAWATER IMMERSION											
Specimen	1	2	3	4	5	6	7	8	9	10	AVE
Width	3.8	3.74	3.76	3.82	3.76	3.84	3.82	3.77			3.79
Thickness	2.11	1.94	2.04	2.09	2.03	2.07	2.06	2.05			2.05
Load	147.67	186.96	209.08	133.04	79.50	167.93	117.45	115.28			144.61
Stress	18.42	25.77	27.26	16.66	10.42	21.13	14.92	14.92			18.69

UNSIZE FIBER – 40 MINUTE ACID TREATMENT THREE MONTHS SEAWATER IMMERSION											
Specimen	1	2	3	4	5	6	7	8	9	10	AVE
Width	3.74	3.9	3.73	3.64	3.64	3.68	3.72	3.6	3.54	3.76	3.70
Thickness	1.96	2.10	2.06	2.12	2.14	2.08	2.04	2.09	2.1	2.06	2.08
Load	72.33	116.58	141.18	99.97	163.10	54.32	108.81	62.18	88.43	81.97	98.89
Stress	9.87	14.23	18.37	12.96	20.94	7.10	14.34	8.26	11.90	10.58	12.85

SIZE FIBER + SILANE – NO ACID TREATMENT NO SEAWATER IMMERSION											
Specimen	1	2	3	4	5	6	7	8	9	10	AVE
Width	3.77	3.94	3.72	3.75	3.66	3.83	3.79	3.78	3.73	3.74	3.77
Thickness	2.09	1.99	2.00	2.05	2.05	2.02	2.14	2.05	2.11	2.01	2.05
Load	193.57	216.71	192.60	195.78	161.81	204.15	218.73	215.07	205.60	171.39	197.54
Stress	24.57	27.64	25.89	25.47	21.57	26.39	26.97	27.76	26.12	22.80	25.52

UNSIZE D FIBER + SILANE – NO ACID TREATMENT NO SEAWATER IMMERSION											
Specimen	1	2	3	4	5	6	7	8	9	10	AVE
Width	3.79	3.88	3.69	3.77	3.81	3.82	3.9	3.87	3.77	3.88	3.82
Thickness	2.07	1.99	2.12	2.08	2.11	2.07	2.08	2.08	2.02	2.02	2.06
Load	203.58	203.96	203.76	206.12	230.02	188.67	222.91	231.16	199.72	209.04	209.89
Stress	25.95	26.42	26.05	26.29	28.61	23.86	27.48	28.72	26.23	26.67	26.63

UNSIZE D FIBER + SILANE – 2.5 MINUTE ACID TREATMENT NO SEAWATER IMMERSION											
Specimen	1	2	3	4	5	6	7	8	9	10	AVE
Width	3.75	3.6	3.72	3.78	3.68	3.71	3.8	3.79	3.68	3.81	3.73
Thickness	1.89	1.97	2.04	1.93	2.08	2.05	1.98	2.05	1.99	2.09	2.01
Load	238.12	297.69	286.20	237.77	281.96	286.56	277.66	193.52	181.45	295.81	257.67
Stress	33.60	41.97	37.71	32.59	36.84	37.68	36.90	24.91	24.78	37.15	34.41

UNSIZE D FIBER + SILANE – 20 MINUTE ACID TREATMENT NO SEAWATER IMMERSION											
Specimen	1	2	3	4	5	6	7	8	9	10	AVE
Width	3.82	3.70	3.64	3.85	3.97	3.68	3.62	3.72	3.65	3.71	3.74
Thickness	2.10	2.13	1.99	2.01	2.12	2.09	2.07	2.01	1.97	2.13	2.06
Load	286.68	236.16	252.84	235.84	249.97	232.47	275.27	225.59	269.31	181.92	244.61
Stress	35.74	29.97	34.91	30.48	29.70	30.22	36.73	30.17	37.45	23.02	31.84

UNSIZE D FIBER + SILANE – 40 MINUTE ACID TREATMENT NO SEAWATER IMMERSION											
Specimen	1	2	3	4	5	6	7	8	9	10	AVE
Width	3.83	3.81	3.82	3.65	3.693	3.88	3.63	3.82	3.71	3.61	3.75
Thickness	2.08	2.09	2.07	2.14	2.16	2.04	2.07	2.09	1.99	2.09	2.08
Load	315.82	273.35	242.22	331.61	269.76	249.93	262.84	295.42	256.00	272.51	276.95
Stress	39.64	34.33	30.63	42.45	33.82	31.58	34.98	37.00	34.67	36.12	35.52

UNSIZE D FIBER + SILANE – NO ACID TREATMENT 3 MONTHS SEAWATER IMMERSION											
Specimen	1	2	3	4	5	6	7	8	9	10	AVE
Width	3.82	3.82	3.81	3.76	3.73	3.77	3.68	3.84	3.78	3.8	3.78
Thickness	2.06	2.00	2.08	2.05	2.01	2.01	2.12	2.08	2.07	1.98	2.05
Load	135.81	214.92	144.79	202.46	164.78	197.76	185.00	132.60	189.63	168.80	173.65
Stress	17.26	28.13	18.27	26.27	21.98	26.10	23.71	16.60	24.23	22.44	22.50

UNSIZE D FIBER + SILANE – 2.5 MINUTE ACID TREATMENT 3 MONTHS SEAWATER IMMERSION											
Specimen	1	2	3	4	5	6	7	8	9	10	AVE
Width	3.56	3.78	3.49	3.78	3.65	3.64	3.57	3.81	3.94	3.65	3.69
Thickness	2.05	2.08	2.08	1.97	1.98	2.07	2.12	2.00	2.08	2.01	2.04
Load	184.23	227.57	226.25	236.53	203.01	222.02	150.47	163.09	226.61	182.98	202.28
Stress	25.24	28.94	31.17	31.76	28.09	29.47	19.88	21.40	27.65	24.94	26.86

UNSIZE FIBER + SILANE – 20 MINUTE ACID TREATMENT 3 MONTHS SEAWATER IMMERSION											
Specimen	1	2	3	4	5	6	7	8	9	10	AVE
Width	3.93	3.61	3.69	3.8	3.78	3.64	3.83	3.72	3.66	3.74	3.74
Thickness	2.01	2.10	2.09	2.09	2.11	2.02	2.01	1.98	2.07	1.86	2.03
Load	185.30	205.32	183.71	145.00	197.58	105.84	215.57	149.04	179.72	141.84	170.89
Stress	23.46	27.08	23.82	18.26	24.77	14.39	28.00	20.23	23.72	20.39	22.41

UNSIZE FIBER + SILANE – 40 MINUTE ACID TREATMENT 3 MONTHS SEAWATER IMMERSION											
Specimen	1	2	3	4	5	6	7	8	9	10	AVE
Width	3.84	3.69	3.71	3.76	3.75	3.66	3.7	3.68	3.67	3.90	3.74
Thickness	2.08	2.05	2.09	2.08	2.09	2.02	1.95	2.08	2.07	2.03	2.05
Load	152.82	150.76	152.91	193.85	148.48	132.36	158.26	150.11	189.97	58.83	148.84
Stress	19.13	19.93	19.72	24.79	18.94	17.90	21.93	19.61	25.01	7.43	19.44

REFERENCES

- 1) W. L. Bradley and T.S. Grant, The Effect of the Moisture Absorption on the Interfacial Strength of Polymeric Matrix Composites, *Journal of Materials Science*, 30, 21, 5537-5542, 1995.
- 2) W. L. Bradley, C. A. Wood, B. A. Pratt, and C. S. Chatawanich, Effect of Seawater on the Interfacial Strength and Durability of Polymer Composites, *Proc. Of Third Int. Conf. on Progress in Durability Analysis of Composite Systems*, Blacksburg, Virginia, Sept. 14-17, 1997.
- 3) W. L. Bradley, P. Chiou, and T. S. Grant, The Effect of Seawater on Polymeric Composite Materials, In: *Composite Materials for Offshore Operations*, Proceedings of the First International Workshop, edited Wang, S.S. and Fitting, D.W., NIST Special Publication 887, National Institute of Standards and Technology, 193–202, 1995.
- 4) Wendon Yachts, Wendon 790 Power Catamaran,
<http://www.wendonyachts.com/wendon790.asp>.
- 5) Brunswick Family Boat Co., Bayliner Division, Online catalog, 20008.
- 6) K. Makinen, S.E. Hellbratt, K.A. Olsson, The Development of Sandwich Structures for Naval Vessels During Years. In: *Mechanics of Sandwich Structures*, Edited by Vautrin, A., Kluwer Academic Publishers: Netherlands, 13-28., 1988.

- 7) P. Goubalt and S. Mayes, Comparative Analysis of Metal and Composite Materials for the Primary Structure of Patrol Boat. Naval Eng J. 108, 3, 387-97, 1996.
- 8) C. S. Smith and A. H. Monks, Design of High Performance Hulls in Fibre-Reinforced Plastics, Proceedings of the Symposium on Small Fast Warships and Security Vessels, London, 95-110, May 1982.
- 9) A. P. Mouritz, E. Gellert, P. Burchill and K. Challis, Review of Advanced Composite Structures for Naval Ships and Submarines, Composite Structures, 53, 21-41, 2001.
- 10) Photograph of KNM Storm Skjold class ship on Sea Trials, Royal Norwegian Navy,
<http://www.aviationweek.com/aw/blogs/defense/index.jsp?plckController=Blog&plckScript=blogScript&plckElementId=blogDest&plckBlogPage=BlogViewPost&plckPostId=Blog%3A27ec4a53-dcc8-42d0-bd3a-01329aef79a7Post%3Aeee080e5-542c-4623-acb9-66973550656f>.
- 11) Photograph of Visby Class Corvette, Royal Swedish Navy,
<http://www.globalsecurity.org/military/world/europe/images/visby-AK0007.jpg>.
- 12) L. B. Nguyen and M. O. Critchfield, Feasibility Study and Fabrication Demonstration of FRP Hull Structures for Naval Surface Combatants, Proceedings of the International Conference on Advances in Marine Structures III, Dunfermline, May 20-23, 1997.

- 13) S. Mayes and B. Scott, Advanced All-composite surface Combatant, Proceedings of the American Society of Naval Engineers (ASNE) Symposium, vol. 1, Biloxi, Mississippi, 16-17, 1995.
- 14) S. Mayes and B. Scott, Advanced All-composite surface Combatant, Proceedings of the American Society of Naval Engineers (ASNE) Symposium, vol. 2, Biloxi, Mississippi, 73-112, 1995.
- 15) D.W. Chalmers, R.J. Osburn and A. Bunney, Hull Construction of CMVs in the United Kingdom, Proceedings of the International Symposium on Mine Warfare Vessels and Systems, London, Paper 13, June 12-15, 1984.
- 16) A.J. Harris, The Hunt Class Mine Countermeasures Vessels, Trans RINA, 122, 485-503, 1980.
- 17) E.C. Pitts and A.L. Dorey, Experience with the Design of GRP MCM Vessels, Proceedings of the International Symposium on Mine Warfare Vessels and Systems, London, Paper 2, June 12-15, 1984.
- 18) D.K. Brown, Design Considerations for MCMV, Naval Forces, 11, 1, 31-8, 1990.
- 19) Photograph of HMS Sandown (M101), <http://www.naval-technology.com/projects/sandown/images/sandown3.jpg>.
- 20) J. Kim and Y. Mai, Engineered Interfaces in Fiber Reinforced Composites, Elsevier Science Ltd, First Edition, ISBN 0-08-042695-0, 1998.
- 21) P. Ehrburger and P. Donnet, Surface treatment of carbon fiber for resin matrices, Strong Fibers, Handbook of Composites, Vol. 1, Elsevier Sci., Amsterdam, 577-608, 1985.

- 22) J. G. Williams, M. E. Donnellan, M. R. James and W. L. Morris, Properties of the Interphase in Organic Matrix Composites, *Materials Science & Engineering*, A126, 1-2, 305-312, 1990.
- 23) M. R. Piggott, The Effect of the Interface/Interphase on Fiber Composite Properties, *Polym. Compos.*, 8, 5, 291-296, 1987.
- 24) L. T. Drzal, M. J. Rich, M. F. Koenig and P. F. Lloyd, Adhesion of graphite fibers to epoxy matrices: II. The effect of fiber finish, 16, 133-152, 1983.
- 25) L. T. Drzal, *Tough Composite Materials: Recent Developments*, Noyes, Park Ridge, NJ, 207-222, 1985.
- 26) A. Kootsookos and A. P. Mouritz, Seawater Durability of Glass- and Carbon-polymer Composites, *Composites Science and Technology*, 64, 1503-1511, 2004.
- 27) Compendium of Chemical Terminology, hydrolysis
(<http://goldbook.iupac.org/H02902.html>). Accessed 23 Jan 2007.
- 28) Compendium of Chemical Terminology, solvolysis
(<http://goldbook.iupac.org/S05762.html>). Accessed 23 Jan 2007.
- 29) J. M. Augl and A. E. Berger, Moisture Effect on Carbon Fiber Epoxy Composites, Naval Surface Weapons Center.
- 30) D. Cripps, L. S. Norwood, *Guide to Composites*, Netcomposites Co.
- 31) A. Letton and W. L. Bradley, Studies in Long Term Durability of Composites in Seawater, National Conference on the use of Composite Materials in Load-bearing Marine Structures, Vol. II: Conference Proceedings, pg. 91, National Academy Press, 1990.

- 32) A. Apicella, C. Migliaresi, L. Nicolais, and S. Roccotelli, The Water Aging of Unsaturated Polyester-based Composites: Influence of Resin Chemical Structure, *Composites*, 14, 387-92, 1983.
- 33) J. Gutierrez, F. Le Lay, and Pl Hoarau, A Study of the Aging of Glass Fibre-resin Composites in a Marine Environment, *Nautical Construction with Composite Materials*, Paris: Ifremer-Centre De Brest, edited by P. Davies and L. Lemoine, 1992.
- 34) E. P. Gellert and D. M. Turley, Seawater Immersion Ageing of Glass-fibre Reinforced Polymer Laminates for Marine Applications, *Composites*, 30A, 1259, 1999.
- 35) Z. D. Jasterzebski, *The Nature and Properties of Engineering Materials*, Second Edition, SI Version, John Wiley & Sons, ISBN 0-471-02859-2, 1977.
- 36) C. Williams, Effect of Water Absorption on the Room Temperature Properties of Carbon Fiber and Glass Fiber Reinforced Polymer Composites, *Ship Materials Engineering Department, David Taylor Research Center, DTRC/SME-88-85*, December 1998.
- 37) R. A. Flinn and P. K. Trojan, *Engineering Materials and Their Applications*, Houghton Mifflin Company, 1975.
- 38) W. F. Smith, *Foundations of Materials Science and Engineering*, Second Edition, McGraw-Hill, Inc., 1993.
- 39) A. P. Mouritz, A. Kootsookos and G. Mathys, Stability of Polyester- and Vinyl Ester-based Composites in Seawater, *Journal of Materials Science*, 39, 6073-6077, 2004.

- 40) C. Baley, P. Davies, Y. Grohens and G. Dolto, Application of Interlaminar Tests to Marine Composites. A Literature Review, *Applied Composite Materials*, 11, 99-126, 2004.
- 41) K. H. G. Ashbee and R. C. Wyatt, Water Damage in Glass Fiber / Resin Composites, *Proceedings of the Royal Society A.312*, 553-564, 1969.
- 42) G. Menges and K. Lutterbeck, Stress Corrosion in Fibre-Reinforced Plastics in Aqueous Media, *Dev. Reinf. Plast.* 3, Elsevier Applied Science Publishers, Ltd., New York, 97-122, 1984.
- 43) Y. Weitsman and M. Henson, Stress Effects on Moisture Transport in an Epoxy Resin and its Composite, Office of Naval Research Report M M 4762-86-15, June 1986.
- 44) B. Ellis, The Effects of Water Absorption on a Polyester Chopped Strand Mat Laminate, *Composites*, 26, 237, 1983.
- 45) K. Liao, C. R. Schultheisz, D. L. Huston, and L. C. Brinson, Long Term Durability of Fiber Reinforced Polymer Matrix Composite Materials for Infrastructure Applications: a Review, *J. Adv Mater*, 54, 1998.
- 46) N. R. Farrer and K. H. G. Ashbee, Self-Stress Enhanced Water Migration in Composites, *Org. Coat. Plast. Chem*, 40, 947-953, 1979.
- 47) Y. J. Weitsman and M. Elahi, Effects of Fluids on the Deformation, Strength and Durability of Polymeric Composites – An Overview, *Mechanics of Time-Dependent Materials* 4: 107-126, Kluwer Academic Publishers, 2000.

- 48) Y. Weitsman, *Moisture in Composites: Sorption and Damage, Fatigue of Composite Materials* edited by K. L. Reifsnider, Elsevier Science Publishers B. V., 1990.
- 49) Y. J. Weitsman and Y. Guo, *A Correlation Between Fluid-induced Damage and Anomalous Fluid Sorption in Polymeric Composites*, *Composites Science and Technology*, 62, 889-908, 2002.
- 50) V. B. Gupta, L. T. Drzal, W. W. Adams, and R. Omlor, *Study of the Morphology of Cured Epoxy Resin*, ARWAL-TR-86-4029, December 1986.
- 51) W. J. Mikols, J. C. Seferis, A. Apicella, and L. Nicolais, *Evaluation of Structural Changes in Epoxy Systems by Moisture Sorption-Desorption and Dynamic Mechanical Studies*, *Polymer Composites*, 3, 3, 118-124, July 1982.
- 52) F. McBagonluri, K. Garcia, M. Hayes, K. N. E. Verghese and J. J. Lesko, *Characterization of Fatigue and Combined Environment on Durability Performance of Glass/Vinyl Ester Composite for Infrastructure Applications*, *International Journal of Fatigue*, 22, 53-64, 2000.
- 53) Y. Weitsman, *A Continuum Model for Viscoelastic Materials*, *The Journal of Physical Chemistry*, 94, 961, 1990.
- 54) L. W. Cai and Y. Weitsman, *Non-Fickian Moisture Diffusion in Polymeric Composites*, Office of Naval Research Technical Report ESM92-6.0-MECH, September 1992.
- 55) T. K. Tsotsis, PhD Dissertation, Texas A and M University, 1989.

- 56) G. Menges and H. W. Gitsner, Proceedings of the Third International Conference on Composite Materials, ICCM-3, Paris, edited by A. R. Bunsell (Pergamon Press, New York) 597, August 1980.
- 57) J. M. Marshall, G. P. Marshall, and R. F. Pinzelli, The Diffusion of Liquids into Resins and Composites, *Polymer Composites*, 3, 3, 131-137, July 1982.
- 58) G. Marom and L. J. Broutman, Moisture Penetration into Composites Under External Stress, *Polymer Composites*, 2, 3, 132-136, 1981.
- 59) A. C. Loos and G. S. Springer, Environmental Effects on Composite Materials, Vol. 1, edited by G. S. Springer (Technomic, Westport, CT, 1981) p. 34.
- 60) R. Kosuri and Y. Weitsman, Sorption Process and Immersed-Fatigue Response of Gr/Ep Composites in Sea Water, Proceedings of ICCM-10, Whistler, B.C., Canada, August 1995.
- 61) G. Marom and L. J. Broutman, Moisture in Epoxy Resin Composites, *Journal of Adhesion*, 12, 2, 153-164, 1981.
- 62) H. Leidheiser, Jr., and R. D. Granata, Ion Transport through Protective Polymeric Coatings Exposed to an Aqueous Phase, *IBM Journal of Research and Development*, 32, 5, 582-90, 1988.
- 63) R. Turoscy, H. Leidheiser, Jr., and J. E. Roberts, Solid-state NMR Studies of Sodium Ions in a Polybutadiene Matrix, *J. Electrochem. Soc.*, 137, 6, 1785-1788, 1990.
- 64) H. Hashida and K. Ganesh, Molecular Characterization of Composite Interfaces, *Polymer Science and Technology Series*, First Edition, Springer, 1985.

- 65) M. Tymichova, Relation Between Toughness and Molecular Coupling at Cross-linked Polymer/Solid Interfaces, PhD Thesis, University of Wollongong, 2005.
- 66) H. A. Clark and E. P. Plueddemann, *Mod. Plast.* 40, 6, 133, 1963.
- 67) P. W. Erickson, A. A. Volpe and E. R. Cooper, SPI, 19th Ann. Tech. Conf. Reinf. Plast. 21-A, 1964.
- 68) E. P. Plueddemann, SPI, 27th Ann. Tech. Conf. Reinf. Plast. 21-B, 1972.
- 69) E. K. Drown, H. Al-Moussawi, and L. T. Drzal, Glass Fiber Sizings and Their Role in Fiber/matrix Adhesion, *J. Adhesion Sci. Technol.* 5, 10, 865-881, 1991.
- 70) P. S. Chua, S. R. Dai and M. R. Piggott, Mechanical Properties of the Glass Fibre-polyester Interphase Part I Effects Due to Silanes, *Journal of Materials Science*, 27, 4, 913-918, 1992.
- 71) P. S. Chua and M. R. Piggott, Mechanical Properties of the Glass Fibre-polyester Interphase Part III Effect of Water on Interface Pressure and Friction, *Journal of Materials Science*, 27, 4, 925-929, 1992.
- 72) E. P. Plueddemann, Present Status and Research Needs in Silane Coupling, In *Proc. ICCI-II, Interfaces in Polymer, Ceramic and Metal Matrix Composites*, Elsevier Sci. Pub., New York, 17-33, 1988.
- 73) T. H. Cheng, F. R. Jones and D. Wang, Effect of Fiber Conditioning on the Interfacial Shear Strength of Glass-fiber Composites. *Composites Sci. Technol.* 48, 89-96, 1993.
- 74) T. C. Chang, Plasma Surface Treatment in Composites Manufacturing, *J. Industrial Technology*, 15, 1, 1998.

- 75) L. Y. Yuan, S. S. Shyu and J. Y. Lai, Plasma Surface Treatments on Carbon Fibers. II. Mechanical Property and Interfacial Shear Strength, *J. Applied Polymer Science*, 42, 2525-2534, 1991.
- 76) B. Z. Jang, Control of Interfacial Adhesion in Continuous Carbon and Kevlar Fiber Reinforced Polymer Composites, *Composites Science and Technology*, 44, 4, 333-349, 1992.
- 77) N. Dilsiz, Plasma Surface Modification of Carbon Fibers: a Review, *J. Adhesion Sci. Technol.*, 14, 7, 975-987, 2000.
- 78) Denise, J. D. Moyer and J. P. Wightman, Characterization of Surface Pretreatments on Carbon Fiber-polyimide Matrix Composites, *Surface and Interface Analysis*, 14, 9, 496-504.
- 79) B. S. Jin, K. H. Lee and C. R. Choe, *Polym. Int.*, 34, 181, 1994.
- 80) L Nohara, G. P. Filho, E. L. Nohara, M. U. Kleinke and M. C. Rezende, Evaluation of Carbon Fiber Surface Treated by Chemical and Cold Plasma Processes, *Materials Research*, 8, 3, 281-286, 2005.
- 81) V. Chirila, G. Marginean, T. Iclanzan, C. Merino and W. Brandl, Method for Modifying Mechanical Properties of Carbon Nano-fiber Polymeric Composites, *Journal of Thermoplastic Composite Materials*, 20, 277-289, May 2007.
- 82) J. C. Goan and S. P. Prosen, Interfacial Bonding in Graphite Fiber-resin Composites, *J. Interfaces in Composites; a Symposium*, 3-26, 1969.
- 83) R. K. Jain, L. M. Manocha and O. P. Bahl, Surface Treatment of Carbon Fibres with Nitric Acid and its Influence on the Mechanical Behaviour of Composites

- made with Phenolic and Furan as Matrices, *Indian Journal of Technology*, 29, 163-172, 1991.
- 84) E. Fitzer, K. H. Geigl, and L. M. Mancho, *Proc. 5th Conf. on Carbon and Graphite*, Vol. 1, p. 405. Society of Chemical Industry, London, 1978.
- 85) C. U. Pittman Jr., G. R. He, B. Wu, and S. D. Gardner, *Chemical Modification of Carbon Fiber Surfaces by Nitric Acid Oxidation Followed by Reaction with Tetraethylenepentamine*. *Carbon*, 35, 3, 317-331, 1997.
- 86) Z. R. Yue, W. Jiang, L. Wang, S. D. Gardner, and C. U. Pittman Jr., *Surface Characterization of Electrochemically Oxidized Carbon Fibers*. *Carbon*, 37, 11, 1785-1796, 1999.
- 87) S. M. Lee, *Handbook of Composite Reinforcements*, ISBN 1-56081-632-5, VCH Publishers, Inc., 1993.
- 88) A. Oberlin and M. Guigon, *The structure of Carbon Fibers*, In A. R. Bunsell, Ed., *Fiber Reinforcements for Composite Materials*, Elsevier, Amsterdam, 1988.
- 89) G. Dagli and N. Sung, *Properties of carbon/graphite fibers modified by plasma polymerization*, *Polym. Composites*, 10, 2, 109-116, 1989.
- 90) M. Chen, T. Yang and Z. Ma, *Investigation of RF Styrene plasma by Emission Spectroscopy*, *IEEE Transactions on Plasma Science*, 23, 2, 151-155, 1995.
- 91) "Phenyl group." *Wikipedia, The Free Encyclopedia*. 28 Mar 2007, 02:43 UTC. Wikimedia Foundation, Inc. 12 Apr 2007
<http://en.wikipedia.org/w/index.php?title=Phenyl_group&oldid=118428015>.
- 92) W. L. Lachman, J. A. Crawford, and L. E. McAllister, in B. Noton, R. Signorelli, K. Street, and L. Phillips, Eds., *Proceedings of the Intl. Conference on Composite*

- Materials, Vol I, Metallurgical Society of the American Institute of Mining, Metallurgical, and Petroleum Engineers, 307, 1976.
- 93) “Carbon Fiber”, Toray Industries Inc., 5/15/07,
<<http://www.torayca.com/index2.html>>.
- 94) “Carbon Fiber Data Sheets, Continuous Fiber”, Hexcel, 5/15/07,
<<http://www.hexcel.com/Products/Downloads/Carbon+Fiber+Data+Sheets.htm?ds=Continuous>>
- 95) E. Fitzer and M. Heine, Carbon Fiber Manufacture and Surface Treatment, In A. R. Bunsell, Ed., Fiber Reinforcements for Composite Materials, Elsevier, Amsterdam, 1988.
- 96) S. C. Bennett and D. J. Johnson, In Proc. 5th London Carbon and Graphite Conference, Vol. 1, Society for Chemical Industry, London, 377, 1978.
- 97) F. A. Ramirez, Evaluation of water degradation of polymer matrix composites by micromechanical and macromechanical tests, Master's thesis, Florida Atlantic University, August 2008.
- 98) P. K. Mallick, Fiber-Reinforced Composites, Materials Manufacturing, and Design, ISBN 0-8247-7796-4, Marcel Dekker, Inc., 1988.
- 99) O. C. Zaske and S. H. Goodman, Handbook of Thermoset Plastics, Unsaturated Polyester and Vinyl Ester Resins, 97-168.
- 100) M. J. Sumner, R. Y. Weyers, A. C. Rosario, J. S. Riffle and U. Sorathia, Synthesis and Characterization of Vinyl Ester Networks Containing Phthalonitrile Moieties, Polymer 45, 5199-5206, 2004.

- 101) Electronegativity, Wikipedia, The Free Encyclopedia. 12 Apr 2007, 01:23 UTC.
Wikimedia Foundation, Inc. 16 Apr 2007
<<http://en.wikipedia.org/w/index.php?title=Electronegativity&oldid=122108764>>
.
- 102) L. Pauling, The Nature of the Chemical Bond, 2nd Ed., Cornell University Press, Ithaca, N.Y., 1948.
- 103) M. Orchin, R. S. Macomber, A. R. Pinhas and R. M. Wilson, The Vocabulary and Concepts of Organic Chemistry, Second Edition, ISBN 0-471-68028-1, John Wiley & Sons, 2005.
- 104) Hydrogen bond, Wikipedia, The Free Encyclopedia. 16 Apr 2007, 21:34 UTC.
Wikimedia Foundation, Inc. 16 Apr 2007
<http://en.wikipedia.org/w/index.php?title=Hydrogen_bond&oldid=123359341>.
- 105) S. P. Prosen, J. V. Duffy, P. W. Erickson and M. A. Kinna, Proc. 21st SPI Annual Technical Conference, Section 8-D, 1966.
- 106) J. W. Herrick, P. E. Gruber, and F. T. Mansur, AVCO Corporation, Lowell, Mass., Technical Report AFML-TR-66-178, part I, July 1966.
- 107) E. Greene and Associates, Marine Composites, Second Edition, 1999.
- 108) J. Vidic, A. Podgornik and A. Strancar, Effect of the Glass Surface on the Strength of Methacrylate Monolith Attachment, Journal of Chromatography A, 1065, 1, 51-58, 2005.
- 109) University of Illinois Imaging Technology Group, How ESEM Works, <http://www.itg.uiuc.edu/ms/equipment/microscopes/esem/how_it_works.htm>.

- 110) Scanning electron microscope, Wikipedia, The Free Encyclopedia. 17 Apr 2007, 16:36 UTC. Wikimedia Foundation, Inc. 19 Apr 2007
<http://en.wikipedia.org/w/index.php?title=Scanning_electron_microscope&oldid=123564139>.
- 111) K. L. Pickering and T. L. Murray, Weak Link Scaling Analysis of High-strength carbon fibre, *Composites: Part A*, 30, 1017-1021, 1999.
- 112) R. A. Johnson, Miller and Freund's Probability and Statistics for Engineers, Fifth Edition, Prentice Hall International Editions, 1994.
- 113) K. K. Phani, *Mat Sci*, 23, 2424, 1988.
- 114) M. S. Akhter, A. R. Chughtai and D. M. Smith, Spectroscopic studies of oxidized soots, *Appl. Spectrosc.* 45, 4, 653-665, 1991.
- 115) M. S. Akhter, A. R. Chughtai and D. M. Smith, The structure of hexane soot I: spectroscopic studies, *Appl. Spectrosc.* 39, 1, 143-153, 1985.
- 116) D. M. Smith and A. R. Chughtai, The surface-structure and reactivity of black carbon, *Colloids Surf. A, Physicochem Eng Aspects*, 105, 1, 47-77, 1995.
- 117) H. P. Boehm, Surface oxides on carbon and their analysis: a critical assessment, *Carbon* 40, 2, 145-149, 2002.
- 118) E. Fuente, J. A. Menendez, D. Suarez and M. A. Montes-Moran, Basic surface oxides on carbon materials: a global view, *Langmuir* 19, 3505-3511, 2003.
- 119) E. Fuente, J. A. Menendez, M. A. Diez, D. Suarez and M. A. Montes-Moran, Infrared spectroscopy of carbon materials: a quantum chemical study of model compounds, *J. of Phys. Chem. B*, 107, 6350, 2003.

- 120) P. E. Fanning and M. A. Vannice, A DRIFTS study of the formation of surface groups on carbon by oxidation, *Carbon*, 31, 721, 1993.
- 121) D. M. Smith, J. R. Keifer, M. Novicky and A. R. Chugtai, An FT-IR study of the effect of simulated solar radiation and various particulates on the oxidation of SO₂, *Appl. Spectrosc.* 43, 1, 103-107, 1989.
- 122) G. S. Szymanski, Z. Karpinski, S. Biniak and A. Swiatkowski, The effect of the gradual thermal decomposition of surface oxygen species on the chemical and catalytic properties of oxidized activated carbon, *Carbon* 40, 2627-2639, 2002.
- 123) E. Raymundo-Pinero, D. Cazorla-Amoros and A. Linares-Solano, Temperature programmed desorption study on the mechanism of SO₂ oxidation by activated carbon and activated carbon fibres, *Carbon*, 39, 2, 231-242, 2001.
- 124) S. Haydar, C. Moreno-Castilla, M. A. Ferro-Garcia, F. Carrasco-Marin, J. Rivera-Utrilla, A. Perrard and J. P. Joly, *Carbon*, 38, 1297, 2000.
- 125) Q. L. Zhuang, T. Kyotani and A. Tomita, DRIFT and TK/TPD analyses of surface oxygen complexes formed during carbon gasification, *Energy & Fuels*, 8, 3, 714-718, 1994.
- 126) Z. X. Jiang, Y. Liu, X. P. Sun, F. P. Tian, F. X. Sun, C. H. Liang, W. S. You, C. R. Han and C. Li, Activated carbons chemically modified by concentrated H₂SO₄ for the adsorption of the pollutants from wastewater and the dibenzothiophene from fuel oils, *Langmuir* 19, 3, 731-736, 2003.
- 127) F. J. Lopez-Garzon, M. Domingo-Garcia, M. Perez-Mendoza, P. M. Alvarez and V. Gomez-Serrano, Textural and chemical surface modifications produced by some oxidation treatments of glassy carbon, *Langmuir*, 19, 7, 2838-2844, 2003.

- 128) L. A. Langley, D. E. Villanueva and D. H. Fairbrother, Quantification of Surface Oxides on Carbonaceous Materials, *Chem. Mater.* 18, 1, 169-178, 2006.
- 129) L. A. Langley and D. H. Fairbrother, Effect of wet chemical treatments on the distribution of surface oxides on carbonaceous materials, *Carbon* 45, 47-54, 2007.
- 130) X-ray photoelectron spectroscopy, Wikipedia, The Free Encyclopedia. 11 Apr 2007, 08:34 UTC. Wikimedia Foundation, Inc. 19 Apr 2007
<http://en.wikipedia.org/w/index.php?title=X-ray_photoelectron_spectroscopy&oldid=121895270>.
- 131) R. P. Popat, I. Sutherland, and E. S. Sheng, Vapor phase chemical derivatization for the determination of surface functional groups by X-Ray photoelectron spectroscopy, *J. Mater. Chem.*, 5, 5, 713-717, 1995.
- 132) A. Chilkoti, B. D. Ratner and D. Briggs, Plasma-deposited polymeric films prepared from carbonyl-containing volatile precursors – xps chemical derivatization and static sims surface characterization, *Chem. Mater.* 3, 1, 51-61, 1991.
- 133) C. D. Batich, Chemical derivatization and surface analysis, *Appl. Surf. Sci.*, 32, 1-2, 57-73, 1988.
- 134) A. P. Ameen, R. J. Ward, R. D. Short, G. Beamson and D. Briggs, A high-resolution X-ray photoelectron spectroscopy study of trifluoroacetic anhydride labeling of hydroxyl groups: demonstration of the β shift due to $-\text{OC}(\text{O})\text{CF}_3$, *Polymer*, 34, 9, 1795-1799, 1993.
- 135) J. McMurry, *J. Organic Chemistry*, 2nd ed., Brooks/Cole Publishing Company, Pacific Grove, CA, 1988.

- 136) S. Zeggane and M. Delamar, XPS study of the penetration and reaction speed of polymer derivatization reagents, *Appl. Surf. Sci.*, 31, 1, 151-156, 1988.
- 137) Y. K. Hamidi, L. Aktas and M. C. Altan, Effect of Packing on Void Morphology in Resin Transfer Molded E-Glass/Epoxy Composites, *Polymer Composites*, 614-627, 2005.
- 138) C. Sellitti, J. L. Koenig and H. Ishida, Surface characterization of graphitized carbon fibers by attenuated total reflection Fourier transform infrared spectroscopy, *Carbon*, 28, 1, 221-228, 1990.
- 139) M. Domingo-Garcia, F. J. L. Garzon and M. J. Perez-Mendoza, On the Characterization of Chemical Surface Groups of Carbon Materials, *Colloid Interface Sci.*, 248, 1, 116-122, 2002.
- 140) K. Niskanen, "Paper Physics", Fapet Oy, 1998.
- 141) R. P. Woodward, Prediction of Adhesion and Wetting from Lewis Acid Base Measurements, presented at TPOs in Automotive, 2000.
- 142) W. Yang, Improvement of Interfacial Adhesion by Plasma Modification in Graphite Fiber/Thermoplastic Composites, Tufts University Master's Thesis, February, 1986.
- 143) D. H. Kaelble, P. J. Dynes and E. H. Cirlin, Interfacial Bonding and Environmental Stability of Polymer Matrix Composites, *Journal of Adhesion*, 6, 6, 23-48, 1974.
- 144) C. Ageorges, K. Friedrich, and L. Ye, "Experiments to relate carbon-fiber surface treatments to composite mechanical properties", *Composites Science and Technology*, 59, 14, 2101-2113, 1999.

- 145) P. S. Chua, S. R. Dai and M. R. Piggott, Mechanical Properties of the Glass Fibre-polyester Interphase Part II Effect of Water on Debonding, *Journal of Materials Science*, 27, 4, 919-924, 1992.
- 146) E. N. Brown and D. M. Dattelbaum, Fracture and Damage Evolution in Polymers, *Nuclear Weapons Journal*, 2, 2006.
- 147) H. C. Tsai, A. M. Arocho and L. W. Gause, Prediction of Fiber/matrix Interphase Properties and their Influence on Interface Stress, Displacement and Fracture Toughness of Composite Material, *Materials Science and Engineering*, A126, 1-2, 295-304, 1990.
- 148) D. Hull, *An Introduction to Composite Materials*, Cambridge University Press, Cambridge, 1981.
- 149) R. Naslain, Fiber/matrix Interphase and Interfaces in Ceramic Matrix Composites Processes by CVI, *Composite Interfaces* 1, 253-286, 1993.
- 150) E. Fitzer, K. H. Geifl, W. Huttner, and R. Weiss, Chemical interactions between the carbon-fiber surface and epoxy resins, *Carbon* 18, 6, 389-393, 1980.
- 151) C. Galiotis, R. J. Young, P. H. J. Yeung, N. Melanitis and D. N. Batchelder, The Study of Model Polydiacetylene/epoxy Composites, Part 1, The Axial Strain in the Fiber, *J. Mater. Sci.* 19, 3640-3648, 1984.
- 152) El. M. Asloun, M. Nardin and J. Schultz, Stress Transfer in Single-fiber Composites: Effect of Adhesion, Elastic Modulus of Fiber and Matrix and Polymer Chain Mobility, *J. Mater. Sci.* 24, 1835-1844, 1989.
- 153) N. Ogata, H. Yasumoto, K. Yamasaki, H. Yu, T. Ogihara, T. Yanagawa, K. Yoshida and Y. Yamada, Evaluation of Interfacial Properties Between Carbon

- Fibers and Semi-crystalline Thermoplastic Matrices in Single Fiber Composites, *J. Mater. Sci.* 27, 5108-5112, 1992.
- 154) K. E. Verghese, *Durability of Polymer Matrix Composites for Infrastructure: The Role of the Interphase*, PhD Dissertation, Virginia Polytechnic Institute and State University, 1999.
- 155) S. Agrawal, R. Singhal, and J. S. P. Rai, *Curing and Rheological Behavior of Vinyl Ester Resins Prepared in the Presence of Tertiary Amines*, *J.M.S. – Pure Appl. Chem.*, A36, 5&6, 741-757, 1999.
- 156) V. I. Povstugar, S. S. Mikhailova, and A. A. Shakov, *Chemical derivatization techniques in the determination of functional groups by X-ray photoelectron spectroscopy*, *J. Anal. Chem.* 55, 5, 405-416, 2000.
- 157) Z. Guo, L. Liu, B. Zhang and S. Du, *Critical Void Content for Thermoset Composite Laminates*, *Journal of Composite Materials*, doi:10.1177/0021998306065289, 2006.
- 158) D. G. Lee and S. S. Cheon, *Impact Characteristics of Glass Fiber Composites with Respect to Fiber Volume Fraction*, *Journal of Composite Materials*, 35, 01, 2001.
- 159) D. Tripathi, N. Lopattananon and F. R. Jones, *A Technological Solution to the Testing and Data Reduction of Single Fibre Fragmentation Tests*, *Composites Part A*, 29A, 1099-1109, 1998.
- 160) J. Donnet, T. K. Wang, S. Rebouillat and J. C. M. Peng, *Carbon Fibers*, Third Edition, Revised and Expanded, Marcel Dekker, Inc., 1998.

- 161) C. M. Laot, Spectroscopic Characterization of Molecular Interdiffusion at a Poly(Vinyl Pyrrolidone) / Vinyl Ester Interface, M. S. Thesis, Virginia Polytechnic Institute and State University, 1997.
- 162) Y. J. Hwang, Characterization of Atmospheric Pressure Plasma Interactions with Textile/Polymer Substrates, PhD Dissertation, North Carolina State University, 2003.
- 163) S. Kajorncheappunngam, The Effects of Environmental Aging on the Durability of Glass/Epoxy Composites, PhD Dissertation, West Virginia University, 1999.
- 164) A. Apicella and L. Nicolais, Effect of Water on the Properties of Epoxy Matrix and Composite, Epoxy Resins and Springer Verlag, NY, 1985.
- 165) S. Aksu, S. Cannon, C. Gardiner and M. Gudze, Hull Material Selection for Replacement Patrol Boats- An Overview, Department of Defence, Maritime Platforms Division, Aeronautical and Maritime Research Laboratory, 2002.
- 166) V. M. Karbhari, J. W. Chin, D. Hunston, B. Benmokrane, T. Juska, R. Morgan, J. Lesko, U. Sorathia and D. Reynaud, Durability Gap Analysis for Fiber-Reinforced Polymer Composites in Civil Infrastructure, Journal of Composites for Construction, ASCE, August, 2003.
- 167) A. H. Nissan and G. L. Batten, Jr., On the Primacy of the Hydrogen Bond in Paper Mechanics, Paper Mechanics, Tappi Journal, 73, 2, 159-164, February 1990.
- 168) A. H. Nissan, V. L. Byrd, G. L. Batten, Jr., and R. W. Ogden, Paper as an H-bond Dominated Solid in the Elastic and Plastic Regimes, Paper Physics, Tappi Journal, 68, 9, 118-124, September 1985.

- 169) J. DiFlavio, R. Pelton, M. Leduc, S. Champ, M. Essig and T. Frechen, The Role of Mild TEMPO-NaBr-NaClO Oxidation on the Wet Adhesion of Regenerated Cellulose Membranes with Polyvinylamine, *Cellulose*, 14, 257-268, 2007.
- 170) Y. Zhao and Y. Duan, The Dispersion of MWCNTs within Epoxy by Treatment with Coupling and Dispersing Agents, *Materials Science Forum*, Vols. 546-549, 2307-2312, 2007.
- 171) H. Watson, P. J. Mikkola, J. G. Matisons and J. B. Rosenholm, Deposition Characteristics of Ureido Silane Ethanol Solutions onto E-glass Fibers, *Colloids and Surfaces, A: Physicochemical and Engineering Aspects*, 161, 183-192, 2000.
- 172) E. P. Plueddemann, *Silane Coupling Agents*, Plenum Press, New York, 1982.
- 173) D. F. Adams, T. R. King and D. M. Blackketter, Evaluation of the Transverse Flexure Test Method for Composite Materials, *Composites Science and Technology*, 39, 341-353, 1990.
- 174) M. S. Madhukar and L. T. Drzal, Fiber/matrix Adhesion and its Effect on Composite Mechanical Properties: II. Longitudinal (0°) and Transverse (90°) Tensile and Flexure Behavior of Graphite/Epoxy Composites, *Journal of Composite Materials*, 25, 958-991, 1991.
- 175) E. J. v. Klinken, the Influence of the Fibre-matrix Interface on the Transverse Mechanical Behaviour and Failure of Carbon Fibre Reinforced Composites, Graduate Report TUE WFW 92.051, Eindhoven University of Technology, 1992.
- 176) T. K. O'Brien and R. Krueger, Analysis of Ninety Degree Flexure Tests for Characterization of Composite Transverse Tensile Strength, NASA/TM-2001-211227 ARL-TR-2568, 2001.

- 177) K. J. Bowles, Transverse Flexural Tests as a Tool for Assessing Damage to PMR-15 Composites From Isothermal Aging in Air at Elevated Temperatures, NASA Technical Memorandum 105848, 1992.
- 178) S. Kajorncheappunngam, R. K. Gupta and H. V. S. GangaRao, Effect of Aging Environment on Degradation of Glass-Reinforced Epoxy, *Journal of Composites for Construction*, 61-69, 2002.
- 179) Y. Yu, X. Yang, L. Wang and H. Liu, Hygrothermal Aging on Pultruded Carbon Fiber/Vinyl Ester Resin Composite for Sucker Rod Application, *Journal of Reinforced Plastics and Composites*, 25, 149, 2006.
- 180) T. Juska, Effect of Water Immersion on Fiber/Matrix Adhesion, CARDEROCKDIV-SME-92/38, R&D Report, 1993.
- 181) K. Luo, G. Li, J. Jin, S. Yang and J. Jiang, Surface Analysis of PBO and Modified SPBO Fiber by Contact Angle Measurements and XPS, *Journal of Macromolecular Science, Part B: Physics*, 45, 631-637, 2006.
- 182) H. Cao, Y. Huang, Z. Zhang and J. Sun, Uniform Modification of Carbon Fibers Surface in 3-D Fabrics using Intermittant Electrochemical Treatment, *Composites Science and Technology*, 65, 1655-1662, 2005.
- 183) C. Moreno-Castilla, M. V. Lopez-Ramon and F. Carrasco-Marin, Changes in Surface Chemistry of Activated Carbons by Wet Oxidation, *Carbon*, 38, 1995-2001, 2000.
- 184) J. Drews, S. Goutianos, P. Kingshott, S. Hvilsted, N. Rozlosnic, K. Almdal and B. F. Sorenson, Plasma Ploymerized Thin Films of Maleic Anhydride and 1,2-

- Methylenedioxybenzene for Improving Adhesion to Carbon Surfaces, *J. Vac. Sci. Technol. A* 25, 4, 1108-1117, 2007.
- 185) J. B. Donnet, E. Papirer and H. Kauksch, Surface Modification of Carbon Fibres and their Adhesion to Epoxy Resins, Paper No. 9, Carbon Fibers, their place in Modern Technology: proceedings of the International Conference Organized by The Plastics Institute, London, 1974.
- 186) S. Pavlidou, K. Krassa and C. D. Papaspyrides, Woven Glass Fabric/Polyester Composites: Effect of Interface Tailoring on Water Absorption, *Journal of Applied Polymer Science*, 98, 843-851, 2005.
- 187) J. B. Donnet, S. Dong, G. Guilpain and M. Brendle, Carbon Fibers Electrochemical and Plasma Surface Treatment and Its Assessment, International Conference on Composite Interfaces, 2nd, Ohio, 1988.
- 188) P. Commercon, Surface Characterization of Plasma Treated Carbon Fibers and Adhesion to Polyethersulfone, PhD Dissertation, Virginia Polytechnic Institute and State University, 1992.
- 189) K. N. E. Verghese, N. S. Broyles, J. J. Lesko, R. M. Davis and J. S. Riffle, Pultruded Carbon Fiber/Vinyl Ester Composites Processed with Different Fiber Sizing Agents. Part II: Enviro-Mechanical Durability, *Journal of Materials in Civil Engineering*, 334-342, 2005.
- 190) L. T. Drzal, M. J. Rich and P. F. Lloyd, Adhesion of Graphite Fibers to Epoxy Matrices: I. The Role of Fiber Surface Treatment, *J. Adhesion*, 16, 1-30, 1982.